CURCUMIN ACTION IN PROSTATE CANCER CELLS AND FIBROBLASTS

By Lauren Giorgio

B.HlthSc (Honours)

A thesis submitted to The University of Adelaide in total fulfilment of the requirements for the degree of Doctor of Philosophy

School of Medicine

Faculty of Health Science

The University of Adelaide

July 2014

This thesis is dedicated to the people

who never stopped believing in me

INVICTUS

Out of the night that covers me
Black as the pit from pole to pole
I thank whatever gods may be
For my unconquerable soul

In the fell clutch of circumstance
I have not winced nor cried aloud
Under the bludgeoning of chance
My head is bloody, but unbowed

Beyond this place of wrath and tears
Looms but the horror of the shade
And yet the menace of the years
Finds, and shall find, me unafraid

It matters not how strait the gate
How charged with punishments the scroll
I am the master of my fate
I am the captain of my soul

-William Ernest Henley

TABLE OF CONTENTS

DECLARATION

This work contains no material which has been accepted for the award of any other degree or diploma in any university or other tertiary institution and, to the best of my knowledge and belief, contains no material previously written by another person, except where due reference has been made in the text.

I give consent to this copy of my thesis when deposited in the University Library, being made available for loan and photocopying, subject to the provisions of the Copyright Act 1968. The author acknowledges that copyright of published works contained within this thesis resides with the Copyright holders of those works.

I also give permission for the digital version of my thesis to be made available on the web, via the University's digital research repository, the Library catalogue, the Australian Digital Theses Program (ADTP) and also through web search engines, unless permission has been granted by the University to restrict access for a period of time.

SIGNATURE: …….. DATE: ……

ACKNOWLEDGEMENTS

First and foremost, I would like to thank the academics who helped me along the way.

I owe my deepest gratitude to Professor Andreas Evdokiou for believing in my ability and trusting me as a scientist. You generously funded the animal study, allowed me full access to all of your resources and reviewed my thesis chapters. The only repayment you wanted was to see me succeed in getting my PhD. I have learnt so much from you and would not have been able to complete this journey without your guidance.

Dr Luke Selth, I thank you from the bottom of my heart for reviewing my data and thesis throughout what was the hardest part of my PhD. I learnt a great deal from the constructive criticism you provided. You were the only person who could get me over those last few hurdles and you selflessly donated your time to doing so. You did this only to see me get my PhD and for this I will always grateful.

Professors Alastair Burt and Richard Russell, I would like to thank you for guiding me through the various challenges I faced throughout my candidature. Your professionalism and approachability was very much appreciated.

Dr Irene Zinonos, thank you for sharing your wealth of animal work knowledge and for always being available to help me, no matter how busy you were. Thank you for all the Greek feasts and for being such a wonderful friend.

Dr Grant Buchanan, thank you for the bioinformatics you performed on my microarray data and for supporting my attendance at national conferences.

Dr Tak Kee and Mr Taka Harada, thank you for giving me the opportunity to work with you on something so novel and exciting. I wish you both the best of luck in the next chapter of this work.

Dr Jeff Holst and Dr Kevin Wang, thank you for having me visit your laboratory, for teaching me everything I needed to know about flow cytometry and for reviewing my paper.

I would also like to thank Dr Eleanor Need and Dr Andrew Trotta, who were co-supervisors for part of my PhD.

When we find someone whose weirdness is compatible with ours, we fall into mutually satisfying weirdness called friendship.

'Classic' Bill Liapis, 'Young' Bill Panagopoulos, Shelley Hay, Sarah Bray, Amanda Drilling, Hilary Dorward, Aneta Zysk and Dijana Miljkovic, thank you for all your help and advice, and for keeping a smile on my face over the years.

Ms Harshani Jayasinghe, thank you for being such an incredible friend. Your visits to my office brightened my days more than you know and your positivity is infectious. I thoroughly enjoyed our adventures and all the Sri Lankan feasts! I wish you all the very best with your PhD.

Dr Tamsin Garrod, I knew you were a true friend when you helped me scrub slimy water bins and pick up horse manure. Thank you for standing by me throughout this journey, it means the world to me. The long walks and coffees were also invaluable in reducing my stress levels! I wish you all the very best with your future endeavours.

Ms Erin Swinstead, I cannot put into words how grateful I am to have had you as a friend throughout this journey. You have always had my back, especially when I did silly things like print ten thousand pages. We laughed together, we cried together and we used the Port Road park bench way too much. Sometimes we needed more than the bench, so off to sushi train we went. Even though you are so far away I still think of us as a great TIEAM! You are an inspirational woman and a true friend, and our legacy at the BHI lives on in the form of a ten metre "promotional poster". I wish you all the very best with your American adventure!

I am fortunate enough to have had the guidance of two wonderful women who kept me sane when nothing seemed to be working. Ms Ann Madigan, words cannot express how grateful I am to have had your unwavering support. I was at rock bottom when I met you but it was with your help that I was able to submit this thesis. I thank you from the bottom of my heart and commend you for being so incredibly talented at your job. Ms Vicki McCoy, thank you for our sessions. It was such a blessing to be able to chat to you, and your words of wisdom and reason were invaluable to my completion. I will carry your advice with me for many years to come!

I am very grateful to the team at The Hospital Research Foundation, especially Paul, Fiona, Bianca, Angela, Chloe, Ali, Jena, Katherine, Briony and Sophia. You have given me so many opportunities to share my research with the wider community, all of which have been invaluable to my personal development. It was an absolute pleasure to have worked with you, I commend you all for your contributions to medical research and I hope that together, we have raised prostate cancer awareness in South Australia.

I am privileged to have been surrounded by many beautiful animals throughout my studies. Ernie, Roxy, Ralph and all the horses, past and present, thank you for keeping me entertained. You were rather therapeutic during the stressful times of my PhD.

Last but certainly not least, my PhD would not have been possible without the unwavering love and support of my family.

Nana, Aunty Sue and Mick, thanks for keeping the fire in my belly and talking me through the obstacles I faced.

Mum and dad, the two most important people in the world to me. You have always inspired me to work hard, stay humble and keep aiming high. I said it in my honours thesis and I will say it again - thank you for providing me with such a peaceful home where I could always forget about all the worries of a PhD. If I can be half the people you are one day, I will be a very lucky person. I love you both very much.

Scott Townley, first of all thank you for reading and editing this thesis multiple times! You have been by my side every step of the journey and this PhD is as much yours as it is mine. You have celebrated the highs but more importantly you were there with me during every single dark day, giving me advice and encouraging me to keep moving forward one step at a time. I admire you as a scientist and for the incredibly kind, gentle and selfless person that you are. You are my pillar of strength and I cannot thank you enough. I love you.

I also wish to respectfully acknowledge the sacrifice of animal life, as without them medical research would not be possible.

ABBREVIATIONS

ABC	ATP binding cassette
ADT	androgen deprivation therapy
amp	ampere
APC	allophycocyanin
AR	androgen receptor
BCR	biochemical relapse
BLI	bioluminescence imaging
BPH	benign prostatic hyperplasia
BSA	bovine serum albumin
$C_6H_5Na_3O_72H_2O$	trisodium citrate dihydrate
CAB	combined androgen blockade
CAF	cancer-associated fibroblast
CAM-DR	cell adhesion-mediated drug resistance
CD	cyclodextrin
CDK	cyclin dependent kinase
cDNA	complementary DNA
ChIP	chromatin immunoprecipitation
cm	centimetre
CMV	cytomegalovirus
CO_2	carbon dioxide
CRPC	castrate resistant prostate cancer
D	day
DAB	3'3'-diaminobenzidine tetrahydrochloride
DCC	dextran-coated charcoal
DcR	decoy receptor
DHT	5α-dihydrotestosterone
DISC	death-inducing signalling complex
DMSO	dimethyl sulfoxide
DNA	deoxyribonucleic acid
DR	death receptor
DRE	digital rectal examination
DTP	drug-tolerant persister
ECL	enhanced chemiluminescence
ECM	extracellular matrix
EDTA	ethylenediamine tetra-acetic acid
eIF	eukaryote initiation factor
EtOH	ethanol
FACS	fluorescent activated cell sorting
FADD	fas-associated death domain
FAP	fibroblast-activated protein
F_c	fragment crystallisable
FCS	fetal calf serum
FSH	follicle stimulating hormone
g	gram
GFP	green fluorescent protein
GSH	glutathione
h	hour
HCl	hydrochloric acid

HGPIN	high-grade prostatic intraepithelial neoplasia
HPG	hypothalamic-pituitary-gonadal
HRP	horse radish peroxidase
IC_{50}	half maximal inhibitory concentration
IgG	immunoglobulin G
IHC	immunohistochemistry
i.p.	intraperitoneal
IPA	ingenuity pathway analysis
kb	kilo base
kD	kilo dalton
kg	kilogram
L	litre
LB	luria broth
LGPIN	low-grade prostatic intraepithelial neoplasia
LH	luteinising hormone
LiCl	lithium chloride
LNCaP	lymph node carcinoma of the prostate
LTC	long-term curcumin
LTV	long-term vehicle
M	molar
MAb	monoclonal antibody
MAPK	mitogen-activated protein kinase
mg	milligram
$MgSO_4$	magnesium sulphate
min	minute
mL	millilitre
mm	millimetre
mM	millimolar
MMP	matrix metalloproteinase
mRNA	messenger ribonucleic acid
mTOR	mammalian target of rapamycin
MTT	methylthiazol tetrazolium
NaCl	sodium chloride
$NaHCO_3$	sodium bicarbonate
Na_2HPO_4	sodium phosphate dibasic
NaH_2PO_4	sodium phosphate monobasic
NCBI	national centre for biotechnology information
ng	nanogram
NHS	normal horse serum
nm	nanometre
nM	nanomolar
NPF	normal prostate fibroblast
PARA	pro-apoptotic receptor agonist
PBS	phosphate buffered saline
PC-3	prostate carcinoma 3
pH	potential hydrogen
PI	propidium iodide
PIN	prostatic intraepithelial neoplasia
PRF	phenol red-free
PSA	prostate specific antigen
qRT-PCR	quantitative real-time polymerase chain reaction
RIPA	radioimmunoprecipitation assay
RNA	ribonucleic acid

RNAse	ribonuclease
RO	reverse osmosis
RP	radical prostatectomy
rpm	revolutions per minute
RPMI	Roswell Park Memorial Institute
RT	room temperature
s.c.	subcutaneous
SCID	severe combined immunodeficiency
SD	standard deviation
SDS	sodium dodecyl sulphate
sec	second
SEM	standard error of the mean
TBS	tris buffered saline
TBST	tris buffered saline-tween 20
TE	tris ethylenediamine tetra-acetic acid
TKR	tyrosine kinase receptor
TNF	tumour necrosis factor
TRAIL	TNF-related apoptosis inducing ligand
Tris	tris(hydroxymethyl)aminomethane
Tris-Cl	tris(hydroxymethyl)aminomethane chloride
tRNA	transfer RNA
UGE	urogenital sinus epithelium
UGM	urogenital sinus mesenchyme
^{o}C	degrees celcius
ΔΔct	delta delta cycle threshold
µg	microgram
µL	microlitre
µM	micromolar
µm	micron

ABSTRACT

Curcumin is a component of the Indian spice turmeric that has shown anti-cancer activity across a range of models. This includes prostate cancer, the most commonly diagnosed cancer in Australia. While much of the current literature relates to epithelial cells, there is no information regarding curcumin activity or resistance in prostate fibroblasts. With curcumin recently entering clinical trials for prostate cancer and being increasingly used as a dietary supplement, it is critical to gain an understanding of curcumin action and potential resistance in these cells, given their reported contribution to cancer progression. Furthermore, with drug resistance being a major setback to cancer therapy, it is also important to investigate curcumin-based combination strategies to enhance efficacy and avoid the development of resistance. The aims of this thesis were therefore to comparatively investigate mechanisms of curcumin action in prostate cancer cells and fibroblasts, to explore the potential for curcumin resistance to occur in prostate fibroblasts and to examine the ability of curcumin to re-sensitise prostate cancers resistant to drozitumab, a monoclonal antibody against death receptor 5 (DR5). Curcumin inhibited prostate cancer cell and fibroblast viability, androgen receptor (AR) activity and androgen-regulated gene expression; effects potentially caused by a decrease in AR residence on DNA. While microarray analysis of curcumin-treated fibroblasts crossed with publically available data from curcumin-treated prostate cancer cells revealed little overlap in genes, both cell lineages underwent cell cycle arrest in response to treatment. However, cell cycle arrest occurred via divergent mechanisms in different prostate cell lines. Long-term culture of prostate fibroblasts in curcumin resulted in curcumin tolerance rather than resistance, characterised by increased cell survival and decreased cell cycle arrest in response to treatment. Curcumin-tolerant fibroblasts were differentiated from sensitive fibroblasts based on a subset of differentially expressed genes, some of which had previously been associated with resistance to cancer therapies, and some of which had lost curcumin-responsiveness in tolerant fibroblasts. Many of the latter genes were androgen-regulated, and tolerant fibroblasts subsequently demonstrated reduced AR function and androgen regulation of genes, concomitant with a decrease in AR residence on DNA. The culture of tolerant fibroblasts in curcumin-free media restored curcumin sensitivity, and partially restored AR function and the ability of androgens to regulate gene expression. Tolerant fibroblasts demonstrated changes in genes responsible for extracellular matrix composition and secretion of growth factors, and when co-cultured with prostate cancer cells, a decrease in cancer cell adhesion and increase in proliferation was observed. Finally, cell line studies confirmed that curcumin re-sensitised drozitumab-resistant prostate cancer cells to drozitumab-induced apoptosis via up-regulation of the drug target DR5. While the same effect was not observed *in vivo*, drozitumab treatment alone demonstrated surprising anti-cancer activity. This thesis provides a greater understanding of curcumin action across multiple prostate cell lines and explores, for the first time, the development and potential implications of curcumin tolerance in prostate fibroblasts. This data provides new insights into how curcumin-based therapies or prevention strategies may affect the whole prostate, and offers considerations for curcumin use in future preclinical and clinical studies.

CONFERENCE PRESENTATIONS

Giorgio. L, Smith. E, Drew. PA & Buchanan. G. Exploring the interaction between fibroblasts and tumour cells in prostate cancer. Basil Hetzel Institute Research Day, Adelaide, October 2011.

Trotta. AP, **Giorgio. L**, Leach. DA, Taylor. RA & Buchanan. G. Androgen receptor function in prostate fibroblasts. Australian Science and Medical Research Conference, Adelaide, June 2012.

Giorgio. L, Leach. DA**,** Smith. E, Drew. PA, Trotta. AP & Buchanan. G. Curcumin inhibits cell growth and androgen receptor function in prostate tumour and fibroblast cell lines. University of Adelaide Faculty of Health Science Postgraduate Research Conference, Adelaide, August 2012.

Giorgio. L, Leach. DA**,** Smith. E, Drew. PA, Trotta. AP & Buchanan. G. Curcumin inhibits cell growth and androgen receptor function in prostate tumour and fibroblast cell lines. Basil Hetzel Institute Research Day, Adelaide, October 2012.

Giorgio. L, Trotta. AP, Need. EF & Buchanan. G. Curcumin targets unique transcriptional programmes in prostate epithelial and fibroblast cell lines. Australian Society for Medical Research, Adelaide, June 2013.

Giorgio. L, Leach. DA**,** Trotta. AP, Wang. Q, Holst. J, Need. EF & Buchanan. G. The anti-proliferative effects of curcumin are mediated by p53-independent BRCA1 signalling in prostate fibroblasts. Prostate Cancer World Congress, Melbourne, August 2013.

Giorgio. L, Leach. DA**,** Trotta. AP, Wang. Q, Holst. J, Need. EF & Buchanan. G. The anti-proliferative effects of curcumin are mediated by p53-independent BRCA1 signalling in prostate fibroblasts. Australian-Canadian Prostate Cancer Research Alliance Symposium, Port Douglas, August 2013.

Giorgio. L, Leach. DA**,** Trotta. AP, Wang. Q, Holst. J, Need. EF & Buchanan. G. The anti-proliferative effects of curcumin are mediated by p53-independent BRCA1 signalling in prostate fibroblasts. University of Adelaide Faculty of Health Science Postgraduate Research Conference, Adelaide, August 2013.

Giorgio. L, Leach. DA, Trotta. AP, Need. EF & Buchanan. G. Curcumin induces divergent mechanisms of cell cycle arrest in prostate fibroblasts and cancer cells. Basil Hetzel Institute Research Day, Adelaide, October 2013.

Giorgio. L, Zinonos. I, Liapis. V, Trotta. AP, Buchanan. G & Evdokiou. A. Drozitumab, a fully humanised agonistic antibody against Apo2L/TRAIL death receptor DR5, exhibits anti-tumour activity in a PC-3 prostate cancer xenograft model. Ninth International Conference of Anticancer Research, Sithonia Greece, October 2014.

PRIZES

Best Poster Presentation in the School of Medicine. University of Adelaide Faculty of Health Science Postgraduate Research Conference, Adelaide, August 2013 ($500 towards travel to Greece)

Best Poster Presentation for the Northern Communities Men's Health Prize. University of Adelaide Faculty of Health Science Postgraduate Research Conference, Adelaide, August 2013 ($300)

Prostate Cancer World Congress Travel Grant, July 2013 ($500 towards travel to PCWC in Melbourne)

SAHMRI Beat Cancer Project Travel Grant, March 2013 ($2,500 towards travel to Greece)

Florey Medical Research Foundation Top Up Cancer Scholarship, June 2011 ($4,000)

Australian Postgraduate Award, January 2011 to July 2014

ENGAGEMENT IN THE SCIENTIFIC COMMUNITY

Radio interview with David Hearn for Coast FM: Research update. June 2014

Invited presentation at the Walkerville Rotary Club for The Hospital Research Foundation Community Awareness Program titled '*Secret men's business: discovering new ways to treat prostate cancer'*. April 2014

Presentation at the Basil Hetzel Institute of Translational Health Research titled *'Curcumin and prostate cancer: hope or hype?'* March 2014

Invited presentation at the Freemason's Foundation for Men's Health titled '*Curcumin and prostate cancer: understanding the mechanisms of action in cancer cells and fibroblasts'*. September 2013

Invited presentation at the Holdfast Bay Rotary Club for The Hospital Research Foundation Community Awareness Program titled '*Secret men's business: discovering new ways to treat prostate cancer'*. August 2013

Radio interview with Belinda Heggen for 5AA: Research update. April 2013

Presentation at the Disciple of Surgery Surgical Science Journal Club titled '*Sipuleucel-T immunotherapy for castrate resistant prostate cancer*'. March 2013

Presentation at the Basil Hetzel Institute of Translational Health Research titled *'Curcumin and prostate cancer: mechanisms of resistance and improving delivery'*. November 2012

University of Adelaide Three Minute Thesis Competition '*Prostate fibroblasts: putting Jeckyll and Hyde to better use'*. August 2012

Radio interview with David Hearn for Coast FM: Research update. June 2012

Presentation at the Basil Hetzel Institute of Translational Health Research titled *'Exploring the interaction between fibroblasts and cancer cells in prostate cancer*'. August 2011

CHAPTER 1

INTRODUCTION

1.1: THESIS OVERVIEW

Curcumin is a biologically active component of the spice turmeric, which has been used in ancient Indian and Chinese medicine for many thousands of years. It has primarily been used as a remedy for inflammatory ailments including wounds, arthritis and gastrointestinal diseases. In recent years, curcumin has been subject to a large amount of preclinical investigation for the treatment of other diseases, including cancer. The aim of this thesis was to investigate curcumin in the context of the human prostate, with particular focus on prostate cancer cells and fibroblasts.

1.2: THE NORMAL PROSTATE

The normal human prostate is a walnut-sized exocrine gland of the male reproductive system that is located immediately beneath the bladder, surrounding the urethra. The function of the prostate is to produce and secrete an alkaline fluid into semen that neutralises the acidity of the vaginal tract, thus prolonging the lifespan of sperm. Secretions from the prostate gland are responsible for 50 to 75% of the volume of semen (Owen and Katz 2005).

1.2.1: Development

All stages of normal prostate growth, development and function are regulated by androgens (Cooke, Young et al. 1987, Cunha, Donjacour et al. 1987). Androgens are steroid hormones responsible for the development and maintenance of male characteristics through binding to the androgen receptor (AR). During embryogenesis, androgens produced by the fetal testes stimulate the formation of prostatic terminal buds, which emerge from the urogenital sinus epithelium (UGE) (Cunha 1994). These prostatic buds grow into the surrounding urogenital sinus mesenchyme (UGM), forming epithelial ducts. Cellular differentiation of the ducts produces epithelial cells, while the surrounding UGM differentiates into smooth muscle. This process occurs from approximately ten weeks gestation until puberty, where the surge of androgens induces full maturation of the prostate gland (Kurzrock, Baskin et al. 1999).

1.2.2: Macroscopic and microscopic structure

The mature prostate gland can be viewed macroscopically as three zones: the peripheral, central and transitional zones comprising approximately 70%, 25% and 5% of the prostate respectively (**Figure 1.1A**) (McNeal 1981). Each zone consists of both an epithelial and stromal (or microenvironment) compartment, separated by a basement membrane. The epithelial compartment contains three cell

types: secretory luminal, basal and neuroendocrine. Secretory luminal cells are androgen-dependent, highly differentiated and functionally active cells that represent the major phenotype of the normal epithelium (Bonkhoff and Remberger 1996). Basal cells are androgen-independent, undifferentiated cells believed to be required for sustaining the renewal of terminally differentiated secretory cells (Signoretti and Loda 2006). Neuroendocrine cells, far less common than secretory luminal or basal cells, are androgen-independent and believed to play a role in providing paracrine signals to luminal secretory cells for growth and function (Huang, Wu et al. 2007). The stromal compartment of the prostate gland contains smooth muscle, lymphatic, vascular and neuronal cells, as well as fibroblasts, embedded into an extracellular matrix (ECM) composed largely of proteoglycans and collagen fibres. **Figure 1.1B** provides a schematic for the microscopic organisation of the prostate gland.

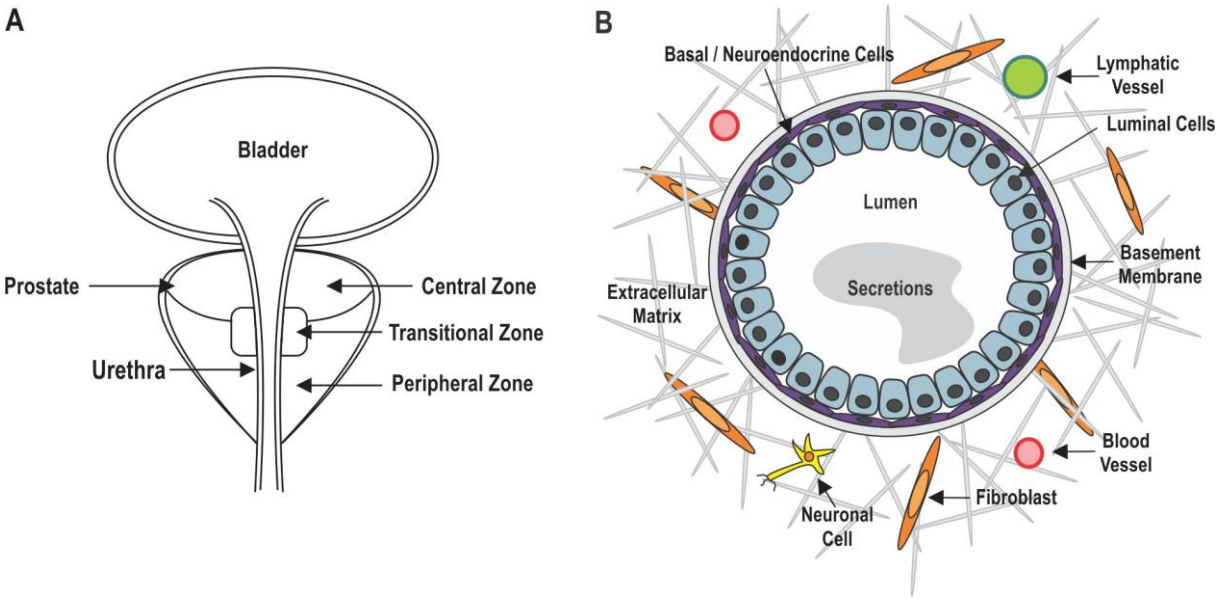

Figure 1.1: Macroscopic and microscopic structures of the normal human prostate gland. A: The prostate gland is located directly under the bladder, surrounding the urethra. There are three anatomical prostatic zones (central, transitional and peripheral), all containing both epithelial and stromal elements. **B**: Microscopic architecture of the normal prostate gland showing separation of the epithelial and stromal compartment by a well-defined basement membrane.

1.2.3: Hormonal control of the normal prostate

Androgens play an essential role in the growth and development of many types of tissue, including the prostate gland. The majority of androgens found in adult males are produced by the co-ordinated action of the hypothalamic-pituitary-gonadal (HPG) axis. The hypothalamus secretes gonadotropin-releasing hormone which stimulates the pituitary gland to release luteinising hormone (LH) and follicle-stimulating hormone (FSH) into the blood stream. In the testes, FSH binds to its receptor on Sertoli cells leading to the regulation of spermatogenesis, and LH binds to its receptor on Leydig cells causing transport of cholesterol from the cell surface to the mitochondrial membrane (Walker and Cheng 2005, Haider

2007). Cholesterol is used to synthesise testosterone, the most abundant male androgen, through a series of steroidogenic enzyme reactions. Testosterone is then released into the blood stream where approximately 97% is bound to serum proteins (such as sex hormone-binding globulin and albumin) and 3% remains free to act on target tissues (Sodergard, Backstrom et al. 1982). Relatively weaker androgens may be synthesised by the adrenal gland under the control of adrenocorticotropic hormone, including dehydroepiandrosterone and androstenedione. These androgens act largely as metabolic intermediates in the conversion of androgen to estrogen (Labrie, Luu-The et al. 2001). Hormonal control of the prostate is represented in **Figure 1.2**.

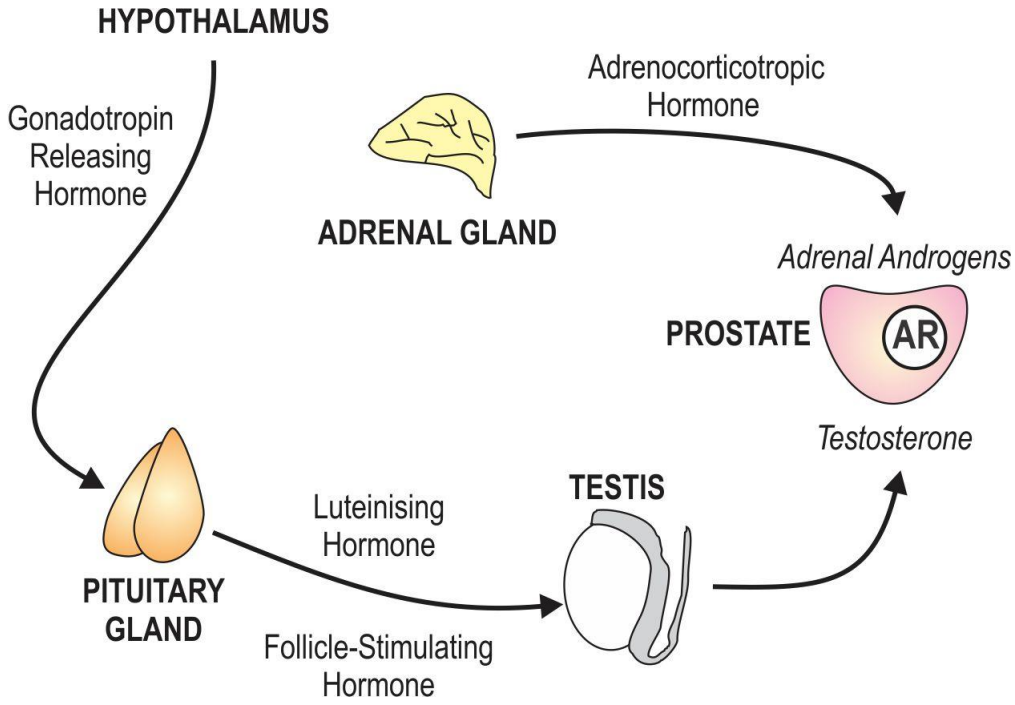

Figure 1.2: Hormonal control of the prostate. The growth and development of the normal prostate requires functional androgen signalling, which is regulated by the hypothalamic-pituitary-gonadal axis. Luteinising hormone and follicle-stimulating hormone, both released from the pituitary gland, act on the testes to synthesise testosterone. Androgens may also be synthesised by the adrenal gland under the control of adrenocorticotropic hormone.

1.2.4: The androgen receptor

Maintenance of the epithelial and stromal compartments of the mature prostate gland is dependent on androgen signalling through AR. Human AR is a member of the steroid receptor superfamily of nuclear receptors. It is encoded by a single 90 kb gene located on the X chromosome at Xq11-12, and is arranged into eight exons. The AR gene has an open reading frame of 2865 nucleotides, encoding a 917 amino acid protein with a molecular weight of 110 kDa (Lubahn, Joseph et al. 1988, Tilley, Marcelli et al. 1989). The AR protein is arranged into four functional domains: an amino terminal transactivation domain, a central DNA-binding domain, a small hinge region and a ligand-binding domain. Upon

translation of AR, un-ligated receptor is localised within the cytoplasm in association with a multi-protein complex consisting of heat shock proteins (e.g. Hsp40, 70 and 90) and chaperones (e.g. p23, TPR and SGTα) that maintain receptor configuration with high affinity for ligand (Pratt and Toft 1997, Vanaja, Mitchell et al. 2002). Circulating testosterone enters the cell and is converted to DHT by 5α-reductase. This conversion enhances the relatively weak androgenic potency of testosterone, as DHT has an approximately ten-fold higher dissociation constant for AR (Wilson and French 1976, Deslypere, Young et al. 1992). Binding of DHT to AR results in the dissociation of this complex, receptor dimerization, phosphorylation and transport to the nucleus (Prins 2000). Within the nucleus, AR binds to DNA sequences known as androgen response elements located in the flanking regions of target genes, and recruits co-regulators (e.g. p160 and p300) and transcriptional machinery required to regulate genes involved in prostate growth, survival and differentiation (Claessens, Verrijdt et al. 2001, Dehm and Tindall 2006). Following dissociation of ligand, AR returns to the cytoplasm where the process may be initiated again (Tyagi, Lavrovsky et al. 2000). Besides ligand-dependent activation, AR can also be activated in the absence of ligand by membrane-bound kinases such as the tyrosine kinase receptor (TKR), via the PI3K-Akt pathway (Weigel and Zhang 1998). The molecular events leading to gene activation in the ligand-independent pathway also include the requirement for receptor maturation, co-factor recruitment to the AR complex and the ability to recognise DNA elements. However, the target genes activated by these mechanisms have not been fully elucidated. **Figure 1.3** provides a schematic for both ligand-dependent and -independent AR signalling.

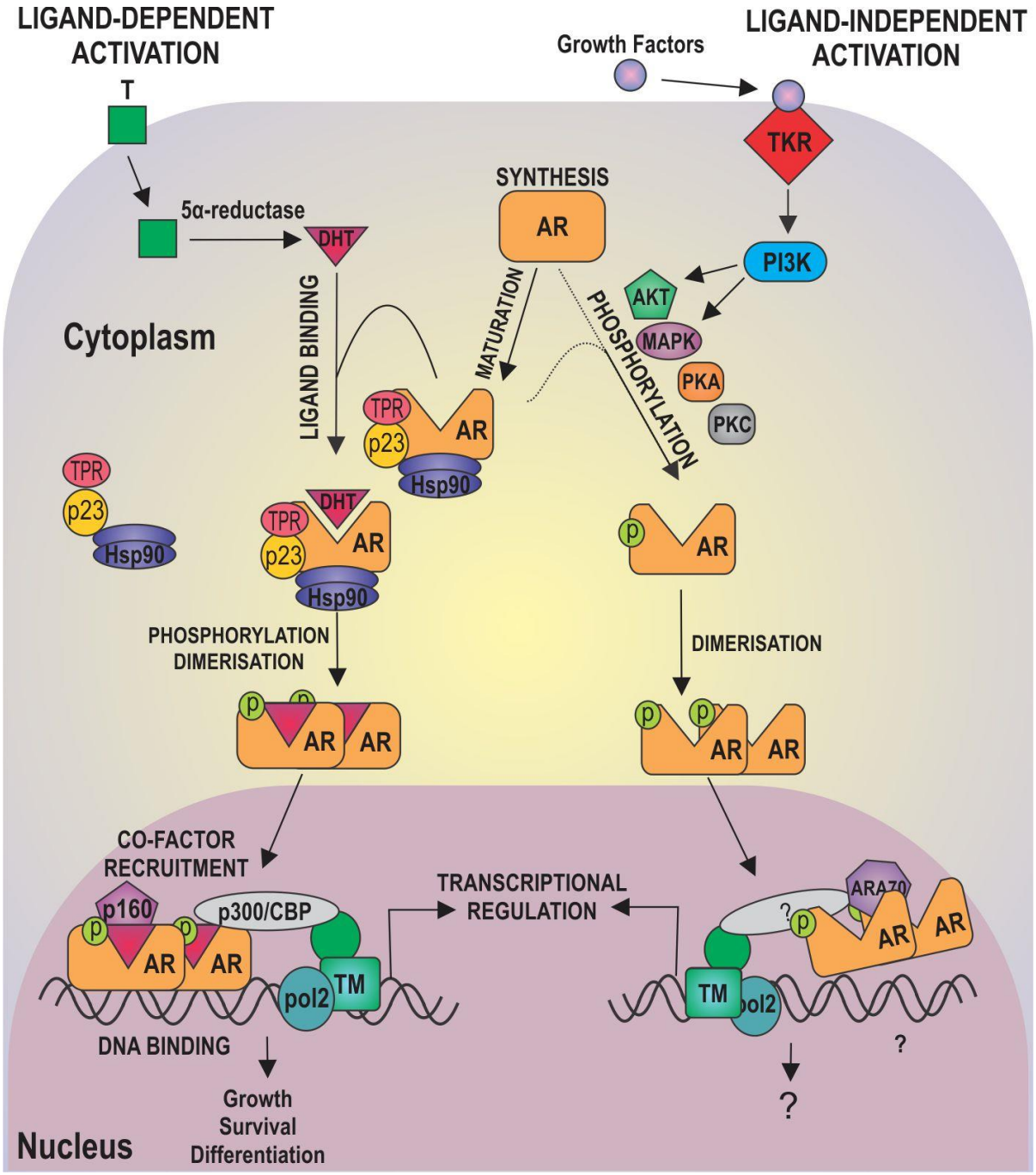

Figure 1.3: Ligand-dependent and -independent androgen signalling in the normal human prostate gland. In the absence of ligand, androgen receptor (AR) is retained in the cytoplasm in association with a multi-protein chaperone complex. Testosterone enters the cell where it is converted to 5α-dihydrotestosterone (DHT) and binds to the AR. This results in dissociation of the chaperone complex, receptor dimerization, phosphorylation and nuclear translocation. Nuclear AR binds to androgen response elements located in the regulatory regions of target genes. Co-factors (e.g. p160 and p300) and transcriptional machinery (TM) are recruited to initiate the transcription of target genes involved in growth, survival and differentiation. The AR may also be activated independent of ligand via tyrosine kinase receptors (TKR). This pathway also involves altered chaperone associations, dimerization, phosphorylation and nuclear translocation; however the target genes activated by this pathway remain unknown.

1.3: PROSTATE CANCER

1.3.1: Epidemiology and risk factors

Prostate cancer is the second leading cause of male cancer-related death in Australia (AIHW 2013). Approximately 18,500 Australian men were diagnosed with prostate cancer in 2012, resulting in 3,200 deaths. There are numerous risk factors that increase the likelihood of developing prostate cancer. Age is by far the biggest, with one in eight men developing the disease by the age of 75 and one in six men by the age of 85 (AIHW 2013). Race is also a large predictor of prostate cancer risk, with the disease affecting more African-American men than any other race (Makridakis, Ross et al. 1999, Freedman, Haiman et al. 2006). Further, African-American men are more likely to be diagnosed at an advanced stage of disease and are more than twice as likely to die of prostate cancer as Caucasian men (Hankey, Feuer et al. 1999). There is also strong evidence that the risk of developing prostate cancer is hereditary, with a positive family history associated with up to a three-fold increased risk (Whittemore, Wu et al. 1995). Like many diseases, the poor diet and sedentary lifestyles associated with developed countries also increases prostate cancer incidence and mortality rates compared to less developed countries (Wolk 2005).

1.3.2: Pathogenesis

The development and progression of prostate cancer is an extremely heterogeneous process involving the accumulation of many genetic and biological alterations. Changes in gene expression, chromosomal abnormalities and increasing DNA instability lead to the activation of oncogenes (e.g. c-myc, HER2, SRC, ABL, RAS and RAF), silencing or deletion of tumour suppressor genes (e.g. p53, Rb, PTEN, BRCA1 and BRCA2) and epigenetic changes (e.g. DNA methylation and histone modification), all which contribute to the uncontrolled proliferation of malignant cells (Konishi, Shimada et al. 2005, Shen and Abate-Shen 2010). Interestingly, 85% of prostate cancers arise in the peripheral zone where prostatic intraepithelial neoplasia (PIN) is most often detected (Häggman, Macoska et al. 1997, Stamey, Yemoto et al. 2000). Believed by some to be a precursor lesion to prostate cancer, PIN is characterised by the neoplastic transformation of secretory luminal cells (Montironi, Mazzucchelli et al. 2007). A diagnosis of PIN indicates a rise in cellular proliferation and disorganisation within secretory luminal cells, often leading to the proliferation of neoplastic cells and eventual formation of a tumour mass. There are two sub-classes of PIN based on cytological characteristics: low-grade PIN (LGPIN) and high-grade PIN (HGPIN). While a direct relationship between PIN and prostate cancer has not been conclusively demonstrated, studies have shown that most patients with HGPIN are likely to develop carcinoma within ten years (De Marzo, Meeker et al. 2003, Bostwick and Qian 2004).

The progression of prostate cancer can also be understood in terms of tumour (T) staging (Borley and Feneley 2009). Tumours termed T1 are too small to be seen by scans or felt by examination of the prostate, and are more likely detected by needle biopsy following a PSA test (discussed further in Section 1.3.3). Tumours termed T2 are palpable and remain entirely within the prostate gland. Locally advanced tumours are classified as T3 if they have broken through the prostate capsule and have either not spread to other organs, or T4 if they have spread to nearby organs such as the bladder or rectum. If malignant cells reach the blood stream, they have the potential to travel to secondary sites such as the bone, lungs, liver, lymph nodes and brain, giving rise to metastatic disease (Bubendorf, Schöpfer et al. 2000). **Figure 1.4** outlines the histological changes characteristic of prostate cancer progression.

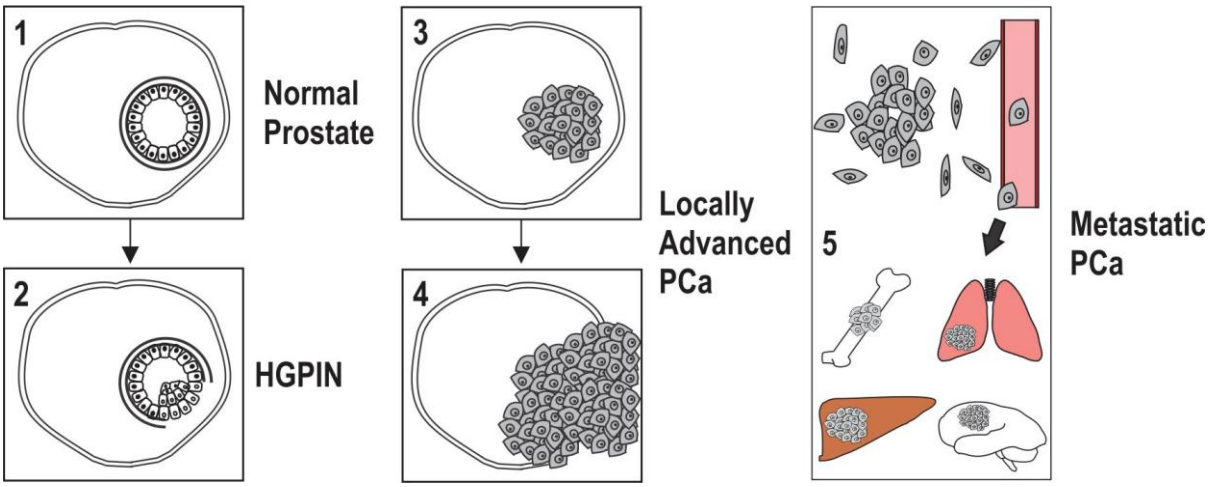

Figure 1.4: The pathogenesis of prostate cancer progression. Representation of the basic histological changes often observed during the progression of prostate cancer including high-grade prostatic intraepithelial neoplasia (HGPIN), locally invasive and advanced disease and metastasis to secondary sites such as bone, lungs, liver and brain.

1.3.3: Diagnosis

The two standard diagnostic tests used to detect prostate cancer are the digital rectal examination (DRE) and the prostate-specific antigen (PSA) blood test. The DRE is used to physically detect enlarged glands and is often an initial assessment of the prostate. The predictive value of DRE is approximately 50%, however the test misses a large number of cancers, many of which at an advanced pathological stage (Stone, DeAntoni et al. 1994, Smith and Catalona 1995). The DRE is therefore often conducted in conjunction with a test for PSA, the most abundantly secreted protein from the normal prostate (Gjertson and Albertsen 2011). While there is typically a small amount of PSA in the blood, high blood PSA levels signify a leakage from disrupted prostate glands, indicating the presence of cancer (Djavan, Zlotta et al. 1999). The use of PSA screening, or the attempt to identify individuals with prostate cancer who otherwise have no reason to suspect they have prostate cancer, has become controversial in recent years as there is much debate on its value in saving lives. In a United States based study, ten

year follow-up results revealed no differences in prostate cancer-related death between men who were screened and those who were not (Berg, Andriole et al. 2009). Likewise, a similar study from the United States found mortality rates from prostate cancer remained unchanged following the introduction of PSA screening, despite one million additional men being diagnosed and treated for prostate cancer (Welch and Albertsen 2009, Shen and Abate-Shen 2010). This study attributed the growth in prostate cancer incidence to the over-diagnosis of men with low-grade carcinomas that only required active surveillance. Conversely, an 11-year European study found that PSA screening significantly reduced prostate cancer-related mortality (Schröder, Hugosson et al. 2012), and the European Goteborg randomised population-based trial showed a reduction in metastatic disease and prostate cancer mortality with screening starting at age 50 (Hugosson, Carlsson et al. 2010).

Not only is there conflicting evidence regarding PSA screening, but there is also no standardised approach to diagnosing prostate cancer. In an attempt to address these issues, a group of leading prostate cancer experts from around the world generated a set of consensus statements at the 2013 Prostate Cancer World Congress regarding the use of PSA testing, with the goal of clarifying existing guidelines (Murphy, Ahlering et al. 2014). The guidelines are as follows: (1) PSA testing reduces prostate cancer-specific mortality and the incidence of metastatic prostate cancer in men aged 50 to 69, (2) prostate cancer diagnoses must be uncoupled from prostate cancer intervention, encouraging the use of active surveillance protocols in men with low-risk cancer, (3) PSA testing should not be considered on its own, but rather as part of a multivariable approach to early prostate cancer detection including use of additional cancer predictors such as DRE, prostate volume, family history and ethnicity to better risk- stratify men, (4) baseline PSA testing for men in their 40s is useful for predicting their future risk of prostate cancer and (5) older men in good health, with greater than a ten-year life expectancy, should be tested on an individual basis that considers co-morbidities.

Following diagnostic tests, confirmation of a prostate cancer diagnosis requires prostatic ultrasound and transrectal ultrasound-guided biopsy. Based on these results, tumour stage and grade are assessed and used to determine the optimal treatment strategy (Gleason, Mellinger et al. 1974). Unfortunately, one of the major challenges in treating prostate cancer is that there is no diagnostic test to discriminate indolent tumours from the life-threatening form of disease. This results in the over-treatment of slow growing disease causing unnecessary side effects to patients, and the under-treatment of aggressive tumours.

1.3.4: Androgen signalling in prostate cancer

Given that normal prostate tissue is reliant on androgens for growth and homeostasis, it is not surprising that the progression of prostate cancer is largely attributed to aberrant androgen signalling that

contributes to all stages of disease (Buchanan, Irvine et al. 2001). The exact role of AR in disease pathogenesis, however, is yet to be defined. The earliest evidence that AR is required for prostate cancer development demonstrated high prostate cancer risk in men with high circulating androgens, and no prostate cancer development in castrated men (Gann, Hennekens et al. 1996, Huggins and Hodges 2002). Further, a single AR mutation (E231G) has been shown to alter AR co-regulator recruitment and increase AR basal transcriptional activity in mice. This mutation caused all mice to develop PIN by 12 weeks of age, and advanced prostate cancer by 50 weeks of age (Han, Buchanan et al. 2005). An association between high AR level and decreased biochemical relapse (BCR)-free survival has also been identified (Li, Wheeler et al. 2004). These data indicate that aberrant AR signalling alone is sufficient to initiate prostate cancer. Historically, scientists believed that the development of prostate cancer no longer responsive to androgen (i.e. castrate-resistant prostate cancer, CRPC, introduced in Section 1.3.5) was due to the androgen-independence of cancer cells. It is now well accepted that the AR is expressed at all stages of prostate cancer, and CRPC remains reliant on AR signalling (Culig, Hobisch et al. 1998, Koivisto, Kolmer et al. 1998). Continued AR signalling observed in CRPC is caused by increased levels of AR, acquisition of AR gain-of-function mutations, altered expression of AR co-regulators and activation of ligand-independent pathways (Culig, Hobisch et al. 1994, Visakorpi, Hyytinen et al. 1995, Tilley, Buchanan et al. 1996, Craft, Shostak et al. 1999, Orio Jr, Térouanne et al. 2002, Chmelar, Buchanan et al. 2007).

1.3.5: Current treatment strategies

Treatment regimens for prostate cancer generally take into consideration the stage and grade of disease, patient age, life expectancy, risk involved with treatment and patient preference. Patients diagnosed with early stage, clinically localised prostate cancer generally undergo active surveillance if the cancer is low risk or radical prostatectomy (RP) and/or radiotherapy if the cancer is higher risk. The latter approach is curative for approximately 75% of patients; however the remaining 25% will experience BCR within five to ten years, as determined by a rise in PSA level (Pound, Partin et al. 1999). Relapse is believed to be due to the presence of micro-metastatic lesions that were undetected at the time of diagnosis (Soloway and Roach Iii 2005). For BCR patients or men who present initially with advanced disease, chemical castration using endocrine-based therapies is the gold standard therapeutic option. This approach is called androgen deprivation therapy (ADT), and exploits the androgen dependence of tumour cells by blocking circulating levels of testosterone. This is achieved by two broad mechanisms: targeting the HPG axis to reduce circulating levels of testosterone, and directly blocking androgen action. When both forms of chemical castration are used, the approach is termed complete androgen blockade (CAB). While CAB offers a reported 5% survival benefit, there have been

mixed reports as to the consistency of its efficacy (Caubet, Tosteson et al. 1997, Schmitt, Wilt et al. 2001).

Almost all patients respond successfully to ADT, however relapse is typically observed within four to five years due to tumours developing the ability to grow and survive despite androgen depletion (Smaletz, Scher et al. 2002). This form of disease is termed CRPC and has an average prognosis of two to three years (Gleave, Bruchovsky et al. 1999, Mellado, Codony et al. 2009). Treatment options for CRPC are limited, and only four agents have been shown to extend life to date: the anti-mitotic doxetaxel (2.4 months), the androgen biosynthesis inhibitor abiraterone acetate (4.4 months), the second-generation androgen antagonist Enzalutamide (4.8 months) and the immunotherapy Sipuleucel-T (4.1 months) (Tannock, De Wit et al. 2004, Kantoff, Higano et al. 2010, Fizazi, Scher et al. 2012, Scher, Fizazi et al. 2012). There is subsequently an urgent need for more effective treatment strategies for men with advanced prostate cancer.

1.4: THE PROSTATE MICROENVIRONMENT

Much of our knowledge into prostate cancer relates to the study of epithelial cells. However, research has become increasingly focussed on how the stroma, or microenvironment, may affect carcinogenesis. It is now evident that paracrine and cell-to-cell interactions between epithelial cells and the microenvironment, termed stromal-epithelial interactions, are required for normal prostate development and function as well as the initiation and progression of cancer.

1.4.1: The normal prostate microenvironment

As described in Section 1.2.1, stromal-epithelial interactions begin in the fetus where androgen stimulation of UGM leads to the differentiation of prostatic epithelium (Cunha 2008). In the mature prostate, the microenvironment provides a supportive framework to the epithelium largely mediated by the action of fibroblasts. Fibroblasts are the principle cellular component of connective tissue, and are heavily involved in the maintenance of epithelial homeostasis through stromal-epithelial interactions (Tarin and Croft 1969). Normal prostate fibroblasts (NPFs) contribute to ECM maintenance by synthesising and secreting collagen, fibronectin and laminin (Rodemann and Muller 1991, Chang, Chi et al. 2002). They are also responsible for ECM degradation via the production of matrix metalloproteinases (MMPs) (Simian, Hirai et al. 2001). Additionally, NPFs maintain the homeostasis of adjacent epithelia through the secretion of soluble growth factors and direct fibroblast-epithelial cell contact that regulates epithelial morphogenesis, movement, organisation and development (Wiseman and Werb 2002, Kalluri and Zeisberg 2006).

1.4.2: The prostate cancer microenvironment

The development of prostate cancer causes several modifications to the adjacent microenvironment. One of those modifications is the activation of fibroblasts, which causes faster proliferation, greater secretion of ECM and altered expression of signalling molecules (Kalluri and Zeisberg 2006). This altered phenotype, termed a cancer-associated fibroblast (CAF), is activated primarily by two mechanisms. The first is through the action of growth factors released from injured epithelial cells and infiltrating macrophages, such as transforming growth factor beta (TGF-β), epidermal growth factor (EGF), platelet-derived growth factor (PDGF) and fibroblast growth factor 2 (FGF-2). The second is through contact with leukocytes via adhesion molecules, such as intracellular adhesion molecule 1 (ICAM-1) and vascular cell adhesion molecule 1 (VCAM-1) (Clayton, Evans et al. 1998, Zeisberg, Strutz et al. 2000).

The activation of fibroblasts allows them to contribute to cancer progression via a number of mechanisms (summarised in **Figure 1.5**). In a cancer setting, CAFs over-secrete ECM degrading proteases MMP-2 and MMP-9, facilitating increased ECM turnover, altered microenvironment composition and ultimately providing an environment permissive of cancer growth and local invasion (Stetler-Stevenson, Aznavoorian et al. 1993). They also over-secrete growth factors that induce the proliferation of adjacent cancer cells, such as TGF-β, hepatocyte growth factor (HGF) and insulin-like growth factor (IGF), and promote microvascular permeability, endothelial and inflammatory cell influx and angiogenesis via the secretion of vascular endothelial growth factor (VEGF) (Dvorak, Sioussat et al. 1991, Bhowmick, Neilson et al. 2004). In addition, CAFs further drive the inflammatory response via the secretion of cytokines and chemokines, such as interleukin 1 (IL-1), monocyte chemo-attractant protein 1 (MCP-1) and stromal cell-derived factor 1 (CXCL12) (Strieter, Wiggins et al. 1989). The secretion of CXCL12 up-regulates its cognate receptors CXCR4 and CXCR7 on tumour cells, and subsequently promotes tumour cell invasion and metastasis to secondary sites bearing high endogenous CXCL12 expression (Arya, Patel et al. 2004, Singh, Singh et al. 2004). This signalling cascade also up-regulates oncogenic proteins (e.g. Her2, ERK, MEK and Akt) that continue to drive tumour growth (Kukreja, Abdel-Mageed et al. 2005, Chinni, Sivalogan et al. 2006, Chinni, Yamamoto et al. 2008). Together these events combine in a positive feedback loop involving further inflammatory responses, ultimately driving cancer cell proliferation and metastasis.

Over the last 15 years, the literature has also become increasingly focussed on defining the role of CAFs in driving prostate cancer initiation. One of the earliest studies demonstrated that initiated but non-tumourigenic BPH-1 prostate cells grown in culture with prostate CAFs acquired the ability to form tumours when transplanted into mice, while BPH-1 cells combined with NPFs did not (Olumi, Grossfeld et al. 1999). More recently, CAFs were shown to alter the differentiation fate of embryonic stem cells,

which was not evident with patient-matched NPFs (Risbridger and Taylor 2008). Further, CAFs were shown to promote the growth of localised tumour cells while NPFs inhibited growth (Paland, Kamer et al. 2009). It is important to note that changes in both stromal and epithelial compartments are required to drive cancer growth. Tissue recombination studies where UGM and UGE were transformed with oncogenes MYC and RAS showed oncogenic introduction into both tissue compartments necessary for carcinoma development (Thompson, Timme et al. 1993). This became further evident in a mouse model of prostate cancer, where the inhibition of oncogenic phosphorylated retinoblastoma in cancer cells induced a paracrine p53 response that suppressed fibroblast proliferation. This triggered the selection and expansion of highly proliferative p53-null fibroblasts, supporting epithelial loss of p53 and cancer progression (Hill, Song et al. 2005). Studies such as these highlight not only the maintenance of stromal-epithelial interactions within a cancer setting, but also the dynamic nature of such interactions.

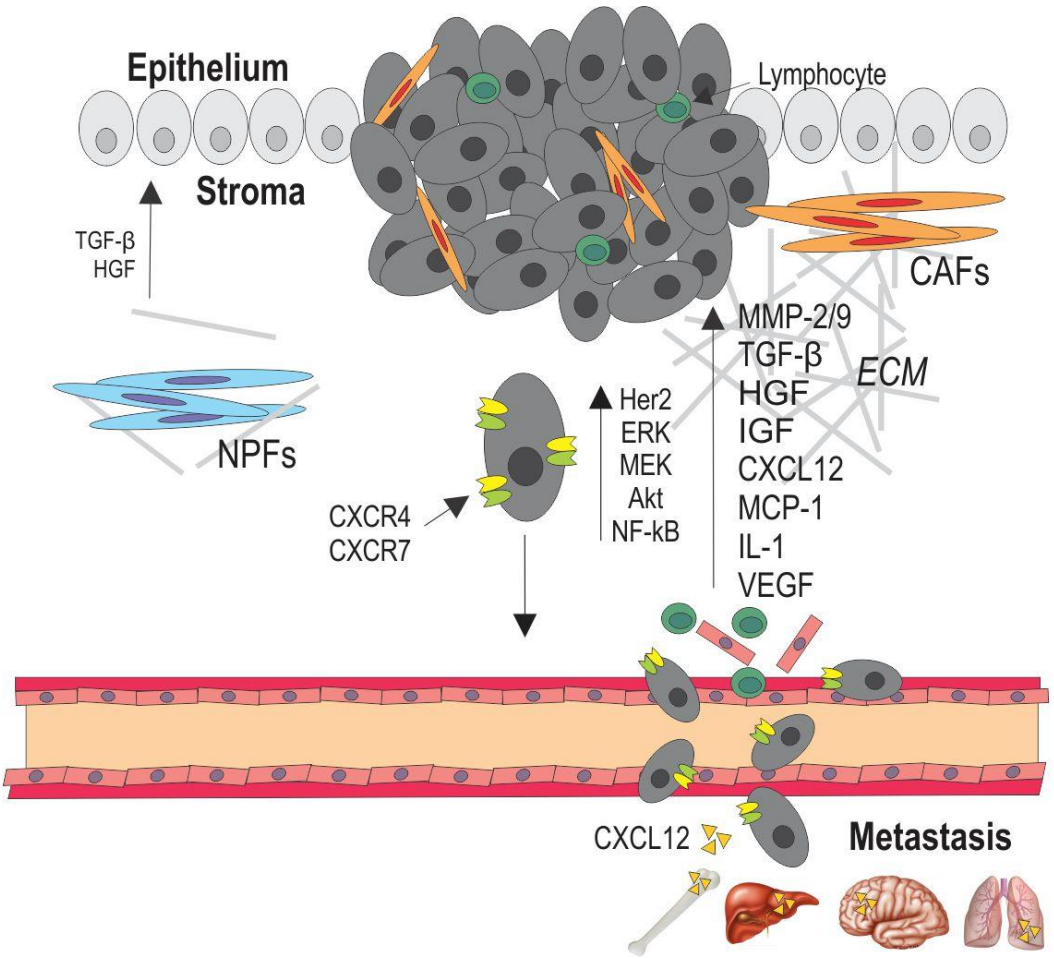

Figure 1.5: Overview of the role of cancer-associated fibroblasts in driving prostate cancer progression. In a cancer setting, cancer-associated fibroblasts (CAFs) re-model the extracellular matrix (ECM) via the over-secretion of matrix metalloproteinases (MMPs). They stimulate cancer cell proliferation, migration and metastasis through over-secretion of growth factors, cytokines, chemokines and angiogenic factors. This, paired with activation of oncogenic proteins, ultimately leads to an environment permissive of cancer growth and metastasis to distant sites such as the bone, liver, brain, lungs and lymph nodes.

1.4.3: Fibroblast-mediated drug resistance

While the role of fibroblasts in cancer initiation and progression is being actively researched, evidence that fibroblasts directly and indirectly contribute to the development of drug resistance is also beginning to emerge. Fibroblast-derived fibronectin is involved in the attachment of epithelial cells to the ECM, a process facilitated by membrane-bound integrins. Interestingly, drug-sensitive human myeloma cells expressing integrin and fibronectin receptors were resistant to chemotherapy when pre-adhered to fibronectin compared to cells grown in suspension, a phenomenon termed cell adhesion-mediated drug resistance (CAM-DR) (Damiano, Cress et al. 1999, Damiano, Hazlehurst et al. 2001). Further, the adherence of small cell lung cancer cells to ECM conferred resistance to chemotherapy via integrin-stimulated tyrosine kinase activation (Sethi, Rintoul et al. 1999). Fibroblasts are also involved in collagen synthesis and deposition, and the excess collagen secreted by CAFs can inhibit the transport of drugs into a tumour. This is further exacerbated by the increased interstitial fluid pressure and subsequent collapse of blood vessels often found within tumours (Heldin, Rubin et al. 2004). The growth factors released by CAFs induce rapid proliferation of cancer cells that is often not matched by the rate of angiogenesis. Not only does this further limit drug delivery to tumours, but the subsequent hypoxia in these areas may decrease the effect of drugs that are oxygen- or free radical-dependent (Brown and Giaccia 1998). Increased hypoxia may induce further genetic instability in cancer cells, and select for highly aggressive and resistant cells often expressing multidrug resistance efflux pumps (Liang, Ma et al. 2012). It has therefore been widely proposed that a combinational approach, targeting both cancer cells and fibroblasts, is likely to be more effective than targeting cancer cells alone.

1.4.4: Fibroblast-targeted therapies

The genetic instability and heterogeneity of cancer cells has caused a great deal of difficulty in targeting them without the development of drug resistance. The genetic stability of fibroblasts combined with their outlined role in carcinogenesis, however, has made them an alluring drug target for cancer therapy (Lee, Fassnacht et al. 2005, Loeffler, Krüger et al. 2006). This is supported by the notion that genetically stable cells do not undergo rapid mutational evolution and are less capable of developing drug resistance. Indeed, molecules that are over-expressed in CAFs such as MMPs and fibroblast-activated protein (FAP) have been investigated as therapeutic targets. As described previously, CAFs over-secrete MMPs which causes ECM remodelling and promote cancer cell migration, invasion and metastasis. This made the development of MMP inhibitors an exciting avenue in the late nineties. However, results from these studies were disappointing, with many clinical trials failing to show anti-cancer efficacy (Pavlaki and Zucker 2003, Leighl, Paz-Ares et al. 2005). Almost all CAFs over-express FAP, believed to increase tumour growth and promote cancer cell invasion (Garin-Chesa, Old et al. 1990, Chen and Kelly 2003, Brennen, Isaacs et al. 2012). Studies into FAP inhibitors, monoclonal

antibodies, targeted vaccines and T-cell therapies have demonstrated promising anti-tumour responses (Welt, Divgi et al. 1994, Scott, Wiseman et al. 2003, Lee, Fassnacht et al. 2005, Loeffler, Krüger et al. 2006, LeBeau, Brennen et al. 2009, Wen, Wang et al. 2010). Small molecule inhibitors against growth factors over-secreted by CAFs (e.g. TGF-β, PDGF and VEGF) have also shown moderate success (Escudier, Eisen et al. 2007, Steeghs, Nortier et al. 2007, Flechsig, Dadrich et al. 2012). In the context of prostate cancer, targeting fibroblasts would most likely occur via neoadjuvant therapy prior to RP (when the cancer microenvironment remains intact), or when the disease is detected at an advanced stage and RP is no longer an option.

1.4.5: Androgen receptor in the prostate cancer microenvironment

While AR has quite a clearly defined role in normal prostate and cancer development, it also plays an important yet somewhat paradoxical role in the prostate cancer microenvironment. There are a number of reports suggesting that stromal AR contributes to prostate cancer initiation. When BPH-1 cells were recombined with rat UGM, grafted to mouse renal capsules and treated with testosterone, invasive carcinoma developed. However when testosterone was removed via castration, epithelial apoptosis was observed (Wang, Sudilovsky et al. 2001). To differentiate the roles of AR in prostate epithelial and stromal cells, Niu et al. generated two inducible AR transgenic adenocarcinoma mouse prostate models where AR could be knocked out in both epithelial and stromal compartments or knocked out in the epithelium only. While the loss of AR in both models caused poorly differentiated primary tumours, AR knock out in the epithelium only resulted in large primary tumours with high proliferation rates, indicating that stromal AR plays a dominant role in promoting tumour initiation (Niu, Altuwaijri et al. 2008). Conversely, there are reports that demonstrate an association between low stromal AR levels and prostate cancer progression (Henshall, Quinn et al. 2001, Olapade-Olaopa, Moscatello et al. 2004, Olapade-Olaopa, Muronda et al. 2004, Ricciardelli, Choong et al. 2005, Wikström, Marusic et al. 2009, Ricke, Williams et al. 2012). Further, a decrease in stromal AR expression has been associated with tumour resistance to ADT and relapse and progression following RP (Henshall, Quinn et al. 2001, Li, Wheeler et al. 2004, Ricciardelli, Choong et al. 2005, Wikström, Marusic et al. 2009). The switch from cancer dependence on stromal AR to the loss of stromal AR promoting cancer progression remains a critical event in prostate cancer pathogenesis and a major predictor of patient outcome. The processes mediating these events, however, have not yet been defined.

1.5: CURCUMIN

1.5.1: Properties and mechanisms of action

Curcumin ($C_6H_{20}O_6$) is a biologically active, polyphenol compound derived from the plant curcuma longa, or turmeric. Turmeric is composed of approximately 5% curcuminoid, a linear form of the plant

secondary metabolite diarylheptanoid. Curcumin accounts for approximately 80% of the curcuminoid content of turmeric, while the remainder is made up of closely related compounds demethoxycurcumin (17%) and bisdemethoxycurcumin (3%) (Gupta, Kismali et al. 2013). The curcumin molecule possesses several functional groups including a pair of phenol aromatic rings connected by two α,β-unsaturated carbonyl groups (schematic presented in **Figure 1.6**).

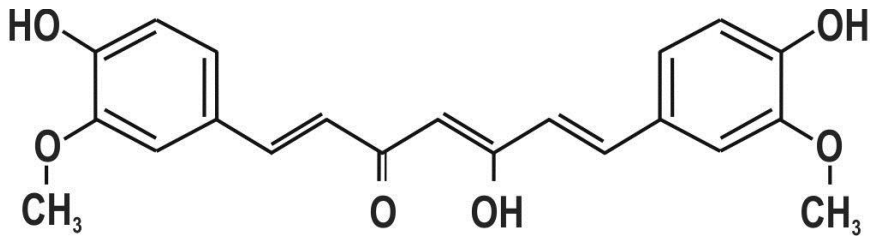

Figure 1.6: Curcumin molecular structure. Curcumin is a natural polyphenol accounting for approximately 80% of the curcuminoid component of the spice turmeric. It contains two aromatic ring systems (phenols) linked by two α,β-unsaturated carbonyl groups.

Curcumin has a long history of use in traditional Indian and Asian medicine, cooking, cosmetics and fabric dye (Hatcher, Planalp et al. 2008). It remains a common remedy for treating infections, wounds and gastrointestinal ailments in these cultures to this day. The first peer reviewed article on curcumin was published in 1937 and identified it as a treatment for human biliary disease (Oppenheimer 1937). Since then, curcumin has become one of the world's most vigorously investigated natural compounds and has been subject to extensive preclinical and clinical studies for a range of medical conditions including inflammatory diseases (e.g. dermatitis and asthma), cognitive disorders (e.g. dementia and depression), vascular disorders and cancer. Indeed, a link has been made between high turmeric consumption (India and Southern Asia) and low cancer incidence (Rao, Rivenson et al. 1995, Sinha, Anderson et al. 2003, Ferlay, Shin et al. 2010). While there is no data reporting the consumption of curcumin in Western countries, the average Indian person is estimated to consume between 60 and 100 mg of curcumin daily (Bar-Sela, Epelbaum et al. 2010).

While curcumin is still considered an alternative medicine, preclinical studies have demonstrated anti-inflammatory, anti-oxidant, anti-septic and anti-angiogenic properties which have become central to its widespread medicinal use (Srimal and Dhawan 1973, Srihari Rao, Basu et al. 1982, Xu, Pindolia et al. 1997, Gururaj, Belakavadi et al. 2002, Weber, Hunsaker et al. 2005, Zhang, Han et al. 2005, Mellado, Codony et al. 2009). These properties have been attributed to a broad range of cellular targets known to modulate many characteristics associated with cancer (summarised in **Figure 1.7**). Curcumin binds to over 30 proteins and targets transcription factors, growth factors, cytokines, enzymes and genes regulating cell proliferation and death pathways (Anand, Thomas et al. 2008). While curcumin-mediated cell death is largely believed to occur via apoptosis, whether this is caspase-dependent or -independent

remains debatable (Piwocka, Bielak-Zmijewska et al. 2002, Thayyullathil, Chathoth et al. 2008, Lu, Lai et al. 2009, Singh, Shrivastav et al. 2009, Hilchie, Furlong et al. 2010, Wu, Hang et al. 2010). Likewise, whether curcumin-mediated cell death is dependent or independent of p53 remains unclear (Jee, Shen et al. 1998, Bush, Cheung Jr et al. 2001, Choudhuri, Pal et al. 2002, Choudhuri, Pal et al. 2005, Liu, Wu et al. 2007, Watson, Greenshields et al. 2010, Jaisin, Thampithak et al. 2011). Despite the precise mechanisms of curcumin-mediated cell death remaining unknown, it is clear from the literature that suppression of transcription factors NF-κB and AP-1 are central mechanisms of curcumin action (Bierhaus, Zhang et al. 1997, Xu, Pindolia et al. 1997, Dickinson, Iles et al. 2003, Divya and Pillai 2006, Dhandapani, Mahesh et al. 2007, Kamat, Sethi et al. 2007, Kunnumakkara, Guha et al. 2007, Lin, Kunnumakkara et al. 2007, Gonzales and Orlando 2008, Hussain, Ahmed et al. 2008, Wang, Veena et al. 2008, Kang, Lee et al. 2009, Hartojo, Silvers et al. 2010, Jutooru, Chadalapaka et al. 2010, Sun, Chen et al. 2011). The majority of curcumin research has been conducted on candidate genes and proteins involved in various disease states. Only over the last few years has microarray and proteomic technology been used to investigate curcumin action in more depth.

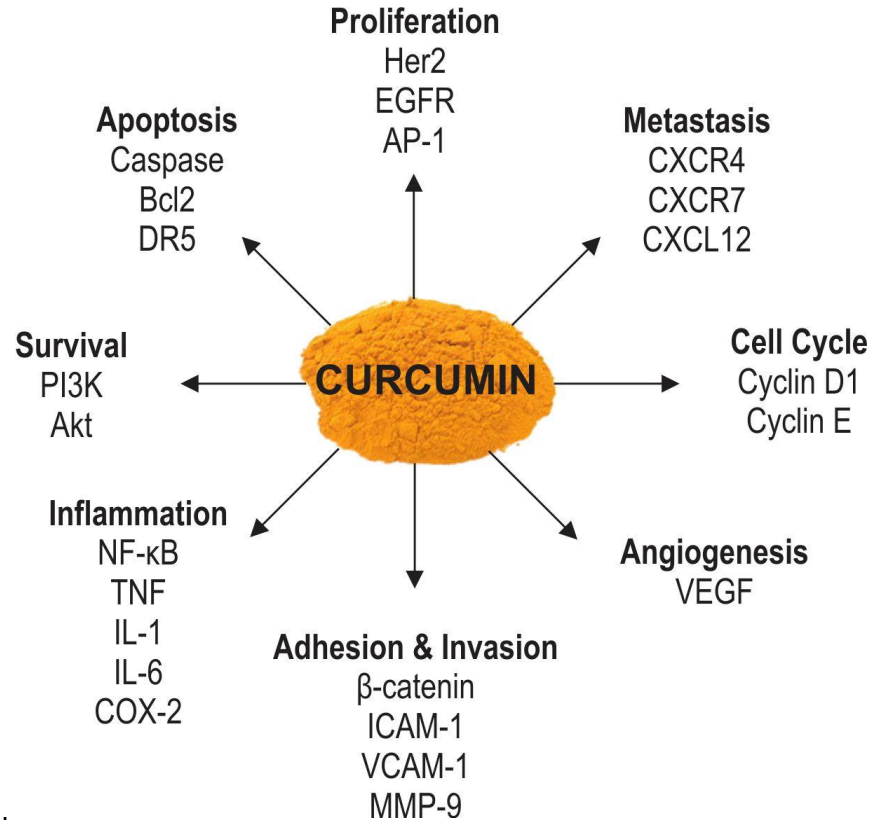

Figure 1.7: Summary of the molecular targets of curcumin. The medicinal properties of curcumin have been attributed to its ability to bind to over 30 proteins. It targets factors involved in cancer cell proliferation, cell cycle, apoptosis, adhesion, invasion, angiogenesis, metastasis and inflammation.

1.5.2: Curcumin and prostate cancer

Curcumin has been shown to inhibit the growth of almost all types of cancer cell, including prostate cancer (Ravindran, Prasad et al. 2009). Consequently, there has been a large body of *in vitro* work investigating the therapeutic efficacy of curcumin in prostate cancer cells. Curcumin has been shown to induce apoptosis in both androgen-dependent (LNCaP and 22Rv1) and androgen-independent (C4-2B, PC-3 and DU-145) prostate cancer cell lines (Dorai, Gehani et al. 2000, Mukhopadhyay, Bueso-Ramos et al. 2001, Thangapazham, Shaheduzzaman et al. 2008, Piantino, Salvadori et al. 2009, Liu, Wang et al. 2011, Teiten, Gaascht et al. 2011). This has been largely attributed to the down-regulation of transcription factors (e.g. NF-κB and AP-1), the targeting of cell growth and survival pathways (e.g. mTOR and EGFR), the activation of pro-caspases (e.g. -3 and -8) and the decreased expression of oncogenic proteins (e.g. Akt and β-catenin) (Korutla, Cheung et al. 1995, Dorai, Gehani et al. 2000, Chaudhary and Hruska 2003, Shankar and Srivastava 2007, Yu, Shen et al. 2008, Piantino, Salvadori et al. 2009, Choi, Lim et al. 2010, Jutooru, Chadalapaka et al. 2010, Killian, Kronski et al. 2012, Sundram, Chauhan et al. 2012). Functionally, curcumin has been shown to decrease the migration and invasion of prostate cancer cells via alterations in MMP-2, MMP-9 and CCL2 (Hong, Ahn et al. 2006, Herman, Stadelman et al. 2009, Cheng, Chen et al. 2013, Piccolella, Crippa et al. 2014). Perhaps most importantly, however, are reports that curcumin decreased AR mRNA, transactivation activity and steady-state protein levels through a structural similarity to AR antagonists and ability to enhance AR degradation (Nakamura, Yasunaga et al. 2002, Ohtsu, Xiao et al. 2002, Shi, Shih et al. 2009, Fajardo, MacKenzie et al. 2012, Guo, Xu et al. 2013). In addition, curcumin has been shown to suppress AR residence on DNA and downstream target gene expression through reduced association of histone acetylation and AR co-activator proteins, both under ligand-dependent and ligand-independent conditions (Shah, Prasad et al. 2012). A xenograft model was used to support these findings; with results indicating that curcumin in combination with ADT reduced tumour growth and delayed the onset of CRPC. Other studies have implicated curcumin as both a DNA hypo-methylating agent and histone acetyltransferase inhibitor in prostate cancer cell lines (Marcu, Jung et al. 2006, Khor, Huang et al. 2011, Shu, Khor et al. 2011).

There have been relatively few studies investigating curcumin efficacy in animal models of prostate cancer. Most have employed xenograft models using various prostate cancer cell lines. One of the earliest studies demonstrated that a diet containing 2% curcumin fed over six weeks caused a decrease in LNCaP xenograft proliferation and an increase in tumour apoptosis (Dorai, Cao et al. 2001). In PC-3 xenografts, curcumin treatment over twenty-eight consecutive days was effective in reducing tumour size when treatment began at the time of tumour inoculation (Khor, Keum et al. 2006). In DU-145 xenografts, curcumin treatment three times weekly over four weeks reduced the size of established

xenografts and prevented the growth of newly inoculated tumours (Hong, Ahn et al. 2006). Finally, in C4-2 xenografts, seven consecutive curcumin injections caused a significant reduction in tumour size (Sundram, Chauhan et al. 2012). While there have been no studies of curcumin in metastatic prostate cancer models, curcumin inhibited the formation of lung metastases when PC-3 cells were injected into mice via intra-cardiac injection (Killian, Kronski et al. 2012).

1.5.3: Curcumin clinical trials for cancer

Despite the promising preclinical efficacy of curcumin, it has had little success in clinical trials. There are currently 15 active clinical trials investigating curcumin for the prevention and treatment of cancer, and results from five trials have been published to date. The first was a Phase I dose-escalation study in 25 patients with high risk or pre-malignant lesions (Chen, Hsu et al. 2001). Individual patients began receiving 500 mg curcumin daily, a dose that was gradually escalated to 12 g daily over three months. No toxicity was reported, however the serum concentration of curcumin peaked at two hours following oral intake and gradually declined within 12 hours. While seven patients showed histological improvement in pre-cancerous lesions, two patients developed malignancies despite curcumin treatment. The second Phase I trial conducted a dose-escalation from 0.45 to 3.6 g curcumin daily for four months in 15 patients with advanced colorectal cancer resistant to standard chemotherapy (Sharma, Euden et al. 2004). Toxicity was not observed but curcumin metabolites were detected in plasma at a very low level. The third study was a Phase II trial that measured the efficacy of curcumin in 21 pancreatic cancer patients (Dhillon, Aggarwal et al. 2008). Patients received 8 g curcumin daily until disease progression. Similarly, no toxicity was reported and curcumin was only detectable in metabolite form at low levels. Three patients showed marked tumour regression and most patients demonstrated a decrease in NF-κB expression in peripheral blood mononuclear cells. The fourth study was another Phase II trial that assessed the effect of curcumin in 41 patients with eight or more aberrant crypt foci, a precursor lesion to colorectal cancer (Carroll, Benya et al. 2011). A daily dose of 4 g over 30 days caused a significant reduction in crypt number. The final Phase II trial investigated the ability of a topical curcumin formulation to eliminate human papilloma virus (HPV) infection from the cervix, which can progress to cervical cancer (Basu, Dutta et al. 2013). Use of curcumin over 30 consecutive days caused a higher rate of HPV clearance than placebo, but the effect was not significant. Given the general lack of efficacy observed in clinical trials, there has been increased interest in improving the bioavailability profile of curcumin.

1.5.4: Challenges associated with curcumin treatment

There are two main causes for the lack of efficacy associated with curcumin: low solubility in water and hydrolysis resulting in degradation within 30 minutes (Kaminaga, Nagatsu et al. 2003, Letchford, Liggins et al. 2008, Leung, Colangelo et al. 2008, Leung and Kee 2009, Wang, Leung et al. 2010, Harada,

Pham et al. 2011). These two challenges must be overcome for curcumin to be considered a realistic therapeutic option for cancer treatment. Various studies have demonstrated effective stabilisation of curcumin using a range of delivery agents including micelles, liposomes, polymers and proteins (Tonneson, Smistad et al. 1993, Barik, Priyadarsini et al. 2003, Leung, Colangelo et al. 2008, Sahu, Kasoju et al. 2008, Chen, Johnston et al. 2009, Leung and Kee 2009, Takahashi, Uechi et al. 2009, Das, Kasoju et al. 2010, Mohanty, Acharya et al. 2010, Tang, Murphy et al. 2010, Wang, Leung et al. 2010, Yallapu, Gupta et al. 2010, Esmaili, Ghaffari et al. 2011). However, there has been concern that large scale molecular assemblies may potentially limit the intracellular delivery of curcumin. The development of molecular scale delivery agents for curcumin has therefore recently been undertaken. Cyclodextrin (CD)-based delivery systems have become a popular means of increasing curcumin bioavailability on a molecular scale. The CD molecule is a naturally occurring, cyclic oligosaccharide with either six (α), seven (β) or eight (γ) glucopyranoside units. They are often used as stabilisers and drug carriers due to their toroidal structure, which has a hydrophobic interior and hydrophilic exterior. This allows hydrophobic drugs such as curcumin to be stably solubilised in water with minimal degradation under physiological conditions (Harada, Pham et al. 2011). Importantly, CDs are approved by both the Therapeutic Goods Administration and the Federal Drug Administration, and are already utilised in the food and cosmetic industries (Szejtli 1998). There have been a number of studies using CD delivery systems to improve curcumin efficacy across a range of malignancies (Yadav, Prasad et al. 2010, Yallapu, Jaggi et al. 2010, Dhule, Penfornis et al. 2012, Michel, Chitanda et al. 2012, Rahman, Cao et al. 2012, Rocks, Bekaert et al. 2012). Recently, Pham et al. synthesised diamide-linked γ-CD dimers in which the diamide link (urea or succinimide) is hydrolysed only within the intracellular environment (Pham, Ngo et al. 2010). This ensures the release of encapsulated material into the cell. Molecular encapsulation of curcumin by the diamide linked γ-CD dimers suppressed the rate of curcumin degradation under physiological conditions by 200-fold (Harada, Pham et al. 2011). Further, curcumin-loaded diamide-linked γ-CD dimers have demonstrated anti-proliferative activity and alterations to gene expression in PC-3 cells comparable to curcumin alone, suggesting encapsulation does not compromise curcumin efficacy (Harada, Giorgio et al. 2013). While further exploration of CD dimers is required, other forms of enhanced curcumin delivery (e.g. nanoparticles and lysosomes) are already being assessed in clinical trials.

1.5.5: Curcumin tolerance and resistance

The development of drug tolerance and resistance is arguably the biggest challenge to cancer therapy. Drug tolerance is defined as a decrease in pharmacologic response following repeated or prolonged drug administration, and can be broadly classed under pharmacokinetic or pharmacodynamic subtypes (Dumas and Pollack 2008). Pharmacokinetic tolerance is characterised by a decreased quantity of drug

reaching the target site, often caused by an increase in drug metabolising enzymes such as CYP450 (Dumas and Pollack 2008). Pharmacodynamic tolerance occurs when the responsiveness of the target receptor diminishes over time, often due to down-regulation or internalisation of the receptor (Raith and Hochhaus 2004). Drug resistance, on the other hand, occurs when cells are no longer killed or inhibited by a drug. This is most often due to spontaneous mutations, which stop the drug from having a biological effect in the target cell (Bock and Lengauer 2012). There are also two main subtypes of drug resistance, acquired and innate, both of which lead to the failure of cancer treatment. Acquired resistance typically develops due to ongoing exposure to a drug and involves a series of changes that allow cancer cells to survive despite continued treatment. One of the most well studied mechanisms of acquired drug resistance is the up-regulation of drug efflux ATP-binding cassette (ABC) transporters such as P-glycoprotein (ABCB1) and multidrug resistance protein 1 (MRP1 or ABCC1) (Juliano and Ling 1976, Beck, Mueller et al. 1979, Roninson, Chin et al. 1986, Shen, Fojo et al. 1986). These transporters are often up-regulated by cancer cells to enhance drug efflux as a first line defence against xenobiotics, substances not normally expected to be found within an organism. Innate drug resistance describes cells that inherently possess mechanisms to counteract treatment, such as p53 or KRAS mutation (Kandioler-Eckersberger, Ludwig et al. 2000, Lièvre, Bachet et al. 2006).

While there is no literature to date describing curcumin tolerance, there are a limited number of reports that curcumin can reverse drug resistance in cancer cells, largely via down-regulation of ABCB1 and ABCG (Shukla, Zaher et al. 2009, Qin, Li et al. 2012, Qiu, Fu et al. 2012, Ye, Zhao et al. 2012, Lu, Qin et al. 2013, Sreenivasan, Ravichandran et al. 2013). There are also three reports in the literature documenting curcumin resistance. The first demonstrated that M14 human melanoma cells were resistant to curcumin-induced apoptosis via over-expression of ABCA1 (Bachmeier, Iancu et al. 2009). Silencing of ABCA1 re-sensitised M14 cells to apoptosis by curcumin. The second study reported that hypoxia in HepG2 hepatocellular carcinoma cells induced curcumin resistance, attributed to an increase in ABCC1, ABCC2 and ABCC3 expression. Again, inhibitors to these transporters reversed hypoxia-induced curcumin resistance (Sakulterdkiat, Srisomsap et al. 2012). Finally, microarray profiling of 60 human cancer cell lines identified genes that determined curcumin sensitivity or resistance (Sertel, Eichhorn et al. 2012). Interestingly, however, correlation analysis between the expression of 48 ABC transporters and the sensitivity or resistance of the cancer cell lines revealed no significant relationships, suggesting ABC transporters may not be a major determinant of resistance to curcumin.

1.5.6: Curcumin activity in fibroblasts

There is also relatively little appreciation for the effect of curcumin on fibroblasts. One study to date has characterised curcumin action in CAFs. In patient-derived breast cancer CAFs, low doses of curcumin up-regulated the tumour suppressor p16 and inactivated the JAK2/STAT3 pathway, thereby reducing

expression of α-smooth muscle actin and the subsequent migration and invasion abilities of fibroblasts (Hendrayani, Al-Khalaf et al. 2013). Curcumin also suppressed expression and secretion of CXCL12, IL-6, MMP-2, MMP-9 and TGF-β, thus impeding CAF paracrine signalling capacity. In non-cancer fibroblasts, curcumin has been shown to reduce proliferation and increase apoptosis, largely through G1-phase cell cycle arrest and inhibition of NF-κB (Tourkina, Gooz et al. 2004, Park, Moon et al. 2007, Sun and Zhao 2011, Hu, Huang et al. 2013, Hwang, Noh et al. 2013, Kloesch, Becker et al. 2013). Furthermore, curcumin can decrease the synthesis of collagen in multiple types of fibroblast (Hu, Hu et al. 2008, Song, Peng et al. 2011, Zhang, Huang et al. 2011, Ryu, Kim et al. 2012). One particular study co-cultured periodontal ligament fibroblasts with oral squamous carcinoma cells in the presence or absence of curcumin (Dudás, Fullár et al. 2013). In curcumin-treated samples, NF-κB and ERK expression were decreased in cancer cells while integrin expression was decreased in CAFs compared to the control. This is interesting given that integrin has been implicated in CAM-DR (discussed in Section 1.4.3). This study also demonstrated that curcumin caused a decrease in the release of mediators associated with epithelial to mesenchymal transition in CAFs, which was subsequently associated with decreased invasion of cancer cells. Recently, however, the curcumin analogue D6 induced cell survival and death pathways in human foreskin fibroblasts despite having no effect on fibroblast proliferation or induction of apoptosis (Rozzo, Fanciulli et al. 2013).

1.6: APOPTOSIS

Apoptosis has largely been proposed as the central mechanism of curcumin-mediated cell death in cancer cells. It is the process of programmed cell death that occurs in multicellular organisms, with the primary outcome to eliminate cells no longer required by the organism or that have sustained irreparable damage to their physical and/or genetic integrity (Ghobrial, Witzig et al. 2005). Apoptotic stimuli include developmental cues, the activation of pro-apoptotic receptors, cellular stress or injury, irradiation, cytotoxic drugs, bacteria and viruses (Gulbins, Jekle et al. 2000). These factors initiate an intracellular proteolytic cascade that causes eventual cell death.

1.6.1: Extrinsic and intrinsic apoptotic pathways

Apoptosis occurs through two principal pathways: the extrinsic or death receptor pathway and the intrinsic or mitochondrial pathway, both summarised in **Figure 1.8** (Jin and El-Deiry 2005). These pathways are mediated by specific cysteine-aspartic proteases called caspases in a two-step process: initiator caspases are activated through biochemical cues, which then cleave and activate effector caspases that drive the apoptotic cell death program (Thornberry and Lazebnik 1998).

The extrinsic pathway is activated from outside of the cell by pro-apoptotic ligands belonging to the tumour necrosis factor (TNF) superfamily, such as fas ligand and Apo2 ligand/TNF-related apoptosis-

inducing ligand (Apo2L/TRAIL or TRAIL). These ligands interact with pro-apoptotic cell surface receptors such as death receptor 4 (DR4) and 5 (DR5), leading to receptor clustering and recruitment of the adaptor molecule fas-associated death domain (FADD). Upon dissociation, initiator caspases -8, -9 and -10 are activated by interaction with FADD to form a death inducing signalling complex (DISC), which then leads to the downstream activation of effector caspases -3, -6 and -7, and subsequent apoptosis (Ashkenazi 2002). Additionally, there are three human decoy receptors for TRAIL: DcR1, DcR2 and osteoprotegrin (Degli-Esposti, Dougall et al. 1997, Degli-Esposti, Smolak et al. 1997, Emery, McDonnell et al. 1998). While DcR1 and DcR2 cannot mediate apoptosis due to a lack of functional death domain, all three receptors compete with DR4 and DR5 for ligand. The extrinsic apoptosis pathway has become a desirable target for cancer therapy because it can circumvent the resistance mechanisms associated with p53 inactivation (Ashkenazi 2002). Surface receptors DR4 and DR5 are particularly interesting targets for cancer therapy as studies have shown that their activation causes apoptosis in cancer cells with minimal effect on normal cells (Fulda and Debatin 2006, Kanwar, Cheung et al. 2010).

The intrinsic pathway is initiated within the cell in response to developmental cues or cellular stress (often p53-mediated) by members of the Bcl-2 family (Cory and Adams 2002). Briefly, these stimuli induce activation of pro-apoptotic factors (e.g. Bax, Bid and Bak) and their translocation to the mitochondria, leading to permeabilisation of the mitochondrial membrane and the release of cytochrome-c and mitochondrial proteins SMAC and DIABLO into the cytosol. These proteins bind to apoptosis protease-activating factor 1, leading to formation of an intracellular DISC-like complex known as the apoptosome (Zou, Li et al. 1999). Within the apoptosome, caspase-9 is cleaved and activated. This leads to activation of effector caspases -3, -6 and -7, with subsequent activation of cytoplasmic endonucleases to degrade nuclear material and proteases that degrade nuclear and cytoskeletal proteins (e.g. poly ADP-ribose polymerase or PARP). Morphologic manifestations of apoptosis such as DNA condensation, fragmentation and membrane blebbing eventually lead to cell death (Cory and Adams 2002). Many conventional chemotherapeutic agents cause cell death via the intrinsic pathway, however cancer cells often become resistant to such treatments via inactivation or mutation of p53 (Strano, Dell'Orso et al. 2007). There is often cross-over between the intrinsic and extrinsic pathways via caspase-8-mediated cleavage of Bid, leading to subsequent release of cytochrome-c (Wang and El-Deiry 2003).

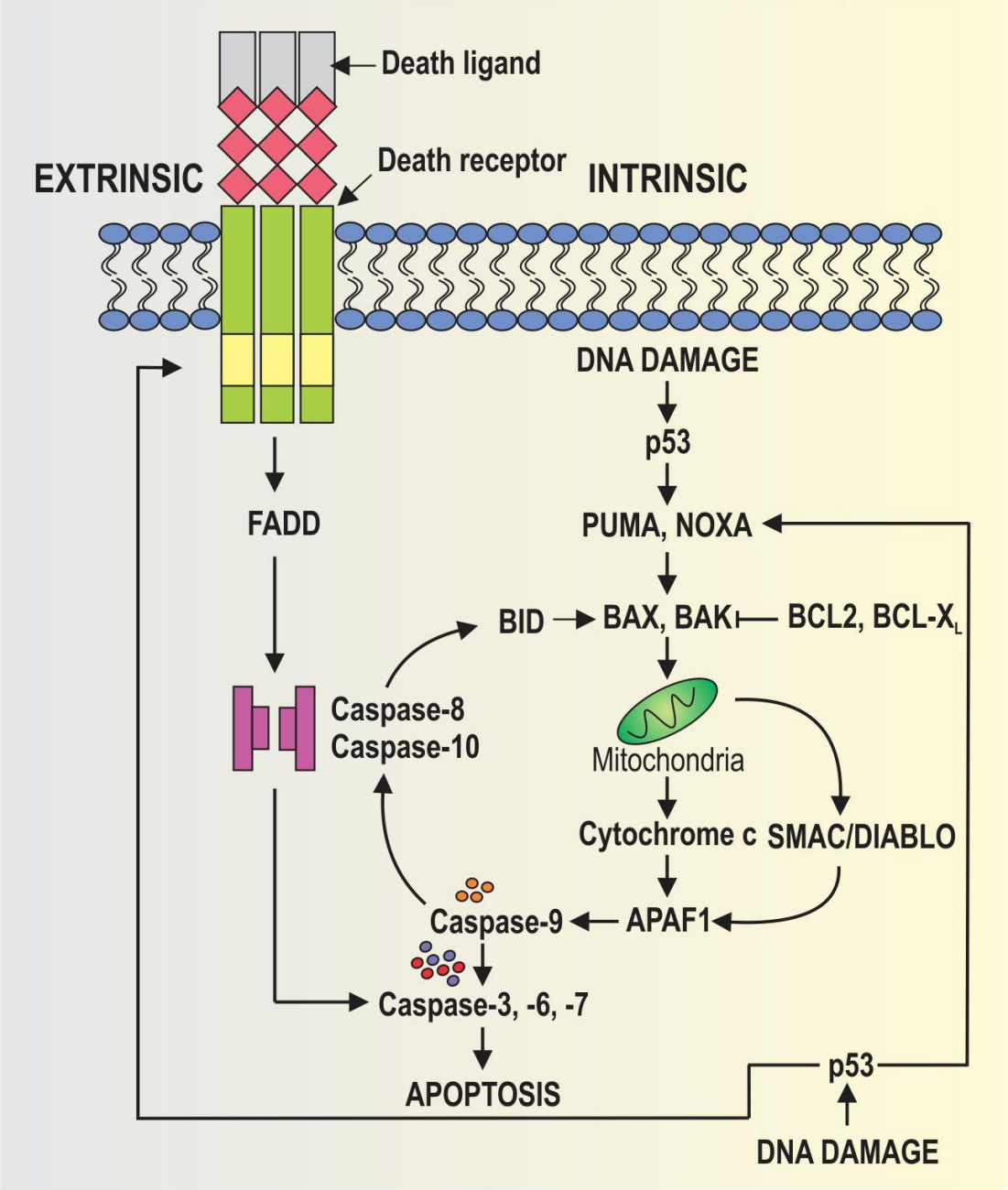

Figure 1.8: The extrinsic and intrinsic apoptosis signalling pathways. The extrinsic pathway triggers apoptosis in response to engagement of death receptors, independent of p53. Ligand activation of death receptors 4 and 5 leads to activation of initiator caspases -8, -9 and -10, which activate effector caspases -3, -6 and -7, causing apoptosis. The intrinsic pathway triggers apoptosis in response to DNA damage or other types of severe cell distress. This pathway involves activation of members of the Bcl2 superfamily, which engage the mitochondria to cause release of pro-apoptotic factors cytochrome c, SMAC and DIABLO. These factors activate initiator caspase-9 through apoptosis protease-activating factor 1 (APAF1), which subsequently activates effector caspases -3, -6 and -7 causing apoptosis.

1.6.2: Targeting apoptosis in cancer

Targeting apoptosis has been a popular approach to treating cancer based on the observation that apoptosis is highly deregulated in cancer cells but not in normal cells (Ashkenazi and Herbst 2008). As mentioned in Section 1.6.1, conventional anti-cancer therapies stimulate apoptosis primarily through the

intrinsic pathway, largely mediated by p53. However, inactivation of p53 is one of the most common events in cancer, and provides a key resistance mechanism to assist cancer cells in avoiding apoptosis (Lee and Bernstein 1995). Therefore therapies targeting the p53-independent extrinsic pathway are widely considered more effective. Several of these strategies, including pro-apoptotic receptor agonists (PARAs), Bcl-2 family inhibitors and caspase modulators have been subject to intensive preclinical and clinical research. Clinical trials have demonstrated that PARAs (including recombinant human TRAIL, drozitumab, lexatumumab and mapatumumab) are safe at high doses, and have shown promising efficacy in causing tumour regression (Tolcher, Mita et al. 2007, Camidge 2008, Hotte, Hirte et al. 2008, Wakelee, Patnaik et al. 2009, Herbst, Eckhardt et al. 2010, Younes, Vose et al. 2010).

1.6.3: Curcumin in combination with pro-apoptotic receptor agonists

Besides the development of novel curcumin delivery systems, there has also been interest in using curcumin in combination with other standard anti-cancer therapies. The combination of agents with synergistic activity is very attractive in anti-cancer therapy because it reduces the possibility of acquired resistance to either therapy and supports lower drug dosage to patients, thereby reducing toxic side effects. Various preclinical studies have demonstrated that curcumin acts in a synergistic manner with multiple anti-cancer agents including genistein, fluorouracil, celecoxib and bortezomib (Verma, Salamone et al. 1997, Lev-Ari, Strier et al. 2005, Du, Jiang et al. 2006, Park, Ayyappan et al. 2008, Majumdar, Banerjee et al. 2009, Altenburg, Bieberich et al. 2011). There are also a myriad of mechanisms by which curcumin may alter the cancer cell to create an environment favourable to toxic therapy, including inhibiting drug-induced DNA repair and the reversal of multi-drug resistance (Saha, Adhikary et al. 2012). The focus of this section will be on the ability of curcumin to modulate apoptosis, thus enhancing cancer cell death.

Some of the most well characterised death ligands (e.g. TNFα and fas ligand) initially carried great promise as anti-cancer agents. However, these agents did not proceed to clinical trials due to their severe toxicity towards normal tissue (Chicheportiche, Bourdon et al. 1997, Marsters, Sheridan et al. 1998). In contrast, recombinant soluble TRAIL is selectively toxic to cancer cells and is safe and well tolerated in patients with advanced tumours (Wiley, Schooley et al. 1995, Pitti, Marsters et al. 1996, Pan, Ni et al. 1997). The loss of TRAIL function has been reported to result in innate or acquired resistance, which may occur via mutation in death receptors, defects in caspase-8 or FADD, over-expression of Bcl2 family members or the loss of Bax and Bak function (Zhang and Fang 2005). Interestingly, several groups have shown that curcumin can sensitise TRAIL-resistant cancer cells to TRAIL-induced apoptosis in a number of cancer models. In human glioma and ovarian cancer cells, the combination of low concentrations of curcumin and TRAIL caused a marked increase in cell death over either agent alone (Gao, Deeb et al. 2005, Wahl, Tan et al. 2007). In LNCaP, DU-145 and PC-3 prostate

cancer cells, curcumin inhibited constitutively active NF-κB and subsequently enhanced TRAIL sensitivity (Deeb, Xu et al. 2003). Animal studies support these findings, with one particular study showing that curcumin sensitised TRAIL-resistant LNCaP xenografts to apoptosis by TRAIL through the up-regulation of DR4 and DR5 (Shankar, Chen et al. 2007, Shankar, Ganapathy et al. 2008). Additionally, curcumin in combination with TRAIL was more effective at inhibiting PC-3 xenograft growth than either agent alone, with the combination significantly reducing expression of Akt and NF-κB (Andrzejewski, Deeb et al. 2008).

1.6.4: Drozitumab

Similar to death ligands, monoclonal antibodies (MAb) designed to target pro-apoptotic receptors are a desirable form of cancer therapy because they are extremely specific in their affinity, thus causing minimal toxicity to patients. Drozitumab is a fully humanised agonistic MAb which has been designed to directly and specifically bind to DR5 on the surface of cancer cells and initiate apoptosis. Drozitumab is advantageous over recombinant soluble TRAIL due to its extended half-life which does not require frequent administration to maintain efficacy (Kelley, Harris et al. 2001). Adams et al. were the first to characterise the anti-cancer activity of drozitumab (Adams, Totpal et al. 2008). Binding studies confirmed a high affinity for DR5, with undetectable binding to other TRAIL receptors. *In vitro*, drozitumab induced apoptosis in various cancer cell lines with no detectable apoptosis in normal human hepatocytes. *In vivo* studies demonstrated potent anti-cancer activity across colorectal, non-squamous cell lung carcinoma and pancreatic ductal cancer xenograft models. Interestingly, addition of an anti-$F_c\gamma$ cross-linking antibody to drozitumab further augmented DISC assembly and caspase-8 activation via enhanced receptor aggregation, thereby enhancing pro-apoptotic signalling (Adams, Totpal et al. 2008). Cross-linking was not found to be necessary *in vivo*, however, due to the abundance of circulating F_c antibodies and the cell-to-cell interactions that enable death receptor aggregation (Adams, Totpal et al. 2008). Other studies have shown drozitumab to be effective against multiple rhabdomyosarcoma cell lines and established xenografts, an effect attributed to high DR5 expression in these cell lines (Kang, Chen et al. 2011). Further, drozitumab has demonstrated efficacy across a panel of breast cancer cell lines, with no effect on normal human primary osteoblasts, fibroblasts or mammary epithelial cells (Zinonos, Labrinidis et al. 2009). The same study characterised drozitumab *in vivo*, showing it caused complete regression of advanced mammary tumours and inhibited osteolysis in a metastatic model of breast cancer. The limited clinical data suggests that drozitumab is well tolerated in patients with solid and haematological malignancies, and is able to prolong stable disease in patients with advanced cancer (Camidge 2008). The promising *in vivo* results from curcumin and TRAIL combination studies provide a strong foundation for studies investigating the combination of curcumin and drozitumab.

1.7: THESIS OBJECTIVES

Taken together, this literature review highlights a number of gaps in knowledge pertaining to curcumin use in prostate cancer. First, there is no understanding of curcumin action in prostate fibroblasts. Given the outlined role of fibroblasts in prostate cancer initiation and progression, an appreciation for how curcumin may affect these cells is critical. The aim of Chapter 3 is therefore to compare and contrast the mechanisms of curcumin action in prostate epithelial cells and prostate fibroblasts. This will be approached in terms of cell viability and cell cycle arrest, androgen signalling and global gene expression analysis. Second, little is understood about curcumin tolerance or resistance, and nothing is known about these phenomena in prostate fibroblasts. Likewise, the impact of drug-tolerant or -resistant fibroblasts on cancer cells has seldom been characterised. Curcumin is already being used in humans and it is therefore imperative to understand not only the likelihood of curcumin tolerance or resistance but also any potential implications associated with them. The aim of Chapter 4 is therefore to characterise the development and mechanisms of curcumin tolerance or resistance in prostate fibroblasts. Potential implications of any tolerance or resistance will be explored in terms of androgen signalling in fibroblasts and effects on prostate cancer cells in co-culture with fibroblasts. Finally, clinical trial outcomes have led to the realisation that curcumin has a poor bioavailability profile. This warrants combination studies where curcumin may enhance the efficacy of other therapeutics. The aim of Chapter 5 is therefore to investigate the ability of curcumin to enhance efficacy of the monoclonal antibody drozitumab both *in vitro* and *in vivo*.

CHAPTER 2

MATERIALS AND METHODS

2.1: MATERIALS

Reagent	Supplier
2-mercaptoethanol	Sigma Aldrich
5α-dihydrotestosterone	Sigma Aldrich
96-well micro-plate reader	BioRad Laboratories
Anti-Annexin V-APC conjugated	BD Biosciences
Anti-AR(N-20) rabbit polyclonal	Santa Cruz
Anti-BRCA1 (C-20) rabbit polyclonal	Santa Cruz
Anti-CDK1 rabbit polyclonal	Bethyl Laboratories
Anti-DR5 rabbit polyclonal	Imgenex
Anti-FKBP51 (H-100) rabbit polyclonal	Santa Cruz
Anti-Gadd45α rabbit polyclonal	Cell Signaling Technology
Anti-GAPDH mouse monoclonal	Millipore
Anti-HMOX1 mouse monoclonal (IHC)	Enzo Lifesciences
Anti-HMOX1 rabbit polyclonal (WB)	Proteintech
Anti-Ki67 mouse monoclonal	Dako
Anti-Lamin A/C rabbit polyclonal	Cell Signaling Technology
Anti-Mek1 rabbit polyclonal	Thermo Scientific
Anti-p21 rabbit polyclonal	Cell Signaling Technology
Anti-p53 mouse monoclonal	Santa Cruz
Anti-PCNA rabbit polyclonal	Bethyl Laboratories
Avidin-Biotin blocking kit	Life Technologies
Bicalutamide	Sigma Aldrich
Bioruptor sonication system	Diagenode
Bradford protein dye reagent	BioRad Laboratories
Bromophenol blue	Sigma Aldrich
CFX 96-well real-time PCR detection system	BioRad Laboratories
CFX manager version 2.1	BioRad Laboratories
Complete protease inhibitor cocktail tablets	Roche Applied Science
Corel draw graphics suite version X5	Corel Corporation
Corn oil	Sigma Aldrich
Curcumin (98% pure)	LKT Laboratories
Deoxycholate	Sigma Aldrich
Dimethyl sulfoxide	Sigma Aldrich
Drozitumab	Genetech
ECL western blotting detection reagent	GE Lifescience
EDTA	Sigma Aldrich
Electronic callipers	Mitutoyo
Endnote version X6	Thomson Reuters
Entellen	Merck Millipore

Ethanol (molecular biology grade)	Sigma Aldrich
FacsCanto II	BD bioscience
Fetal calf serum	Sigma Aldrich
FlowJo version 10	Treestar Inc
FLUOStar optima luminometer	BMG Labtech
Formalin (10% neutral buffered)	Fronine Laboratory Supplies
GeNorm	Biogazelle
Glass coverslips	Thermo Scientific
Glycerol	Sigma Aldrich
Glycine	Sigma Aldrich
Goat anti-human IgG $F_c\gamma$ fragment	Jackson Laboratories
GraphPad statistical software version 6	GraphPad Software Incorporated
Haematoxylin (Gill's No. 2)	Sigma Aldrich
Hydrogen peroxide	Sigma Aldrich
Igepal	Sigma Aldrich
Image J version 1.47	National Institute of Health
iQ SYBR green supermix	BioRad Laboratories
iScript cDNA synthesis kit	BioRad Laboratories
Isofluorane	Faulding Pharmaceuticals
Isopropanol	Ajax Finechem
IVIS 100 imaging system	Xenogen
LAS4000 imaging system	GE Healthcare
Lipofectamine LTX with Plus reagent	Life Technologies
Lithium chloride	Sigma Aldrich
Living image version 2.50.1	Calliper Lifesciences
Luciferase assay system	Promega Corporation
Luria broth	Sigma Aldrich
Magnesium sulphate	Sigma Aldrich
Matrigel-HC	BD Bioscience
Methanol	Ajax Finechem
Microscope	Olympus CX41
Microtome	Microm
Microwave	Panasonic
Mini protean tetra cell	BioRad Laboratories
Mini protean TGX precast gels	BioRad Laboratories
Monosodium phosphate	Sigma Aldrich
MTT reagent	Sigma Aldrich
NanoDrop 1000 spectrophotometer	NanoDrop Technologies
Nanozoomer digital slide scanner	Hamamatsu
NDP Scan software	Hamamatsu
Needles (25G)	Becton Dickinson
Normal horse serum	Sigma Aldrich
Normal rabbit IgG	Santa Cruz
Nuclease-free water	Applied Biosystems
Passive lysis buffer (5X)	Promega Corporation

Penicillin-streptomycin	Sigma Aldrich
Phenol chloroform isoamyl alcohol	Sigma Aldrich
Phenol red-free RPMI-1640 culture medium	Life Technologies
Phosphatase inhibitor cocktail	Roche Applied Science
Phosphate buffered saline	Life Technologies
Precision plus protein kaleidoscope standards	BioRad Laboratories
Propidium iodide	Sigma Aldrich
Propidium iodide (filter sterilised)	BD Biosciences
Protein G sepharose 4 fast flow	GE Healthcare
Proteinase K	Sigma Aldrich
QIAprep spin miniprep kit	QIAGEN
RNeasy spin kit	QIAGEN
RPMI-1640 culture medium	Life Technologies
Skim milk powder	Diploma
Sodium bicarbonate	Sigma Aldrich
Sodium chloride	Sigma Aldrich
Sodium dodecyl sulphate	Sigma Aldrich
Sodium phosphate dibasic	Sigma Aldrich
Sterilisation filters (0.2 µm)	Pall Corporations
Superfrost plus glass slides	Thermo Scientific
Syringe	Becton Dickinson
Thermal cycler	MJ Research
Tissue processing cassettes	Sigma Aldrich
Trans-blot turbo mini nitrocellulose transfer packs	BioRad Laboratories
Trans-blot turbo transfer system	BioRad Laboratories
Transfer RNA	Sigma Aldrich
Tri-sodium citrate dihydrate	Sigma Aldrich
Tris	Sigma Aldrich
Triton-X 100	Sigma Aldrich
Trypan blue	Sigma Aldrich
Trypsin-EDTA	Life Technologies
Tween 20	Sigma Aldrich
Ultra-pure water	Millipore
Universal LSAB+ Kit	Dako
Vector NTi computer suite	Life Technologies
Venny	BioInfoGP (J.C. Oliveros)
Whatman filter paper	Whatman International
Xylene	Sigma Aldrich
Z-VAD-fmk	Calbiochem

2.2: BUFFERS AND SOLUTIONS

Acid Alcohol

Concentrated HCl	1 mL
EtOH	99 mL

5% Blotto

Skim milk powder	5 g
TBST	95 mL

Dilute to 1 or 3% as required.

10×Citrate buffer (0.1 M)

$C_6H_5Na_2O_72H_2O$	29.4 g
→ pH to 6	
RO H_2O	Make up to 1 L

Solution diluted to 1× (10 nM) prior to use.

3% Normal Horse Serum

NHS	3 mL
PBS	97 mL

6×protein loading dye

Tris-Cl/SDS	7 mL
SDS	1 g
Glycerol	3 mL
2-mercaptoethanol	600 µL
Bromophenol blue	1.2 mg

20×PBS (0.2 M)

$Na2HPO_4$	21.8
$NaH2PO_4$	6.4
NaCl	180
→ pH to 7.4	
RO H_2O	Make up to 1 L

Solution diluted to 1× (20 mM) prior to use.

RIPA lysis buffer

Tris	0.79 g
NaCl	0.9 g
→ pH to 7.4	
Triton X-100	1 mL
100 mM EDTA	1 mL
RO H_2O	Make up to 100 mL

Add 2 protease inhibitor tablets

10×Running buffer

Tris	30.3 g
Glycine	144 g
SDS	10 g

RO H_2O	Make up to 1 L

Scott's Water

$NaHCO_3$	20 g
$MgSO_4$	3.5 g
RO H_2O	Make up to 1 L

10×TBS (pH 7.4)

Tris	60.6 g
NaCl	87.6 g
→ pH to 7.4	
RO H_2O	Make up to 1 L

TBS + Tween 20 (TBST)

TBS	2.5 L
Tween 20	5 mL

4×Tris-Cl/SDS

Tris-Cl	3.025 g
→ pH to 6.8	
SDS	0.2 g
RO H_2O	Make up to 50 mL

0.01% Trypan Blue

Trypan blue	100 µL
PBS	10 mL

ChIP Dilution Buffer

10% Triton X-100	1100 µL
10% SDS	10 µL
500 mM EDTA pH 8.1	24 µL
500 mM Tris-HCl pH 8.1	334 µL
5M NaCl	334 µL
100×Protease Inhibitor	100 µL
RO H_2O	8098 µL

ChIP Elution Buffer

10% SDS	1000 µL
1 M $NaHCO_3$	1000 µL
RO H_2O	8000 µL

ChIP High Salt Immune Complex Wash Buffer

10% SDS	100 µL
10% Triton X-100	1000 µL
500 mM EDTA pH 8.1	40 µL
500 mM Tris-HCl pH 8.1	400 µL
5M NaCl	1000 µL
RO H_2O	7460 µL

ChIP LiCl Immune Complex Wash Buffer

1 M LiCl	4000 µL
10% Igepal CA-630	1000 µL
10% Deoxycholate	1000 µL
500 mM EDTA pH 8.1	20 µL
500 mM Tris-HCl pH 8.1	200 µL
RO H_2O	3780 µL

ChIP Low Salt Immune Complex Wash Buffer

10% SDS	100 µL
10% Triton X-100	1000 µL
500 mM EDTA pH 8.1	40 µL
500 mM Tris-HCl pH 8.1	400 µL
5 M NaCl	300 µL
RO H_2O	8160 µL

ChIP SDS Lysis Buffer

10% SDS	1000 µL
500 mM EDTA pH 8.1	200 µL
500 mM Tris-HCl pH 8.1	1000 µL
100×Protease Inhibitor	200 µL
RO H_2O	7600 µL

ChIP TE pH 8.1

500 mM EDTA pH 8.1	200 µL
500 mM Tris-HCl pH 8.1	20 µL
RO H_2O	9780 µL

2.3: GENERAL METHODS

2.3.1: Cell culture

Cell lines

The cell lines used throughout this thesis are detailed below. All cell lines were maintained in RPMI-1640 media containing 1% penicillin-streptomycin at 37^{O}C with 5% CO_2. All procedures involving cell lines were performed under aseptic conditions in a laminar flow cabinet. All experiments were plated and treated using RPMI-1640 containing the percentage of fetal calf serum (FCS) detailed below, unless otherwise stated in individual chapter methods. Phenol red-free (PRF) RPMI-1640, with or without dextran-coated charcoal FCS (DCC-FCS), was used for experiments treated with hormone or measuring curcumin uptake.

Cell Line	Origin	AR	Supplier	FCS
LNCaP	Lymph node metastasis of a 50 year old male with prostate adenocarcinoma	+	ATCC	10%
C4-2B	Derived from sub-cutaneous LNCaP xenografts in castrated nude mice	+	Chung, LW, University of Texas	5%
PC-3	Bone metastasis of a 62 year old male with prostate adenocarcinoma	-	American Type Culture Collection	5%
PShTert-AR	Telomerase immortalised human prostate myofibroblast expressing AR	+	Lee, PL, New York University	5%
PShTert-ctrl	Telomerase immortalised human prostate myofibroblast expressing empty vector	-		

Table 2.1: Origin, supplier and growth conditions of the cell lines used in this thesis.

PShTert-AR and PShTert-ctrl fibroblasts were derived from prostate with benign prostatic hyperplasia, and have been described previously (Li, Li et al. 2008). Long-term vehicle-treated (LTV) or long-term curcumin-treated (LTC) fibroblasts were generated by culturing PShTert-AR fibroblasts in escalating doses of DMSO (0.025 to 0.06%) or curcumin (5 μM increments up to 30 μM) over a period of 12 weeks. These fibroblasts were maintained as per PShTert-AR fibroblasts. Luciferase-expressing PC-3 cells (PC-3-luc) were generated in Professor Andreas Evdokiou's laboratory using the retroviral expression vector SFG-NES-TGL, giving rise to a single fusion protein encoding herpes simplex virus thymidine kinase, GFP and firefly luciferase (luc). Briefly, virus particle-containing supernatants were generated from cultured HEK-293 cells transfected with a viral vector, filtered to remove any cellular debris and then used to transduce PC-3 cells as described previously (Zannettino, Rayner et al. 1996, Labrinidis, Diamond et al. 2009). The retrovirally-transduced cells were grown as bulk cultures for 48 h and subsequently sorted for positive GFP expression using fluorescent-activated cell sorting (FACS). Positive cells were allowed to proliferate and the 10% of cells expressing the most GFP were obtained by FACS to generate the sub-line PC-3-luc.

Passaging cells

Cell lines were maintained in T75 or T150 sterile tissue culture flasks and were passaged at regular intervals, or when cells were approximately 80 to 90% confluent. Culture medium was aspirated from the flasks and cells were washed with 5 to 10 mL 1×PBS. PBS was aspirated, 1.5 mL (T75) or 3 mL (T150) 1×trypsin-EDTA was added and cells were incubated at 37^{o}C for approximately 1 min, or until cells had detached. An equal volume of RPMI-1640 medium containing 5% FCS was added and the cell suspension centrifuged at 1500 rpm for 5 mins. The supernatant was aspirated, the cell pellet resuspended in an appropriate volume of RPMI-1640 medium and cells were counted manually using a haemocytometer. Cells were either passaged into a new flask with fresh RPMI-1640 medium containing FCS or plated into the appropriate culture plate at the specific density indicated for each experiment.

Freezing and thawing cells

Cells were harvested, washed and centrifuged as outlined above, and were gently resuspended in freezing mix prepared using 65% FCS, 25% RPMI-1640 and 10% DMSO. A confluent T75 flask was divided into three 1 mL cryovials and a confluent T150 flask was divided into six 1 mL cryovials. Cryovials were placed into a controlled rate freezing unit containing isopropanol at -80^{o}C overnight followed by long-term storage in liquid nitrogen. Stored vials containing frozen cell lines were removed from liquid nitrogen and slowly thawed in a 37^{o}C water bath. Cells were added to 9 mL pre-warmed RPMI-1640 containing 5% FCS in a 15 mL tube and centrifuged at 1500 rpm for 5 mins. The supernatant was aspirated, the cell pellet was resuspended in fresh medium and cells were plated into a T25 culture flask containing RPMI-1640 and FCS.

Drug stocks and treatments

Curcumin powder was dissolved in molecular biology-grade DMSO and kept as a 50 mM stock in the dark. 5α-dihydrotestosterone (DHT) was dissolved in molecular biology-grade ethanol and was kept as a 10 mM stock at -20^{o}C. Drozitumab was dissolved in 0.5 mol/L arginine succinate, 20 mmol/L Tris and 0.02% Tween 20 (pH 7.2) and was kept at -80^{o}C. Affinity-pure goat anti-human IgG $F_c\gamma$ fragment was kept at 4^{o}C and ZVAD-fmk was kept at -20^{o}C. Drugs were prepared freshly for each experiment in RPMI-1640 medium. Preparation of drozitumab required a 1:1 dilution with IgG $F_c\gamma$ fragment followed by 30 min incubation at 4^{o}C prior to use. Cells were treated 24 to 48 h after seeding, and treatment volumes were 100 µL per well (96-well plate), 1 mL per well (24-well plate) or 2 mL per well (6-well plate).

2.3.2: Cell proliferation and viability assays

Trypan blue dye exclusion assay

Cell proliferation was assessed at required time points using the trypan blue dye exclusion method, and was conducted in technical quadruplicate using 24-well plates. Trypan blue selectively stains dead cells due to their porous membrane. For proliferation assays, the culture medium from each well was removed and placed in a 15 mL clear tube. Cells were washed with 0.5 mL PBS per well, which was then removed and placed in the corresponding tube. Cells were trypsinised using 250 µL trypsin-EDTA per well for 1 min at 37^{o}C. After ensuring all cells had detached from the plate, 250 µL RPMI-1640 medium (containing 5% serum) was added to the well and the cell suspension was then transferred into the corresponding tube. A further 250 µL PBS was used to wash the well and collect any remaining cells, before the tubes were centrifuged at 1500 rpm for 5 mins. The supernatant was carefully aspirated and the cell pellet resuspended with 50 to 500 µL RPMI-1640 medium, depending on cell confluency. A volume of cell suspension was added to an equal volume of 1×trypan blue in a 96-well round bottom plate and 10 µL of this mix was placed onto a haemocytometer and manually counted.

MTT assay

Cell viability was assessed at the required time points using the MTT assay, and was conducted in at least technical quadruplicate using 24- and 96-well plates. The MTT assay is a colorimetric assay utilising cellular mitochondrial activity (via the amount of oxido-reductase enzyme) as a measure of cell viability. These enzymes are capable of reducing the tetrazolium dye MTT to its insoluble formazan, which is purple in colour. The amount of insoluble formazin dye released by cells is directly proportionate to cell number, and whilst MTT is theoretically a measure of mitochondrial metabolism, many peer-reviewed articles and biotechnology companies refer to it as a measure of cell viability. As such, the term cell viability will be used throughout this thesis. The MTT reagent was made up by placing 2.5 mg MTT powder into 10 mL serum-free PRF RPMI-1640 medium and pre-warming to 37^{o}C. Culture medium was aspirated from each well and replaced with either 100 µL (96-well plate) or 500 µL (24-well plate) MTT reagent. Cells were incubated at 37^{o}C for 2 h. Following incubation, MTT reagent was aspirated and replaced with 100 or 500 µL DMSO and gently shaken until all dye was released. For experiments conducted in 24-well plates, the DMSO was pipetted into a 96-well plate, and plates were scanned at 570 nm using a plate reader.

2.3.3: Preparation of plasmid DNA

Expression vectors

The three expression vectors used in this thesis were pCMV-AR3.1 (8081 base pairs), pGL4.14-PB3Luc (6530 base pairs) and enhanced GFP (eGFP; 3798 base pairs). pCMV-AR3.1 contains the entire coding

sequence of the human wild-type AR cDNA cloned into the Eco RI restriction sites of the pCMV3.1 parental expression vector, under control of the cytomegalovirus (CMV) promoter, and has been described previously (Buchanan, Craft et al. 2004, Butler, Centenera et al. 2006, Need, Scher et al. 2009). pGL4.14-PB3Luc is an AR reporter construct containing luciferase linked to three copies of the androgen-responsive minimal rat probasin promoter, ligated to the thymidine kinase enhancer element. The eGFP construct was created in Professor Eric Gowan's laboratory by insertion of eGFP into the pVAX1 vector (commercially available from Life Technologies), under control of a CMV promoter.

Transformation of chemically competent cells

Chemically competent DH5α cells (100 µL frozen aliquot) were thawed on ice for 10 mins and transferred to an ice-cold 1.5 mL tube. Approximately 10 ng plasmid DNA was added to the cells and incubated on ice for 20 mins. Cells were then heat shocked at 42^{O}C for 45 secs and incubated on ice for a further 2 mins, before 400 µL luria broth (LB) medium was added to the cells and the mixture was incubated at 37^{O}C for 1 h on an orbital shaker at 225 rpm. Following incubation, 200 µL of culture was spread onto LB agar plates containing 100 µg/mL ampicillin and incubated overnight at 37^{O}C.

Isolation of plasmid DNA from bacterial cultures

Bacterial cultures were prepared by inoculation of 5 mL LB medium containing 100 µg/mL ampicillin with a single colony transformed according to the method described above. These cultures were grown for 16 h at 37^{O}C on an orbital shaker at 225 rpm. Plasmid DNA was prepared using the QIAprep miniprep kit according to the manufacturer's instructions. The DNA was eluted in 50 µL TE buffer (pH 8) and quantified using the Nanodrop 1000 spectrophotometer.

2.3.4: Transfection

Transfections were conducted in technical sextuplet using 96-well plates, unless otherwise stated. Cells were plated in RPMI-1640 medium containing FCS and were incubated for 24 h. Prior to transfection, cells were washed with serum-free PRF RPMI-1640 medium. Transfection was performed for 4 h in the same medium with the appropriate DNA plasmids mixed with Lipofectamine LTX (0.4 µL per well) and Plus reagent (0.1 µL per well), according to the manufacturer's instructions. Following transfection, the reaction mix was carefully removed and cells were overlaid with the appropriate treatment, made up in PRF RPMI-1640 containing 5% DCC-FCS, for 20 h. Following removal of treatment medium, cells were lysed using 30 µL 1×Passive Lysis buffer per well with 10 mins orbital shaking and overnight storage at -80^{O}C. To assess luciferase activity, plates were thawed on ice and 10 µL from each well was transferred to an opaque 96-well plate and read for reporter activity with the luciferase assay system using a FLUOstar optima luminometer. Remaining sample was pooled into respective treatment groups

and cleared via centrifugation at 10,000 rpm for 10 mins at 4^{O}C. Lysate was transferred to new, ice-cold tubes and stored at -80^{O}C until required for immunoblot analysis.

2.3.5: Flow cytometry

All flow cytometry-based assays were conducted in at least technical duplicate using 6-well plates.

Uptake assays

For the luminometer-based method, cells were treated and then washed twice in ice-cold PBS. Next, 400 µL ice-cold methanol was added to each well and cells were harvested using a cell scraper and lysed using a 1 mL syringe fitted with 25-gauge needle. This process was performed as quickly as possible to ensure minimal methanol evaporation. Lysates were transferred to an opaque walled, clear-bottomed 96-well plate and fluorescence was read on a FLUOstar optima luminometer under the following conditions: excitation filter 420 nm; emission filter 540 nm; bottom reading; 4 mm orbital scan; 5 scans per well (Harada, Pham et al. 2011). Vehicle control-treated samples were used to measure background fluorescence. For the flow cytometry-based uptake method, cells were treated, washed twice in 1 mL ice-cold PBS and harvested in 500 µL trypsin-EDTA. Following detachment, 500 µL RPMI-1640 containing 5% FCS was added to the well and the cell suspension pipetted into an ice-cold 15 mL tube. Each well was washed with 1 mL ice-cold PBS to collect any remaining cells and the cell suspension was centrifuged at 1,500 rpm for 5 mins at 4^{O}C. Supernatant was removed and cells were washed again in 1 mL ice-cold PBS. Following centrifugation and removal of PBS, cells were fixed in ice-cold 70% ethanol with gentle vortexing. Cells were analysed immediately for green fluorescent intensity using the FITC channel on a FacsCanto II running DIVA software. All steps of the uptake protocols were performed in the dark.

Cell cycle analysis

Cells were treated, washed, harvested and fixed as described above, and stored at -20^{O}C overnight. The following day, fixed cells were washed in PBS twice before being incubated in 50 µg/mL propidium iodide (PI), 40 µg/mL RNAse A and 0.1% Tween 20 in PBS for 2 h in the dark. Cell cycle analysis was conducted using the FacsCanto II running DIVA software. DNA frequency histograms were obtained in FlowJo using the Dean-Jett-Fox model.

Annexin/PI assay

Following treatment, cells were washed and harvested as described above, and stained with 0.25 µg annexin V-APC and 0.1 µg PI per sample on ice for 15 mins. Fluorochrome compensation was conducted using unstained, healthy cells and single stained (annexin V or PI only) apoptotic cells. Apoptosis was induced by heating cells to 43^{O}C for 60 mins (Stankiewicz, Lachapelle et al. 2005).

Analysis was conducted using the FacsCanto II running DIVA software. FlowJo software was used to determine percentages of Annexin V^+/PI^- cells (apoptosis) and Annexin V^-/PI^- (healthy cells).

2.3.6: Immunoblot

Lysate preparation

Cells for immunoblot analysis were harvested using trypsin-EDTA as described in Section 2.3.1, and resuspended in 150 µL ice-cold RIPA buffer with added protease inhibitors. Lysates were passed through cold 1 mL syringes fitted with a 25G needle at least 5 times before being centrifuged at 10,000 rpm for 10 mins at 4^OC. Supernatant was collected, placed into a clean, ice-cold 1.5 mL tube and stored at -80^OC until required.

Bradford protein assay

Protein was quantified using the Bradford protein assay in a 96-well plate. This method involves the addition of a dye which binds to basic and aromatic amino acid residues. Upon binding of proteins, there is a corresponding change in dye colour. For each protein sample, 1 µL lysate was mixed with 159 µL water in technical duplicate. Protein standards were prepared in duplicate using increasing concentrations of 1 to 16 µg/mL BSA (to a final volume of 160 µL with water). To each protein sample, 40 µL Bradford reagent was added and carefully pipetted up and down to mix reagents. Samples were incubated at room temperature (RT) for 5 mins before being read on a micro-plate reader at 595 nm. A standard curve was created by plotting the increasing BSA concentrations against their respective values, thus allowing determination of the unknown sample concentration. Once quantified, the appropriate volume of protein equivalent to 20 to 50 µg per sample was added to a new tube on ice. An appropriate volume of 6×loading dye was then added to the lysate, and the remainder of volume was completed with water (a total volume of 15 µL for 15-well gels and 30 µL for 10-well gels). Samples were placed on a heating block at 95^OC for 5 mins to denature protein and stored at -20^OC until required.

Electrophoresis and transfer

Samples were loaded into either a 10-well or 15-well 4 to 15% gradient TGX Stain-Free precast gel, set up in a Mini Protean Tetra Cell. The first lane of each gel was loaded with 10 µL Precision Plus Protein Kaleidoscope Standard molecular weight marker. Proteins were electrophoresed in 1×running buffer at 150 volts for approximately 30 mins. Protein was transferred using the Trans-Blot Turbo Transfer System and the Trans-Blot Turbo Mini Nitrocellulose transfer packs, according to the manufacturer's instruction (1.3 amps for 3 to 10 mins).

Antibody incubations

Following transfer, Ponceau S stain was used to confirm efficient transfer of proteins. After extensive washing in water to remove the Ponceau S stain, membranes were blocked in TBST containing 5% skim milk powder for 1 h. This was followed by incubation with a primary antibody overnight and then the appropriate HRP-conjugated secondary antibody for 1 hr, each diluted in TBST containing 1% skim milk powder. Membranes were washed three times for 5 mins in TBST following incubation with each antibody. All steps were performed with gentle rotation at RT, except for overnight incubations which were performed at 4^{O}C. Bound antibody was visualised using ECL Western Blotting Detection Reagent according to the manufacturer's instructions, and exposed on a LAS4000 imager for the necessary time.

2.3.7: Quantitative real-time PCR

RNA isolation

Following treatment, cells were harvested and centrifuged as described in Section 2.3.1**,** followed by resuspension in 350 µL RLT lysis buffer from the RNeasy RNA isolation kit. This kit was then used to isolate RNA according to the manufacturer's instructions, which included an on-column DNA removal treatment using the RNase-free DNAse kit. Elution of RNA was performed with 35 µL nuclease-free water, before RNA was gently vortexed and placed on ice. Quantification and assessment of RNA quality was then performed using the Nanodrop 1000 spectrophotometer, and RNA was stored at -80^{O}C until required.

cDNA synthesis

The iScript cDNA synthesis kit was used for all cDNA reactions and was performed on 500 to 1000 ng RNA, according to the manufacturer's instructions. Briefly, each reaction was incubated at 25^{O}C for 5 mins, 42^{O}C for 30 mins and 85^{O}C for 5 mins using a thermal cycler. Control samples lacking either RNA or reverse transcriptase were included in the synthesis reactions. Following incubation, cDNA samples were diluted 1:10 (500 ng) or 1:20 (1000 ng) in nuclease-free water. Both neat and diluted cDNA were stored at -20^{O}C until required.

Primer design and efficiency

Primer sequences were designed using Vector NTi software and purchased from Geneworks (Thebarton, Adelaide). All sequences were created according to the following four criteria: length between 19 and 23 base pairs, melting temperature between 55^{O}C and 60^{O}C, G-C content between 35% and 65%, and amplicon length between 80 and 120 base pairs. All sequences were checked for specificity prior to ordering using Primer-BLAST (NCBI). Standard curves were performed on all new primers using a five-fold serial dilution of cDNA (1:5 to 1:3125), and primers were assessed again for

specificity (a single amplicon) and efficiency (90 to 110%) prior to use by qRT-PCR. All primer sequences are listed in Appendix B.

qRT-PCR reactions

The CFX96 Real-Time Detection System was used for all qRT-PCR reactions. A master-mix containing 5 µL SYBR green, 0.4 µL each of 20 µM forward and reverse primers and 2.2 µL nuclease-free water was prepared and deposited into each well, followed by 2 µL cDNA (10 µL reaction). All reactions were performed in technical duplicate with controls for exclusion of RNA and reverse transcriptase, and no template control (nuclease-free water and master-mix only). The cycling parameters were as follows: 95^{o}C for 3 mins, 40 cycles at 95^{o}C for 15 secs, 60^{o}C for 15 secs and 72^{o}C for 30 secs. The housekeeping genes *GAPDH* and *RPL32* were selected as the optimal normalisation controls following geNorm analysis of seven housekeeping genes (*ALAS1*, *GAPDH*, *HPRT*, *MRPL19*, *PPIA*, *RAC1* and *RPL32*). Gene expression was presented as relative to the geometric mean of *GAPDH* and *RPL32* unless otherwise stated, and shown as fold-change relative to the vehicle control. The 2-(ΔΔCT) method was used to analyse all qRT-PCR data.

2.3.8: Chromatin immunoprecipitation

Treatment, cross-linking and sonication

Cells were plated in RPMI-1640 containing 5% FCS, and were allowed to adhere for 24 h. Media was replaced with PRF RPMI containing 5% DCC-FCS for a further 24 h, and then cells were treated for 4 h. Treatment was aspirated and cells were fixed with 20 mL 1% formaldehyde in PBS for 10 mins at RT. Upon completion of the fixation process, formaldehyde was aspirated and fixed cells were washed twice with 20 mL ice-cold PBS. Following the washes, 500 µL ice-cold PBS containing protease inhibitor was added to the dish, and cells were scraped and transferred to an ice-cold 1.5 mL tube. Cells were pelleted by pulse spinning for 15 secs at RT. The supernatant was aspirated and 700 µL SDS lysis buffer was added to each tube. Tubes were incubated for 10 mins on ice. Sonication was then performed under the following conditions: five cycles of 30 secs maximum power followed by 30 secs break. The chromatin immunoprecipitation performed for this thesis was conducted by Mr Damien Leach.

Immunoprecipitation

Following sonication, all steps were performed on ice unless otherwise stated. A 20 µL aliquot of soluble chromatin was placed into a new 1.5 mL tube and stored at -20^{o}C for later use as the DNA input control. Next, a 200 µL aliquot of soluble chromatin was placed into a new 2 mL tube for the immunoprecipitation reaction. To each sample, 1800 µL ice-cold dilution buffer was added containing protease inhibitor and samples were vortexed. Protein G sepharose slurry beads were prepared by

washing the required volume of beads in an equal volume of 1×TE buffer (pH 8.1) three times, spinning gently and resuspending at a 1:1 ratio of beads to TE buffer. Using a cut tip to avoid damaging the beads, 45 µL of beads were added to the 2 mL tube with 200 µg tRNA to block non-specific interactions with the beads. Samples were placed on a rotator for 1 h at 4^{O}C and were then centrifuged at 13,000 rpm for 30 secs at 4^{O}C. The resulting supernatant was transferred to a new 2 mL tube. To each tube, 4 µg AR N-20 antibody was added. A normal rabbit IgG negative control was included for each lysate. Samples were incubated overnight at 4^{O}C with continual inversion of the samples.

Washes and reverse cross-linking

The following day, 45 µL of beads were added to each sample, as well as 200 µg tRNA. Samples were incubated on a rotator for 1 h at 4^{O}C to allow antibody-protein complexes to attach to the beads. Beads were pelleted with gentle centrifugation at 4^{O}C for 1 min. Supernatant was aspirated without dislodging the beads. Each sample was then washed for 5 mins at 4^{O}C on a rotator with 1 mL of the following ice-cold buffers in order, followed by gentle centrifugation at 4^{O}C for 1 min and removal of supernatant: low salt immune complex wash buffer (one wash), high salt immune complex wash buffer (one wash), lithium chloride immune complex wash buffer (one wash) and 1×TE buffer (pH 8.1, two washes). Following the washes, the beads were resuspended in 250 µL of freshly prepared elution buffer. The mixture was vortexed briefly and rotated for 15 mins at RT. Samples were then centrifuged at 13,000 rpm for 1 min at RT and supernatant was transferred to a new 1.5 mL tube. The elution step was repeated and eluates were combined, making a total of 500 µL. At this point, the 20 µL input samples were thawed and 480 µL elution buffer was added to each sample. Finally, 20 µL 5 M sodium chloride was added to each sample and vortexed. Samples were incubated at 65^{O}C overnight to reverse DNA-protein crosslinks.

Phenol chloroform purification and ethanol precipitation

The following day, 10 µL 500 mM EDTA (pH 8.1), 20 µL 1 M Tris-HCl (pH 6.5) and 1 µL RNAse were added to each sample and incubated at 37^{O}C for 90 mins. Following the incubation, 20 µg proteinase K was added to each sample, mixed by flicking and incubated at 55^{O}C for 1 h. Using a fume hood, 500 µL phenol chloroform was added to each sample and shaken vigorously by hand for 15 secs. Samples were allowed to incubate for 5 mins at RT to allow the mixture to settle. Samples were then centrifuged at 13,000 rpm for 10 mins at 4^{O}C. The top aqueous layer of the sample was transferred to a new tube, and 1 mL 100% ethanol and 40 µg glycogen were added to each tube and vortexed before samples were incubated at -20^{O}C overnight. The following day, samples were centrifuged at 13,000 rpm at 4^{O}C for 30 mins and the supernatant was carefully pipetted from the pellet. The pellet was washed in 500 µL 70% ethanol and vortexed to ensure pellet dislodgement from the tube. Samples were centrifuged again

at 13,000 rpm at 4^{O}C for 10 mins. Supernatant was carefully pipetted off and the pellet was air dried. Once dry, 100 µL of nuclease-free water was added to each pellet, vortexed and allowed to incubate at RT for 1 h. Samples were vortexed again and stored at -20^{O}C until required. qRT-PCR was performed as described in Section 2.3.7. Data was normalised to DNA input to control for uneven sample quantities and the non-specific binding region *NC2,* as described previously (Need, Selth et al. 2012). Data was not normalised to IgG as no binding activity was detected in these samples.

2.3.9: Immunohistochemistry

Preparation of tissues

Collected tissue was placed into cassettes and immersed in 10% neutral buffered formalin immediately after excision. Tissue was processed within a week of removal, embedded into paraffin and was cut at 6 µm sections onto super frost plus slides using a microtome. Prior to staining, slides were heated to 65^{O}C for approximately 15 mins or until wax had melted. Slides were de-waxed in xylene (3×5 mins), rehydrated in graded ethanol (100%, 90%, 70% and 50% for 5 mins each) and washed in PBS (2×3 mins).

Immunostaining

Slides were immersed in 10 mM sodium citrate buffer, and antigen retrieval was conducted using a microwave set on high power for 2.5 mins (or until boiling) followed by low power for 20 mins. On completion of antigen retrieval, slides were allowed to cool in sodium citrate buffer for a further 20 mins before being washed in PBS (2×3 mins). Endogenous peroxidase activity was quenched by incubation of slides in 3% hydrogen peroxide in 200 mL methanol for 10 mins at RT. Slides were then washed in PBS (2×3 mins), outlined with a PAP pen and endogenous avidin-biotin activity was blocked using an avidin-biotin blocking kit according to the manufacturer's instruction. Slides were washed in PBS thoroughly (3×5 mins) before being incubated with 3% normal horse serum for 1 h at RT in a humid chamber to block non-specific binding. Following blocking, slides were incubated in the primary antibody diluted in 3% NHS in a humid chamber overnight at 4^{O}C. The following day, slides were washed in PBS (2×3 mins) and biotinylated anti-mouse-rabbit-goat link (Universal LSAB+ HRP kit) was applied for 15 mins at RT. Following washes in PBS (2×3 mins), streptavidin-HRP (Universal LSAB+ HRP kit) was applied for a further 15 mins at RT. Slides were washed thoroughly in PBS (2×5 mins) before being incubated in DAB (Universal LSAB+ HRP kit) for exactly 1 min at RT. Slides were washed thoroughly in running tap water before being counterstained with haemotoxylin (3 dips). Slides were rinsed further in tap water before being dehydrated in graded ethanol (90% and 100%), cleared in xylene and cover slipped using entellin.

Haemotoxylin and Eosin

Slides were heated, de-waxed and rehydrated as described above, before being placed in haemotoxylin for 10 mins. Slides were then washed thoroughly in running water, stripped in 2 dips of 1% acid alcohol, washed again in running tap water and blued using Scott's water for 2 dips. Slides were washed again in running tap water before being placed in eosin for 2 dips. Slides were washed for a final time in running tap water before being rehydrated, cleared and cover-slipped as described above.

CHAPTER 3

CURCUMIN ACTION IN PROSTATE CANCER CELLS AND FIBROBLASTS

3.1: INTRODUCTION

Curcumin has become one of the world's most vigorously investigated natural compounds for cancer prevention and treatment. The anti-cancer activity of curcumin has been well characterised across a range of *in vitro* and *in vivo* cancer model systems, particularly colorectal, breast and pancreatic cancers. There has also been a moderate amount of research investigating the efficacy of curcumin for the prevention and treatment of prostate cancer. However the current literature relating to curcumin and the prostate is largely focussed on cancer cells, and the effect of curcumin on cells of the broader prostate microenvironment, such as fibroblasts, has not been comprehensively investigated.

The current understanding of curcumin action in fibroblasts is derived largely from studies of inflammatory disease. Scleroderma is a chronic auto-immune condition where fibroblasts are recruited and activated by cytokines and growth factors, leading to excessive collagen deposition and fibrosis. Curcumin has been shown to cause apoptosis in scleroderma lung fibroblasts while leaving normal lung fibroblasts unaffected (Tourkina, Gooz et al. 2004). This was attributed to the lack of heme oxygenase-1 (HMOX1) and glutathione s-transferase enzymes in synovial lung fibroblasts. The anti-fibrotic activity of curcumin in scleroderma fibroblasts has also been linked to inhibition of TGF-β signalling (Song, Peng et al. 2011). Synovial fibroblasts are potential therapeutic targets in rheumatoid arthritis due to their role in joint destruction. Curcumin was shown to reduce proliferation and increase apoptosis in these fibroblasts through G1-phase cell cycle arrest and inhibition of NF-κB signalling (Park, Moon et al. 2007). Curcumin has also been shown to down-regulate the clinical arthritis score in mice, partly by decreasing NF-κB transcriptional activity in fibroblast-like synoviocytes (Moon, Kim et al. 2010). Further, the curcumin derivative 2,6-bis(2,5-dimethoxybenzylidene)-cyclohexanone inhibited collagenase activity through suppression of MMP-1 and MMP-3, as well as NF-κB nuclear translocation and DNA binding (Lee, Abas et al. 2014). The evidence for curcumin-mediated inhibition of collagen synthesis is relatively strong, with this effect having also been shown in human keloid, lung and skin fibroblasts (Hu, Hu et al. 2008, Zhang, Huang et al. 2011, Ryu, Kim et al. 2012). Similarly to studies in epithelial cells, it appears NF-κB inhibition is also a central mechanism of curcumin action in fibroblasts. Interestingly, a recent study demonstrated that the curcumin derivative D6 induced both cell survival and death pathways in

human foreskin fibroblasts despite having no effect on proliferation or induction of apoptosis (Rozzo, Fanciulli et al. 2013). This raises the possibility that curcumin may affect various cell types differently.

Curcumin is already being widely used as a supplement as well as being the subject of three clinical trials for prostate cancer. It is therefore important to gain an understanding of how curcumin may affect cells of the prostate microenvironment, including its effect on AR in both epithelial and stromal compartments. In cancer cells, increased AR levels and function drive the production of PSA (KLK-3), tumour growth and resistance to hormonal therapies (Chen, Sawyers et al. 2008). In contrast, AR in fibroblasts is believed to contribute to prostate cancer initiation, despite low stromal AR levels being indicative of cancer progression and poor patient outcome (Henshall, Quinn et al. 2001, Ricciardelli, Choong et al. 2005, Yu, Yeh et al. 2012). Curcumin is known to target AR mRNA and protein in prostate cancer cells (Nakamura, Yasunaga et al. 2002); however its effect on fibroblast AR has not yet been investigated.

The overall aim of this chapter is to critically investigate the transcriptomic mechanisms of curcumin action in human prostate fibroblasts. This chapter also endeavours to compare the intracellular effects of curcumin in prostate fibroblasts and prostate cancer cells based on experiments conducted in this thesis, as well as publically available data. These comparisons include investigating how curcumin affects cell viability, AR function, gene expression and cell cycle arrest mechanisms. Finally, a model is proposed to explain the divergent curcumin responses to cell cycle arrest in prostate cancer cells and fibroblasts observed in this chapter.

3.2: MATERIALS AND METHODS

3.2.1: Cell culture and reagents

Human prostate cancer cells (LNCaP, PC-3 and C4-2B) and immortalised human prostate fibroblasts (PShTert-AR and PShTert-ctrl) were maintained as described in Section 2.3.1. Immortalised fibroblasts were chosen over primary fibroblasts due to both low levels and poorly functional AR in primary fibroblasts (Shaw, Papadopoulos et al. 2006, Cano, Godoy et al. 2007, Tanner, Welliver Jr et al. 2011). Curcumin and DHT were stored as described in Section 2.3.1. The data presented in this chapter was conducted on PShTert-AR fibroblasts treated with 0.06% DMSO (LTV fibroblasts, described in Section 2.3.1). These fibroblasts served as the control for the long-term curcumin-treated (LTC) fibroblasts studied in Chapter 4. The morphology and DHT-responsiveness of LTV fibroblasts remained comparable to the original PShTert-AR fibroblasts throughout the entire study. For simplicity, LTV fibroblasts will be referred to as PShTert-AR in this chapter. Some of the experiments were conducted at high doses of curcumin (30 μM). Whilst the dose of curcumin used in combination with DHT was relatively low (10 μM), a higher dose (30 μM) was used in some experiments assessing curcumin alone. This is not a physiologically relevant dose, but was chosen to study the acute effects of curcumin over a short time-frame. This dose did not severely affect reference genes GAPDH and RPL32 or β-actin protein expression over the time period that these experiments were conducted.

3.2.2: MTT assay

LNCaP, C4-2B and PC-3 cells (5×10^3 cells per well), and PShTert-AR and PShTert-ctrl fibroblasts (3×10^3 cells per well), were plated in RPMI-1640 containing FCS in 24-well plates and were allowed to adhere for 24 h. Culture medium was aspirated and cells were treated with vehicle control or 5 to 25 μM curcumin for 2 to 6 days. Cell viability was measured at D2, D4 and D6 by MTT assay as described in Section 2.3.2. Results are the average of 2 to 3 independent experiments. Non-linear regression analysis (log inhibitor versus normalised response) and IC_{50} calculations were performed using GraphPad Prism Software.

3.2.3: Transactivation assay

LNCaP, C4-2B and PC-3 cells (2.5×10^4 per well), and PShTert-AR and PShTert-ctrl fibroblasts (5×10^3 per well), were plated in RPMI-1640 containing FCS in 96-well plates and were allowed to adhere for 24 h. Culture medium was aspirated and cells were transfected in serum-free PRF RPMI-1640 containing 50 ng pGL4.14-PB3Luc per well either alone (C4-2B and PShTert-AR) or in combination with 5 ng pCMV-AR3.1 (PC-3 and PShTert-ctrl), as described in Section 2.3.4. Following transfection, cells were treated with PRF RPMI-1640 containing DCC-FCS and treatment (vehicle control or 0.01 to 100 nM DHT in the presence or absence of 10 μM curcumin) for 20 h, a time frame that has been optimised for

the assessment of DHT-mediated AR transactivation activity in prostate cancer cells previously (Buchanan, Craft et al. 2004). Luciferase activity was measured as described in Section 2.3.4. Results are the average of 2 to 3 independent experiments.

3.2.4: Flow cytometry

For flow cytometry-based uptake assays, C4-2B, PC-3, LNCaP, PshTert-AR and PShTert-ctrl cells were plated in RPMI-1640 containing FCS at a density of 2×10^5 cells per well in 6-well plates and were allowed to adhere for 24 h. Cells were treated with vehicle control or 25 µM curcumin in serum-free PRF RPMI-1640 for 10 mins. Results are the average of 4 to 5 independent experiments. For luminometer-based uptake assays, cells were plated and treated as described above for 0 to 60 mins. Cells were harvested and analysed as described in Section 2.3.5. For cell cycle analysis, LNCaP/C4-2B cells (3×10^5 cells per well) and PShTert-AR fibroblasts (5×10^4 cells per well) were plated in RPMI-1640 containing FCS into 6-well plates and allowed to adhere for 24 h. Cells were treated with serum-free PRF RPMI-1640 containing vehicle control or 30 µM curcumin for 16 h. Results are the average of 3 independent experiments. For Annexin/PI assays, PShTert-AR fibroblasts were plated in RPMI-1640 containing FCS at a density of 5×10^4 cells per well in 6-well plates and treated with vehicle control or 30 µM curcumin over a time course of 4 to 48 h. Results are representative of 3 independent experiments. For all flow cytometry experiments, cells were prepared and analysed as described in Section 2.3.5.

3.2.5: Quantitative real-time PCR

LNCaP (3×10^5 cells per well) or PShTert-AR (5×10^4 cells per well) were plated in RPMI-1640 containing FCS into 6-well plates. Cells were allowed to adhere for 24 h before being treated with RPMI-1640 containing FCS or PRF RPMI-1640 containing DCC-FCS and either (1) vehicle control or 0.1-1000 nM DHT for 16 h, (2) vehicle control, 10 nM DHT, 0.1 to 10 µM curcumin or the combination of 0.1 to 10 µM curcumin with 10 nM DHT for 16 h, (3) vehicle control, 10 nM DHT, 30 µM curcumin or the combination of DHT and curcumin for 16 h or (4) vehicle control or 30 µM curcumin for 4 to 16 h. The 16 h time frame was chosen for hormone experiments because the laboratory has previously shown this to be optimal for evaluating DHT-mediated changes to RNA and protein expression (Trotta, Need et al. 2012, Trotta, Need et al. 2013). The concentration of 1000 nM DHT was included in QPCR experiments to determine whether, as in prostate cancer cells, this dose was inhibitory to AR activity in PShTert-AR fibroblasts. RNA was extracted and cDNA synthesised as described in Section 2.3.7. Results are the average of 2 independent experiments and are normalised to *GAPDH* (1) or the geometric mean of *GAPDH* and *RPL32* (2-4). Primer sequences are listed in Appendix B.

3.2.6: Chromatin immunoprecipitation

PShTert-AR fibroblasts were plated in RPMI-1640 containing FCS into 15 cm sterile culture dishes at a density of 5×10^5 per dish and were allowed to adhere for 24 h. Media was replaced with PRF RPMI-1640 containing DCC-FCS for a further 24 h. Cells were treated using this media containing vehicle control, 10 nM DHT, 10 μM curcumin or the combination of DHT and curcumin for 4 h, a time frame which had previously been optimised for assessing DHT-mediated AR binding to DNA (Need, Selth et al. 2012). Chromatin immunoprecipitation was performed as described in Section 2.3.8. Results are the average of 4 independent experiments. Primer sequences are listed in Appendix B.

3.2.7: Immunoblot

LNCaP and PC-3 cells (3×10^5 cells per well) and PShTert-AR fibroblasts (5×10^4 cells per well) were plated in RPMI-1640 containing FCS into 6-well plates were allowed to adhere for 24 h. Cells were treated with vehicle control or 30 μM curcumin for 16 h. Lysate preparation and protein quantification was performed as described in Section 2.3.6. Membranes were probed with antibodies recognising BRCA1 (1:200), p53, Gadd45α, p21, CDK1, PCNA, HMOX1 (1:1000) and GAPDH (1:2000). Results are representative of 2 independent experiments. Where relevant, densitometry was performed using Image J.

3.2.8: Microarray analysis

PShTert-AR fibroblasts were plated in RPMI-1640 containing FCS at a density of 2.5×10^4 cells per well in 6-well plates for 48 h. Cells were treated with vehicle control or 30 μM curcumin for 4 to 16 h. RNA was extracted as described in Section 2.3.7. Triplicate RNA samples were pooled and sent to the Adelaide Microarray Centre to assess RNA integrity (Agilent bioanalyser) prior to being hybridised to Affymetrix GeneChip Human Gene 1.0 st Arrays. The pooling of RNA samples extracted from biological replicates has been shown to be statistically valid for gene microarrays, and helps to reduce the cost of these otherwise expensive experiments (Peng, Wood et al. 2003). Bioinformatics were performed by Dr Grant Buchanan in R using Bioconductor and the Limma package (Smyth, Michaud et al. 2005). Figures 3.5A and 3.5B were originally generated by Dr Buchanan in R and redrawn by Ms Giorgio using Corel Draw. Briefly, array data was normalised using RMA, filtered by mapped probes and an arbitrary minimum expression threshold (± 0.5 log fold change), and genes significantly affected over time identified by a Benjamini-Hochberg adjusted p-value of 0.05, determined from Bayesian linear regression modelling. Genes were segregated into eight profile categories by unanchored k-means clustering using R. The data presented in this chapter conform to MIAME guidelines, have been deposited in NCBI's Gene Expression Omnibus and are accessible through GEO series accession number GSE50618. Microarray results were validated using an independently extracted set of RNA

samples by qRT-PCR. Curcumin-affected genes at the 12 h time-point in PShTert-AR fibroblasts were compared to those published for LNCaP and C4-2B cells at 12 h (Thangapazham, Shaheduzzaman et al. 2008), and the overlap determined using Venny software. Gene pathway analysis was conducted using Ingenuity Pathway Analysis (IPA) software to predict enriched canonical pathways significantly altered by curcumin treatment.

3.3: RESULTS

3.3.1: Identification of qRT-PCR reference genes for curcumin-treated samples.

Curcumin targets a large number of molecules and signalling pathways within cells (Hasima and Aggarwal 2012). It was therefore important that appropriate reference genes were selected prior to performing qRT-PCR with curcumin-treated samples. PShTert-AR fibroblasts were treated with vehicle control or 30 µM curcumin for 4 to 16 h and the expression of well-established reference genes *MPRL19*, *ALAS1*, *HPRT1*, *PPIA*, *RAC1*, *GAPDH* and *RPL32* were analysed across the dataset by qRT-PCR. The most stable genes with the highest expression (lowest Ct values) in curcumin-treated PShTert-AR fibroblasts were *GAPDH* and *RPL32* (**Figure 3.1A**). GeNorm, a program that determines the most stable reference genes from a set of tested candidate reference genes in a given sample panel, confirmed that *GAPDH* and *RPL32* were the most stable genes and recommended using the geometric mean of these genes for normalization of qRT-PCR data (**Figure 3.1B**).

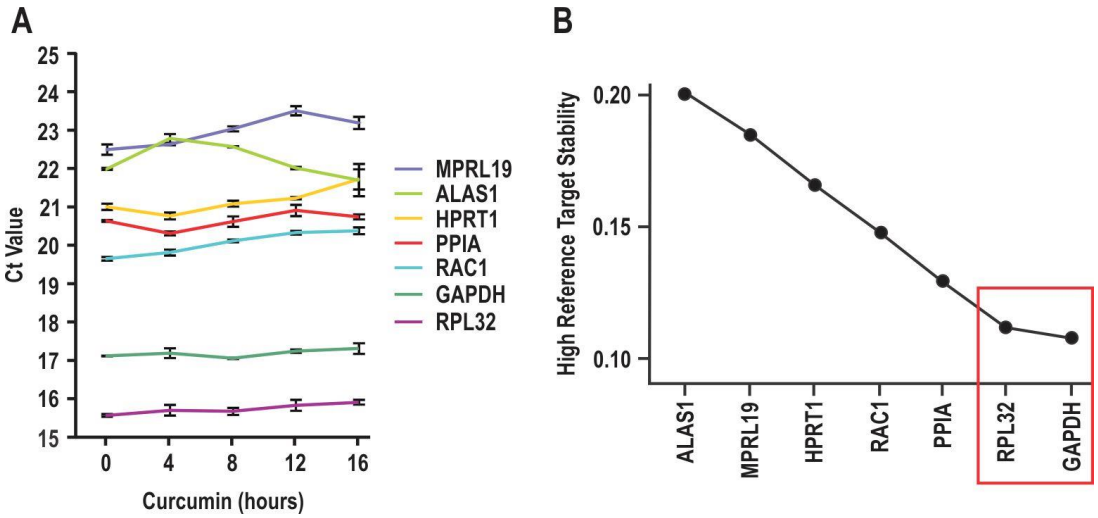

Figure 3.1: Identification of qRT-PCR reference genes for curcumin-treated samples. A: PShTert-AR fibroblasts were treated with vehicle control or 30 µM curcumin for 4 to 16 h and *MPRL19*, *ALAS1*, *HPRT1*, *PPIA*, *RAC1*, *GAPDH* and *RPL32* gene expression was assessed by qRT-PCR. Data is presented as mean expression (Ct value) ± SEM of triplicate samples. **B:** GeNorm analysis demonstrated *RPL32* and *GAPDH* were the most stable reference genes for future curcumin experiments.

3.3.2: The sensitivity of prostate epithelial and fibroblast cell lines to curcumin.

The literature presents mixed reports as to the curcumin sensitivity of different cell lines and lineages. Curcumin is often reported to be cancer cell-specific, leaving normal cells largely unaffected (Ravindran, Prasad et al. 2009). To compare the relative sensitivity of different prostate cells to curcumin, three epithelial (LNCaP, C4-2B and PC-3) and two fibroblast (PShTert-AR and PShTert-ctrl) cell lines were treated with 5 to 25 µM curcumin over a 6 day period. Curcumin inhibited the viability of all cell lines across each time-point in a dose-dependent manner (**Figure 3.2A**). To assess the relative effect of

curcumin on cell viability, the IC_{50} value was calculated for each cell line at each time-point using the non-linear regression function in GraphPad. These values were averaged across time-points and presented relative to PShTert-AR (**Figure 3.2B**). This method of presenting the data allowed comparison of the curcumin sensitivities of each cell line relative to the main cell type of interest, PShTert-AR. Interestingly, curcumin appeared to be more effective in reducing the viability of AR-negative cells (PShTert-ctrl and PC-3) compared to AR-positive cells (PShTert-AR, LNCaP and C4-2B). Specifically, PC-3 cells were significantly more sensitive to curcumin than PShTert-AR fibroblasts ($p<0.01$) and LNCaP cells ($p<0.05$). Further, PShTert-ctrl fibroblasts were more sensitive than LNCaP cells ($p<0.05$). In order to test the hypothesis that cells were differentially sensitive to curcumin via differences in cellular curcumin uptake, two assays were performed, both of which utilised the natural fluorescence of curcumin. Curcumin is reported to possess excitation and emission spectra of 405 nm and 470 to 600 nm respectively, making intracellular curcumin detectable in the FITC channel (Harada, Pham et al. 2011). In the first assay, PShTert-AR fibroblasts were treated with 25 μM curcumin (the highest dose from Figure 3.2A) for a time course of 0 to 60 mins. Following treatment, cells were lysed in methanol to release intracellular curcumin and the resulting fluorescence was measured using a luminometer. This experiment demonstrated that intracellular curcumin fluorescence peaked at approximately 10 mins post-treatment, and levels remained unchanged for up to 60 mins (**Figure 3.2C**). While this assay was effective when investigating curcumin uptake in one cell line, comparing multiple cell lines was not ideal due to variability in cell densities, which would potentially affect results. Further, the rapid evaporation of methanol made the assay technically difficult and did not allow time for testing multiple cell lines at once. Therefore to measure curcumin uptake across the five cell lines simultaneously, flow cytometry was performed. This assay was deemed more accurate to detect intracellular curcumin, as curcumin has previously been shown to localise in the cytoplasm of prostate cancer cells following treatment (Harada, Giorgio et al. 2013). To establish the optimal dosing range, PShTert-AR fibroblasts were treated with 10 to 50 μM curcumin for 10 mins, and mean FITC fluorescence was quantified. There was a linear relationship between the dose of curcumin and the mean fluorescence quantified (**Figure 3.2D**). The concentration of 25 μM was chosen for subsequent experiments as it fell within the linear range, meaning differences across cell lines could be readily quantified. Importantly, the level of fluorescence detected in vehicle-treated samples was very similar across cell lines. However at 25 μM curcumin, there were no significant differences in uptake between the five cell lines, even when individual cell line data was normalised to the respective vehicle control (**Figure 3.2E**).

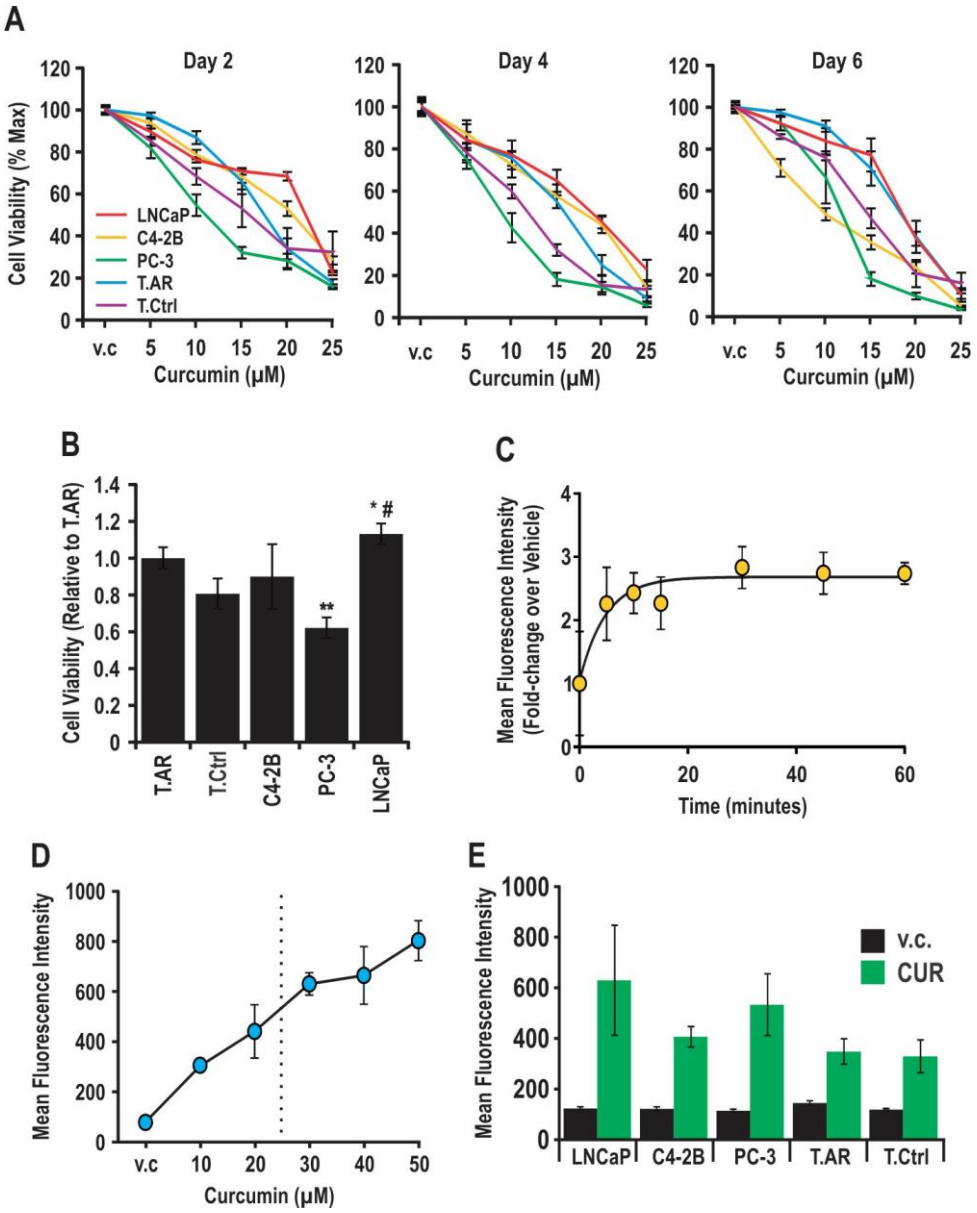

Figure 3.2: The sensitivity of prostate epithelial and fibroblast cell lines to curcumin. A: LNCaP, C4-2B, PC-3, PShTert-AR (T.AR) and PShTert-ctrl (T.Ctrl) cells were treated with vehicle control (v.c.) or 5 to 25 μM curcumin, and cell viability was measured by MTT assay at D2, D4 and D6. Data is presented as mean cell viability ± SEM relative to the maximal response of each cell line and is the average of 2 (LNCaP, T.Ctrl) or 3 (C4-2B, PC-3, T.AR) independent experiments. **B:** Using the data presented in Figure 3.2A, IC_{50} values were calculated for each cell line at each time point, averaged and presented relative to PShTert-AR. * $p<0.05$ PShTert-ctrl compared to LNCaP; ** $p<0.01$ PC-3 compared to PShTert-AR; # $p<0.05$ PC-3 compared to LNCaP (Unpaired *t*-test). **C:** PShTert-AR fibroblasts were treated with v.c. (60 mins) or 25 μM curcumin for 5 to 60 mins. Cells were lysed in methanol and analysed for green fluorescence at 420 nm on a luminometer. Data is presented as mean fluorescence intensity ± SEM relative to the v.c. and is the average of 4 independent experiments. **D:** PShTert-AR fibroblasts were treated with v.c. or 10 to 50 μM curcumin for 10 mins. Cells were analysed for green fluorescence using flow cytometry. Data is presented as mean fluorescence intensity ± SD of duplicate samples. **E:** LNCaP, C4-2B, PC-3, PShTert-AR (T.AR) and PShTert-ctrl (T.Ctrl) cells were treated with v.c. or 25 μM curcumin for 10 mins. Cells were analysed for green fluorescence using flow cytometry. No statistical significance was observed for all comparisons (Unpaired *t*-test). Data is presented as mean fluorescence intensity ± SEM and is the average of 4 (T.AR, T.Ctrl) or 5 (LNCaP, C4-2B, PC-3) independent experiments.

3.3.3: Effect of curcumin on AR transactivation in prostate epithelial cells and fibroblasts.

Given the previously reported inhibitory effects of curcumin on epithelial AR transactivation and gene expression (Nakamura, Yasunaga et al. 2002), the activity of AR in response to curcumin was compared between prostate cancer cells and fibroblasts. Transactivation assays were used to quantify the function of AR in endogenous (C4-2B), stably over-expressed (PShTert-AR) and transiently transfected (PC-3 and PShTert-ctrl) settings. LNCaP cells were not included in the transactivation assays because, given their poorly adhesive nature, the process of transfection, treatment and washing meant that there were few cells left to assay by the end of the experiment. In each cell line, curcumin significantly suppressed the AR response to DHT ($p<0.001$, **Figure 3.3A**). At 100 nM DHT, curcumin reduced DHT-mediated AR transactivation by 42.9 ± 3.7% (C4-2B), 76.4 ± 9.1% (PC-3), 59.0 ± 4.8% (PShTert-AR) and 68.6 ± 7.6% (PShTert-ctrl). Results for PShTert-ctrl fibroblasts were the average of 2 experiments (rather than 3) due to difficulty with transfection. Relatively lower luciferase values were recorded for this cell line, which may explain the higher basal AR transactivation activity. Curcumin had little effect on cell viability over the 20 h treatment period, as determined by concurrent MTT assays (**Figure 3.3B**). While there was a slight increase in C4-2B cell viability in response to DHT, this was unsurprising given that these cells are stimulated by androgen. Importantly, this experiment eliminated the possibility that decreases in AR transactivation activity were due to a decrease in cell viability. Further, curcumin treatment alone did not influence luciferase activity over vehicle control, also eliminating the possibility that curcumin impacts luciferase activity.

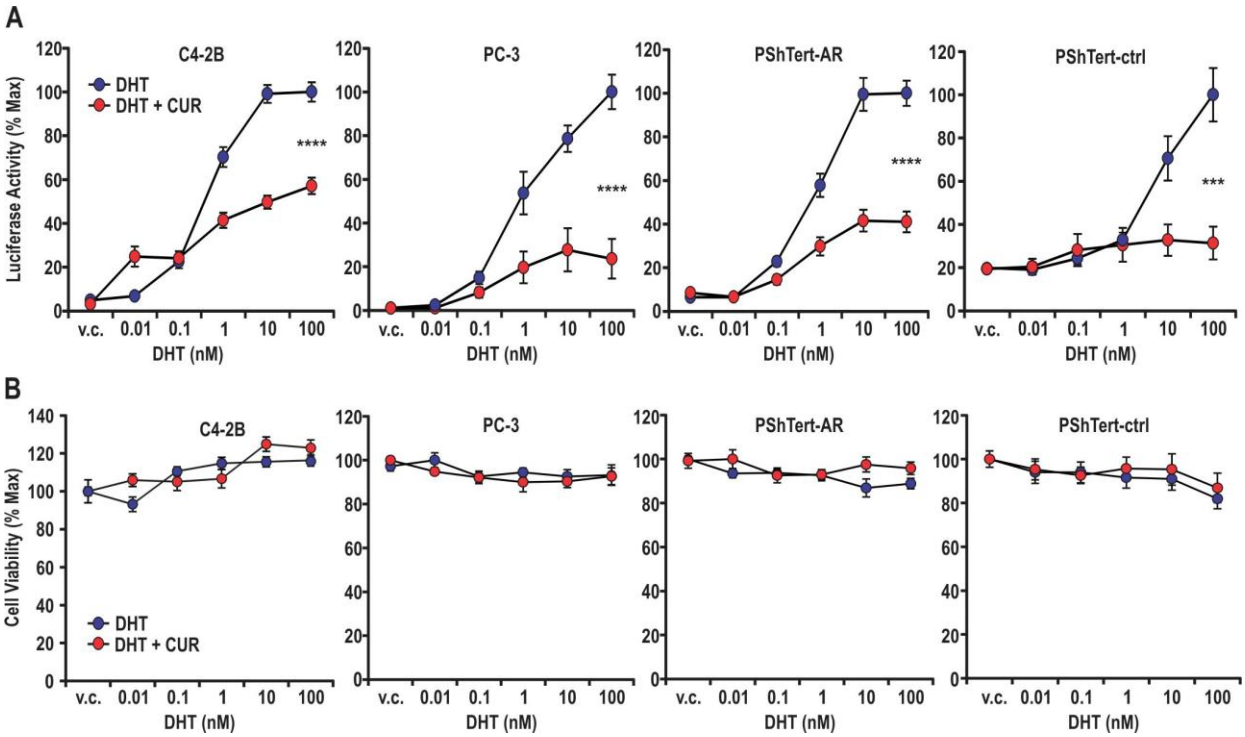

Figure 3.3: The effect of curcumin on AR transactivation activity in prostate epithelial cells and fibroblasts. A: C4-2B/PShTert-AR cells were transfected with 50 ng of androgen-responsive pGL4.14-PB3Luc and PC-3/PShTert-ctrl cells were transfected with 50 ng pGL4.14-PB3Luc and 5 ng pCMV-AR3.1. Cells were treated with vehicle control (v.c.) or 0.01 to 100 nM DHT alone or in combination with 10 µM curcumin (CUR) for 20 h. *** $p<0.001$, **** $p<0.0001$ DHT + CUR compared to DHT alone (Two-way ANOVA). Data is presented as mean luciferase activity ± SEM relative to the maximal response of each cell line and is the average of 2 (PShTert-ctrl) or 3 (C4-2B, PC-3, PShTert-AR) independent experiments. **B:** Cell lines were treated as described above and cell viability was measured by MTT assay at 20 h. No significance for DHT compared to DHT+CUR for all cell lines (Two-way ANOVA). Data is presented as mean cell viability ± SEM relative to the v.c. and is the average of 2 independent experiments.

3.3.4: Effect of curcumin on androgen-regulated gene expression in prostate epithelial cells and fibroblasts.

To support the demonstrated inhibitory effect of curcumin on AR transactivation activity, the ability of curcumin to inhibit DHT-mediated androgen-regulated gene expression was investigated in both an epithelial (LNCaP) and fibroblast (PShTert-AR) cell line. Prior to this experiment, however, optimal concentrations of DHT and curcumin needed to be identified. First, a DHT dose-response was conducted in PShTert-AR fibroblasts and expression of the androgen-regulated gene *TGFB3* was assessed by qRT-PCR (**Figure 3.4A**). This demonstrated a dose-dependent increase in gene expression in response to DHT, with 100 nM causing the maximal response. The decrease in gene expression at 1000 nM DHT was likely due to hormone saturation. The dose of 10 nM DHT was therefore chosen for future experiments as data from this experiment, as well as Figure 3.3A and previous unpublished data from this laboratory (Leach et al.), indicated that 10 nM DHT was a non-

saturating dose that provided a near maximal response in PShTert-AR fibroblasts. To optimise the dose of curcumin required to see an inhibitory effect in combination with DHT, PShTert-AR fibroblasts were treated with 10 nM DHT and curcumin in the ratio of 1:1000, 1:10,000 or 1:100,000; and expression of *TGFB3* was again assessed by qRT-PCR (**Figure 3.4B**). A concentration of curcumin 1000 times greater than DHT (i.e. 10 μM) was required to cause a 53.0 ± 0.22% decrease in DHT regulation of *TGFB3* gene expression in PShTert-AR fibroblasts ($p<0.001$). In addition to the observation that 10 μM curcumin did not have a large effect on cell viability (shown in Figures 3.2A and 3.3B), this dose of curcumin was subsequently chosen for further experiments. Interestingly, the low curcumin doses in combination with DHT (i.e. 0.1 to 1 μM) stimulated *TGFB3* expression over DHT alone. This was a surprising result, however may potentially be explained by the proposed hormetic effect of curcumin (Demirovic and Rattan 2011).

Treatment of LNCaP and PShTert-AR cells with 10 nM DHT and 10 μM curcumin resulted in the inhibition of all androgen-regulated genes tested (**Figure 3.4C**), including *FBXO32* ($p<0.0001$; 55.5 ± 2.3%), *TGFB3* ($p<0.0001$; 93.0 ± 2.7%), *FKBP51* ($p<0.001$; 74.9 ± 2.8%) and *KLK3* ($p>0.05$, 62.8 ± 12.1%). It has also been shown that curcumin reduces AR binding to DNA in LNCaP cells (Shah, Prasad et al. 2012). To investigate whether this was the case in PShTert-AR fibroblasts, chromatin immunoprecipitation for *FKBP51*, the most studied AR binding site in our laboratory, was performed. As expected, DHT caused a 14.82 ± 0.92 fold increase in AR DNA binding to an *FKBP51* DNA regulatory region, and curcumin reduced DHT-mediated binding of AR by 52.86 ± 9.17% ($p<0.01$, **Figure 3.4D**). Together, these data suggest that curcumin can target AR DNA binding in prostate fibroblasts, which may affect AR transactivation activity and androgen-regulated gene expression.

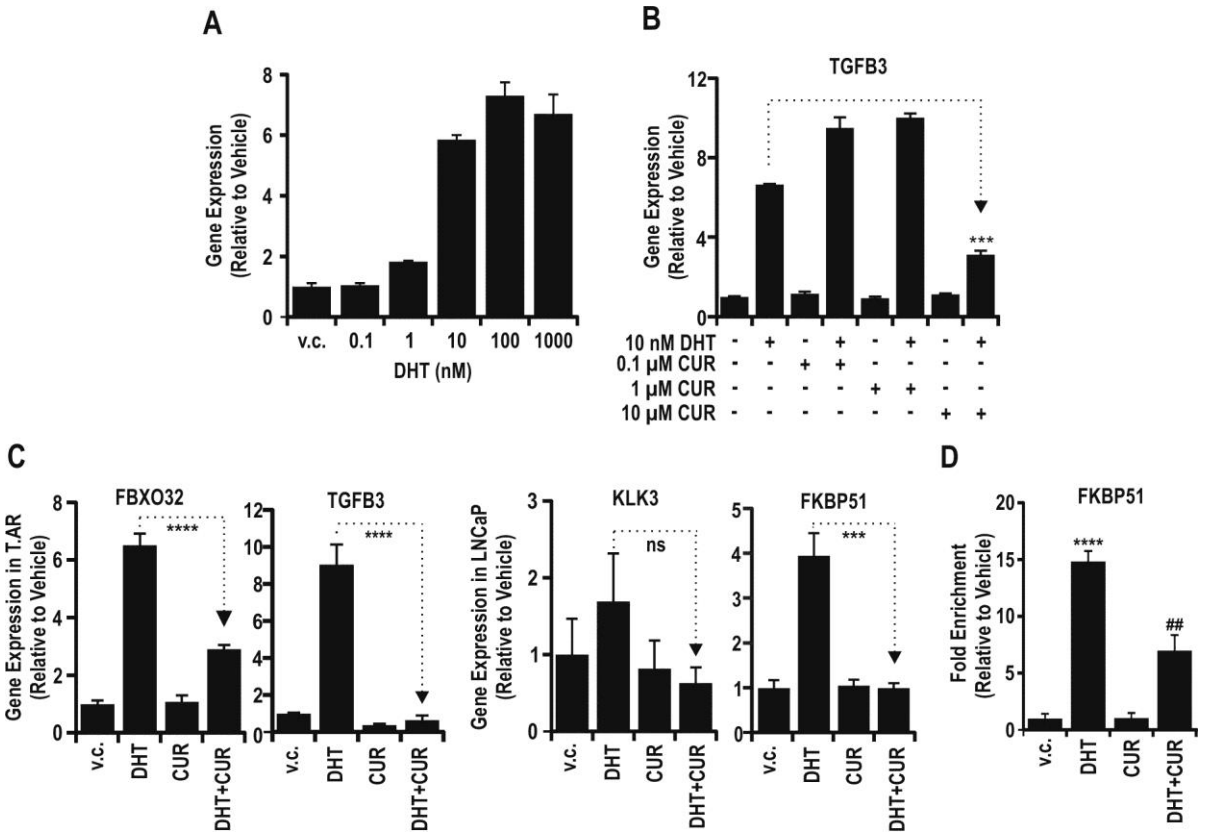

Figure 3.4: The effect of curcumin on DHT-mediated gene expression in prostate epithelial cells and fibroblasts. A: PShTert-AR fibroblasts were treated with vehicle control (v.c.) or 0.1 to 1000 nM DHT and the expression of androgen-regulated gene *TGFB3* was measured by qRT-PCR. Data is presented as mean expression ± SEM of triplicate samples relative to v.c. and reference gene *GAPDH*. **B:** PShTert-AR fibroblasts were treated with v.c., 10 nM DHT alone or 10 nM DHT combined with 0.1 to 10 µM curcumin (CUR) for 16 h, and *TGFB3* gene expression was assessed by qRT-PCR. *** p<0.001 DHT + CUR compared to DHT (Unpaired I-test). Data is presented as mean expression ± SEM relative to v.c. and reference genes *GAPDH* and *RPL32*. **C:** PShTert-AR (T.AR) fibroblasts and LNCaP cells were treated with v.c., 10 nM DHT, 10 µM CUR or DHT+CUR and expression of androgen-regulated genes *FBXO32* and *TGFB3* (T.AR), and *KLK3* and *FKBP51* (LNCaP) were measured by qRT-PCR. ** p<0.01 ****; p<0.0001 DHT compared to DHT + CUR (Unpaired *t*-test). Data is presented as mean expression ± SEM relative to v.c. and reference genes *GAPDH* and *RPL32,* and is the average of 2 independent experiments. **D:** PShTert-AR fibroblasts were treated with v.c., 10 nM DHT, 10 µM CUR or DHT+CUR and chromatin immunoprecipitation was performed at a regulatory region on the androgen-regulated *FKBP51* gene. ** p<0.01 DHT + CUR compared to DHT (Unpaired *t*-test). Data is presented as mean AR fold enrichment ± SEM relative to v.c., total DNA input and the non-specific binding region *NC2*, and is the average of 4 independent experiments.

3.3.5: Genome-wide analysis of curcumin action in prostate fibroblasts over time.

In order to gain a more detailed insight into the global mechanisms of curcumin action in prostate fibroblasts, microarray analysis was performed. The analysis was performed on RNA from PShTert-AR fibroblasts treated with vehicle control or 30 μM curcumin for 4, 8, 12 and 16 h, a timeframe over which curcumin did not overtly affect cell viability (Figure 3.3B). ANOVA identified 1205 genes to be significantly affected by curcumin treatment over time, with 43.9% (529 genes) up-regulated and 56.1% (676 genes) down-regulated at 12 h ($p<0.05$). Ingenuity Pathway Analysis applied to all significantly affected genes identified enrichment of pathways involved in DNA damage responses including Gadd45 signalling (p=1.74E-06), BRCA1 in DNA damage (p=3.24E-06), ATM signalling (p=9.33E-05) and double-strand break repair (p=3.31E-03), and cell cycle arrest pathways including both G1/S and G2/M checkpoint regulation (p=2.29E-03 and 1.62E-02 respectively) and CHK proteins in checkpoint control (p=3.89E-03) (**Table 3.1**). The pathways significantly altered are consistent with the inhibitory effect of curcumin on cell viability.

To dissect the patterns of curcumin response, non-hierarchical cluster analysis was performed on curcumin-affected genes, which yielded eight independent responses (**Figure 3.5A**). These arbitrary clusters were then collapsed by temporal similarity into three main groups (**Figure 3.5B**). Group 1 represented sustained down-regulation (clusters 4 and 5: 439 genes), Group 2 represented sustained up-regulation (clusters 2, 3 and 8: 319 genes) and Group 3 genes underwent rapid down-regulation and return to baseline by 16 h (clusters 1 and 7: 415 genes). A fourth group consisting of 32 genes showed acute up-regulation at 4 h and return to baseline at 16 h (**Figure 3.5A**; Cluster 6). Using an independently generated set of RNA samples, gene responses were validated in representative genes chosen from groups 1-3 (**Figure 3.5C**). The fourth group of genes were not found to be responsive to curcumin at validation, perhaps indicating a response to time in culture or effect of collection, and were not considered further. Additional IPA analysis was then used to investigate the biological importance of genes in Groups 1, 2 and 3 (**Table 3.2**). Similar to the overall response, Group 1 was enriched for genes involved in cell cycle pathways including BRCA1 in DNA damage (p=7.94E-09), double-strand break repair (p=8.71E-05), and Gadd45 signalling (p=3.89E-04). Group 2 was enriched for genes involved in oxidative stress response pathways such as NRF2 signalling (p=8.51E-06) and p38 MAPK signalling (p=1.32E-03). Group 3 was enriched for genes involved in prolactin signalling (p=3.16E-03), estrogen-mediated S-phase entry (p=4.07E-03) and anti-proliferative role of TOB in T-cell signalling (p=5.13E-03). Taken together, these data suggest that the effect of curcumin on prostate fibroblasts may be the result of early initiation of oxidative stress, decreased tolerance of DNA damage and altered cell cycle regulation.

Pathway	P-value	Ratio
GADD45 Signalling	1.74E-06	3.48E-01
Role of BRCA1 in DNA Damage Response	3.24E-06	2.00E-01
Estrogen-mediated S-phase Entry	8.32E-05	2.50E-01
ATM Signalling	9.33E-05	1.77E-01
Hereditary Breast Cancer Signalling	1.02E-04	1.25E-01
Pancreatic Adenocarcinoma Signalling	1.38E-04	1.25E-01
Granzyme A Signalling	1.66E-04	3.00E-01
Bladder Cancer Signalling	8.91E-04	1.30E-01
Antiproliferative Role of TOB in T Cell Signalling	1.07E-03	2.31E-01
p38 MAPK Signalling	1.26E-03	1.19E-01
p53 Signalling	1.32E-03	1.25E-01
Cell Cycle: G1/S Checkpoint Regulation	2.29E-03	1.34E-01
DNA Double-Strand Break Repair by Homologous Recombination	3.31E-03	2.35E-01
Role of CHK Proteins in Cell Cycle Checkpoint Control	3.89E-03	1.40E-01
NRF2-mediated Oxidative Stress Response	4.79E-03	8.85E-02
Prostate Cancer Signalling	5.37E-03	1.01E-01
Mismatch Repair in Eukaryotes	5.50E-03	1.67E-01
Small Cell Lung Cancer Signalling	5.75E-03	1.01E-01
ERK5 Signalling	9.77E-03	1.21E-01
DNA damage-induced 14-3-3σ Signalling	1.05E-02	1.90E-01
Cyclins and Cell Cycle Regulation	1.23E-02	1.00E-01
Cell Cycle: G2/M DNA Damage Checkpoint Regulation	1.62E-02	1.22E-01
TWEAK Signalling	1.78E-02	1.32E-01
IL-6 Signalling	2.04E-02	8.87E-02
Glucocorticoid Receptor Signalling	2.14E-02	6.80E-02
TNFR1 Signalling	2.19E-02	1.15E-01

Table 3.1: Ingenuity pathway analysis of the 1205 curcumin-affected genes in PShTert-AR fibroblasts. Pathway analysis of these genes revealed DNA damage and cell cycle arrest pathways to be amongst the most enriched in response to curcumin treatment.

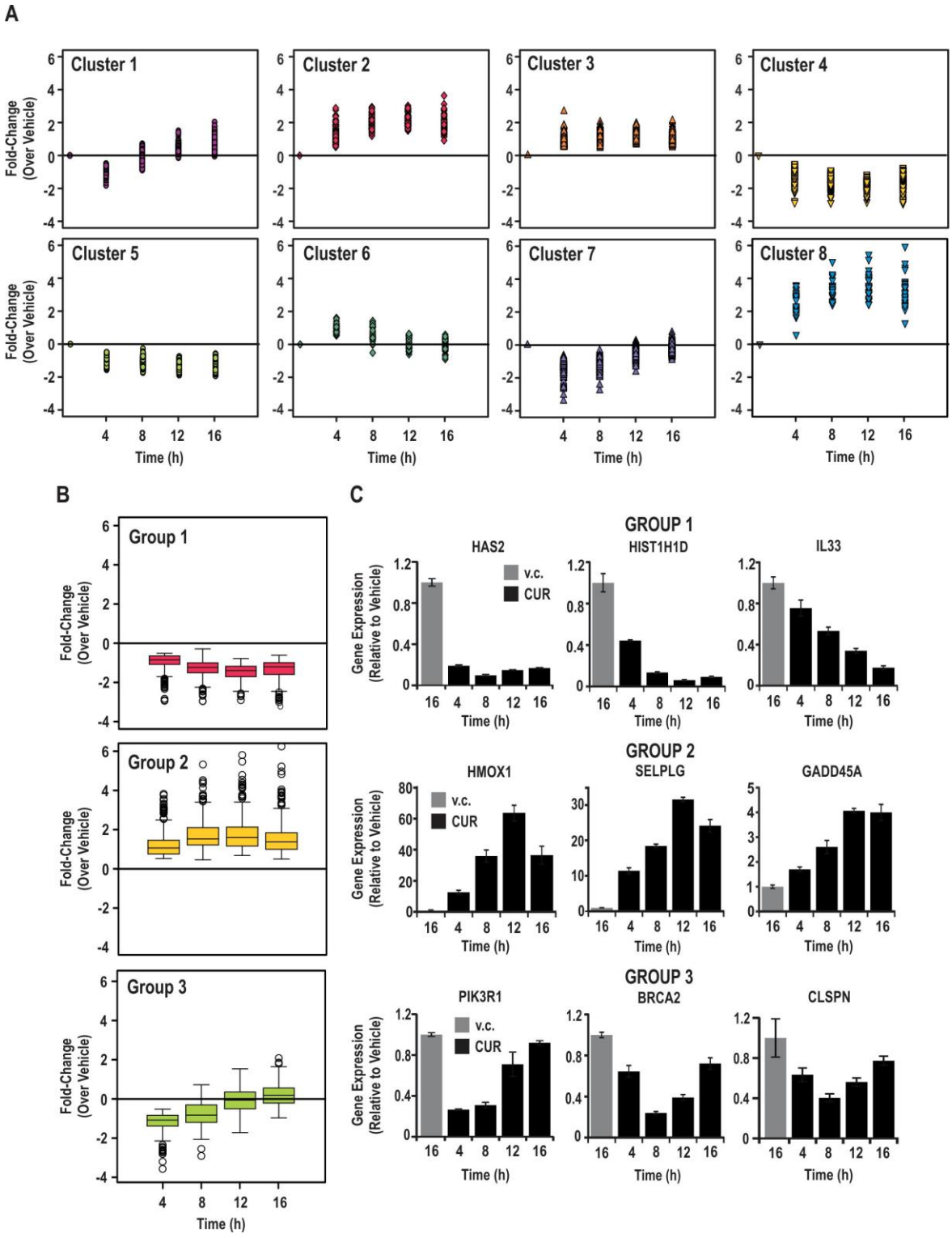

Figure 3.5: Genome-wide analysis of curcumin action in prostate fibroblasts over time. Triplicate RNA samples from vehicle control (v.c.) or 30 μM curcumin-treated PShTert-AR fibroblasts were pooled and analysed on Affymetrix Human 1.0st Gene Arrays. A cut-off of $p<0.05$ was applied to analyse genes. **A:** Non-hierarchical cluster analysis revealed eight distinct clusters of genes, presented as fold-change over v.c. at 4, 8, 12 and 16 h. **B:** The eight clusters were further classified into four sub-groups based on similar responses and presented as boxplots of fold-change over v.c. at 4, 8, 12 and 16 h. Group 4 was unable to be validated and was excluded from further analysis. **C:** Groups 1, 2 and 3 were validated by qRT-PCR using an independent set of RNA produced under identical conditions. Data is presented as mean expression ± SEM relative to v.c. and reference genes *GAPDH* and *RPL32*.

	Pathway	P-value	Ratio
Group 1 (439 genes)	Role of BRCA1 in DNA Damage Response	7.94E-09	1.69E-01
	Granzyme A Signalling	6.92E-07	3.00E-01
	Hereditary Breast Cancer Signalling	7.59E-06	8.59E-02
	DNA Double-Strand Break Repair by Homologous Recombination	8.71E-05	2.35E-01
	Mismatch Repair in Eukaryotes	1.55E-04	1.67E-01
	GADD45 Signalling	3.89E-04	1.74E-01
	Role of CHK Proteins in Cell Cycle Checkpoint Control	4.37E-04	1.05E-01
	DNA damage-induced 14-3-3σ Signalling	4.47E-03	1.43E-01
	Estrogen-mediated S-phase Entry	8.71E-03	1.07E-01
	Cell Cycle Control of Chromosomal Replication	1.35E-02	9.38E-02
	Cyclins and Cell Cycle Regulation	1.45E-02	5.56E-02
	Cell Cycle: G1/S Checkpoint Regulation	2.51E-02	5.97E-02
	Cell Cycle: G2/M DNA Damage Checkpoint Regulation	4.37E-02	6.12E-02
Group 2 (319 genes)	NRF2-mediated Oxidative Stress Response	8.51E-06	6.25E-02
	Bladder Cancer Signalling	2.45E-04	7.61E-02
	ERK5 Signalling	2.63E-04	9.09E-02
	p38 MAPK Signalling	1.32E-03	5.93E-02
	ATM Signalling	1.48E-03	8.06E-02
	GADD45 Signalling	2.57E-03	1.30E-01
	LPS-stimulated MAPK Signalling	3.55E-03	6.10E-02
	ERK/MAPK Signalling	4.90E-03	3.85E-02
	ErbB Signalling	6.76E-03	5.75E-02
	Toll-like Receptor Signalling	7.59E-03	6.45E-02
	p53 Signalling	9.77E-03	5.21E-02
	HGF Signalling	1.29E-02	4.72E-02
Group 3 (415 genes)	Prolactin Signalling	3.16E-03	6.25E-02
	Estrogen-mediated S-phase Entry	4.07E-03	1.07E-01
	Antiproliferative Role of TOB in T Cell Signalling	5.13E-03	1.15E-01
	Small Cell Lung Cancer Signalling	1.58E-02	4.49E-02
	Prostate Cancer Signalling	2.63E-02	4.04E-02

Table 3.2: Ingenuity pathway analysis of the three classes of curcumin response. Pathway analysis of Groups 1 and 2 revealed DNA damage and cell cycle arrest pathways to be associated with the sustained down-regulation of genes while cellular stress pathways were associated with the sustained up-regulation of genes. Acute gene changes (Group 3) did not appear to play much of a role in curcumin action.

3.3.6: Comparing genome-wide curcumin action in LNCaP, C4-2B and PShTert-AR cells.

In order to assess the congruence between curcumin-responsive genes in prostate fibroblast and cancer cells, the microarray data presented above was overlapped with previously published microarray data for both LNCaP and C4-2B prostate cancer cells that had been treated with 10 μM curcumin for 12 h (Thangapazham, Shaheduzzaman et al. 2008) (**Figure 3.6A**). Only 7.6% of the curcumin-responsive genes in PShTert-AR fibroblasts were also regulated by curcumin in both LNCaP and C4-2B cancer cells, and only 0.94% of genes were common across all three cell lines (common genes listed in **Table 3.3**). The limited overlap of curcumin-responsive genes between LNCaP and C4-2B cells was surprising given their common origin and similar relative sensitivity to curcumin (Figure 3.2A) (Wu, Hsieh et al. 1994). Despite the limited overlap at the gene level, IPA analysis showed that the majority of pathways regulated by curcumin in PShTert-AR fibroblasts were also affected in both LNCaP and C4-2B cells (**Table 3.4**). However, four pathways were found to be specific to fibroblasts: bladder cancer signalling (p=8.91E-04), p38 MAPK signalling (p=1.26E-03), small cell lung cancer signalling (p=5.75E-03) and ERK5 signalling (p=9.77E-03).

Given that cell cycle pathways were significantly affected across all three cell lines, cell cycle analysis was performed to closer examine the phases in which each cell line underwent arrest. There was a significant increase in C4-2B (31.8 ± 9.0%; $p<0.05$), LNCaP (61.2 ± 8.8%; $p<0.001$) and PShTert-AR (24.5 ± 8.9%; $p<0.05$) cells arresting in the G2/M-phase of the cell cycle in response to curcumin treatment (**Figure 3.6B**). Cell cycle changes were congruent with a curcumin effect on the expression of cell cycle regulatory genes including *CLSPN*, *RAD17* and *PCNA* (8 h), and *ATR* (16 h), results which also validate microarray data ($p<0.05$; **Figure 3.6C**). Consistent with an effect on G2 arrest, flow cytometry demonstrated a significant increase in the number of apoptotic PShTert-AR fibroblasts over 8 to 48 h of curcumin treatment compared to vehicle ($p<0.001$), and a decrease in the healthy fraction of cells ($p<0.01$) (**Figure 3.6D**). These results suggest that curcumin can induce apoptosis in prostate fibroblasts within 8 h of treatment.

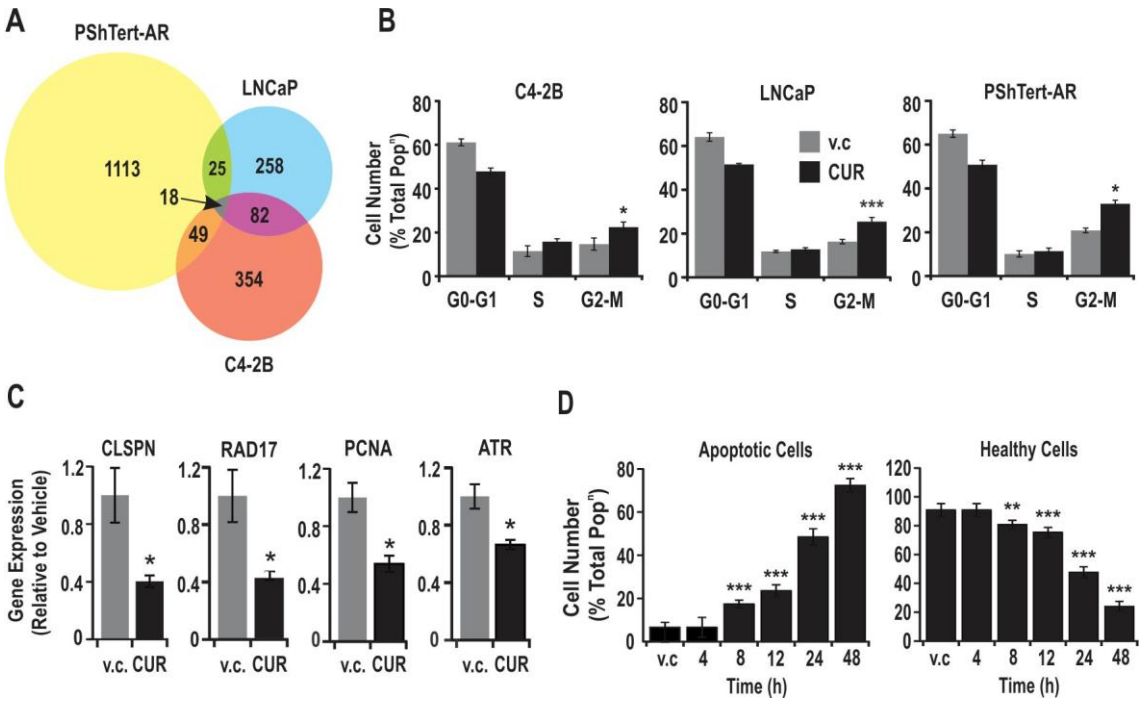

Figure 3.6: Comparing genome-wide curcumin action in LNCaP, C4-2B and PShTert-AR cells. A: Genes from the 12 h time-point were overlayed with publicly available data where LNCaP and C4-2B prostate cancer cells were treated with 10 μM curcumin for 12 h. There were 92 genes (7.6%) in common between fibroblast and epithelial cell lineages and only 18 genes (less than 1%) in common between the three cell lines. **B:** C4-2B, LNCaP and PShTert-AR cells were treated with vehicle control (v.c.) or 30 μM curcumin (CUR) for 16 h. Cells were fixed, labelled with PI and analysed by flow cytometry. Cell cycle distribution was determined using FlowJo software. * $p<0.05$; ***$p<0.001$ CUR compared to v.c. (Unpaired *t*-test). Data is presented as mean cell number (percentage of cells in each phase of the total population) ± SEM and is the average of 3 independent experiments. **C:** PShTert-AR fibroblasts were treated as described in Figure 3.5 and *CLSPN*, *RAD17, PCNA* and *ATR* gene expression were measured by qRT-PCR. * $p<0.05$ CUR compared to v.c. (Unpaired *t*-test). Data is presented as mean expression ± SEM relative to v.c. and reference genes *GAPDH* and *RPL32*. Data represents validation of the microarray. **D:** PShTert-AR fibroblasts were treated with v.c. or 30 μM CUR for 4 to 48 h. Cells were labelled with PI and Annexin V, and assessed for apoptosis by flow cytometry. ** $p<0.01$, *** $p<0.001$ CUR compared to v.c. (Unpaired *t*-test). Data is presented as mean cell number (apoptotic or healthy cells as a percentage of the total population) ± SEM and is representative of 3 independent experiments.

All (18)	PShTert-AR & C4-2B (67)		PShTert-AR & LNCaP(43)		C4-2B & LNCaP (100)		
ADAMTS1	ADAMTS1	KIF20A	ADAMTS1	KIF20A	AADAT	FTH1	PBK
ASPM	AP1	KIF4A	AKAP1	KLHL3	ABCC4	GADD45A	PCANAP6
ATF3	ASF1B	KIFC1	AMPD1	MAP1LC3B	ACSL3	GALNT7	PPIF
BUB1B	ASPM	LMNB1	ASPM	MDM2	ADAMTS1	GGH	PPP3CA
CDCA3	ATF3	LRRFIP1	ATF3	MELK	ADRB2	GTF3A	PSF1
CDKN1A	BRCA1	MCM10	AURKB	MSH5	ANKH	Hcap-d3	RFC4
CENPF	BRCA2	MCM3	BTG1	PDIA6	ANLN	HDLBP	RNU47
DDIT3	BUB1B	MELK	BUB1B	RIOK3	ARID5B	HMG20B	RRM2
FEN1	CCNA2	MIKI67	CDCA3	SEC24A	ARL6IP	HMOX1	SEPP1
GADD45A	CDC7	MRE11A	CDK5R1	SECISBP2	ASPM	IQGAP3	SESN2
HMOX1	CDCA2	NNMT	CDKN1A	SERPINC1	ATAD2	KIAA0286	SFPQ
KIF20A	CDCA3	OSR2	CENPF	SESN2	ATF3	KIF20A	SLC43A1
MELK	CDCA4	PNRC2	CETP	SLC25A37	BUB1B	KLK2	SLC4A4
SESN2	CDCA8	POLE2	DDIT3	SLC2t6A2	C1orf116	LBR	SNRPB
TMEFF2	CDKN1a	RAD51	DUSP1	SPRY4	C1orf79	LOC146909	ST6GALNAC1
TRIB3	CDKN1B	RFC3	EGR1	TMEFF2	CAMKK2	LRIG1	STC2
TROAP	CENPF	RGS2	EIF5	TNXIP	CCNB1	MAD2L1	TDG
TXNIP	DDIT4	SESN2	FEN1	TRIB3	CDC2	MCCC2	TFP1
	DDIT3	SIX1	GADD45A	TROAP	CDCA3	MCM2	TK1
	DEPDC1	SNRPA1	HMOX1	UHRF1	CDKN1A	MCM7	TMEFF2
	E2F8	THBS1	ID1	ZNF12	CDKN3	MELK	TMEM48
	EIF2C2	TIFA	JUNB		CENPF	MGC14376	TMEPAI
	ESPL1	TMEFF2			CREB3L4	MIPEP	TMPRSS2
	FBXO5	TMPO			DC13	MYC	TncRNA
	FEN1	TRIB3			DDIT3	NASP	TNFRSF19
	FIGNL1	TRIM59			DDR2	NETO2	TRIB3
	GADD45A	TRIM68			DKFZP586A052	NKX3-1	TROAP
	GCNT1	TROAP			DUT	NMU	TXNIP
	GMNN	TTK			EBP	NUP88	UAP1
	GTSEQ	TXNIP			EMP2	NUSAP1	UBE2T
	H1F0	WDHD1			EXTL2	OACT2	VPS13A
	HMGB2	WEE1			FEN1	OIP5	ZA20D2
	HMOX1	YEATS4			FKBP5	ORC5L	
	KIF14				FLJ10719	OVOS2	

Table 3.3: Common curcumin-responsive genes between PShTert-AR, C4-2B and LNCaP cells.

Pathway	PShTert-AR	C4-2B	LNCaP
GADD45 Signalling	1.74E-06	8.32E-06	4.57E-04
Role of BRCA1 in DNA Damage Response	3.24E-06	1.59E-14	3.09E-2
Estrogen-mediated S-phase Entry	8.32E-05	2.57E-06	1.15E-02
ATM Signalling	9.33E-05	3.16E-12	1.95E-05
Hereditary Breast Cancer Signalling	1.02E-04	5.01E-11	2.14E-03
Pancreatic Adenocarcinoma Signalling	1.38E-04	2.82E-02	n/s
Granzyme A Signalling	1.66E-04	01.45E-02	n/s
Bladder Cancer Signalling	8.91E-04	n/s	n/s
Antiproliferative Role of TOB in T Cell Signalling	1.07E-03	5.13E-03	n/s
p38 MAPK Signalling	1.26E-03	n/s	n/s
p53 Signalling	1.32E-03	4.68E-05	n/s
Cell Cycle: G1/S Checkpoint Regulation	2.29E-03	2.57E-02	n/s
DNA Double-Strand Break Repair by Homologous Recombination	3.31E-03	1.02E-06	n/s
Role of CHK Proteins in Cell Cycle Checkpoint Control	3.89E-03	1.26E-11	4.57E-03
NRF2-mediated Oxidative Stress Response	4.79E-03	n/s	6.17E-05
Prostate Cancer Signalling	5.37E-03	n/s	1.17E-03
Mismatch Repair in Eukaryotes	5.50E-03	2.63E-06	3.55E-03
Small Cell Lung Cancer Signalling	5.75E-03	n/s	n/s
ERK5 Signalling	9.77E-03	n/s	n/s

Table 3.4: Ingenuity pathway analysis for curcumin-affected genes in PShTert-AR fibroblasts compared to C4-2B and LNCaP cells. Comparative pathway analysis revealed genes involved in Gadd45 signalling, role of BRCA1 in DNA damage and ATM signalling pathways common to all three cell lines.

3.3.7: Mechanisms of curcumin-mediated cell cycle arrest in prostate cancer cells and fibroblasts.

The small transcriptional overlap between PShTert-AR, LNCaP and C4-2B cell lines may be indicative of cell-specific mechanisms of curcumin action. To gain further insight into the mechanisms of curcumin-mediated cell cycle arrest in prostate fibroblast and cancer cells, steady-state levels of proteins in the BRCA1 pathway were studied in response to curcumin treatment for 16 h (**Figure 3.7A**). This time-point was chosen because it was 8 hours before the large increase in apoptosis occurred, meaning cells were still alive but likely committed to death (Figure 3.6D). This pathway was significantly affected in response to curcumin treatment in all three cell lines used in the current study, and has been shown to play a role in cell cycle control (Mullan, Quinn et al. 2006). In PShTert-AR fibroblasts, curcumin reduced levels of BRCA1 and caused a concomitant decrease in BRCA1 target proteins Gadd45α and p53, as well as downstream PCNA, a processivity factor for DNA polymerase whose rate of synthesis correlates directly with the proliferation state of cells (Celis, Madsen et al. 1987). These changes are consistent with decreased PCNA-mediated cellular proliferation. Conversely in LNCaP cells, while curcumin also decreased BRCA1, it increased Gadd45α and p53 protein levels causing an induction of p21. These responses are more consistent with initiation of a p53/p21-driven cell cycle arrest. It became clear that the p53 status of cells may play an important role in these results. Therefore to understand how curcumin may cause death in the absence of p53, the pathway was re-assessed in PC-3 cells which lack functional p53 (Scott, Earle et al. 2003, Alimirah, Panchanathany et al. 2007). While BRCA1 expression was again decreased in response to curcumin treatment, Gadd45α expression was increased in a similar manner to LNCaP cells. However PCNA levels were also decreased and there was no change in p21, similarly to PShTert-AR fibroblasts. This suggests that there is some cross-over between pathways in curcumin-treated cells lacking p53. All changes in protein expression were confirmed by densitometry (**Figure 3.7B**). Diagrammatic representation for the proposed divergent mechanisms of cell death in prostate cancer cells and fibroblasts is presented in **Figure 3.7C**. The above data provides insight into the divergent induction of cell-cycle arrest pathways by curcumin in prostate fibroblast and epithelial cells, and once again highlights the cell-specific nature of curcumin action.

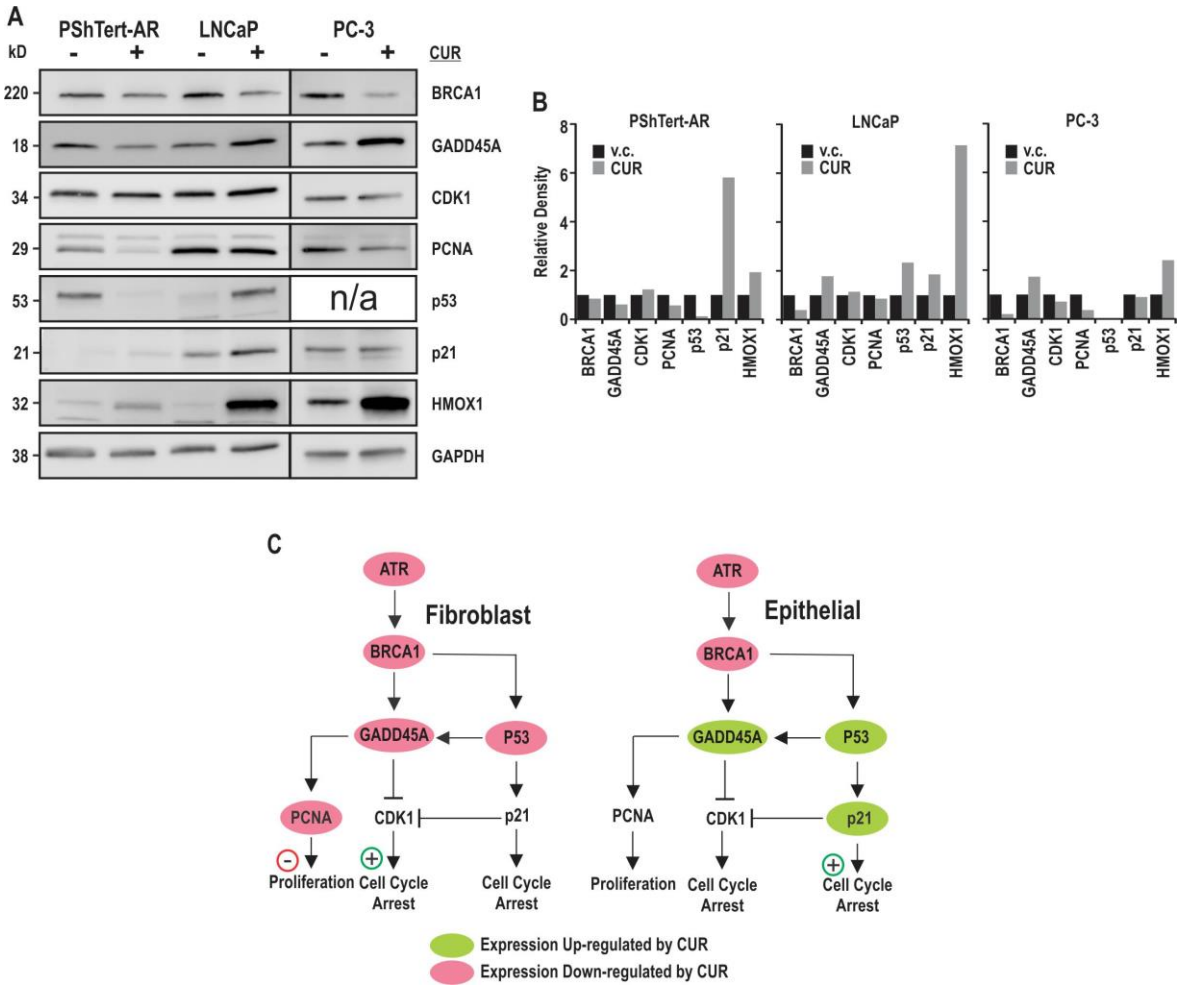

Figure 3.7: Mechanisms of curcumin-mediated cell cycle arrest in prostate cancer cells and fibroblasts. A: PShTert-AR, LNCaP and PC-3 cells were treated with vehicle control (-) or 30 μM curcumin (CUR; +) for 16 h. Lysates were probed for BRCA1, Gadd45α, CDK1, PCNA, p53, p21, HMOX1 and GAPDH. Results are representative of 2 independent experiments. **B:** Densitometry was performed on the immunoblots from Figure 3.7A using Image J software. Data represents density relative to vehicle control and GAPDH. **C:** A proposed model for the divergent mechanisms of curcumin-induced cell cycle arrest observed between PShTert-AR fibroblasts and LNCaP cancer cells.

3.4: DISCUSSION

The growth, differentiation and progression of solid tumours are mediated by complex bi-directional interactions between cancer cells and the surrounding microenvironment. As discussed in Chapter 1 fibroblasts are the main cellular constituents of the microenvironment, and supply cancer cells with pro-proliferative and anti-apoptotic signals via secreted paracrine factors and actively remodel the ECM (Kalluri and Zeisberg 2006). Deleterious genetic changes to tumour suppressors within fibroblasts, such as loss of PTEN, have been shown to accelerate tumour initiation, progression and malignant transformation (Trimboli, Cantemir-Stone et al. 2009). Further, it is now recognised that the microenvironment is an important component in predicting therapeutic efficacy. Fibroblasts have been shown to mediate *de novo* drug resistance, resulting in the protection of cancer cells from the initial effects of therapy and contributing to permanent, acquired drug resistance (Meads, Gatenby et al. 2009). Given the important role of fibroblasts in these processes and the lack of insight into fibroblasts in terms of drug efficacy studies, the aim of this chapter was to characterise the effect of curcumin on prostate fibroblasts compared to prostate cancer cells.

Cell cycle control and DNA damage responses are largely controlled by BRCA1 (Mullan, Quinn et al. 2006). Data from this chapter implicates BRCA1 as a key mediator of curcumin response in prostate cells. Not only did curcumin down-regulate its protein expression, the BRCA1 pathway was significantly affected by curcumin in both prostate cancer cells and fibroblasts. This finding is consistent with other studies associating DNA damage response proteins such as ATM, ATR and BRCA1 with curcumin action rather than curcumin-induced DNA damage *per se* (Cao, Jia et al. 2006, Landais, Hiddingh et al. 2009, Rowe, Ozbay et al. 2009, Lu, Cai et al. 2011, Blakemore, Boes et al. 2013). This study is the first to identify divergent responses of fibroblasts and epithelial cells to curcumin downstream of BRCA1, with Gadd45α appearing to be central in this process. Regulation of Gadd45α may occur in a p53-mediated, DNA damage-inducible manner, as well as via p53-independent mechanisms such as Oct-1 and NF-YA binding to the Gadd45α promoter (Jin, Zhao et al. 2000). In this study, Gadd45α protein levels decreased with curcumin treatment in fibroblasts, proposed to cause a decrease in both cell cycle mediators and downstream proliferation. In p53 wild-type epithelial cells however, there was a clear increase in Gadd45α and p53, factors known to increase p21, suggestive of cell cycle arrest in a p53-dependent manner (Xiong, Hannon et al. 1993, Zhang, Xiong et al. 1993, Vairapandi, Balliet et al. 1996, Rozzo, Fanciulli et al. 2013). When p53 is not present in epithelial cells, there appeared to be some cross-over between the two proposed pathways where Gadd45α was still activated (similar to p53 wild-type epithelial cells) but arrest appeared to be via a decrease in PCNA (similar to prostate fibroblasts). Indeed, curcumin-mediated induction of p53-dependent cell cycle arrest has been previously demonstrated in breast and basal

cell carcinoma cells (Jee, Shen et al. 1998, Choudhuri, Pal et al. 2005). This data suggests that curcumin-induced up-regulation of p53 and p21 drives cell cycle arrest via this pathway in p53 wild-type epithelial cells rather than the p53-independent pathway observed in fibroblasts. These results also indicate that p53 may prove to be an important marker of curcumin efficacy specifically within prostate cancer cells expressing wild-type p53. These findings are encouraging as they demonstrate that curcumin may cause death in cancer cells regardless of their p53 status, which is often associated with drug resistance.

Despite previous evidence that curcumin is taken up by cancer cells more favorably than non-cancer cells (Syng-Ai, Kumari et al. 2004, Kunwar, Barik et al. 2008), the data in this chapter demonstrated that prostate fibroblasts are dose-dependently sensitive to curcumin treatment, suggesting that curcumin may also target the fibroblasts within a solid tumour. This is of particular interest as CAFs have been implicated in cancer initiation, progression, supporting the metastatic colonisation of cancer cells in distant organs and drug resistance (Bhowmick, Neilson et al. 2004, Loeffler, Krüger et al. 2006, Brennen, Rosen et al. 2012, Karagiannis, Poutahidis et al. 2012, Sebens and Schäfer 2012). Differential curcumin uptake by fibroblasts and epithelial cells was excluded as a possible cause of the varied sensitivities to curcumin and subsequently variable transcriptional responses. In previous studies, variable sensitivity to curcumin has been attributed to differential expression of NF-κB and AP-1, heat shock proteins (Hsp90, 70 and 27) and BRCA1, or on compromised mismatch repair function (Aggarwal 2000, Rauh-Adelmann, Lau et al. 2000, Mukhopadhyay, Bueso-Ramos et al. 2001, Shaulian and Karin 2001, Rashmi, Santhosh Kumar et al. 2003). Future studies may consider investigating these results more thoroughly using other methodologies such as tritium-labelling. This is a well-established technique used to measure amino acid uptake, and has also been useful in measuring curcumin excretion (Holder, Plummer et al. 1978, Tomi, Mori et al. 2005, Wang, Bailey et al. 2011).

Data from this chapter indicated that AR activity and DNA binding was inhibited by curcumin in prostate fibroblasts as effectively as in prostate cancer cells (Dorai, Gehani et al. 2000, Nakamura, Yasunaga et al. 2002, Lin, Shi et al. 2006, Shi, Shih et al. 2009, Shah, Prasad et al. 2012). Targeting AR is the gold standard therapeutic option for advanced prostate cancer, and simultaneously inhibiting AR in both compartments of the prostate may be advantageous in patients. However, given the dual roles of fibroblast AR in prostate cancer initiation and progression, the timing of curcumin treatment may become an important consideration. As described previously, fibroblasts expressing AR contribute to prostate cancer initiation yet the loss of AR in fibroblasts has been associated with higher clinical stage, higher pre-treatment PSA level and earlier relapse after radical prostatectomy

(Henshall, Quinn et al. 2001, Ricciardelli, Choong et al. 2005). Curcumin may therefore be more safely used at later stages of disease. Future studies into the effect of curcumin action on AR activity may be strengthened by assessing endogenous markers of AR activity, such as PSA. Specifically, assessment of AR protein levels would reinforce the transactivation data, and potentially eliminate the possibility that changes in curcumin-mediated inhibition of AR were due to different AR protein expression. Future studies should also use a dual luciferase assay or constitutively active reporter plasmid as a transfection control. These assays were attempted for the purpose of this thesis, however were not part of a standard protocol for this laboratory and could not be successfully established within the time-frame of the study. Regardless of these limitations, the data presented in this chapter highlights the importance of understanding the cellular mechanisms of curcumin responses in the normal and neoplastic tissue microenvironment prior to use as a cancer preventative or treatment.

Curcumin initiated early gene responses resulting in G2/M-phase cell cycle arrest and apoptosis of prostate fibroblasts analogous to epithelial cells, despite large differences in the induced transcriptional response between the two cell types (Dorai, Cao et al. 2001, Mukhopadhyay, Bueso-Ramos et al. 2001, Piantino, Salvadori et al. 2009). Some of the commonly affected genes between prostate cancer cells and fibroblasts included cell cycle regulators *CDKN1A*, *MYC* and *MCM2,* in accordance with previous observations (Thangapazham, Shaheduzzaman et al. 2008). However, the limitation of using the Thangapazham *et al.* dataset was the comparison of different curcumin doses. The disparity in the number of genes compared between these studies may have been due to the lower dose used in epithelial cells, or different criteria used to identify differentially expressed genes. Furthermore, Thangapazham et al. did not publish their methods in full, making a true comparison between their study and the current study difficult to make. For example, the culture conditions for LNCaP and C4-2B cells were not described, and may differ from the conditions used for this thesis. The limited methodological information provided in their paper does indicate that curcumin was sourced from the same company (LKT Laboratories), that RNA was extracted in the same manner and that RNA was also hybridised to Affymetrix GeneChip Human Gene Arrays. However, they used 2.0 ST arrays, reported to capture approximately 4,600 more RefSeq transcripts than the 1.0 ST arrays used in this thesis. It was encouraging, however, to also observe little overlap between the closely related LNCaP and C4-2B cell lines within the same study, providing further evidence for the cell-specific nature of curcumin action. Ideally, analysis and processing of the Thangapazham *et al*. raw data should have been performed identically to the data in this chapter; however the authors would only provide gene lists. To address this limitation, a direct, global comparison of curcumin responses within these different epithelial and fibroblast cells across a range of curcumin doses and

times is required. However, the observation of similar pathway enrichment between cancer cells and fibroblasts in terms of cell cycle is in accordance with two recent studies that demonstrated similar biological pathways affected by the curcumin derivative D6 in cancer cells and fibroblasts (Pisano, Pagnan et al. 2010, Rozzo, Fanciulli et al. 2013). Future studies should also consider performing a dose-response microarray, to better understand the mechanisms associated with mild or low-dose curcumin treatment.

The inducible stress response gene HMOX1 is commonly up-regulated with curcumin treatment (Bachmeier, Mohrenz et al. 2008, Panchal, Vranizan et al. 2008, Thangapazham, Shaheduzzaman et al. 2008, Rozzo, Fanciulli et al. 2013). This study demonstrated strong HMOX1 gene and protein induction by curcumin in fibroblasts over 16 hours, supporting curcumin activity in these cells comparable to epithelial cells. Interestingly, HMOX1 has been implicated in enhanced survival of neoplastic cells and drug resistance, and is considered a novel therapeutic target (Gleixner, Mayerhofer et al. 2009). It is possible that curcumin in combination with HMOX1-targeting agents may prove more beneficial in targeting cancer cells than either agent alone.

In summary, the findings of this chapter provide a global view of how curcumin affects gene transcription in prostate fibroblasts, and the common pathways initiated by this agent towards cell death in fibroblasts and cancer cells. These data suggest a potential benefit of curcumin in the treatment of prostate cancers regardless of p53 status, particularly in cases where CAFs may be contributing to cancer growth, invasion and metastasis. However, the inhibition of fibroblast AR activity might paradoxically aid growth of adjacent cancer cells. As such, the use of curcumin as a therapy or preventative agent warrants careful consideration.

CHAPTER 4

CURCUMIN TOLERANCE IN PROSTATE FIBROBLASTS

4.1: INTRODUCTION

The previous chapter identified that curcumin has a dual effect on prostate cancer cells and fibroblasts, which may be advantageous from a clinical perspective. However, while curcumin has been studied as a therapeutic agent in multiple types of cancer, there has been very little characterisation of curcumin tolerance or resistance in cancer cells. There is also no understanding for whether tolerance or resistance may develop in fibroblasts.

Tumours are heterogeneous, with cellular differences often arising due to genetic instability. Historically, this was based on the idea that dominant clones in the cell population survive through genetic mutation and subsequent selection (Nowell 1976). In recent times, this model has become somewhat simplistic as evidence is now suggesting many other factors contributing to tumour heterogeneity including epigenetics, cancer stem cells and stromal-epithelial interactions (Greaves 2009, Hanahan and Weinberg 2011, Bock and Lengauer 2012). Drug treatment also provides selective pressure and may result in drug tolerance or resistance through mechanisms such as altered drug uptake, metabolism, target receptor expression and cellular repair mechanisms, ultimately causing treatment failure (Sawyers 2007, Redmond, Wilson et al. 2008). As described in Section 1.5.5, drug tolerance and resistance are caused by different molecular mechanisms.

The literature presents no information on whether CAFs contribute to drug tolerance. However, recent evidence and retrospective analyses are beginning to define a role for CAFs in the development of drug resistance (Bhowmick, Neilson et al. 2004, Karagiannis, Poutahidis et al. 2012). Most notably, the paracrine action of CAF-secreted mediators has been shown to influence adhesions between cancer cells and fibroblasts, subsequently affecting the sensitivity of cancer cells to apoptosis (Thomas, Anglaret et al. 1998, Shain and Dalton 2001). Further, head and neck squamous cell carcinoma cells demonstrate a decreased sensitivity to cetuximab in the presence of CAFs (Johansson, Ansell et al. 2012). In this particular study, CAF-conditioned media protected the cancer cells from cetuximab treatment in a dose-dependent manner, suggesting resistance to treatment was mediated by CAF-derived soluble factors. Indeed, CAF-derived fibronectin and integrin have been shown to cause tamoxifen resistance in breast cancer cells (Pontiggia, Sampayo et al. 2012), and microenvironment-derived WNT16B was shown to promote tumour cell survival and

disease progression in a prostate cancer mouse model (Sun, Campisi et al. 2012). Interestingly, pancreatic ductal adenocarcinoma cells in long-term co-culture with pancreatic fibroblasts resulted in chemo-resistant cancer cells, marked by reduced expression of caspases (-3, -7, -8 and -9) and caspase-inducing transcription factor STAT-1 (Müerköster, Werbing et al. 2008). This was confirmed in SCID mice, where tumours arising from cancer cells co-inoculated with fibroblasts responded less towards chemotherapy than tumours containing cancer cells alone (Müerköster, Werbing et al. 2008).

Given the role of fibroblasts in cancer progression and drug resistance, targeting them is becoming an attractive option for cancer therapy. However, targeting fibroblasts in a cancer setting may cause drug tolerance and/or resistance in fibroblasts because their proximity to blood vessels makes them likely to receive treatment first, at least when tumour angiogenesis is minimal. The aim of this chapter is therefore to expose prostate fibroblasts to long-term culture in curcumin and establish whether tolerance or resistance occurs. Specifically, this chapter aims to characterise both the functional and transcriptomic mechanisms by which any tolerance or resistance may occur through microarray profiling, examination of candidate genes and comparison of current data with publically available microarray data defining mechanisms of chemotherapeutic drug resistance. Further, the dynamic interaction between cancer cells and fibroblasts indicates that changes to one cell type may strongly impact the other. Therefore this chapter also aims to investigate potential implications of curcumin tolerance or resistance in fibroblasts in terms of androgen signalling and effects on the activity of cancer cells.

4.2: MATERIALS AND METHODS

4.2.1: Cell culture and reagents

Long-term curcumin-treated fibroblasts (LTC) and aged-matched, DMSO-treated vehicle control fibroblasts (LTV) were generated using the AR-positive, immortalised prostate fibroblast cell line PShTert-AR (full method described in Section 2.3.1). Fibroblasts were maintained in 30 μM curcumin because, despite tolerance, this was the highest dose that cells could survive in. That is, tolerant cells struggled to grow at doses above 30μM. Long-term curcumin withdrawn (LTC-w) fibroblasts were generated by culturing LTC fibroblasts in curcumin-free RPMI-1640 media containing 5% FCS for a minimum of four weeks (eight passages). Curcumin and DHT were stored as described in Section 2.3.1. All experiments comparing LTV, LTC and LTC-w fibroblasts were conducted at the same time but for the purpose of clarity, the results for LTC-w fibroblasts (Figure 4.6) have been presented separately from LTV and LTC fibroblasts (Figure 4.5).

4.2.2: MTT assay

LTV, LTC and LTC-w fibroblasts were plated in RPMI-1640 containing FCS at a density of $3x10^3$ cells per well in 24-well plates and allowed to adhere for 24 h. Culture medium was aspirated and cells were treated with vehicle control or 15 to 35 μM curcumin for 4 days. Cell viability was measured at D4 by MTT assay as described in Section 2.3.2. Results are the average of 3 independent experiments.

4.2.3: Flow cytometry

For uptake assays, LTV and LTC fibroblasts were plated in RPMI-1640 containing FCS at a density of 1×10^5 cells per well in 6-well plates and were allowed to adhere for 24 h. Cells were treated with serum-free PRF RPMI-1640 containing vehicle control or 25 μM curcumin for 10 mins. Results are the average of 3 independent experiments. For cell cycle analysis, LTV and LTC fibroblasts were plated in RPMI-1640 containing FCS at a density of $5x10^4$ cells per well in 6-well plates and were allowed to adhere for 24 h. Cells were treated with vehicle control or 30 μM curcumin for 16 h. Results are the average of 3 independent experiments. For all flow cytometry experiments, cells were prepared and analysed as described in Section 2.3.5

4.2.4: Quantitative real-time PCR

LTV and LTC fibroblasts were plated in RPMI-1640 containing FCS at a density of $5x10^4$ cells per well in 6-well plates and were allowed to adhere for 24 h. Cells were treated with (1) vehicle control or 30 μM curcumin for 4 to 16 h or (2) vehicle control or 0.1 to 10 nM DHT in PRF RPMI-1640 containing 5% DCC-FCS for 16 h. RNA was extracted and cDNA synthesised as described in

Section 2.3.7. Results are the average of 2 independent experiments and are relative to *GAPDH* (2) or the geometric mean of *GAPDH* and *RPL32* (1). Primer sequences are listed in Appendix B.

4.2.5: Microarray analysis

LTV and LTC fibroblasts were plated in RPMI-1640 containing FCS at a density of $3x10^4$ cells per well in 6-well plates and were allowed to adhere for 48 h. Cells were treated with vehicle control or 30 µM curcumin for 4 to 16 h. RNA was extracted and cDNA synthesised as described in Section 2.3.7, and bioinformatics were performed by Dr Grant Buchanan as described in Section 3.2.8. Microarray results were validated using an independently extracted set of RNA samples by qRT-PCR. Genes identified in the current study were overlayed with publically available microarray data (Györffy, Surowiak et al. 2006) using Venny software, and gene pathway analysis was conducted using IPA software.

4.2.6: Transactivation assay and transfection efficiency

For transactivation assays, LTV, LTC and LTC-w fibroblasts were plated in RPMI-1640 containing FCS at a density of $5x10^3$ cells per well in 96-well plates and were allowed to adhere for 24 h. Culture medium was aspirated and cells were transfected in serum-free PRF RPMI-1640 containing 50 ng pGL4.14-PB3Luc per well, as described in Section 2.3.4. Following transfection, cells were treated with PRF RPMI-1640 containing 5% DCC-FCS and vehicle control or 0.01 to 100 nM DHT in the presence or absence of 10 µM curcumin for 20 h. Luciferase activity was assayed as described in Section 2.3.4. Results are the average of 3 to 5 independent experiments. Transfection efficiency was measured by plating cells at a density of $2x10^4$ cells per well in 24-well plates, which were allowed to adhere for 24 h. Cells were transfected with 0 to 2 µg eGFP vector for 4 h as described above. Mean GFP fluorescence was quantified using flow cytometry. Results are the average of 2 independent experiments.

4.2.7: Chromatin immunoprecipitation

LTV and LTC fibroblasts were plated in RPMI-1640 containing 5% FCS into 15 cm sterile culture dishes at a density of 5×10^5 per dish and were allowed to adhere for 24 h. Media was replaced with PRF RPMI-1640 containing 5% DCC-FCS for a further 24 h. Cells were treated using this media with vehicle control, 10 nM DHT, 10 µM curcumin or the combination of DHT and curcumin for 4 h. Chromatin immunoprecipitation was performed as described in Section 2.3.8. Results are the average of 4 independent experiments. Primer sequences are listed in Appendix B.

4.2.8: Immunoblot and fractionation

For immunoblot experiments, LTV and LTC fibroblasts were plated in RPMI-1640 containing FCS at a density of $5x10^4$ cells per well in 6-well plates and were allowed to adhere for 24 h. Cells were treated with either (1) vehicle control or 30 μM curcumin for 16 h or (2) vehicle control or 0.1 to 10 nM DHT in PRF RPMI-1640 + 5% DCC-FCS for 16 h. Lysate preparation and protein quantification was performed as described in Section 2.3.6. Membranes were probed with antibodies recognising BRCA1 (1:200), p53, Gadd45α, p21, CDK1, PCNA, HMOX1 (all 1:1000) and GAPDH (1:2000). Results are representative of two independent experiments. For fractionation experiments, LTV and LTC cells were plated in RPMI-1640 containing FCS at $1x10^5$ cells per 10 cm diameter dish and incubated for 48 h. Cells were treated with vehicle control, 10 nM DHT, 30 μM curcumin or the combination of DHT and curcumin, and processed as previously described (Suzuki, Bose et al. 2010). Briefly, cells were washed twice with PBS, collected in 1 mL PBS and pelleted by pulse centrifugation. Supernatant was replaced with 0.1% NP40 and an aliquot for whole cell fraction was removed. Supernatant collected after pulse centrifugation constituted the cytoplasmic fraction. The remaining pellet was resuspended in NP40 and sonicated at low power for 5 seconds to generate the nuclear fraction. Suzuki et al. demonstrated the efficient separation of nuclear from cytoplasmic proteins with no detectible cross-contamination of the nucleoporin and lamin A/C markers or the pyruvate kinase and tubulin cytoplasmic markers (Suzuki, Bose et al. 2010). Samples underwent immunoblot analysis with antibodies recognising AR (1:2000), cytoplasm-specific MEK1 (1:4000), nuclear-specific lamin A/C (1:4000) and β-actin (1:2000). Results are representative of 2 independent experiments.

4.2.9: Matrix adhesion assay

LTV and LTC fibroblasts were plated in RPMI-1640 containing FCS at a density of $1x10^4$ cells per well in 24-well plates and were allowed to adhere for 24 h. Cells were treated with vehicle control or 10 nM DHT in PRF RPMI-1640 containing 5% DCC-FCS and 1 mM ascorbic acid, every second day for six days. Fibroblasts were removed by incubation in 100 mM EDTA for 30 mins, leaving the ECM intact in the well. PC-3 cells were plated on top of the fibroblast ECM in PRF RPMI-1640 containing 5% DCC-FCS at a density of $1x10^4$ cells per well and allowed to adhere for 4 h. Adhesion of PC-3 cells was measured as previously described, with minor modifications (Kucik and Wu 2005). Briefly, cells were washed with PBS and the remaining cells adhered to the culture plate were counted manually using the trypan blue dye exclusion assay and a haemocytometer, as described in Section 2.3.2. Results are the average of 2 independent experiments.

4.2.10: Conditioned media experiments

LTV and LTC fibroblasts were plated in RPMI-1640 containing FCS at a density of $2x10^5$ cells in 10 cm dishes and were allowed to adhere for 24 h. Cells were treated with vehicle control or 10 nM DHT in PRF RPMI-1640 containing 5% DCC-FCS for 72 h. Conditioned media was collected, centrifuged, filtered using a 0.2 µm filter and stored at -80^oC. PC-3 cells were plated in RPMI-1640 at a density of $5x10^3$ cells per well in 24-well plates and allowed to adhere for 24 h. Media was aspirated and replaced with conditioned media used in a 1:1 dilution with PRF RPMI-1640 containing 5% DCC-FCS. Cell proliferation was counted manually at D5 using the trypan blue dye exclusion assay and a haemocytometer. Results are the average of 2 independent experiments.

4.3: RESULTS

4.3.1: Characterisation of prostate fibroblasts grown long-term in curcumin.

The first experiment in this chapter aimed to establish whether curcumin tolerance or resistance was more likely to occur in response to the long-term culture of prostate fibroblasts in curcumin. To compare the relative curcumin sensitivity of LTV and LTC fibroblasts, cells were treated with 15 to 35 µM curcumin for 4 days. The doses were increased over those in Figure 3.1 to include 30 µM (the dose LTC cells were maintained in), and 35 µM (a higher dose that would define whether cells were tolerant or resistant). Two-way ANOVA analysis revealed LTV fibroblasts were significantly more sensitive to curcumin compared to LTC fibroblasts (**Figure 4.1A**; $p<0.0001$). At 30 µM, curcumin inhibited LTV viability by 80.1 ± 7.7%, while LTC fibroblasts were only inhibited by 29.0 ± 10.6%. At 35 µM, LTV viability was inhibited by 91.6 ± 2.9%, while LTC viability was inhibited by 49.4 ± 18.8%. Given LTC viability was inhibited by approximately 20% more at 35 µM than 30 µM, the cells were considered more likely curcumin-tolerant. Cell cycle analysis identified both a significant reduction in LTV fibroblasts remaining in S-phase and an increase in cells arresting in G2/M-phase after treatment with 30 µM curcumin ($p<0.001$; **Figure 4.1B**). However, there was no significant effect of curcumin treatment on S- or G2/M-phase in LTC fibroblasts. These data suggest that while chronic curcumin exposure results in fibroblasts that are less sensitive to its anti-proliferative effects, cells remain susceptible to treatment with higher doses indicating that they are tolerant rather than resistant.

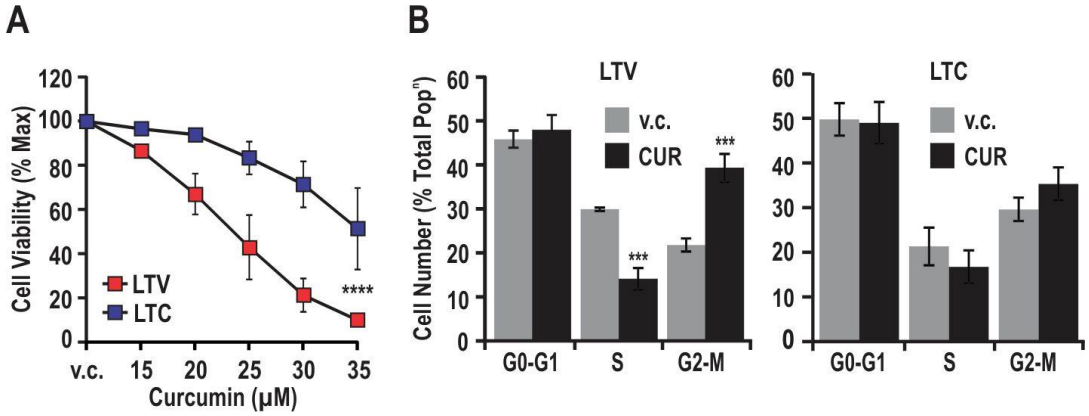

Figure 4.1: Characterisation of prostate fibroblasts grown in long-term curcumin. A: LTV and LTC fibroblasts were treated with vehicle control (v.c.) or 15 to 35 µM curcumin and cell viability was measured by MTT assay at D4. **** $p<0.0001$ (Two-way ANOVA). Data is presented as mean cell viability ± SEM, relative to the maximal response for each cell line, and is the average of 3 independent experiments. **B:** LTV and LTC fibroblasts were treated with v.c. or 30 µM curcumin (CUR) for 16 h. Cells were fixed, labelled with PI and analysed by flow cytometry. Cell cycle distribution was determined using FlowJo software. *** $p<0.001$ (Unpaired *t*-test). Data is presented as mean cell number (percentage of cells in each phase of the total population) ± SEM and is the average of 3 independent experiments.

4.3.2: Functional analysis of LTV and LTC fibroblasts.

It was hypothesised that the curcumin tolerance demonstrated in LTC fibroblasts could be due to the alteration of proteins involved in causing cell death and/or decreased curcumin cellular uptake. In Chapter 3, the BRCA1 pathway was identified to be one of the most significantly affected pathways in curcumin-treated PShTert-AR fibroblasts. Therefore this pathway was assessed again in LTV and LTC fibroblasts. There were no directional differences in curcumin response between LTV and LTC fibroblasts in terms of BRCA1, Gadd45a, CDK1, PCNA, p53 and p21 steady state protein levels (**Figure 4.2A**). Upon qualitative analysis, untreated LTC fibroblasts did show increased BRCA1 and decreased PCNA, CDK1 and p53 steady-state levels compared to LTV fibroblasts. They also demonstrated enhanced HMOX1 protein levels in response to curcumin. Curcumin uptake in LTV and LTC fibroblasts was also assessed in cells treated with vehicle control or 30 μM curcumin for 10 mins (the optimal time to capture curcumin uptake identified in Figure 3.1). However, there was no significant difference in the amount of intracellular curcumin in LTV and LTC fibroblasts (**Figure 4.2B**). The data in Figure 4.2B indicates much higher intracellular fluorescence than the data in Figure 3.2E. It is important to note that there was an extended period of time between these two sets of experiments due to flow cytometer malfunction, which may explain this. Regardless, the current data suggests that while curcumin still enters LTC fibroblasts, there may be intracellular mechanisms such as HMOX1 up-regulation and PCNA down-regulation that potentiate tolerance to curcumin.

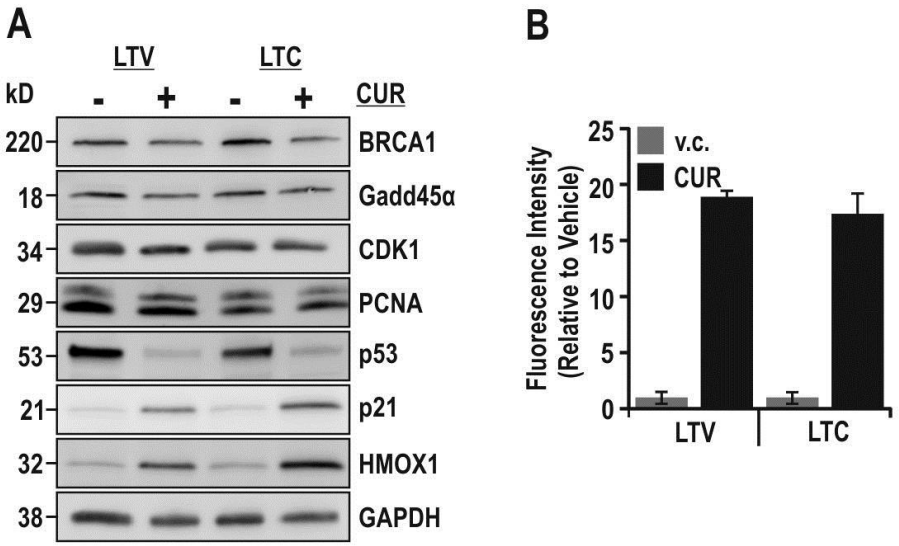

Figure 4.2: Functional analysis of LTV and LTC fibroblasts. A: LTV and LTC fibroblasts were treated with vehicle control (-) or 30 μM curcumin (CUR; +) for 16 h. Lysates were probed for BRCA1, Gadd45α, CDK1, PCNA, p53, p21, HMOX1 and GAPDH. Results are representative of 2 independent experiments**. B:** LTV and LTC fibroblasts were treated with vehicle control (v.c.) or 30 μM CUR for 10 mins. Cells were analysed for green fluorescence using flow cytometry. $p>0.05$ LTV compared to LTC (Unpaired *t*-test). Data is presented as mean fluorescence intensity ± SEM relative to the v.c. of each cell line and is the average of 3 independent experiments.

4.3.3: Genome-wide analysis of differential LTV and LTC response to curcumin.

To further investigate the changes associated with curcumin tolerance, time course microarray experiments were performed where LTV and LTC fibroblasts were treated with 30 μM curcumin for 4 to 16 h. Microarray results were validated using an independent sample set generated under identical conditions (**Figure 4.3A**). Validation results confirmed a larger increase in *HMOX1* gene expression in LTC fibroblasts (200.5-fold over vehicle at 12 h compared to 65.5-fold over vehicle in LTV fibroblasts), concomitant with the increased protein levels observed in Figure 4.2A. Analysis of the microarray revealed 2207 genes differentially expressed between LTV and LTC fibroblasts, irrespective of treatment (**Figure 4.3B**). To identify whether these genes had been associated with acquired drug resistance in the literature previously, they were crossed with genes identified by Gyorffy et al. found to be associated with resistance to at least four clinically used anti-cancer agents across 30 cancer cell lines (Györffy, Surowiak et al. 2006). This analysis revealed that 23 of the 65 genes (35.4%) identified in the Gyorffy study were also associated with curcumin tolerance in prostate fibroblasts ($p<0.0001$ Yate's chi squared**; Figure 4.3C**). The genes in common between the two studies are listed in **Table 4.1**. It is important to note that this comparison of genes was conducted on two microarray datasets that had undergone different analyses, and the number of common genes is likely to be dependent on the statistics and cut-offs used. Ingenuity pathway analysis of the 2207 genes associated with curcumin tolerance revealed eIF2 signalling (p=3.16E-16) and mTOR signalling (p=3.39E-07) as the most significantly enriched pathways differentiating LTV and LTC fibroblasts (**Table 4.2**).

Interestingly, 133 genes identified to be curcumin-responsive in LTV fibroblasts (Chapter 3) were no longer significantly responsive in LTC fibroblasts. These may represent a subset of curcumin-responsive genes where regulation by curcumin is lost with the development of tolerance (genes listed in **Table 4.3**). Pathway analysis of these genes showed ERK5 signalling (p=6E-03), p38/MAPK signalling (p=3.09E-02) and role of BRCA1 in DNA damage (p=4.67E-2) pathways to be significantly enriched (**Table 4.4**). Taken together, these data suggest that there are numerous gene expression modifications that drive the development of curcumin tolerance. Specifically, these changes appear to increase the protein synthesis capacity of tolerant fibroblasts through enhanced eIF2 and mTOR signalling, thereby allowing the proliferation of cells exposed to curcumin. Tolerance is also associated with the loss of curcumin responsiveness in a sub-set of genes, having a downstream effect on pathways that regulate DNA damage and cell death.

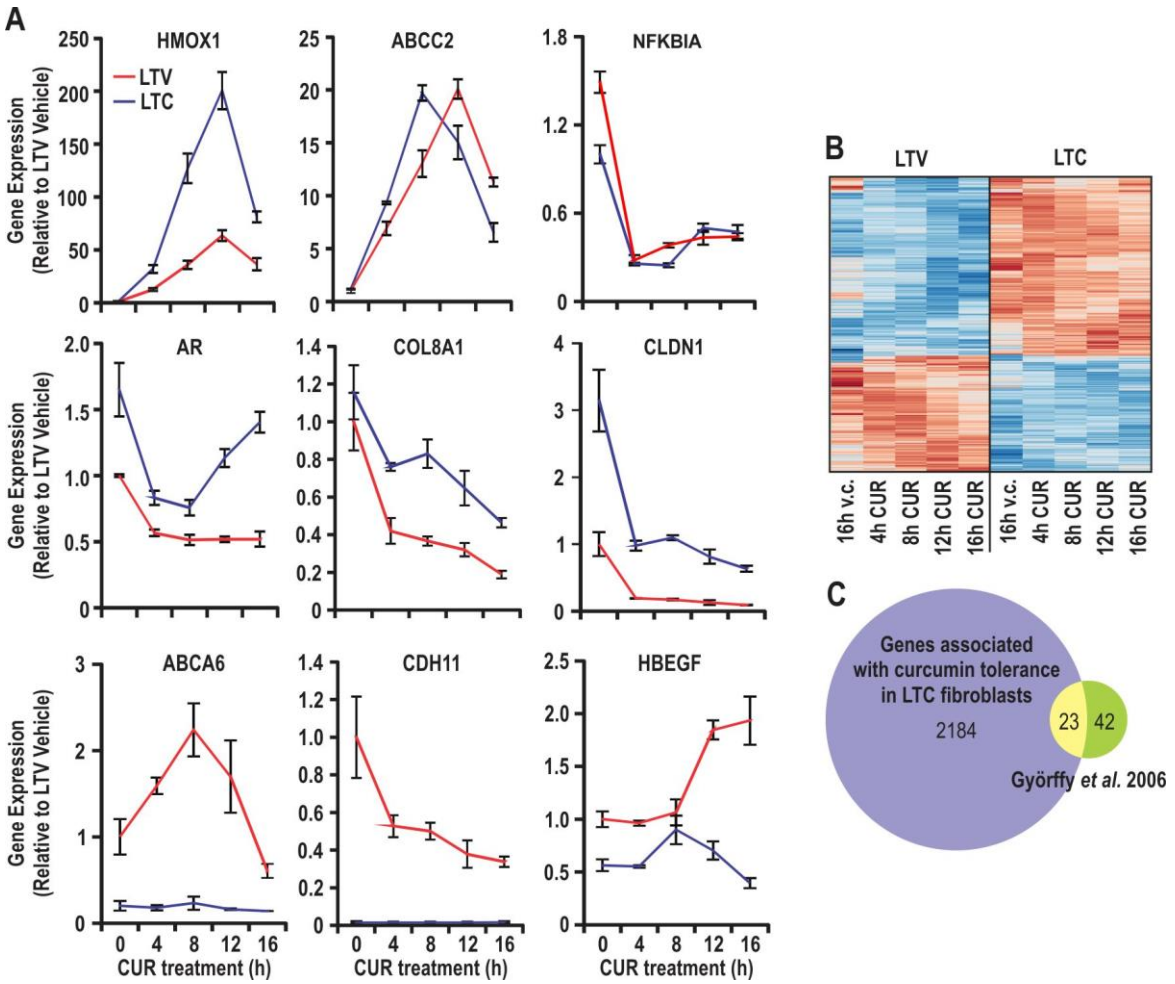

Figure 4.3: Genome-wide analysis of differential LTV and LTC response to curcumin. Triplicate RNA samples from vehicle control (v.c.) or 30 μM curcumin (CUR) treated PShTert-AR fibroblasts were pooled and analysed on Affymetrix 1.0st Gene Arrays. A cut-off of $p<0.05$ was applied to analyse genes. **A:** Microarray results were validated by qRT-PCR using an independent set of RNA produced under identical conditions. Data is presented as mean expression ± SEM relative to LTV v.c. and housekeeper genes *GAPDH* and *RPL32*. **B:** Heat map of the 2207 genes differentially expressed between LTV and LTC fibroblasts (red = up-regulated, blue = down-regulated). **C:** Twenty three out of sixty five (35%) genes identified in the Gyorffy et al. study were in common with the 2207 differentially expressed genes between LTV and LTC fibroblasts in the current study ($p<0.0001$, Yate's chi squared).

AKAP12	DUSP4	IGFBP7	SERPINE1
AOX1	ERBB3	MAGEA6	SKP2
BIRC2	FANCL	MCAM	TFPI
CTH	FDFT1	MMP1	TFPI2
DDIT4	FYN	MXI1	TRIM2
DKK3	HMGA2	SERPINB2	

Table 4.1: Genes associated with curcumin tolerance common to the drug resistance study by Gyorffy et al. The overlap in genes demonstrates some commonality between mechanisms of drug tolerance and resistance. Many of these genes have important roles in apoptosis (BIRC2), cell cycle and proliferation (DUSP4, ERBB3, SKP2), DNA damage (DDIT4, FANCL), cellular adhesion (MCAM, FYN, IGFBP7) and matrix remodelling (MMP-1).

Pathway	P value	Ratio
eIF2 Signalling	3.16E-16	2.89E-01
mTOR Signalling	3.39E-07	2.02E-01
Hepatic Fibrosis/Hepatic Stellate Cell Activation	3.47E-07	2.19E-01
Axonal Guidance Signalling	7.08E-07	1.55E-01
Regulation of eIF4 and p70S6K Signalling	1.10E-06	2.0E-01
Ephrin Receptor Signalling	7.24E-06	1.76E-01
Integrin Signalling	7.41E-05	1.78E-01
RhoGDI Signalling	5.50E-04	1.59E-01
TWEAK Signalling	8.71E-04	2.56E-01
Ephrin B Signalling	8.71E-04	2.07E-01
Signalling by Rho Family GTPases	1.02E-03	1.45E-01
Epithelial Adherens Junction Signalling	1.05E-03	1.75E-01
ILK Signalling	1.41E-03	1.56E-01
Remodelling of Epithelial Adherens Junctions	2.00E-03	2.14E-01
Actin Cytoskeleton Signalling	2.24E-03	1.45E-01
TNFR2 Signalling	4.27E-03	2.35E-01
TNFR1 Signalling	4.68E-03	2.04E-01
IL-17A Signalling in Fibroblasts	5.37E-03	2.25E-01
IL-8 Signalling	6.03E-03	1.33E-01
Regulation of Actin-based Motility by Rho	6.76E-03	1.76E-01
Death Receptor Signalling	9.12E-03	1.76E-01
Molecular Mechanisms of Cancer	1.45E-02	1.21E-01
CXCR4 Signalling	2.34E-02	1.38E-01
Androgen Signalling	2.95E-02	1.24E-01

Table 4.2: Pathway analysis of genes associated with curcumin tolerance in prostate fibroblasts. Analysis revealed eIF2 and mTOR signalling as the most significant pathways associated with curcumin tolerance. These pathways are heavily involved in cellular proliferation and protein synthesis.

ABCA6	CDCA2	ETS2	IL8	MRM1	RBMY1A1	STK38
AGBL3	CDCA4	FABP4	KIF18B	MSC	RFPL4A	SUV39H1
AKAP6	CDCA8	FAM117B	KRTAP2-4	MTBP	RNF34	TAF7L
ALKBH2	CHAC1	FAM154A	LDHC	MTERFD1	ROPN1L	TCF21
AMIGO2	CHAF1A	FAM154B	LEAP2	NAV3	RPL34	THBS1
ANKFN1	CKAP2L	FAM209A	LINC00152	OASL	RPS6KA5	TLL2
ANKRD45	COA5	FAM5C	LINC00161	OLR1	RSPH10B	TMCO2
ARHGAP11B	CPNE9	FANCL	LINC00310	OSGIN2	SCARNA17	TMEM60
AURKB	CREB5	FERMT3	LOC285033	PARP2	SEMA7A	TNC
BARD1	CRTAM	FILIP1L	LRFN5	PDCD1LG2	SERPINB10	TNFRSF11B
BORA	CYP2R1	FNDC7	LRRFIP1	PDE7B	SERPINE1	TRNAU1AP
C17orf53	DDIT4	FOXR2	MAFF	PDIA6	SH3D19	TROAP
C1orf189	DET1	GABRE	MAP1A	PDLIM5	SKA1	TTK
C5orf34	E2F8	GRID2	MASTL	PIP5K1A	SKA3	UGCG
C5orf4	EGF	GTSE1	MCM10	PMAIP1	SLC25A37	VPS33B
C5orf64	ELTD1	HIST1H2AK	MCOLN3	PNLDC1	SLC26A2	ZNF334
CARD16	EML1	IER3	MIR224	POLH	SNORA21	ZNF623
CCNF	ENC1	IL33	MOBP	PPP1R27	SNORA62	ZNF780B
CD274	EPHA7	IL6	MPZL2	PRKCG	SPHK1	ZNF93

Table 4.3: Genes no longer curcumin-responsive in tolerant fibroblasts. There were 2207 genes differentially expressed between LTV and LTC fibroblasts. Of these, 133 genes that were significantly affected by curcumin in LTV fibroblasts (Chapter 3) were no longer significantly affected in LTC fibroblasts. These may represent a subset of curcumin-responsive genes where regulation is lost with the development of curcumin tolerance.

Pathway	P value	Ratio
Bladder Cancer Signalling	1.62E4	5.15E-02
Hepatic Cholestasis	1.26E3	2.73E-02
Hepatic Fibrosis	1.26E3	3.23E-02
IL-6 Signalling	4.57E3	3.23E-02
ERK5 Signalling	6.03E3	4.41E-02
HMGB1 Signalling	1.66E2	2.75E-02
HGF Signalling	2.00E2	2.70E-02
ERK/MAPK Signalling	2.34E2	1.90E-02
p38 MAPK Signalling	3.09E2	2.50E-02
Role of BRCA1 in DNA Damage Response	4.68E2	2.82E-02

Table 4.4: Pathway analysis of genes no longer curcumin-responsive in tolerant fibroblasts. Analysis revealed decreased ERK5, p38 MAPK and BRCA1 signalling to be associated with the development of curcumin tolerance. MAPK signalling (including ERK5) is involved in regulating cellular proliferation, differentiation, survival and apoptosis in eukaryotes.

4.3.4: Functional implications of curcumin tolerant prostate fibroblasts on PC-3 cells.

The microarray analysis conducted in this study also revealed a number of static gene changes between LTV and LTC fibroblasts, identified by comparison of the vehicle treatment groups. Specifically, there were differences between LTV and LTC expression of ECM-regulating genes *COL1A2* ($p<0.01$), *VCAN* (not significant) and *COL4A6* ($p<0.001$), validated by qRT-PCR (**Figure 4.4A**). Unpublished data from our laboratory has shown that when PShTert-AR fibroblasts are treated with DHT, they secrete an ECM more adhesive to cancer cells than vehicle treatment (Leach et al.). Experiments were therefore conducted to measure PC-3 cell adherence to ECM secreted by LTV and LTC fibroblasts in the presence of DHT. PC-3 cells were significantly more adherent to ECM secreted from DHT-treated LTV fibroblasts compared to vehicle-treated LTV fibroblasts ($p<0.05$; **Figure 4.4B**). There was no significant difference, however, in PC-3 adherence to LTC fibroblast ECM in response to DHT.

Further, the microarray data revealed differences in the expression of secreted growth factor genes *EGF* ($p<0.001$), *FGF1* (not significant) and *HGF* ($p<0.001$) between LTV and LTC fibroblasts, also validated by qRT-PCR (**Figure 4.4C**). The influence of secreted growth factors on PC-3 cell proliferation was subsequently investigated using conditioned media from both LTV and LTC fibroblasts. The presence of fibroblast conditioned media decreased the overall growth of PC-3 cells compared to the non-conditioned media control. In the presence of LTV conditioned media, PC-3 cell growth was significantly less than the control ($p<0.01$; **Figure 4.4D**), however there was no significant difference between PC-3 growth in LTC conditioned media and the control. Taken together, these data further support the notion that LTC fibroblasts have undergone changes in gene expression in response to ongoing curcumin treatment, including genes responsible for growth factor expression and ECM composition. These changes may play a functional role in enhancing prostate cancer cell proliferation and reducing adhesion to surrounding matrix.

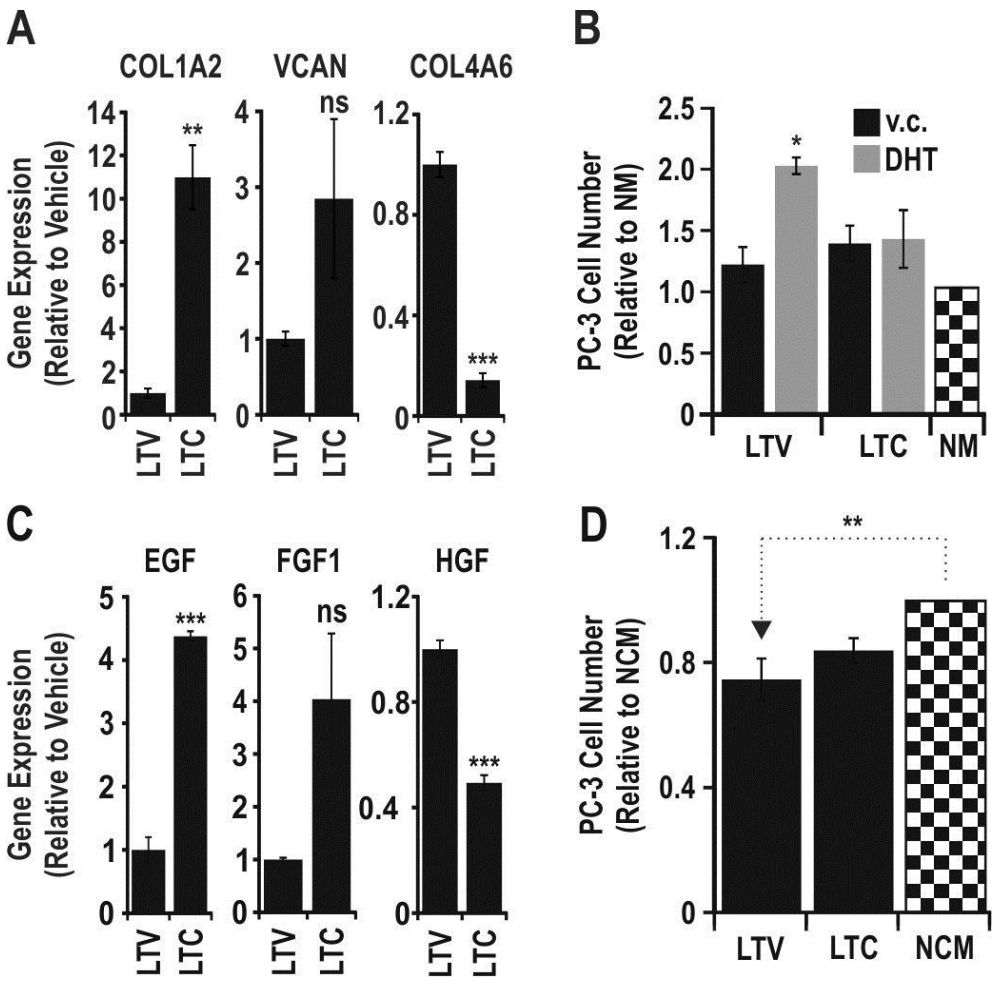

Figure 4.4: Functional implications of curcumin tolerance in prostate fibroblasts on PC-3 cells. A: LTV and LTC fibroblasts were treated with vehicle control (v.c.) for 16 h and *COL4A6, VCAN* and *COL1A2* expression was measured by qRT-PCR. ** p<0.01 *** p<0.001 LTC compared to LTV (Unpaired *t*-test). Data is presented as mean expression ± SEM relative to LTV v.c. and reference genes *GAPDH* and *RPL32,* and represents microarray validation. **B:** Cultured LTV and LTC fibroblasts were treated with v.c. or 10 nM DHT for 6 days. Cells were removed from the culture dish and PC-3 cell attachment to the deposited ECM was counted using trypan blue dye exclusion after 4 h. * p<0.05 LTV DHT compared to LTV v.c. (Unpaired *t*-test). Data is presented as mean cell number ± SD relative to no matrix (NM) and LTV v.c., and is the average of 2 independent experiments **C:** LTV and LTC fibroblasts were treated with v.c. for 16 h and *EGF, FGF* and *HGF* expression was measured by qRT-PCR. *** p<0.001 LTC compared to LTV (Unpaired *t*-test). Data is presented as mean expression ± SEM relative to LTV v.c. and reference genes *GAPDH* and *RPL32,* and represents microarray validation. **D:** Cultured LTV and LTC fibroblasts were treated with v.c. or 10 nM DHT for 72 h. Fibroblast-conditioned and non-conditioned control media was placed on PC-3 cells in a separate plate and PC-3 cell proliferation was measured at D5. Bars represent DHT-conditioned media only. ** p<0.01 LTV compared to non-conditioned media (NCM), p>0.05 LTC compared to NCM (Unpaired *t*-test). Data is presented as mean cell number ± SEM relative to NCM and is the average of 2 independent experiments.

4.3.5: The effect of curcumin tolerance on AR signalling in prostate fibroblasts.

Androgen signalling plays an important role in prostate fibroblast function. The observation that DHT-treated, LTC-derived ECM did not significantly increase PC-3 adhesion over vehicle (Figure 4.4B) indicated a potential impairment to androgen signalling with the development of curcumin tolerance. To investigate this further, the 133 genes no longer significantly curcumin-responsive in LTC fibroblasts (Table 4.3) were overlapped with microarray data previously generated in our laboratory where PShTert-AR fibroblasts were treated with vehicle control or DHT (Leach et al.; 2612 genes identified with a log fold-change greater than ± 0.5 over vehicle). Interestingly, 54/133 genes (40.6%) were androgen-regulated in PShTert-AR fibroblasts ($p<0.0001$ Yate's chi squared; **Figure 4.5A**; common genes listed in **Table 4.5**). Androgen signalling in LTV and LTC fibroblasts was therefore further analysed using AR transactivation assays.

First, the transfection efficiency between LTV and LTC fibroblasts was compared to ensure any effect seen in the transactivation assay was due to differences in AR activity alone. A standard curve using an eGFP vector was chosen over the pLG4.14-PB3Luc vector to ensure efficiency was measured independent of AR activity. The amount of pLG4.14-PB3Luc DNA used in this thesis (50 ng in a 96-well plate) was approximately equivalent to 250 ng eGFP (250 ng in a 24-well plate). Two-way ANOVA analysis demonstrated no significant differences between the transfection efficiencies of LTV and LTC fibroblasts, despite a small difference between the two cell lines at 500 ng DNA (**Figure 4.5B**). Figure 4.5B presents data as the amount of GFP as a percentage of the maximum GFP taken up by cells. LTV and LTC fibroblasts were then assessed for AR transactivation activity in response to DHT, alone or in combination with curcumin. Two-way ANOVA analysis demonstrated a significant reduction in LTV AR transactivation with curcumin and DHT in combination compared to DHT treatment alone ($p<0.0001$; **Figure 4.5C**). However there was no reduction in LTC AR transactivation activity with curcumin and DHT in combination, suggesting that curcumin was no longer able to decrease DHT-mediated activity in LTC fibroblasts. Interestingly, at 100 nM DHT treatment alone there was 75.4 ± 1.3% less AR transactivation activity in LTC compared to LTV fibroblasts ($p<0.0001$). Immunoblot analysis of the transactivation assay lysates confirmed similar AR levels across vehicle-treated LTV and LTC fibroblasts (**Figure 4.5C**). To gain a better perspective of the difference in AR activity between LTV and LTC fibroblasts, data from Figure 4.5C was presented relative to each cell line's vehicle control. At 100 nM DHT, curcumin reduced LTV AR transactivation by 26.5 ± 4.3% while in LTC fibroblasts only 11 ± 6.8% inhibition was observed (**Figure 4.5C**). While the AR transactivation studies may have been somewhat affected by the small difference in transfection efficiency highlighted in Figure 4.5B, it is unlikely to account for the profound differences observed between LTV and LTC fibroblasts in Figure 4.5C. Curcumin had little

effect on cell viability over the 20 h treatment period, eliminating the possibility that a decrease in AR activity was due to a decrease in cell number (**Figure 4.5D**). While there was a significant difference in cell viability between DHT treatment alone and in combination with curcumin for LTV ($p<0.01$) and LTC ($p<0.05$) fibroblasts, this significance was presumably due to differences at low DHT concentrations which could not explain the profound effect observed in Figure 4.5C at 10 to 100 nM DHT.

ABCA6	CD274	ENC1	KIF18B	PDCD1LG2	SNORA62
AMIGO2	CDCA2	EPHA7	KRTAP2-4	PDE7B	SPHK1
ARHGAP11B	CDCA4	FAM117B	LRRFIP1	PDLIM5	SUV39H1
AURKB	CDCA8	GRID2	MASTL	POLH	TCF21
BARD1	CHAF1A	GTSE1	MCM10	SEMA7A	THBS1
C17orf53	CKAP2L	HIST1H2AK	MTBP	SH3D19	TNC
C5orf34	DDIT4	IER3	MTERFD1	SKA1	TNFRSF11B
C5orf4	E2F8	IL6	NAV3	SKA3	TROAP
CCNF	ELTD1	IL8	PARP2	SLC26A2	TTK

Table 4.5: Androgen and curcumin-regulated genes no longer curcumin-responsive in tolerant fibroblasts.

Next, cells were assessed for DHT responsiveness in terms of gene expression (*AR* and androgen-regulated genes *FBXO32* and *FKBP51*). Two-way ANOVA analysis revealed no differences in *AR* gene expression with DHT treatment in LTV or LTC fibroblasts (**Figure 4.5E**). At 10 nM DHT, LTV fibroblasts demonstrated a 7.0-fold increase in *FBXO32* expression while only a 2.1-fold increase was observed in LTC fibroblasts ($p<0.001$; **Figure 4.5E**). Similarly at 10 nM DHT, LTV fibroblasts demonstrated a 16.0-fold increase in *FKBP51* expression while only a 9.6-fold increase was observed in LTC fibroblasts (not significant, **Figure 4.5E**). Analysis of steady-state protein levels for AR and FKBP51 supported mRNA results, demonstrating AR stabilisation and FKBP51 induction with DHT treatment across both cell lines. The transactivation assay results and qRT-PCR data presented above indicate that curcumin tolerance causes a decrease in androgen responsiveness, the ability of AR to regulate gene expression and the ability for curcumin to reduce DHT-mediated AR transactivation.

To gain an understanding for the mechanism behind the loss of androgen responsiveness observed in LTC fibroblasts, chromatin immunoprecipitation was performed at a site on the regulatory region of the androgen-regulated gene *FKBP51*. As described in Figure 3.4D, LTV fibroblasts demonstrated a significant increase in AR binding to *FKBP51* upon DHT treatment ($p<0.0001$; 14.8-fold over vehicle) and decrease in binding when curcumin was added to DHT ($p<0.01$). In LTC fibroblasts, however,

there was no difference in the amount of AR binding to *FKBP51* in response to DHT alone or in combination with curcumin. The lack of AR binding to this site in LTC fibroblasts may be a potential mechanism for decreased AR activity. It was therefore hypothesised that the reduction in AR DNA binding may be due to defects in cytoplasmic-nuclear AR translocation, which was subsequently assessed by cell fractionation and immunoblot. In vehicle-treated cells, AR was predominately localised in the cytoplasmic compartment in both LTV and LTC fibroblasts, as expected (**Figure 4.5G**). In response to 4 h DHT treatment, AR localised predominantly within the nucleus in both cell lines, with no apparent reduction in cytoplasmic AR levels in either cell line. Curcumin treatment decreased both nuclear and cytoplasmic AR levels in LTV and LTC fibroblasts compared to vehicle control, and DHT in combination with curcumin restored nuclear AR translocation without altering cytoplasmic AR levels in either cell line. It is important to note that the comparisons made were across treatments in LTV and LTC fibroblasts, and data should not be compared between the cellular fractions as they were assessed on different blots. Taken together, these data suggest that the impairment in AR signalling caused by curcumin tolerance may be due to decreased AR binding to DNA, despite AR nuclear translocation remaining intact. However, there are other possibilities that require exploration in future experiments, including the effect of curcumin on the distribution of AR binding sites and AR pioneer factors, and the timing of AR nuclear translocation in response to curcumin and androgen treatment. Further, analysis of MEK in the nuclear fraction and LMNA in the cytoplasmic fraction should be made to ascertain the level of contamination between cellular compartments.

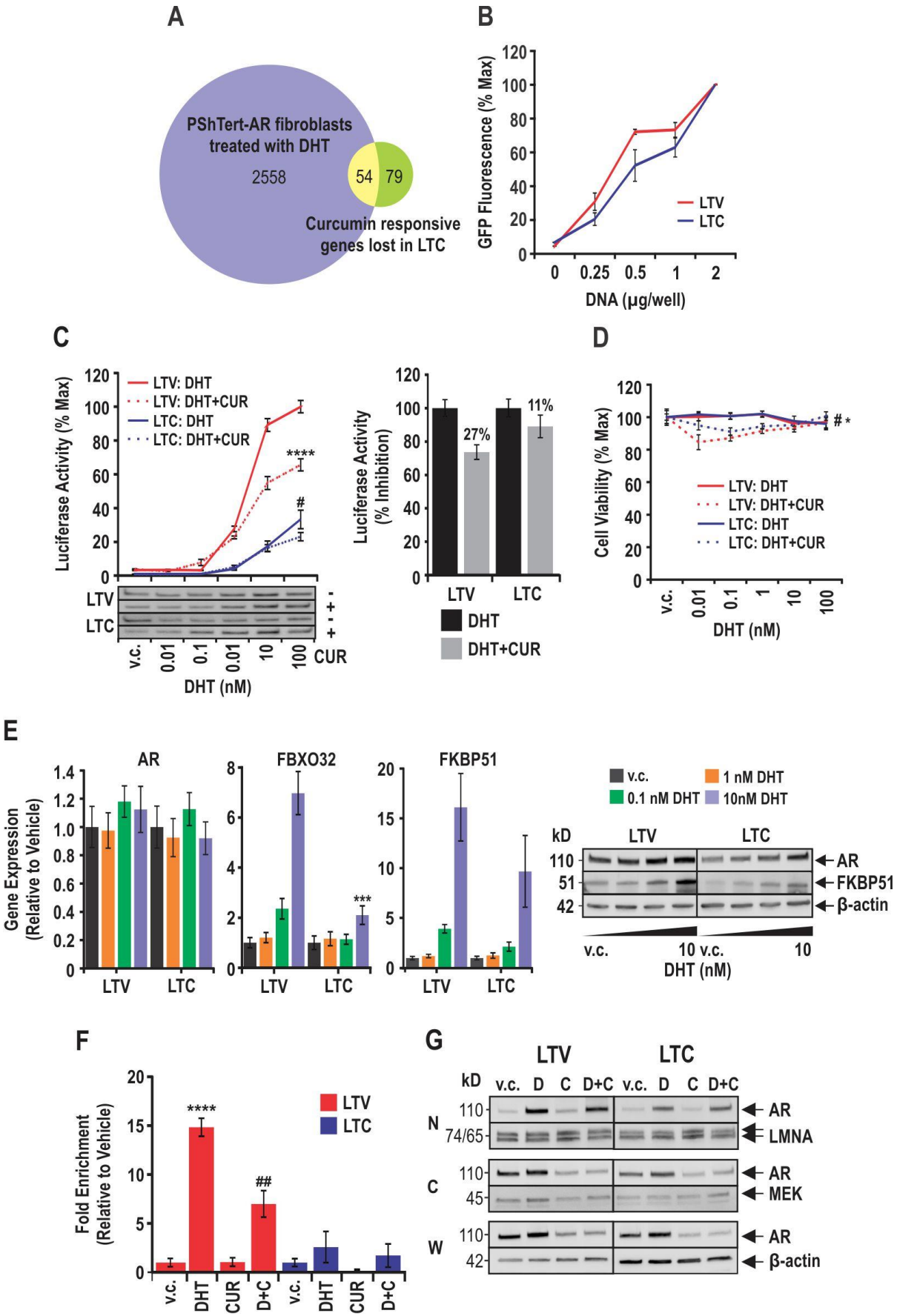
A
PShTert-AR fibroblasts treated with DHT
2558
54
79
Curcumin responsive genes lost in LTC
B
GFP Fluorescence (% Max)
DNA (µg/well)
LTV
LTC
C
Luciferase Activity (% Max)
LTV: DHT
LTV: DHT+CUR
LTC: DHT
LTC: DHT+CUR
DHT (nM)
CUR
Luciferase Activity (% Inhibition)
27%
11%
DHT
DHT+CUR
D
Cell Viability (% Max)
DHT (nM)
E
AR
FBXO32
FKBP51
Gene Expression (Relative to Vehicle)
v.c.
1 nM DHT
0.1 nM DHT
10nM DHT
kD
AR
FKBP51
β-actin
F
Fold Enrichment (Relative to Vehicle)
G
N
C
W
AR
LMNA
MEK
β-actin

Figure 4.5 The effect of curcumin tolerance on AR signalling in prostate fibroblasts. A: One hundred and thirty three curcumin-responsive genes no longer regulated in LTC fibroblasts were crossed with genes that were androgen-regulated in the original PShTert-AR fibroblast cell line. Of them, 92 genes (69%) were in common between the two datasets ($p<0.0001$; Yate's chi squared). **B:** LTV and LTC fibroblasts were transfected with 0 to 2 µg eGFP vector and GFP fluorescence was measured by flow cytometry. $p>0.05$ LTC compared to LTV (Two-way ANOVA). Data is presented as mean GFP fluorescence ± SD relative to the maximal response of each cell line and is the average of 2 independent experiments. **C:** Top panel: LTV and LTC fibroblasts were transfected with 50 ng androgen-responsive pLG4.14-PB3Luc and treated with vehicle control (v.c.) or 1 to 100 nM DHT in the presence or absence of 10 µM curcumin (CUR) for 20 h. **** $p<0.0001$ LTV DHT compared to DHT+CUR (Two-way ANOVA), # $p<0.0001$ LTV DHT compared to LTC DHT (Two-way ANOVA). Data is presented as mean luciferase activity ± SEM relative to the maximal LTV response and is the average of 5 independent experiments. Bottom panel: Lysates from transactivation assays were collected and probed for AR. Data is representative of 2 independent experiments. **D:** LTV and LTC fibroblasts were treated as described in Figure 4.5C and viability was measured by MTT assay at 20 h. * $p<0.01$ LTV DHT compared to DHT+CUR; # $p<0.05$ LTC DHT compared to DHT+CUR (Two-way ANOVA). Data is presented as mean cell viability ± SEM relative to the v.c. of each cell line and is representative of 2 independent experiments. **E:** LTV and LTC fibroblasts were treated with v.c. or 0.1 to 10 nM DHT and *AR*, *FBXO32* and *FKBP51* gene expression was measured by qRT-PCR. ** $p<0.01$ LTV compared to LTC (Two-way ANOVA). Data is presented as mean expression ± SEM relative to the v.c. of each cell line and housekeeping gene *GAPDH*. Data is representative of 2 independent experiments. Immunoblot analysis for AR, FKBP51 and β-actin supports mRNA results and is representative of 2 independent experiments. **F:** LTV and LTC fibroblasts were treated with v.c., 10 nM DHT, 30 µM CUR or the combination of DHT and CUR (D+C) and chromatin immunoprecipitation was performed at a regulatory region in the *FKBP51* gene. **** $p<0.0001$ LTV DHT compared to LTV v.c. (Unpaired *t*-test), ## $p<0.01$ LTV DHT+CUR compared to LTV DHT (Unpaired *t*-test). Data is presented as mean AR fold-enrichment ± SEM relative to v.c., total DNA input and expression of non-specific binding region NC2, and is the average of 4 independent experiments. Note: LTV data was already presented in Figure 3.4D and was used in this figure for comparative purposes. Experiments on LTV and LTC were conducted at the same time. **G:** LTV and LTC fibroblasts were treated with v.c., 10 nM DHT, 30 µM CUR or D+C for 4 h and immunoblot for AR was performed in nuclear (N), cytoplasmic (C) and whole (W) cell fractions. LMNA and MEK were used as respective nuclear and cytoplasmic-specific controls, and β-actin was used as the whole lysate loading control. Data is representative of 2 independent experiments.

4.3.6: The reversible nature of curcumin tolerance.

To establish whether curcumin tolerance was reversible and whether this impacted AR signalling, curcumin was withdrawn from LTC fibroblasts for a minimum of four weeks (cells termed LTC-w). This process caused curcumin-tolerant fibroblasts to return to their original sensitivity, where approximately 80% of cells died when treated with 30 μM curcumin (**Figure 4.6A**; $p>0.05$ compared to LTV). All experiments comparing LTV, LTC and LTC-w were completed concurrently, but have been separated into two figures for simplicity. The transfection efficiency of LTC-w fibroblasts was not significantly different to LTV or LTC fibroblasts (**Figure 4.6B**). Two-way ANOVA analysis demonstrated no significant ability of curcumin to reduce DHT-mediated AR transactivation in LTC-w fibroblasts (**Figure 4.6C**). When assessing the relative difference in AR activity between 100 nM DHT alone and in combination with curcumin, LTC-w fibroblasts demonstrated a 21 ± 8.2% decrease in AR activity with curcumin compared to 26.5 ± 4.3% (LTV) and 11.0 ± 6.8% (LTC) shown in Figure 4.5C. It appeared that some DHT responsiveness had returned to LTC-w fibroblasts, with significantly more AR activity upon DHT treatment compared to LTC fibroblasts ($p<0.0001$). Immunoblot analysis of the transactivation assay lysates confirmed no visible increases in AR levels across treatments (**Figure 4.6C**). Curcumin had no effect on cell viability over the 20 h treatment period used, again eliminating the possibility that a decrease in AR activity was due to a decrease in cell number (**Figure 4.6D**).

LTC-w fibroblasts were also assessed for DHT responsiveness in terms of gene expression (*AR* and androgen-regulated genes *FBXO32* and *FKBP51*). Two-way ANOVA analysis revealed no differences in *AR*, *FBXO32* or *FKBP51* gene expression compared to LTV fibroblasts (**Figure 4.6E**). At 10 nM DHT, LTC-w fibroblasts demonstrated an 8.8-fold increase in *FBXO32* expression (compared to 7.0-fold in LTV) and a 14.6-fold increase in *FKBP51* expression (compared to 16.0-fold in LTV). Analysis of steady-state protein levels for AR and FKBP51 supported mRNA results, demonstrating AR stabilisation and FKBP51 induction with DHT treatment in LTC-w fibroblasts. In summary, curcumin sensitivity in LTC fibroblasts appears transient, and may be restored by removal of curcumin from the culture media. In this scenario, DHT-mediated AR transactivation activity and regulation of genes partially returns, however curcumin remains unable to decrease DHT-mediated AR transactivation activity.

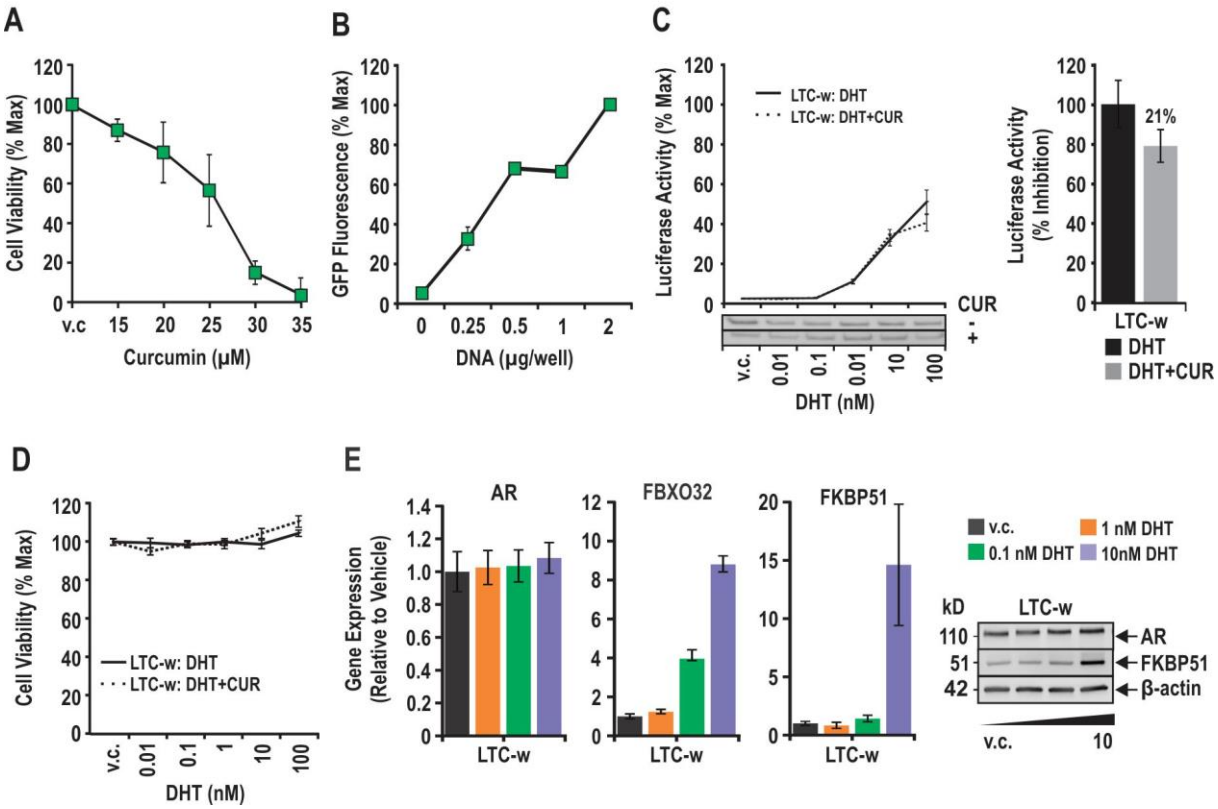

Figure 4.6: The effect of reversed curcumin tolerance on AR signalling in prostate fibroblasts. LTC-w fibroblasts were generated by withdrawing LTC fibroblasts from curcumin for four weeks. **A**: LTC-w fibroblasts were treated with vehicle control (v.c.) or 15 to 35 μM curcumin and cell viability was measured by MTT assay at D4. $p>0.05$ LTC-w compared to LTV (Two-way ANOVA; not shown on figure). Data is presented as mean viability ± SEM relative to the maximal response and is the average of 3 independent experiments. **B:** LTC-w fibroblasts were transfected with 0 to 2 μg eGFP vector and GFP fluorescence was measured by flow cytometry. $p>0.05$ LTC-w compared to LTV and LTC (Two-way ANOVA). Data is presented as mean GFP expression ± SD and is the average of 2 independent experiments. **C:** Top panel: LTC-w fibroblasts were transfected with 50 ng androgen responsive pLG4.14-PB3Luc and treated with v.c. or 1 to 100 nM DHT in the presence or absence of 10 μM curcumin for 20 h. $p>0.05$ DHT+CUR compared to DHT (Two-way ANOVA), $p<0.0001$ LTC-w DHT compared to LTC DHT (Two-way ANOVA, not shown on figure). Data is presented as mean luciferase activity ± SEM relative to the LTV maximal response and is the average of 3 independent experiments. Bottom panel: Lysates from transactivation assays were collected and probed for AR. Data is representative of 2 independent experiments **D:** LTC-w fibroblasts were treated as described in Figure 4.6C and viability was measured by MTT assay at 20 h. $p>0.05$ DHT compared to DHT+CUR (Two-way ANOVA). Data is presented as mean cell viability ± SEM relative to v.c. and is representative of 2 independent experiments. **E:** LTC-w fibroblasts were treated with v.c. or 0.1 to 10 nM DHT and *AR*, *FKBP51* and *FBXO32* gene expression was measured by qRT-PCR. $p>0.05$ LTC-w compared to LTV (Two-way ANOVA; not shown on figure). Data is presented as mean expression ± SEM relative to v.c. and housekeeping gene *GAPDH*. Data is the average of 2 independent experiments. Immunoblot analysis for AR, FKBP51 and β-actin supports mRNA results and is representative of 2 independent experiments.

4.4: DISCUSSION

Current knowledge relating to drug tolerance and resistance in cancer has largely been derived from early studies characterising antibiotic resistance. These studies clearly and categorically defined antibiotic tolerance and resistance as separate processes; tolerance involving the survival of phenotypic variants and resistance involving mutational target modification and drug efflux (Lewis 2013). Indeed, similarities between drug-tolerant cancer cells and bacteria have been discussed previously (Sharma, Lee et al. 2010, Dawson, Intapa et al. 2011, Lambert, Estévez-Salmeron et al. 2011, Glickman and Sawyers 2012). However the concept of drug-tolerant cancer cells is quite new, and there is a paucity of literature characterising them. The data presented in this chapter demonstrates, for the first time, evidence indicating curcumin tolerance in prostate fibroblasts that are treated chronically with curcumin.

The cell viability experiments performed in this chapter revealed two observations indicating that fibroblasts had become curcumin tolerant rather than resistant. First, a proportion of tolerant fibroblasts died in response to a dose higher than the maintenance dose. Second, the tolerance observed in prostate fibroblasts was shown to be reversible, with removal of curcumin from culture medium restoring curcumin sensitivity. These factors, combined with no observable differences in curcumin uptake between tolerant and sensitive cells, fit the definition of drug tolerance more so than resistance. The development and mechanisms of drug tolerance in cancer cells are only beginning to emerge, and the results from this study are at least partly supported by other studies investigating drug tolerance in cancer cells (Sharma, Lee et al. 2010, Yan, Chen et al. 2011). Interestingly, Sharma et al. described a sub-population of reversibly drug-tolerant human lung cancer cells. Specifically, treatment of cells with a tyrosine kinase inhibitor caused rapid death, but consistently left a small viable drug-tolerant population, termed drug-tolerant persister (DTP) cells. While most DTPs did not proliferate, there were a proportion of DTPs termed drug-tolerant expanded persisters (DTEPs) that continued to proliferate normally in the presence of drug, demonstrating 500-fold less sensitivity than the original cells. Following drug withdrawal, DTEPs remained resistant for up to 90 cell divisions, after which drug sensive cells dominated the population. A schematic from the proposed process is presented in **Figure 4.7**.

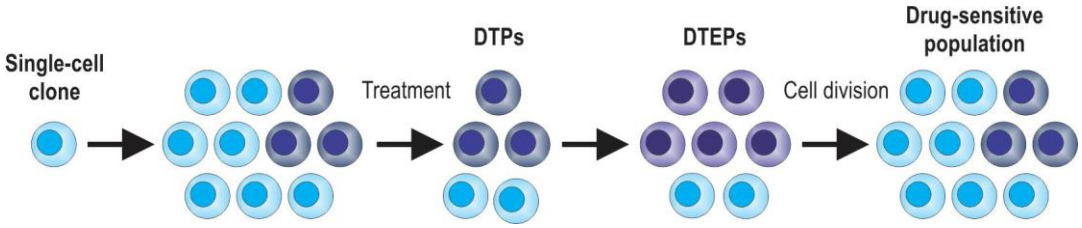

Figure 4.7: Desensitisation and resensitisation of cancer cells, as proposed by Sharma et al. The expansion of a single-cell clone from a drug-sensitive cancer cell line generates a population of cells called drug-tolerant persisters (DTPs). This population can be expanded in the presence of drug to yield a population of drug-tolerant expanded persisters (DTEPs), that remain drug-resistant following withdrawal of drug until sensitive cells outnumber them.

Results from the Sharma et al. study highlight the possibility that DTPs and DTEPs were also involved in the curcumin tolerance observed in prostate fibroblasts. While the technique for generating tolerance in the current study is a well-described technique for generating acquired drug resistance, future studies may benefit from adaptation of the Sharma et al. technique where cells were repeatedly treated with drug in the same plate, resulting in the isolation and subsequent expansion of approximately 50 tolerant clones after 30 days of treatment. Confirmation of DTPs may be gained from assessing IGF-1 receptor activity in curcumin-tolerant fibroblasts, as activation has been observed in drug tolerance and resistance studies previously (Chakravarti, Loeffler et al. 2002, Buck, Eyzaguirre et al. 2008, Dallas, Xia et al. 2009, Eckstein, Servan et al. 2009, Sharma, Lee et al. 2010). In the current study, LTC-w fibroblasts were cultured in curcumin-free media for eight passages before being re-assessed for sensitivity. Future studies may also benefit from re-assessing tolerant fibroblasts at more regular intervals following withdrawal of curcumin to more accurately gauge when sensitivity is reversed.

The reversal of curcumin tolerance observed in this study begs the question whether the transcriptomic changes associated with tolerance are also reversed when cells transition back to a sensitive state. This may lead to the identification of curcumin-mediated genomic plasticity. Indeed, the plasticity of human ovarian cancer genomes in adapting to changes in the environment has recently been established (Hoogstraat, De Pagter et al. 2014). To further investigate the potential for curcumin-mediated genomic plasticity, future experiments should assess a panel of genes in LTC-w fibroblasts that were differentially expressed between LTV and LTC fibroblasts. Reversible curcumin tolerance potentially indicates that curcumin use in patients may follow the “re-treatment response” observation where patients who respond well to treatment and who later experience treatment failure demonstrate good secondary responses after a break from the drug (Cara and Tannock 2001, Kurata, Tamura et al. 2004, Yano, Nakataki et al. 2005). Drug cycling has previously proven

successful in prostate cancer patients, with various cyclical androgen depletion strategies causing successive declines in PSA level (Feltquate, Nordquist et al. 2006). While the current observation is in a fibroblast model, it certainly warrants further investigation in cancer cells.

Future clinical studies should be aware of the potential implications of curcumin tolerance, particularly for prostate cancer. First, co-culture studies suggested that curcumin-tolerant fibroblasts may promote cancer growth and a loss of cancer cell adhesion to ECM through alterations to collagens, potentially creating an environment permissive of metastasis. The COL1A2 gene encodes Collagen Type I, a fibrillar collagen found in most connective tissues, and the COL4A6 gene encodes a chain of Collagen Type IV, the major structural component of basement membranes. While the relevance of each individual gene alteration remains unclear, functional studies in this chapter demonstrate that curcumin-tolerant fibroblasts deposit a different ECM to non-tolerant fibroblasts, with potential implications for cancer growth. The ability of curcumin to target collagen synthesis was described in Chapter 3, and it is entirely feasable that long-term curcumin treatment of prostate fibroblasts may modify the composition of ECM. Future studies may analyse the differences between the matrices further, possibly using proteomics or secretomics. Second, curcumin-tolerant fibroblasts demonstrated decreased AR function and the impairment of AR activity. As discussed in Chapter 3, targeting the AR signalling axis in both compartments of the prostate may be advantageous, but also warrants careful consideration due to the dual roles of fibroblast AR in cancer initiation and progression. The development of curcumin tolerance in men with intact prostates, either as a supplement or neoadjuvant, could potentially contribute to prostate cancer progression. Curcumin may therefore be better used in combination with hormonal therapy in advanced disease where the prostate microenvironment is no longer present.

Microarray profiling of curcumin-tolerant fibroblasts revealed a moderate percentage of genes in common with the Györffy drug resistance study (Györffy, Surowiak et al. 2006). Likewise, four genes that differentiated curcumin tolerance from sensitivity (*RBBP4*, *AK2*, *RABEPK* and *BTAF1*) were also associated with curcumin resistance in a study using the NCI60 panel of cell lines (Sertel, Eichhorn et al. 2012). Retinoblastoma-binding protein 4 (RBBP4) is involved in histone acetylation, chromatin assembly and transcriptional silencing (Yarden and Brody 1999, Nicolas, Morales et al. 2000). The differential expression of RBBP4 in the current study is interesting given epigenetic alterations have also been linked to drug resistance (Glasspool, Teodoridis et al. 2006, Sharma, Lee et al. 2010). Further, eight out of 35 genes differentiating breast CAFs before and after chemotherapy were associated with curcumin tolerance in the current study (Rong, Kang et al. 2013). These

comparisons suggest that there may be some commonality between genes involved in cancer cell drug tolerance and resistance, regardless of the drug.

Microarray analysis also revealed the differential expression of numerous stress response and cell death-mediating genes between curcumin-tolerant and -sensitive fibroblasts. The transcription factor NF-κB (*NFKBIA*) is involved in cellular response to stress, and plays an important role in tumour development and progression through consitutive activation (Liu, Chiang et al. 2012). Inhibition of NF-κB and members of its signalling pathway are central to curcumin efficacy in most cell lines and clinical studies (Aggarwal, Kumar et al. 2003). Interestingly, curcumin-tolerant fibroblasts displayed comparatively lower *NFKBIA* gene expression in untreated samples compared to sensitive fibroblasts. As outlined in the previous chapter, HMOX1 (haem oxygenase 1 or heat-shock protein 32) is also a stress response gene known to be one of the most highly up-regulated genes in response to curcumin treatment (Bachmeier, Mohrenz et al. 2008, Panchal, Vranizan et al. 2008, Thangapazham, Shaheduzzaman et al. 2008, Rozzo, Fanciulli et al. 2013). Over-expression of *HMOX1* is reported to provide cancer cells and fibroblasts protection against various forms of DNA damage, and inhibitors have been shown to restore cell death (Rothfuss and Speit 2002, Mayerhofer, Gleixner et al. 2008, Rushworth and MacEwan 2008, Scharstuhl, Mutsaers et al. 2009). In this study, curcumin-tolerant fibroblasts showed almost four-fold more *HMOX1* gene expression in response to curcumin than sensitive fibroblasts. Interestingly, higher Hsp70 production in curcumin-resistant cancer cell lines has been shown to protect cells from apoptosis (Khar, Ali et al. 2001). Future studies investigating the effect of HMOX1 knockdown or HMOX1 inhibitors on reversing curcumin tolerance are warranted. Taken together, these data suggest that alterations in stress response and cell death-mediating genes are likely to contribute to curcumin tolerance in prostate fibroblasts by providing mechanisms for cytoprotection against curcumin.

Protein synthesis pathways mTOR and eIF2 signalling were also strongly associated with curcumin tolerance. Uncontrolled cell growth and proliferation is characteristic of all cancers, which is dependent on the rate of protein synthesis (Rosenwald 1996). Protein synthesis occurs in three stages: initiation, elongation and termination, where initiation is the most complex and tightly regulated step (Hershey 1991). Up-regulation of protein synthesis, a hallmark of cancer, is due to the increased expression and function of translation initiation factors such as eIF2. The role of translation initiation factors are to escort initiation specific forms of transfer RNA onto the ribosome and identify the translational start site (Rosenwald, Hutzler et al. 2001). Indeed, transient curcumin treatment has previously been shown to target the mTOR pathway and down-regulate eIF2 protein expression in other forms of cancer (Beevers, Li et al. 2006, Beevers, Chen et al. 2009, Chen, Tian et al. 2010,

Sun, Chen et al. 2011). It is possible that curcumin-tolerant fibroblasts have developed an enhanced protein synthesising capacity to survive high doses of curcumin. The development of curcumin tolerance may be inhibited by the combination of curcumin and mTOR inhibitors, however drugs targeting mammalian protein synthesis are often very toxic.

In summary, the findings of this chapter provide proof of principle that curcumin tolerance may be achieved in prostate fibroblasts. Tolerance is characterised by a decrease in the proportion of cells dying in response to curcumin, which may be attenuated with higher doses, and a loss of responsiveness to curcumin-responsive genes charactersied in sensitive fibroblasts. Microarray analysis provided a broad mechanistic insight into the mechanisms of curcumin tolerance, including enhanced protein synthesis and alterations in the activity of stress response genes. This chapter also explored the decrease in AR activity associated with curcumin tolerance, and identified potential implications of tolerance in terms of enhancing cancer cell proliferation and decreasing adhesion to the surrounding microenvironment. The data presented in this chapter provides important considerations for current and future curcumin use in men with prostate cancer.

CHAPTER 5

THE EFFICACY OF CURCUMIN IN COMBINATION WITH DROZITUMAB

5.1: INTRODUCTION

Curcumin has been subject to a large amount of *in vitro* investigation across multiple prostate cancer cell lines, however there has been relatively few studies using prostate cancer animal models to verify efficacy. A review of the literature reveals that while curcumin-mediated prevention of prostate cancer is most often studied using transgenic mice (Barve, Khor et al. 2008, Narayanan, Nargi et al. 2009), most studies investigating curcumin as a treatment employ xenograft models. One of the earliest studies demonstrated that 2% dietary curcumin over six weeks caused a significant decrease in LNCaP xenograft proliferation and micro-vessel density, as well as an increase in tumour cell apoptosis (Dorai, Cao et al. 2001). Another study used a PC-3 xenograft model to examine how the timing of curcumin treatment via intraperitoneal (i.p.) injection may impact efficacy (Khor, Keum et al. 2006). A daily dose of 8 µg/kg for four weeks commencing one day prior to tumour inoculation significantly decreased tumour growth, while the same dose given three times weekly for four weeks commencing three weeks following tumour inoculation was insufficient to decrease tumour growth. Further, the effect of curcumin on prostate cancer invasiveness has been investigated using a DU-145 xenograft model (Hong, Ahn et al. 2006). The study demonstrated that 5 mg/kg curcumin administered three times weekly for four weeks via oral gavage caused a significant reduction in both tumour volume and MMP-2 and MMP-9 activity. Most recently, curcumin significantly reduced the size of C4-2 xenografts with a single 1 g/kg intratumoural injection 40 days following tumour inoculation, and also reduced the size of PC-3 xenografts following 100 mg/kg i.p curcumin administered daily for three weeks, two weeks following tumour inoculation (Sundram, Chauhan et al. 2012, Cheng, Chen et al. 2013). Taken together, these data suggest that curcumin does show efficacy in various xenograft models of prostate cancer, however factors such as cell line, dose, administration method and timing of treatment appear to be important factors for efficacy.

Despite the promising preclinical evidence for curcumin efficacy, clinical trials to date have been disappointing. This has been clear since 2001 when peak curcumin excretion was shown two hours following treatment, resulting in little effect on pre-cancerous lesions at a dose of 12 grams daily (Chen, Hsu et al. 2001). There are currently three active clinical trials assessing curcumin in men with prostate cancer. However, the pilot data for the first of those trials appears disappointing (Hejazi, Rastmanesh et

al. 2013). Briefly, 40 prostate cancer patients undergoing radiotherapy were given three grams of curcumin daily for 20 weeks. This dose caused no differences to urinary, bowel or treatment-related symptoms compared to placebo. One criticism of the clinical trials conducted since the Chen et al. study is the use of low curcumin doses, especially when 12 grams of daily curcumin has already proven ineffective.

To combat disappointing results in clinical trials, curcumin is now being utilised and administered differently via methods that were discussed in Section 1.5.4. One example is combination studies that manipulate the ability of curcumin to re-sensitise drug-resistant cancer cells to therapy. This has been observed with various chemotherapeutics, but the example most pertinent to this chapter is the combination of curcumin with death ligand TRAIL. Recombinant soluble TRAIL has shown promising anti-cancer activity in preclinical studies and has been well tolerated in Phase I trials due to its ability to induce apoptosis in cancer cells with minimal toxicity to normal cells (Wiley, Schooley et al. 1995, Pitti, Marsters et al. 1996, Pan, Ni et al. 1997, Ashkenazi, Pai et al. 1999, Walczak, Miller et al. 1999, Herbst, Eckhardt et al. 2010). However many types of cancer have shown resistance to TRAIL-induced apoptosis through both innate and acquired mechanisms, including the presence of decoy receptors (Thakkar, Chen et al. 2001, Voelkel-Johnson, King et al. 2002, Riccioni, Pasquini et al. 2005, Zhang and Fang 2005, Sallman, Chen et al. 2007). Resistance to TRAIL has been attenuated by curcumin across numerous cancer cell lines. Specifically, curcumin re-sensitised TRAIL-resistant breast cancer cell lines MCF-7, T47D and SK-BR-3 to TRAIL-mediated apoptosis via enhanced mobilisation of DR5 to the plasma membrane (Park, Cho et al. 2013). Similarly, curcumin was shown to restore TRAIL-induced cytotoxicity in TRAIL-resistant LNCaP cells by down-regulation of NF-κB, a factor known to cause TRAIL resistance (Deeb, Jiang et al. 2004, Braeuer, Büneker et al. 2006). These findings were validated in an LNCaP xenograft model where curcumin up-regulated DR4 and DR5 expression, and inhibited NF-κB activation (Shankar, Chen et al. 2007, Shankar, Ganapathy et al. 2008). The up-regulation and mobilisation of DR4 and DR5, combined with inactivation of NF-kB, are therefore possible mechanisms behind TRAIL resensitisation.

The data surrounding curcumin and TRAIL suggest that curcumin may be better used in combination rather than as a monotherapy for the treatment of cancer. Drozitumab, as outlined in Section 1.6.4, is a monoclonal DR5 antibody with more potent activity than TRAIL. This is due to a higher binding affinity for DR5 (with undetectable binding to DR4 and decoy receptors), and a serum half-life of up to 20 days compared to 30 minutes for TRAIL (Salvesen and Duckett 2002, Plummer, Attard et al. 2007, Takeda, Okumura et al. 2007, Adams, Totpal et al. 2008, Hanahan and Weinberg 2011Hanahan, 2000 #676). The aim of this chapter is therefore to investigate whether curcumin can re-sensitise drozitumab-

resistant prostate cancer cells to drozitumab-mediated apoptosis, using both cell line studies and a xenograft model.

5.2: MATERIALS AND METHODS

5.2.1: Cell culture and reagents

Human luciferase-expressing prostate PC-3 cells (PC-3-luc) were generated and maintained as described in Section 2.3.1 (Zinonos, Labrinidis et al. 2009). The PC-3 cell line was chosen on the basis of unpublished data from the Evdokiou laboratory demonstrating higher drozitumab resistance and DR5 protein levels in PC-3 compared to LNCaP and DU-145 cells (Liapis et al.). Curcumin, drozitumab, goat anti-human IgG $F_c\gamma$ fragment and ZVAD-fmk were stored as described in Section 2.3.1. For all *in vitro* experiments, drozitumab was cross-liked with goat anti-human IgG $F_c\gamma$ fragment for 30 mins at 4^oC before use to ensure DR5 aggregation at the cell surface (Adams, Totpal et al. 2008). The dose of 100 ng/mL (used in the Evdokiou laboratory) was converted to 700 nM for consistency within this thesis.

5.2.2: Cell viability assays

PC-3-luc cells were plated in RPMI-1640 containing 5% FCS at a density of 1×10^4 cells per well in 96-well culture plates and allowed to adhere for 24 h. Culture medium was aspirated and cells were treated with (1) vehicle control or 10 to 50 μM curcumin alone or in combination with 700 nM drozitumab, (2) vehicle control or 700 nM drozitumab in combination with increasing amounts of IgG $F_c\gamma$ antibody, (3) vehicle control or 0.25 to 4 μM curcumin or (4) vehicle control, 10 to 50 μM curcumin or 44 to 700 nM drozitumab. All treatments were for 48 h, and cell viability was measured by MTT assay as described in Section 2.3.2. Results are the average of 2 independent experiments.

5.2.3: Flow cytometry

For Annexin/PI assays, PC-3-luc cells were plated in RPMI-1640 containing FCS at a density of 2×10^5 cells per well in 6-well plates. Cells were treated with (1) vehicle control or 10 to 30 μM curcumin for 24 h or (2) vehicle control, 20 μM curcumin, 700 nM drozitumab or the combination of curcumin and drozitumab for 24 h. The 24 h time-point was used to capture cells while they were in the process of dying. Results are the average of 2 independent experiments. Cells were prepared and analysed as described in Section 3.2.4. For detection of DR5, cells were plated and treated as described above (2) and harvested as described in Section 3.2.5. Cells were stained with 0.25 μg PE-conjugated human anti-DR5 antibody per sample, and were analysed for PE fluorescence using DIVA and FlowJo software. Results are the average of 2 independent experiments.

5.2.4: Animal study

Male five-week old athymic nude mice were acclimatised to the animal housing facility for a minimum of one week prior to experimentation. Mice were housed under pathogen-free conditions and general physical well-being and animal weight was monitored continuously throughout the experiment. All experimental procedures on animals were carried out with strict adherence to the rules and guidelines

for the ethical use of animals in research, and were approved by the University of Adelaide Animal Ethics Committees and the Institute of Medical and Veterinary Science. PC-3-luc cells were cultured in RPMI-1640 containing FCS in T150 flasks until they reached approximately 80% confluence. Cells were removed from flasks with 3 mL trypsin-EDTA, centrifuged and resuspended in 2 mL PBS at 5×10^4 cells per 25 µL. Matrigel-HC (2mL) was added to the cells and the cell suspension remained on ice during the procedure. Mice were anaesthetised with isoflurane and the flanks wiped with ethanol. A 25-gauge needle was inserted into the flank and 50 µL of cell suspension was injected. Mice were allowed to recover under a heat lamp before being transferred into cages. Mice were randomly assigned into six treatment groups each consisting of eight mice, and treatment commenced three days following tumour inoculation. Treatment groups were as follows: vehicle control (corn oil only), low curcumin (50 mg/kg), high curcumin (100 mg/kg), drozitumab (3 mg/kg), low curcumin and drozitumab, and high curcumin and drozitumab. Curcumin was administered three times weekly via i.p. injection while drozitumab was given once weekly via i.p. injection. Intraperitoneal injection was chosen over dietary curcumin to facilitate more efficient drug delivery and a reproducible dose to the tumour site. Non-invasive, whole body imaging was conducted weekly to monitor PC-3-luc bioluminescence using the Xenogen IVIS 100 Imaging System. Mice were injected with 100 µL D-luciferin via i.p. injection at a final dose of 150 mg/kg (as per the manufacturer's instructions) and then anaesthetised with isoflurane. Images were acquired for between one and 30 secs from the front angle, and the photon emission transmitted from mice was captured and quantitated in photons/s/cm^2/sr using Xenogen Living Image software. On the final day of imaging, mice were sacrificed and the tumours were harvested and weighed. The lungs and livers were also harvested and imaged separately for the presence of metastases for between one sec and five mins.

5.2.5: Histology and immunohistochemistry

Tumours were fixed, embedded, cut and stained as described in Section 2.3.9. Primary antibodies were applied in the following dilutions: mouse anti-Ki67 (1:500), rabbit anti-DR5 (1:100) and mouse anti-HMOX1 (1:50). Sections were imaged using a Nanozoomer digital slide scanner and analysed using NDP Scan software. For positive Ki67 staining, three random 0.25cm^3 areas from vehicle and drozitumab-treated groups (eight per group) were selected at 10x magnification and positive cells were counted using Image J.

5.3: RESULTS

5.3.1: Effect of curcumin, alone and in combination with drozitumab, on PC-3-luc cell viability.

Unpublished data from the Evdokiou laboratory shows that treatment-naïve PC-3-luc cells are relatively resistant to drozitumab, with approximately 10 to 15% cell death observed following 700 nM treatment for 48 h (Liapis et al.). To establish whether curcumin could re-sensitise PC-3-luc cells to drozitumab-induced apoptosis, cells were treated with 10 to 50 μM curcumin both alone and in combination with 700 nM drozitumab for 48 h. At 20 μM curcumin cell viability was inhibited by 33.5 ± 10.3%, which increased to 67.6 ± 7.7% when in combination with 700 nM drozitumab (**Figure 5.1A**). Two-way ANOVA analysis revealed a significant difference between treatment with curcumin alone and the combination of curcumin and drozitumab ($p<0.01$). A dose of 20 μM curcumin was therefore chosen for future experiments as higher doses (40 to 50 μM) were considered too toxic.

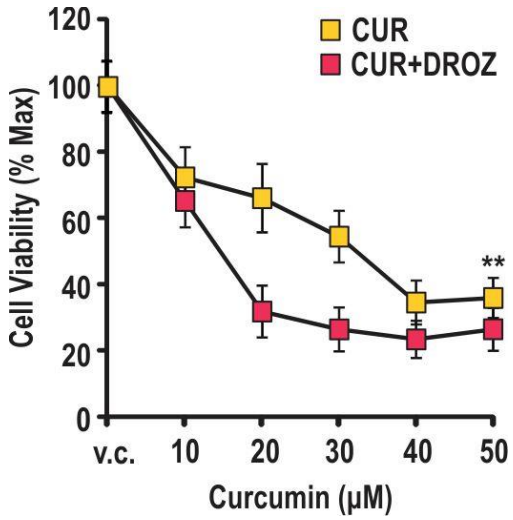

Figure 5.1: Effect of curcumin, alone and in combination with drozitumab, on PC-3-luc cell viability. PC-3-luc cells were treated with vehicle control (v.c.) or 10 to 50 μM curcumin (CUR) either alone or in combination with 700 nM drozitumab (DROZ). Cell viability was measured by MTT assay at D2. ** $p<0.01$ CUR compared to CUR+DROZ (Two-way ANOVA). Data is presented as mean cell viability ± SEM relative to the maximal response and is the average of 2 independent experiments.

5.3.2: Effect of curcumin, alone and in combination with drozitumab, on PC-3-luc apoptosis.

As described in Section 1.5.1, the mechanism of curcumin-induced cell death is a highly debated topic in the literature. It was therefore necessary to gain an understanding for how curcumin causes cell death in PC-3-luc cells, despite some evidence already pointing to apoptosis (Liu, Wang et al. 2011). Cells were treated with vehicle control or 10 to 30 μM curcumin for 24 h and analysed for apoptosis using Annexin V/PI assay. Firstly, the lack of PI staining across all samples indicated no presence of necrosis and minimal cellular debris. Further, less than 5% of vehicle-treated cells were undergoing apoptosis in any given experiment, which was considered the basal level of cell death. All doses of

curcumin significantly increased the proportion of apoptotic cells over vehicle, with 10 μM curcumin causing apoptosis in 9.3 ± 1.9% of the population and 20 and 30 μM curcumin causing apoptosis in 19.1 ± 3.7% and 19.1 ± 3.6% of the population respectively ($p<0.05$; **Figure 5.2A**). This was paired with a significant decrease in the proportion of healthy cells at all curcumin concentrations compared to vehicle ($p<0.05$; **Figure 5.2B**). Visual representation of the dot-plots generated using flow cytometry is provided in **Figure 5.2C**. Next, apoptosis was assessed in PC-3-luc cells treated with vehicle control, 20 μM curcumin, 700 nM drozitumab and the combination of curcumin and drozitumab to establish whether the combination could increase apoptosis over either agent alone. The combination caused significantly more apoptosis than drozitumab alone ($p<0.0001$; **Figure 5.2D**). While curcumin and drozitumab alone caused 12.5 ± 0.8% and 25.7 ± 0.95% apoptosis respectively, the combination caused apoptosis in 49.3 ± 3.5% of the cell population. There was also a concomitant reduction in the healthy fraction of cells between drozitumab alone and the combination ($p<0.0001$; **Figure 5.2E**). Visual representation of the dot-plots generated using flow cytometry is provided in **Figure 5.2F**.

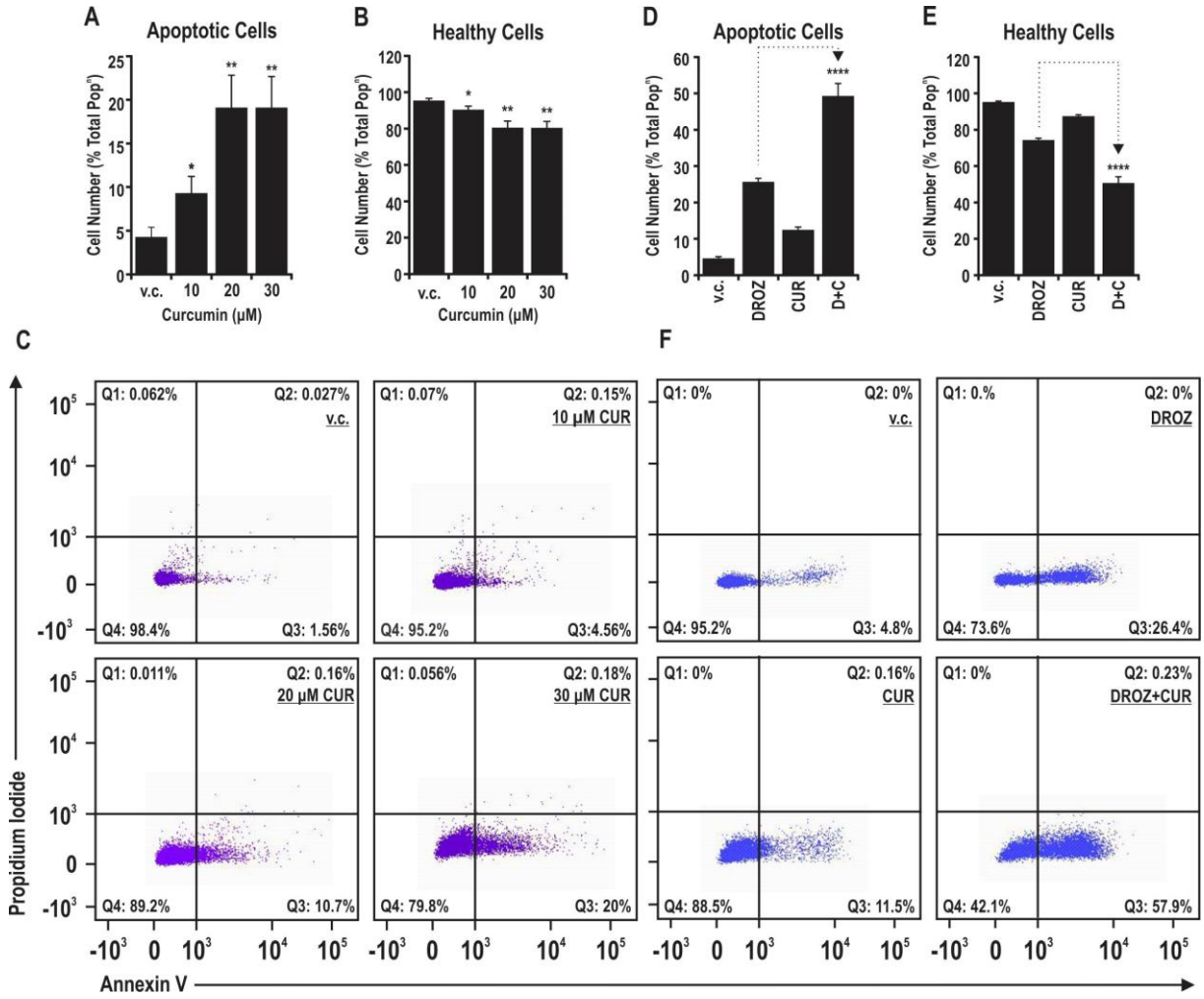

Figure 5.2: Effect of curcumin, alone and in combination with drozitumab, on PC-3-luc apoptosis. **A-B**: PC-3-luc cells were treated with vehicle control (v.c.) or 10 to 30 μM curcumin (CUR) for 24 h. Cells were labelled with Annexin V/PI and assessed for apoptosis by flow cytometry. * $p<0.05$; ** $p<0.01$ CUR compared to v.c. (Unpaired *t*-test). Data is presented as mean cell number (apoptotic or healthy) as a percentage of the population ± SEM and is the average of 2 independent experiments. **C**: Representative dot plots demonstrating the dose-dependent increase in apoptosis in CUR-treated PC-3-luc cells. **D-E**: PC-3-luc cells were treated with v.c., 700 nM drozitumab (DROZ), 20 μM CUR or the combination (DROZ+CUR) for 24 h and were assessed for apoptosis as described above. ** $p<0.01$ DROZ+CUR compared to DROZ (Unpaired *t*-test). Data is presented as mean cell number (apoptotic or healthy) as a percentage of the population ± SEM and is the average of 2 independent experiments. **F**: Representative dot plots demonstrating DROZ+CUR causing more apoptosis than CUR or DROZ alone.

5.3.3: Mechanisms of drozitumab resensitisation in PC-3-luc cells.

As described previously, there is much debate surrounding whether curcumin-mediated cell death is caspase-dependent or independent. To determine whether apoptosis in PC-3-luc cells was caspase-dependent, cells were treated with 10 μM zVAD-fmk (pan caspase inhibitor), 20 μM curcumin or the combination of curcumin and zVAD-fmk (**Figure 5.3A**). Treatment with zVAD-fmk alone had no effect on cell viability and, as expected, 20 μM curcumin moderately inhibited cell viability (29.1 ± 7.8%; $p<0.05$). Interestingly, however, zVAD-fmk in combination with curcumin did not significantly restore cell viability to vehicle level (24.0 ± 9.1%), suggesting curcumin-mediated cell death is caspase-independent in PC-3-luc cells. Further, a number of studies have observed death receptor up-regulation upon curcumin treatment. As DR5 is the target of drozitumab, the effect of curcumin on membrane-bound DR5 expression was measured by flow cytometry (**Figure 5.3B**). Curcumin-treated cells demonstrated 2.5-fold up-regulation of DR5 over vehicle-treated cells ($p<0.0001$). Likewise, the combination of curcumin and drozitumab up-regulated DR5 3.2-fold over vehicle ($p<0.0001$). Visual representation of the histograms generated using flow cytometry is provided in **Figure 5.3C**.

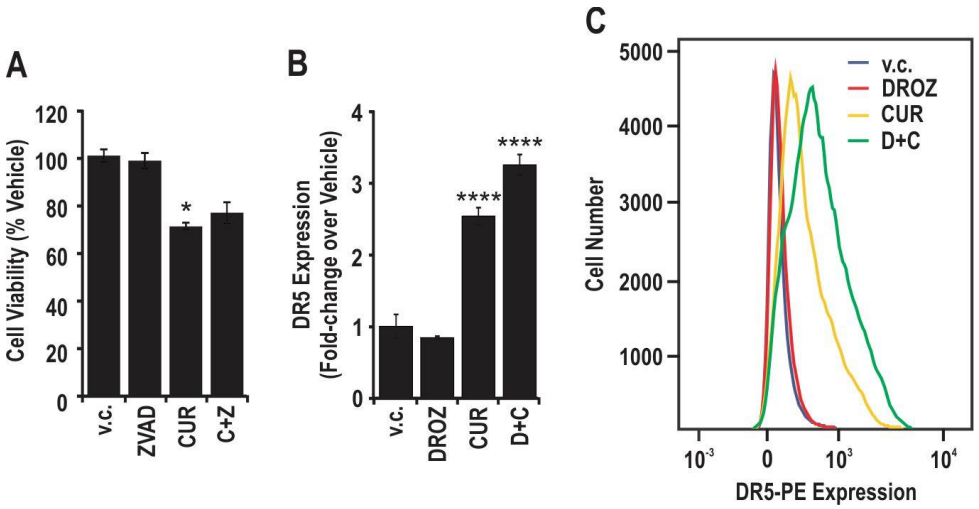

Figure 5.3: Mechanisms of drozitumab resensitisation in PC-3-luc cells. **A**: PC-3-luc cells were treated with vehicle control (v.c.), 10 μM zVAD-fmk, 20 μM curcumin (CUR) or the combination of CUR and zVAD-fmk (C+Z). Cell viability was assessed by MTT assay at D2. *$p<0.05$ CUR compared to v.c. (Unpaired *t*-test). Data is presented as mean cell survival ± SEM relative to v.c. and is the average of 2 independent experiments. **B**: PC-3-luc cells were treated with v.c., 700 nM DROZ, 20 μM CUR or the combination of drozitumab and curcumin (D+C) and were examined for DR5 expression using flow cytometry. **** $p<0.0001$ CUR and D+C compared to v.c. (Unpaired *t*-test). Data is presented as mean DR5-PE expression ± SEM relative to v.c. and is the average of 2 independent experiments. **C**: Representative histogram demonstrating the CUR-induced increase in DR5 expression in PC-3-luc cells.

5.3.4: Optimisation of a PC-3-luc xenograft model.

In order to evaluate the above observations *in vivo*, a PC-3-luc xenograft model was established. The sub-cutaneous (s.c.) xenograft model was chosen over orthotopic or genetically engineered prostate cancer models because it had already been established in the Evdokiou laboratory, was considered likely to metastasise and was cost effective and time efficient. Unfortunately, this meant the role of the prostate microenvironment could not be considered. Prior to this animal study, there were no peer-reviewed articles assessing the effect of curcumin on PC-3 xenografts so an optimisation study was initially undertaken. A luciferase assay revealed that PC-3-luc cells maintained strong luciferase expression after thawing (**Figure 5.4A**). Based on the Evdokiou xenograft model protocol, four male BALB/c nude mice were injected into the flank with 1×10^5 PC-3-luc cells in 100 µL Matrigel-HC via s.c. injection. The time-line for this study is presented in **Figure 5.4B**. Ten days post-inoculation, mice underwent non-invasive bioluminescence imaging (BLI) repeatedly over a 50 min time course to establish when optimal tumour bioluminescence occurred following D-luciferin injection (**Figure 5.4C**). The data indicated that the optimal time to image mice was 10 min post-injection. Mouse 4 presented with no signal, likely due to improper injection of D-luciferin, and was subsequently removed from the figure. From D10 to D19, two mice were treated with vehicle control (mice 1 and 4) and two mice were treated with 50 mg/kg curcumin (mice 2 and 3) by i.p. injection five times (approximately every second day). The growth of PC-3-luc tumours was aggressive in all mice, and by D21 tumour volume was greater than 1 cm^3 and mice had to be sacrificed. Tumour growth is demonstrated by representative bioluminescence images (**Figure 5.4D**), and quantification of tumour size over the experimental period (**Figure 5.4E**). The small number of animals used in this optimisation study, combined with inexperience in performing s.c. injections, gave rise to the variable luciferase activity evident in Figures 5.4C-E. Importantly, all mice maintained their weight over the experimental period indicating that curcumin treatment was well tolerated (**Figure 5.4F**).

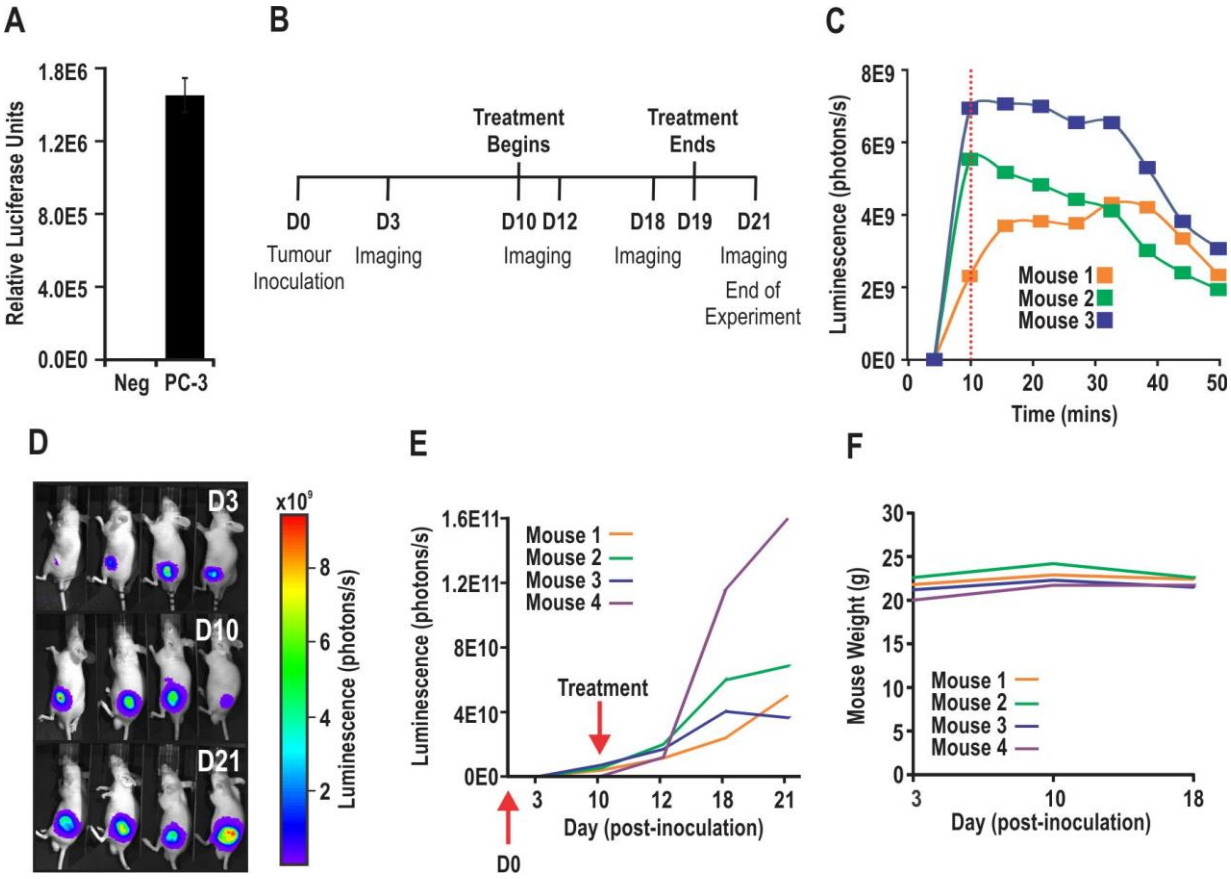

Figure 5.4: Optimisation of a PC-3-luc xenograft model. Four six-week old male BALB/c nude mice were injected sub-cutaneously into the flank with 1×10^5 PC-3-luc cells in 100 µL Matrigel-HC (D0). Mice were treated with either 50 mg/kg curcumin (CUR: mice 2 and 3) or equivalent vehicle control (v.c.: mice 1 and 4) via intraperitoneal injection on D10, D12, D14, D17 and D19. Mice were imaged on D3, D10, D12, D18 and D21 using the Xenogen IVIS 100 bioluminescence imaging system and were sacrificed on D21. **A**: PC-3-luc cells were thawed, lysed and assessed for luciferase activity. Data is presented as mean relative luciferase units ± SEM of 3 technical replicates. **B**: Time-line for the study. **C**: On D10, mice were injected i.p. with D-luciferin and tumour bioluminescence was measured over a time course of 50 mins to ascertain the optimal timing for future experiments. Data is presented as luminescence (photons/s) over the 50 min time period. **D**: Representative bioluminescence images of PC-3-luc tumours from each mouse at D3, D10 and D21. **E**: Growth of PC-3-luc tumours in mice. Data is presented as luminescence (photons/s) over the 21 day time period. **F**: Mouse weights over the experimental period. Data is presented as weight (g) on D3, 10 and 18.

5.3.5: The effect of curcumin, drozitumab, and the combination on tumour burden *in vivo.*

To examine whether the curcumin-mediated resensitisation of drozitumab-resistant PC-3-luc cells could be replicated *in vivo*, the PC-3-luc xenograft model established above was used with minor modifications. In order to extend the experimental time-frame to approximately five weeks, 5×10^4 PC-3-luc cells were injected with 50 µL Matrigel-HC into mice by s.c. injection. Two doses of curcumin were chosen: 50 mg/kg and 100 mg/kg. These were based on effective doses found in non-prostate xenograft studies (Choi, Chun et al. 2006, Su, Yang et al. 2010, Chen, Lai et al. 2012, Datta, Halder et al. 2013). Treatment commenced on D3 post-inoculation rather than D10, as curcumin was shown to be less effective in reducing the size of established tumours (Khor, Keum et al. 2006). The dose of drozitumab (3 mg/kg) was selected from a previous breast cancer xenograft study (Zinonos, Labrinidis et al. 2009). A time-line for the study is presented in **Figure 5.5A**. The take-rate for PC-3-luc xenografts was 100%. Mouse weight was maintained for the duration of the experiment, indicating all treatments were well tolerated (**Figure 5.5B**). The more dramatic increase in mouse weight observed in Figure 5.5B compared to Figure 5.4F was most likely because the experiment was conducted over a longer time-frame, and tumour sizes were much larger. Tumour growth was measured by BLI (**Figure 5.C**) and calliper measurements (**Figure 5.5D**), both producing congruent results. By D31, neither 50 nor 100 mg/kg curcumin treatment significantly altered tumour growth compared to vehicle control. Surprisingly however, drozitumab treatment had reduced tumour volume by an average of 78.1 ± 5.6% compared to vehicle at D31 ($p<0.01$). While 50 mg/kg curcumin in combination with drozitumab also significantly decreased tumour growth (62.8 ± 11.1%; $p<0.05$), this could not be attributed to curcumin given the marked efficacy of drozitumab alone. *Ex vivo* tumour wet weights supported the BLI and calliper results, yet there were no significant differences in tumour weight between any of the treatment groups (**Figure 5.5E**). Drozitumab-treated mice, however, demonstrated an average 46.1 ± 8.7% reduction in wet tumour weight compared to vehicle at D31.

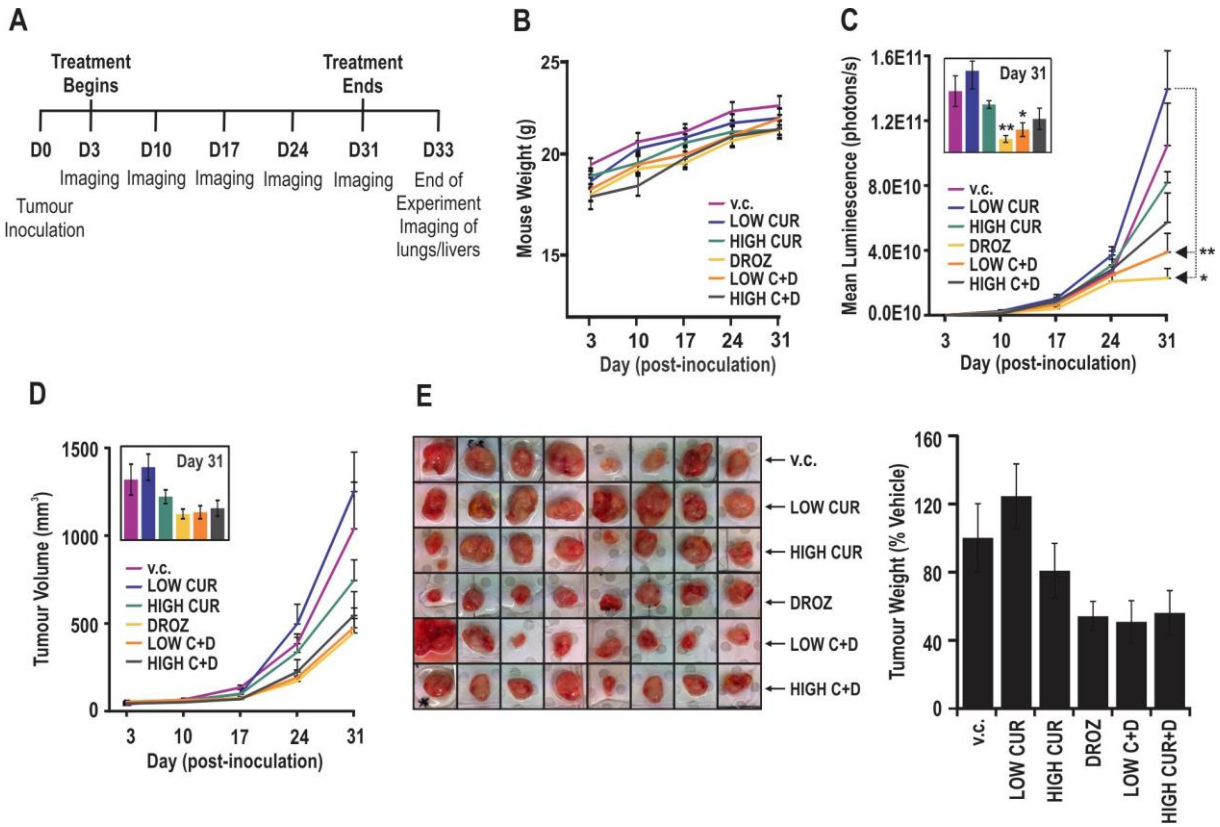

Figure 5.5: The effect of curcumin, drozitumab, and the combination on tumour volume *in vivo*. Forty eight six-week old male BALB/c nude mice were injected sub-cutaneously into the flank with 5×10^4 PC-3-luc cells in 50 µL Matrigel-HC (D0). Mice were randomly assigned to six treatment groups each containing eight mice: vehicle control (v.c.), low curcumin (LOW CUR; 50 mg/kg), high curcumin (HIGH CUR; 100 mg/kg), drozitumab (DROZ; 3 mg/kg), low curcumin and drozitumab (LOW C+D) or high curcumin and drozitumab (HIGH C+D). Treatment via intraperitoneal injection began on D3 post tumour inoculation and continued three times weekly for four weeks. Mice were imaged weekly on the Xenogen IVIS 100 bioluminescence imaging system and were humanely sacrificed on D33. **A**: Time-line for the study. **B**: Mouse weights over the duration of the experiment. Data is presented as mean weight (g) ± SEM of eight mice. **C**: Mean luminescence (photons/s) of PC-3-luc xenograft tumours over the duration of the experiment. * $p<0.05$ LOW C+D compared to v.c. (D31); ** $p<0.01$ DROZ compared to v.c. (D31) (Unpaired *t*-test). Data is presented as mean luminescence + SEM of eight mice. **D**: Calliper measurements over the duration of the experiment. $p>0.05$ for all comparisons of tumour volume (Unpaired *t*-test). Data is presented as mean volume (mm^3) + SEM of eight mice. **E**: Photographs of tumours taken from mice on D33 and tumour wet weights *ex vivo*. $p>0.05$ for all comparisons of tumour weight (Unpaired *t*-test). Data is presented as mean weight ± SEM of eight mice as a percentage of the vehicle control.

5.3.6: *In vitro* investigation of xenograft study observations.

There were two unexpected observations from the animal study: the *in vivo* effectiveness of drozitumab in reducing tumour burden and the lack of curcumin efficacy. To closer examine these findings, further *in vitro* work was performed. Until this point, all *in vitro* experiments involved cross-linking drozitumab with anti-$F_c\gamma$ IgG prior to treatment in a 1:1 ratio, which enhances drug efficacy by promoting DR5 aggregation. PC-3-luc cells were therefore treated with increasing amounts of anti-$F_c\gamma$ IgG combined with a constant dose of 700 nM drozitumab. While the agents in a 1:1 ratio reduced cell viability by 22.1 ± 1.8%, in a 1:2 ratio (drozitumab: anti-$F_c\gamma$ IgG) this was increased to 38.8 ± 2.8% compared to vehicle control ($p<0.001$; **Figure 5.6A**). This suggested that enhanced antibody cross-linking may increase drozitumab efficacy. While there were no statistical differences between vehicle control and curcumin treatment in the animal study, 50 mg/kg curcumin appeared to promote tumour growth. To confirm that curcumin was not acting in a hormetic manner PC-3-luc cells were treated with low doses in culture, however 0.25 to 4 µM curcumin did not stimulate cell growth (**Figure 5.6B**). The increase in tumour size with 50 mg/kg curcumin treatment over vehicle control was more likely due to the high variability in tumour sizes seen across treatment groups (see **Figure 5.5E**).

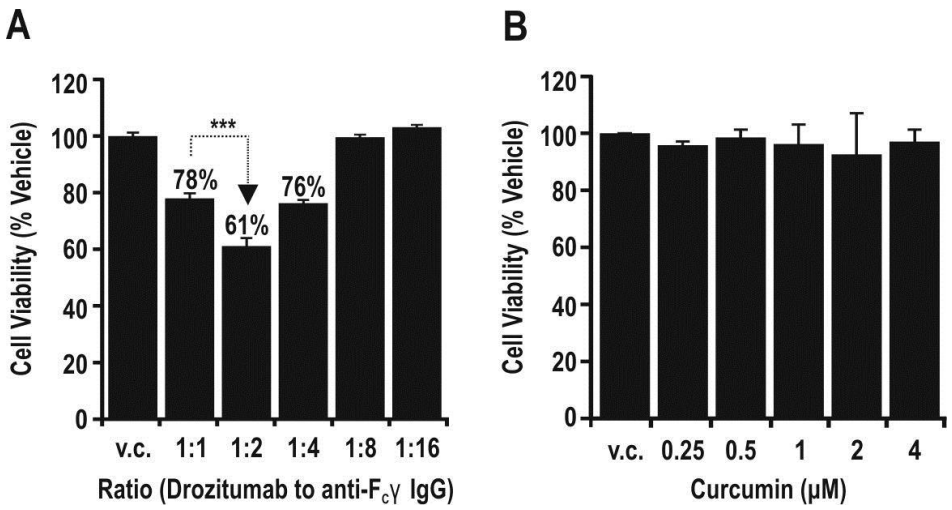

Figure 5.6: *In vitro* investigation of xenograft study observations. A: PC-3-luc cells were treated with vehicle control (v.c.) or 700 nM drozitumab with increasing amounts of anti $F_c\gamma$ IgG. Cell viability was assessed by MTT assay at D2. *** $p<0.001$ 1:2 compared to 1:1 (Unpaired *t*-test). Data is presented as mean cell viability ± SEM relative to v.c. and is the average of 3 independent experiments. **B**: PC-3-luc cells were treated with v.c. or 0.25 to 4 µM curcumin. Cell viability was assessed by MTT assay at D2. $p>0.05$ for all comparisons (Unpaired *t*-test). Data is presented as mean cell viability ± SEM relative to v.c. and is the average of 2 independent experiments.

5.3.7: Development of metastatic lesions in the PC-3-luc xenograft model.

Upon conclusion of the animal study, the lungs and livers were removed from all mice and subjected to BLI to detect any metastasis. While there were no liver metastases detected in the control group, between 37.5 (3/8) and 50 (4/8) percent of mice from each treatment group had developed liver metastases (**Figure 5.7A**). Conversely, while 50% of the control group had developed lung metastases, all treatments decreased the incidence of lung lesions, with the combination of high curcumin and drozitumab being completely free of lung metastases (**Figure 5.7A**). Quantification of the lung and liver BLI data confirmed that high curcumin and drozitumab treatment prevented the development of lung metastasis and all treatments except HIGH CUR+DROZ promoted liver metastases (**Figure 5.7B**). However, upon histological examination of representative lung and liver sections stained with haematoxylin and eosin, no liver metastases and only a few small lung metastases were observed (examples provided in **Figure 5.7C**). This potentially indicated the presence of micro-metastases, where newly formed tumours were too small to be detected by histology but were identified upon BLI.

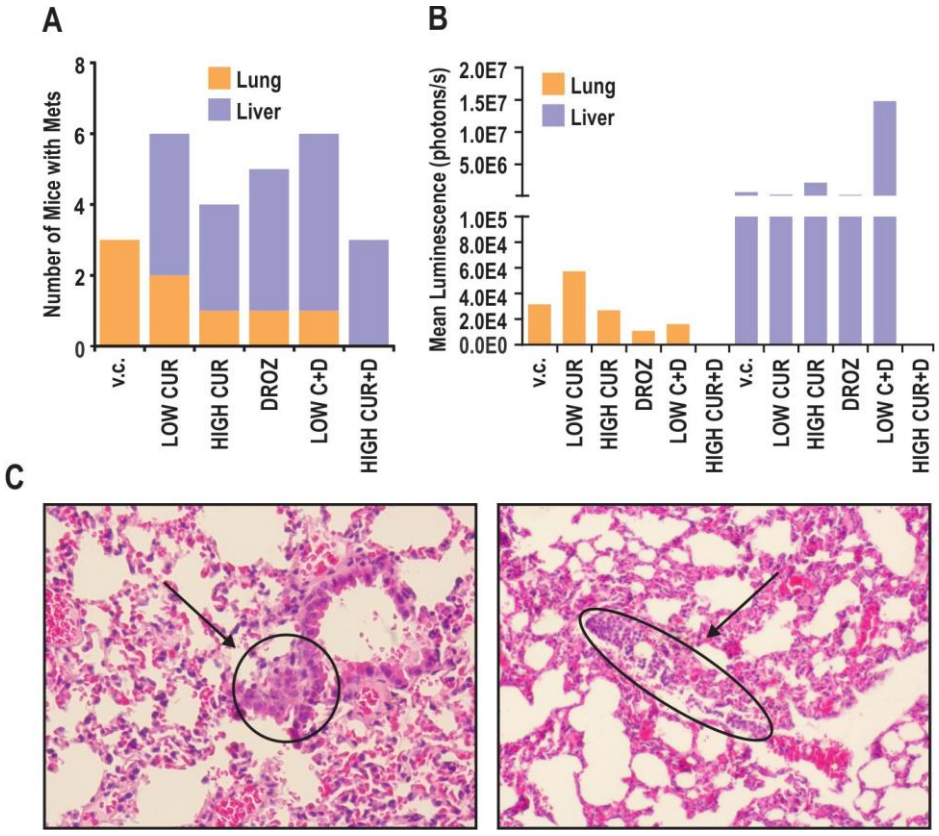

Figure 5.7: Development of metastatic lesions in the PC-3-luc xenograft model. On D33, the lungs and livers were removed from all mice and were subjected to bioluminescence imaging. **A**: Quantification of the number of mice per treatment group that developed lung or liver metastatic lesions. **B**: Mean luminescence (photons/s) of PC-3-luc xenograft metastatic lesions on D33 of the experiment. Data is presented as the mean luminescence of eight mice. **C**: Representative haematoxylin and eosin stained sections demonstrating the presence of small lung metastases in the PC-3-luc xenograft model, indicated by arrows.

5.3.8: Analysis of tumour histology and immunohistochemistry.

Histology was performed on tumour samples to assess intra-tumoural changes in response to each treatment. Haemotoxylin and eosin staining confirmed the growth of poorly differentiated tumours within a connective tissue capsule, and no glandular structures were observed (**Figure 5.8A**). All tumours possessed varying levels of necrotic tissue at the centre, indicated by strong eosin staining. This was likely due to ischemia, as blood vessels were only found throughout the outer, healthy tissue. Immunohistochemistry for Ki67, HMOX1 and DR5 was also performed (**Figure 5.8B**). Negative control images demonstrated only a small amount of background staining due to red blood cells remaining in xenografts causing high endogenous peroxidase activity. First, Ki67 staining was conducted to ascertain whether intra-tumoural proliferation rates matched the BLI and tumour volume data. Positive cells were predominantly present in the outer areas of tumour and the qualitative proportions of proliferating cells correlated with results from Figure 5.5C-E. Given the promising anti-tumour activity observed with drozitumab treatment in Figure 5.5C, Ki67 staining was manually counted for vehicle and drozitumab-treated mice. The results demonstrated an average 44.4 ± 16.9% reduction in the number of cancer cells actively proliferating in the drozitumab-treated tumours ($p<0.001$; **Figure 5.8C**).

Data from this thesis and others studies show that HMOX1 is one of the most highly affected curcumin targets identified to date, with curcumin treatment causing large up-regulation of HMOX1 mRNA and protein (Balogun, Hoque et al. 2003, Thangapazham, Shaheduzzaman et al. 2008, Teiten, Gaigneaux et al. 2012). Therefore HMOX1 staining was used as an indirect, qualitative assessment of curcumin activity in tumours. Staining was detected mostly near the edges of the xenografts where cellular proliferation was highest. Interestingly, curcumin treatment increased HMOX1 staining intensity over vehicle, particularly when combined with drozitumab. This indicated that perhaps some curcumin was reaching the tumour site despite other factors limiting its efficacy. Staining for DR5 was also assessed to ascertain whether the treatments had caused any change to its expression within the tumour. However there did not appear to be any visible differences in DR5 expression across treatment groups.

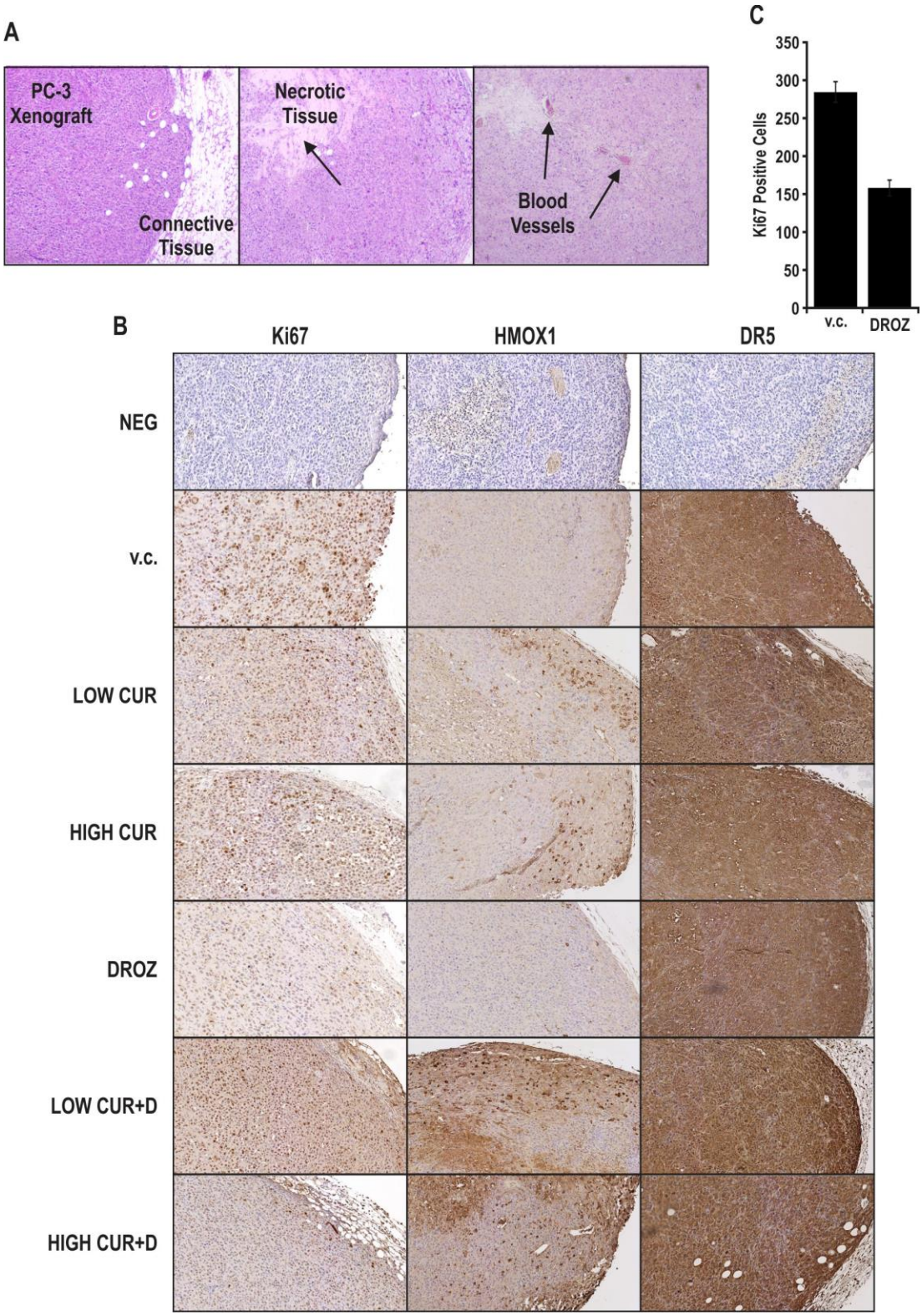

Figure 5.8: Analysis of tumour histology and immunohistochemistry. A: Haematoxylin and eosin staining on PC-3-luc xenografts demonstrate the formation of poorly differentiated, non-glandular tumours confined within a connective tissue capsule. All tumours demonstrated necrosis within the core, likely due to ischemia. Blood vessels were present, however, in the outer areas of tissue where proliferation rates were highest. **B**: Representative immunohistochemistry staining for Ki67, HMOX1 and DR5 across all treatment groups. **C**: Quantification of positive Ki67 staining in vehicle control (v.c.) and drozitumab (DROZ) treatment groups. $p<0.001$ DROZ compared to v.c. (Unpaired *t*-test). Data is presented as mean cell number ± SEM of eight tumours.

5.3.9: Re-assessment of curcumin and drozitumab sensitivity in PC-3-luc explant cells.

To better understand the treatment responses seen *in vivo*, as well as establishing whether any drug tolerance may have developed, a small piece of healthy tumour was taken from a representative mouse from each treatment group and cultured *ex vivo*. Images of the explant culture process are presented in **Figure 5.9A**. Prior to beginning these experiments, the vehicle control-treated explant was compared to original PC-3-luc cells to ensure cells had not changed after being grown in mice. While there appeared to be some differential response to drozitumab between the original and vehicle-treated explant, two-way ANOVA analysis revealed no significant differences between them with either treatment (**Figure 5.9B-C**). Next, all explant cell lines were re-assessed for drug sensitivity. All explant cells responded to curcumin treatment (20 μM and above) in a dose-dependent manner ($p<0.0001$) but there were no differences in curcumin response between explant cell lines (**Figure 5.9D**). This indicated that cells did not acquire any tolerance to treatment throughout the animal study, possibly due to poor curcumin delivery to the tumour site. In drozitumab-treated cells, however, the vehicle and 50 mg/kg curcumin-treated explants demonstrated a significant reduction in viability at 700 nM drozitumab while all other explant cells failed to respond ($p<0.01$, **Figure 5.9E**). This indicated that while drozitumab treatment significantly reduced tumour size, cells were possibly becoming tolerant to treatment by the end of the study.

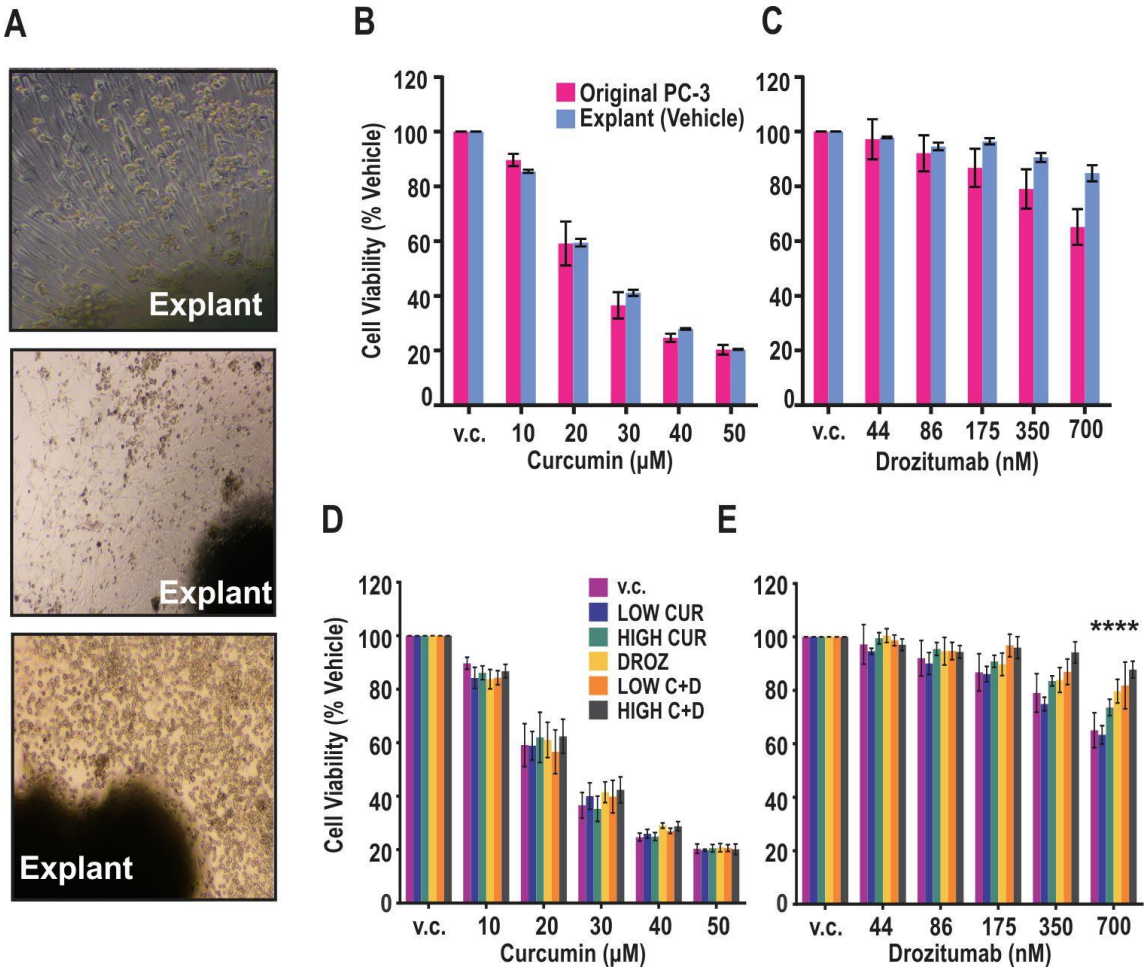

Figure 5.9: Re-assessment of curcumin and drozitumab sensitivity in PC-3-luc explant cells. A: Photographs of PC-3-luc cells growing out of explant tissue in culture. **B-C**: Original PC-3-luc and vehicle-treated explant PC-3-luc cells were treated with either vehicle control (v.c.), curcumin (10 to 50 μM; B) or drozitumab (44 to 700 nM; C). Cell viability was assessed by MTT assay at D0 and D2. $p>0.05$ original compared to explant (Two-way ANOVA). Data is presented as mean ± SEM relative to v.c. and is the average of 2 (original) or 3 (explant) independent experiments. **D-E**: Representative PC-3-luc explant cells from each treatment group were cultured *ex vivo*. Cells were treated with either v.c., curcumin (10 to 50 μM; D) or drozitumab (44 to 700 nM; E). Cell viability was assessed by MTT assay at D2. **** $p<0.0001$ drozitumab-treated explant compared to vehicle-treated explant at 700 nM drozitumab (Two-way ANOVA). Data is presented as mean ± SEM relative to v.c. and is the average of 3 independent experiments.

5.4: DISCUSSION

Given the poor bioavailability profile of curcumin, many studies are now investigating curcumin as part of combinatorial therapeutic strategies to enhance its efficacy. One of the earliest and most successful studies of this kind found that piperine, an inhibitor of hepatic and intestinal metabolism found in black pepper, increased curcumin bioavailability by 2000% in humans (Shoba, Joy et al. 1998). This led to the widespread addition of piperine to curcumin supplements. Rather than increasing curcumin potency, the aim of this chapter was to use curcumin to increase the potency of the monoclonal antibody drozitumab.

The data presented in this chapter demonstrated that curcumin could re-sensitise drozitumab-resistant prostate cancer cells to death via up-regulation of DR5, thereby validating previous studies (Shankar, Chen et al. 2007, Shankar, Ganapathy et al. 2008). However, this effect was not observed in the xenograft model. The absence of a decrease in tumour size in curcumin-treated mice, paired with minimal HMOX1 staining within tumours and no apparent curcumin tolerance *ex vivo*, suggested that curcumin did not effectively reach the tumour. This is illustrated in **Figure 5.10**, where small deposits of curcumin can be seen in the abdominal area of most mice throughout the course of the study. Additional curcumin build up within fatty abdominal areas was observed upon dissection at the end of the study, indicating that the full dose of curcumin was not reaching the tumour site.

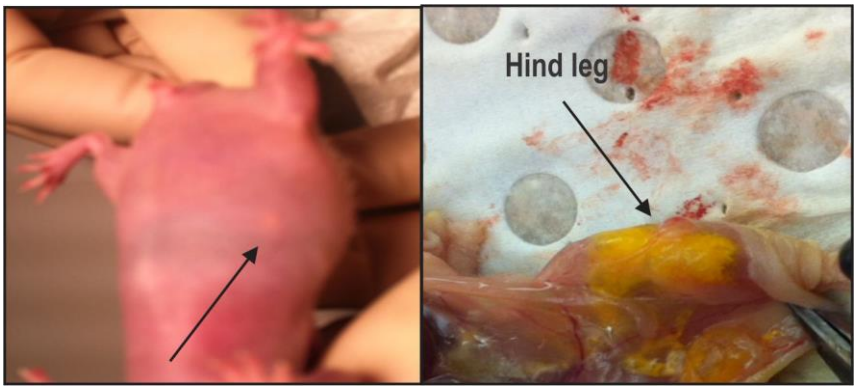

Figure 5.10: Curcumin deposits within the abdominal areas of mice observed both during the study (left) and upon completion of the study (right).

Besides compromised curcumin delivery, additional factors may have contributed to the lack of efficacy including incorrect dosing, sub-optimal drug administration and the aggressiveness of the cell line. The doses used in this study were selected based on previous studies where curcumin showed anti-cancer efficacy in various xenograft models. However, publications following the completion of these experiments have been inconclusive in identifying whether the doses used were appropriate. One study reported that 200 mg/kg curcumin administered five times weekly for three weeks via i.p. injection failed to significantly reduce the size of A549 lung cancer xenografts (Wang, Zhang et al. 2013), yet another study observed a significant reduction in PC-3 xenograft size following 100 mg/kg i.p. injection daily for

three weeks (Cheng, Chen et al. 2013). While there are a multitude of factors that may have contributed to variability when comparing published studies (such as curcumin purity or treatment duration), it is clear that an effective dose in one type of cancer cell will not be effective in another. This provides further evidence towards the notion presented in Chapter 3 that the mechanism of curcumin action is cell-type dependent.

While many xenograft studies have used i.p. injection for curcumin delivery, this may not be the most efficient method of curcumin administration. Upon delivery to the peritoneal cavity, a drug must pass into and out of the circulation, thereby lengthening the time to reach the target tissue. Curcumin undergoes rapid degradation in circulation, first by hydrolysis and then by molecular fragmentation (Wang, Pan et al. 1997). Therefore i.p. injection may allow more time for curcumin to degrade before reaching the target tissue. Curcumin also has a high affinity for binding serum proteins in blood. Binding of curcumin to BSA reduces its half-life to approximately six hours *in vitro* and impairs curcumin delivery to cell membranes (Leung and Kee 2009, Sneharani, Singh et al. 2009, Harada, Giorgio et al. 2013).

The timing of curcumin treatment is also a critical factor in whether treatment will produce significant results (Khor, Keum et al. 2006). It may also be possible that commencing treatment three days post-inoculation was insufficient against the aggressive PC-3 cell line. There was also a large amount of variability observed in the xenograft study. Given the aggressive nature of the PC-3 cell line, only a small number of cells were injected into mice which probably contributed to the inconsistency in tumour sizes prior to treatment. Further, the variable nature of peritoneal drug transport between individuals may have further contributed to the variability in results seen in this study (Davies 2000). Taken together, the dose, method and timing of treatment may have affected curcumin delivery, and the effect of novel curcumin analogues and delivery systems on death receptor expression should therefore be considered in future studies. Indeed, curcumin encapsulated by diamide-linked γ-cyclodextrin dimers did not compromise efficacy or regulation of DR5 in PC-3 cells (Harada, Giorgio et al. 2013).

The marked reduction in tumour size observed with drozitumab treatment was surprising given the relative resistance of PC-3 cells in culture. It is important to note that the PC-3 cells used in this study were termed drozitumab-resistant by the Evdokiou laboratory due to their lack of response to high doses of drug, despite no investigation into the mechanisms behind such observations. These cells may have been drug-tolerant, but this was not considered relevant for the nature of this chapter. While drugs displaying *in vitro* sensitivity and *in vivo* resistance are relatively common, the opposite scenario is quite rare. One particular study observed this using fluconozole for the treatment of candida albicans, with the effect caused by inactivation of cholesterol biosynthesis enzymes *in vitro* (Miyazaki, Miyazaki et al. 2006). There are a multitude of possibilities for why this may have occurred in the current study, but one

plausible hypothesis is that the naturally circulating F_c fragment found in mouse serum enhanced drozitumab efficacy (Khayat, Dux et al. 1984, Pure, Durie et al. 1984). This was supported by the observation that increasing the amount of F_c fragment increased drozitumab efficacy *in vitro*.

As described in Section 1.3.5, there is an urgent need for new therapeutics to treat advanced prostate cancer. As such, the efficacy of drozitumab against PC-3 xenografts warrants further investigation in metastatic and CRPC models. Prostate cancer has been described as a good candidate for antibody-based therapy (Jakobovits 2008). First, the prostate is a non-essential organ which allows for the targeting of antigens in both normal and cancer cells. Second, metastases in bone and lymph nodes are accessible by circulating antibodies. Further, early diagnosis allows treatment to be initiated when tumours are small, thereby facilitating antibody penetration. Monoclonal antibodies against prostate-specific membrane antigen have already shown promise in animal models of advanced prostate cancer and clinical trials (Sokoloff, Norton et al. 2000, Nanus, Milowsky et al. 2003, Smith-Jones, Vallabhajosula et al. 2003, Henry, Wen et al. 2004, Milowsky, Nanus et al. 2004, Bander, Milowsky et al. 2005). Future studies should investigate the molecular events associated with drozitumab action in prostate cancer, including effects on the androgen signalling axis and the value of drozitumab in combination with ADT. Future studies would also benefit from performing immunohistochemistry for a human-specific protein marker, or analysing luciferase or GFP expression, to allow for more sensitive detection of metastases. While the data presented in this study shows drozitumab arrested tumour growth following three weeks of treatment, culture of tumour cells *ex vivo* indicated that tolerance may have developed. It will therefore also be important to extend the timeline of future animal studies to investigate this.

In summary, the results of this chapter highlight the potential for curcumin to re-sensitise drozitumab-resistant cancers to cell death via up-regulation of DR5. However, the poor bioavailability of curcumin represents a significant set-back in being able to achieve this and warrants the investigation of enhanced curcumin delivery systems in combination with drozitumab. The study did, however, identify drozitumab as a potential therapy for advanced prostate cancer. This is an exciting, novel therapeutic avenue given the current lack of effective treatment options for men with advanced prostate cancer.

CHAPTER 6

GENERAL DISCUSSION

6.1: OVERVIEW

Androgen deprivation therapy has been the primary treatment strategy for advanced prostate cancer for over sixty years (Huggins and Hodges 2002). While initially effective, the majority of patients relapse due to the development of castrate resistance. Research over the last ten years has demonstrated that the failure of ADT is due to acquired mechanisms that maintain AR signalling, not a decreased requirement for androgen signalling as previously thought (Scher and Sawyers 2005). In short, the AR remains a major mediator of prostate cancer cell growth and a viable target for the treatment of all stages of disease. Current research is therefore becoming increasingly focussed on the development of agents that target the AR signalling axis at multiple levels, including androgen synthesis, metabolism and action at all relevant sites (gonadal, adrenal and intra-tumoural). The efficacy of these agents, including abiraterone acetate and enzalutamide, supports the concept of continued AR signalling in CRPC.

Natural agents, particularly phytochemicals (derived from plants), have a long history of use in the treatment of cancer. In fact, some leading anti-cancer agents are derived from nature, including taxanes (e.g. paclitaxel, docetaxel), anthracyclines (e.g. doxorubicin, epirubicin) and vinca alkaloids (e.g. vincristine, vindesine). Research into natural compounds as cancer therapies has gained much interest over the last 60 years due to the chemical diversity found in millions of species of plants, as well as marine and micro-organisms (Butler 2004). Curcumin is one such compound that has garnered interest as an anti-cancer therapy. This is, in part, due to the low incidence of gastrointestinal cancers in countries that consume high amounts of curcumin. Curcumin has demonstrated efficacy in animal models of prostate cancer, believed to be at least partially due to the anti-androgenic activity of curcumin and its structural analogues which inhibit AR expression, reduce AR residence on DNA, enhance AR degradation and target androgen-regulated genes (Nakamura, Yasunaga et al. 2002, Ohtsu, Xiao et al. 2002, Thangapazham, Shaheduzzaman et al. 2008, Shi, Shih et al. 2009, Sharma, Lee et al. 2010, Xu, Chu et al. 2012). However, while there has been a large amount of research into curcumin action in prostate cancer cells, our understanding of how curcumin may affect the prostate microenvironment, including fibroblasts, is very limited. Prostate fibroblasts are key regulators of epithelial cell function, and can progress to an activated form in a cancer setting where they help drive cancer initiation and progression. Most therapeutic studies, however, do not consider the mechanisms

of drug action in normal or cancer-associated fibroblasts that surround a tumour. This thesis therefore investigated curcumin in the context of both prostate cancer cells and fibroblasts.

6.2: MAJOR FINDINGS OF THIS THESIS

The mechanisms of curcumin action are cell-specific, despite similar biological outcomes.

The studies presented in Chapter 3 demonstrate that curcumin has the potential to target both prostate cancer cells and fibroblasts in a tumour setting. This comes at a time when the role of cancer-associated fibroblasts in driving cancer growth and progression is becoming increasingly recognised. The mechanisms dictating curcumin action amongst prostate cell lines are diverse, indicating that cell lines should be considered on an individual cell basis. This was particularly evident upon investigation of the BRCA1 pathway, whereby three different prostate cell lines displayed cell cycle arrest through alternative means within this pathway, regardless of their p53 status. Identifying these differences will provide valuable information in recognising cancers or diseases that will most likely benefit from curcumin treatment.

The data gathered in this chapter highlights the cell-specific nature of curcumin action, and potentially provides an explanation for inconsistencies found in the literature when describing curcumin action in different cell types. Not only were there large transcriptomic differences in curcumin response between epithelial and fibroblast lineages in the current study, there were also differences in curcumin sensitivity across a panel of prostate cancer cell lines. Indeed, similar observations have been made with curcumin in other cancer cell lines (O'Sullivan-Coyne, O'Sullivan et al. 2009, Sertel, Eichhorn et al. 2012). Interestingly, exposure to the same drug may cause differential drug responses amongst individual cells, highlighting how differences in drug toxicity and efficacy may not be the collective cellular response (Kuang and Walt 2005).

One of the most favourable aspects of curcumin reported in the literature is its ability to specifically target cancer cells whilst having minimal impact on normal cells. There are studies to support this in normal mammary epithelial cells, dermal fibroblasts and hepatocytes at similar curcumin doses used in this thesis (Ramachandran and You 1999, Syng-Ai, Kumari et al. 2004, Choudhuri, Pal et al. 2005, Watson, Hill et al. 2008). However, the data presented in this thesis indicates that despite genotypic and phenotypic differences in prostate cell lines, curcumin-treated prostate fibroblasts and cancer cells both undergo cell cycle arrest and subsequent death. There are also reports supporting curcumin-induced death in normal cells, including human foreskin fibroblasts, retinal endothelial cells and lymphocytes (Bielak-Zmijewska, Koronkiewicz et al. 2000, Magalska, Brzezinska et al. 2006, Premanand, Rema et al. 2006, Scharstuhl, Mutsaers et al. 2009). There are a number of arguments presented in the literature to support the cancer-specific action of curcumin. First, absorption and fluorescence spectroscopic

methods have shown that cellular uptake of curcumin is higher in cancer cells than normal cells, hypothesised to be a result of differences in membrane structure, protein composition and cell size (Kunwar, Barik et al. 2008). The data presented in this thesis, however, suggests there is no difference in curcumin uptake between prostate cancer and non-cancer cell types of variable size. Second, the increased generation of reactive oxygen species mediated by depletion of glutathione (GSH) has been shown to sensitise cancer cells, but not normal cells, to curcumin (Syng-Ai, Kumari et al. 2004). Glutathione is an endogenous antioxidant involved in the neutralisation of free radicals and reactive oxygen species. While a decrease in GSH may lead to increased susceptibility to oxidative stress implicated in the progression of cancer, many cancer cells display elevated GSH that increases the antioxidant capacity and resistance to oxidative stress (Traverso, Ricciarelli et al. 2013). Future studies may consider investigating the relative GSH levels in the models used in this thesis to determine whether GSH influences curcumin sensitivity in prostate cancer. Finally, most cancer cells express constitutively active NF-κB, a well-established curcumin target that is proposed to increase curcumin sensitivity (Shishodia, Amin et al. 2005). However the data presented in this thesis indicates that curcumin remains able to inhibit NF-κB in prostate fibroblasts, which may also be a central mechanism of inducing death in these cells. As discussed in Chapter 3, variable curcumin sensitivity has also been attributed to differential expression of heat shock proteins and compromised mismatch repair function (Aggarwal 2000, Rauh-Adelmann, Lau et al. 2000, Mukhopadhyay, Bueso-Ramos et al. , Shaulian and Karin 2001, Rashmi, Santhosh Kumar et al. 2003). Given the demonstrated effect of curcumin on non-malignant prostate fibroblasts, it is highly likely that curcumin also has effects on other cells in the broader prostate microenvironment such as immune and vascular cells. This presents an incredibly complex system whereby curcumin may induce biological responses from many different cell types, ultimately having some impact on prostate cancer cells. It is therefore important to consider that curcumin action may not be cancer cell-specific and is likely to be different across all cell types due to a host of factors that contribute to differential drug responses.

Despite all prostate cells being sensitive to curcumin in the current study, investigating the mechanisms of curcumin action within each individual cell was valid due to the diverse roles played by different cell types. One example is the observation that curcumin inhibits fibroblast AR activity. As described throughout this thesis, AR expressed in prostate cancer cells is a major mediator of disease progression and is subsequently the primary therapeutic target for all stages of disease. Expression of AR in CAFs has also been shown to be a critical player in prostate cancer initiation (Wang, Sudilovsky et al. 2001, Niu, Altuwaijri et al. 2008, Yu, Yeh et al. 2012). The data from this thesis suggests that curcumin may simultaneously target AR in both the epithelial and fibroblast compartments of the prostate, resulting in a more efficient AR targeting strategy. While these findings have not been validated in primary prostate

CAFs, they demonstrate that curcumin may be beneficial in targeting a single protein across multiple cell types at the same time. Curcumin in combination with second generation AR targeting agents may therefore more effectively inhibit the AR signalling axis than either agent alone. This may allow for lower doses of each agent to be used, thereby decreasing drug toxicity and potential tolerance or resistance.

Paradoxically, however, low fibroblast AR levels have been associated with accelerated disease progression and poor patient outcome (Henshall, Quinn et al. 2001, Ricciardelli, Choong et al. 2005). The use of curcumin in an intact prostate may therefore further decrease fibroblast AR levels leading to a poor outcome. The likelihood of this scenario is difficult to gauge. On one hand, RP is often conducted prior to manipulation of androgen signalling via ADT, meaning prostate fibroblasts would no longer be present. On the other hand, patients have often relapsed when given ADT and the value of targeting AR in non-prostate fibroblasts is not understood. This observation may be of foreseeable concern in men taking curcumin supplements prior to being diagnosed with prostate cancer. It is therefore important to assess the effect of curcumin in primary fibroblasts and tissue recombination models where the paracrine interactions between cancer cells and fibroblasts can be considered.

Results from the Shah et al. study investigating curcumin in combination with ADT are quite relevant to this thesis, and provide context for the current study (Shah, Prasad et al. 2012). In androgen-sensitive cell lines, curcumin augmented the effect of ADT and reduced cell number compared to ADT alone. This occurred through suppression of AR and AR pioneer factors (GATA2 and FOXA1) at enhancers of AR target genes, without affecting AR protein accumulation or localisation. To support these findings, immunocompromised mice harbouring established human prostate xenografts were castrated and treated with vehicle or 50 mg/kg curcumin daily for five weeks (Shah, Prasad et al. 2012). Curcumin significantly reduced the tumour growth and weight of castrated mice, demonstrating not only that it obstructs the transition of ADT-sensitive disease to castrate-resistance, but also that it can effectively block the growth of established castrate-resistant tumours. This study highlights a number of factors pertinent to the current data. First, the frequency of curcumin administration used in Chapter 5 (three times per week) was evidently too little to see a significant effect on tumour growth. Further, the results provide evidence to support the curcumin-mediated reduction in AR binding to FKBP51 in prostate fibroblasts observed in this thesis. Considering the potentially detrimental effect of curcumin on prostate fibroblasts presented in this thesis, and the data presented by Shah et al., perhaps curcumin is best used to target androgen receptor signalling in cancers that lack prostate stroma, such as those that recur following RP.

In summary, the data presented in Chapter 3 highlights the value of investigating curcumin action across multiple cell types and lineages, to find not only unknown advantages of curcumin treatment but also to ensure that curcumin does not have detrimental effects on cancer progression.

Tolerance may occur when fibroblasts are treated with curcumin over an extended time-frame.
While the advantages and considerations for curcumin use in a prostate setting were outlined above, curcumin use is already widespread, both as a supplement as well as through clinical trials. The potential for curcumin tolerance or resistance to occur in prostate fibroblasts was therefore investigated. Studies from this thesis demonstrated the development of curcumin tolerance *in vitro*, characterised by a number of transcriptomic and physiological changes. The physiological changes observed were reversible upon curcumin withdrawal, opening up a whole new perspective on the transient nature of curcumin action. Examination of curcumin sensitivity and tolerance in prostate fibroblasts led to the identification of some potential pitfalls of curcumin use in a clinical setting, including the impairment of fibroblast AR activity and the unfavourable effect of tolerant fibroblasts on the growth and adhesion of cancer cells. However, the literature surrounding these findings is inconclusive and further investigation is required before these observations can be considered major drawbacks.

There is limited data on the response of fibroblasts to cancer therapy, and their potential impact on cancer outcome. However, researchers are now attempting to use CAFs as predictors of chemotherapy efficiency and resistance, rationalised by their frequent association with drug resistance (Sonnenberg, van der Kuip et al. 2008, Rong, Kang et al. 2013). Indeed, this study identified genes associated with curcumin tolerance, some of which were also associated with resistance to curcumin and other drugs. The transcriptomic alterations associated with curcumin tolerance were believed to contribute to the observation that tolerant fibroblasts altered the growth and adhesive characteristics of PC-3 prostate cancer cells. While the effect of treated fibroblasts on treatment-naïve cancer cells has not been well investigated, one particular study found radiation-induced senescent fibroblasts stimulated the proliferation of co-cultured breast cancer cells (Tsai, Stuart et al. 2009). This was due to the ability of fibroblasts to induce expression of mitogenic genes in the cancer cells. The ability of fibroblasts to modulate the activity of cancer cells is further evidence to support research into this area, as well as targeting fibroblasts during therapy.

Data from this chapter indicates that curcumin tolerance is reversible upon its withdrawal from culture media. Not only does curcumin sensitivity return in terms of cell viability, but some androgen responsiveness is restored. This reversible, drug-tolerant state has been observed previously in tyrosine kinase inhibitor-resistant PC-9 human lung adenocarcinoma cells where, following several passages in drug-free media, drug sensitivity was restored to parental levels (Chmielecki, Foo et al. 2011).

Tolerance to anti-cancer drugs is a relatively new field of research, with limited data to draw upon. However one proposed mechanism of drug tolerance is the presence of drug-tolerant persister (DTP) cells, responsible for propagating the cellular population via an intrinsic ability to tolerate drug exposure not involving drug efflux (Sharma, Lee et al. 2010). Indeed, altered curcumin uptake was eliminated as a potential mechanism of curcumin action and tolerance in Chapters 3 and 4. This, paired with minimal changes to ABC transporters in the microarray data, suggests that curcumin tolerance is more likely a result of cells being better equipped to survive high doses of drug rather than making permanent alterations to drug influx and efflux pathways. The characteristics observed were also supported by definitions of drug tolerance described in Section 1.5.5 (Raith and Hochhaus 2004, Dumas and Pollack 2008). As described by Sharma et al, a transiently drug-tolerant state mediated by DTPs may allow a small population of cancer cells to withstand initial drug treatment and enable survival until more permanent resistance mechanisms are established. It is therefore possible that curcumin tolerance may develop into a more permanent form of resistance, involving mutational alterations to drug transport, if cells are exposed to curcumin for longer periods of time. It would be interesting to investigate whether the transcriptomic changes associated with curcumin tolerance were also reversed upon curcumin withdrawal, results of which may link curcumin to genomic plasticity. Theoretically, curcumin tolerance in cancer cells may not be detrimental to patients given the androgen signalling axis becomes impaired. However, the partial restoration of androgen responsiveness with curcumin withdrawal means that curcumin may be best used in combination with other androgen targeting agents.

Curcumin has the potential to re-sensitise prostate cancer cells to drozitumab.

The previous two chapters investigated curcumin used on its own, to closely examine intracellular mechanisms of action and tolerance. Clinical trial data, however, indicates that curcumin is unlikely to be used as a monotherapy due to its poor oral bioavailability. Efforts are now being made to increase the bioavailability profile, as well as utilise curcumin to reverse drug resistance and enhance other anti-cancer agents. There are reports in the literature describing an effect of curcumin on death receptor expression; therefore the combination of curcumin and drozitumab, a monoclonal antibody targeted to DR5, was investigated in prostate cancer cells resistant to drozitumab. While the combination of curcumin and drozitumab showed efficacy in the xenograft model, the effect was no better than drozitumab treatment alone. There are many possible reasons behind the lack of curcumin efficacy demonstrated *in vivo* (discussed in Section 5.4), however the ability of curcumin to re-sensitise drozitumab-resistant cancer cells was evident in cell line studies and worthy of further preclinical investigation.

Drozitumab showed promising efficacy against PC-3 xenografts, despite PC-3 cells being resistant in culture. This was believed to be due to F_c fragment known to circulate in mouse serum. Monoclonal

antibodies have garnered much interest in their efficacy in prostate cancer, but it is unclear whether they will be a realistic treatment option. Antibodies directed against established targets in other tumours such as Her2 (trastuzumab) and EGFR (cetuximab) have been investigated in prostate cancer clinical trials, albeit with poor outcomes (Ziada, Barqawi et al. 2004, Slovin, Kelly et al. 2009). It was promising that drozitumab caused a large reduction in tumour size in highly aggressive, androgen-independent PC-3 xenografts, which may be an indication of its efficacy in models of advanced prostate cancer. Theoretically, drozitumab could be investigated at all stages of prostate cancer, including localised, advanced and castrate-resistant disease, and has already shown no toxicity to normal cells (Adams, Totpal et al. 2008, Zinonos, Labrinidis et al. 2009). However, any future combination studies involving curcumin should be wary of the potential implications of curcumin use in an intact prostate setting, as outlined above.

6.3: FUTURE DIRECTIONS

While a number of limitations and future directions have already been discussed throughout this thesis, this section will outline studies that may enable progression of this work. One of the most obvious limitations of this thesis was the use of immortalised fibroblasts, derived from benign prostatic hyperplasia and engineered to over-express AR (Li, Li et al. 2008). The unnaturally high levels of AR within these fibroblasts may have skewed the data as prostate cancer cell lines over-expressing AR show greater AR and Polymerase II recruitment to DNA, earlier induction of transcription and enhanced gene transcription of AR target genes (Urbanucci, Marttila et al. 2012). While the results generated in the current study were, at times, extrapolated to normal and cancer-associated fibroblasts, future studies must validate these findings in primary prostate fibroblasts expressing natural levels of AR. Following this, studies investigating curcumin in the context of cancer cells and fibroblasts (e.g. the effect of targeting fibroblast AR on cancer cells or the effect of tolerant fibroblasts on cancer cells) should consider *in vivo* experiments that may involve a tissue recombination or inducible knock down model, whereby paracrine interactions between both cell lineages can be studied.

Chromatin immunoprecipitation studies revealed a large decrease in AR binding to FKBP51 in curcumin-treated fibroblasts, proposed to be a potential mechanism of targeting AR function. The chromatin immunoprecipitation protocol used in the laboratory generated only a small amount of DNA, which limited the number of AR binding sites that could be investigated. Future studies should assess more AR binding sites to be confident about the hypothesis that curcumin reduces AR binding to DNA in prostate fibroblasts. It is somewhat reassuring, however, that this has already been observed in prostate cancer cells at multiple sites (Shah, Prasad et al. 2012). Fractionation experiments demonstrated no apparent dysfunction in AR nuclear translocation in curcumin-tolerant fibroblasts, despite far less binding of AR to FKBP51. It would therefore be interesting to investigate factors that may explain

curcumin-mediated inhibition of AR activity and DNA binding following nuclear translocation, including curcumin's AR antagonistic activity, action on AR co-activators and repressors and epigenetic effects such as histone modification.

The analysis of curcumin tolerance in prostate fibroblasts was the first of its kind, and was therefore considered a preliminary study. However, the observation that curcumin-tolerant fibroblasts may influence the characteristics of cancer cells is noteworthy and warrants further investigation using primary fibroblasts and tissue recombination models. This would ensure that people using curcumin are not potentially creating an environment favourable to cancer proliferation and metastasis. A number of curcumin tolerance mechanisms were identified in this thesis, including the decreased response to curcumin-responsive genes, enhanced protein synthesis and alterations in the activity of stress response and cell death-mediating genes. However, there are a multitude of biochemical and molecular events associated with drug tolerance that could be explored in future studies including drug metabolism, DNA repair mechanisms and the presence of DTPs. It is important to consider that while identifying these mechanisms in cell lines is important, tumour heterogeneity plays a substantial role in drug tolerance and resistance. While mechanisms of drug tolerance or resistance identified *in vitro* could be therapeutically targeted to delay resistance, the clinical relevance of these mechanisms must first be established. Further, if the DTP hypothesis is correct, mechanisms allowing drug tolerance and resistance may only affect a proportion of the cell population, thus allowing the remaining cells to re-populate (Baguley 2010).

The development of curcumin tolerance was associated with an impairment to AR function in prostate fibroblasts. First and foremost, this phenomenon should be assessed in curcumin-tolerant prostate cancer cells. While the outcome of AR impairment in fibroblasts is questionable, an impairment of AR signalling in prostate cancer cells would presumably benefit patient outcome. Following this, xenograft studies should be employed to assess both curcumin tolerance generated *in vitro*, as well as whether tolerance can be achieved by treating mice with equivalent human doses. Subsequently, the effect of tolerance on prostate cancer progression may be explored. Further, new curcumin analogues and enhanced delivery systems which are more likely to show efficacy in patients should be investigated in the context of tolerance and androgen signalling.

The microarray studies performed in this thesis were central to investigating mechanisms of curcumin action in fibroblasts, and were used primarily for their cost-effectiveness. Microarrays have been used to study multiple diseases since their introduction in the nineties. They have allowed for the development of personalised medicine and have transformed the way cancer therapies are investigated. In recent years, however, RNA-seq has become advantageous over microarray profiling due to its ability to

sequence entire genes (known or unknown) over a large dynamic range (Hoheisel 2006). This means RNA-seq can identify gene splice variants, post-transcriptional modifications and mutations/single nucleotide polymorphisms (Maher, Kumar-Sinha et al. 2009, Tang, Barbacioru et al. 2010). A modification of RNA-seq, GRO-seq, only sequences newly synthesised transcripts and identifies polymerase activity and pausing at promoters (García-Martínez, Aranda et al. 2004, Core and Lis 2008). This avoids capturing transcription secondary to the treatment being tested. Future studies into curcumin action may consider using RNA-seq or GRO-seq for a more detailed view of the transcriptional changes associated with curcumin treatment, as well as identifying potential mutations associated with curcumin tolerance.

Drozitumab demonstrated encouraging efficacy in PC-3 xenograft studies, and future studies should investigate the effect of drozitumab in models of advanced prostate cancer, including CRPC. Future studies should also consider assessing drozitumab in transgenic mouse models given the limitations of xenograft studies. A xenograft model was used in this study for its simplicity and cost-effectiveness. However, there are clear limitations to the model including the absence of immune response and tumour microenvironment, and the poor adaptation of human cancer cells to grow in mice.

6.4: CONCLUSION

The findings from this thesis provide a novel insight into the mechanisms of curcumin action in the human prostate gland. This body of work offers an unbiased view of the potential benefits of curcumin use in advanced prostate cancer, and the potential drawbacks of curcumin use in early stage prostate cancer. This thesis also provides a foundation for future investigations that assess how curcumin, as well as new analogues and delivery systems, affect prostate cancer cells and fibroblasts. Despite curcumin's status as an alternative medicine, curcumin use is growing rapidly in western countries. It is therefore important that research in this area continues to ensure that curcumin will not cause any unforseen side effects, both in people who are already using supplements and those who may use it as a treatment for cancer in the future.

APPENDIX A

The following publication reflects data generated from collaboration with the Adelaide University Chemistry Department. It describes the preclinical investigation of diamide-linked γ-cyclodextrin dimers as novel, molecular scale delivery agents for curcumin (described in Section 1.5.4). I was involved in the conceptualisation of cell line experiments, performed the lab work for Figure 3, wrote the methods surrounding Figure 3 and critically reviewed the manuscript.

Diamide Linked γ-Cyclodextrin Dimers as Molecular-Scale Delivery Systems for the Medicinal Pigment Curcumin to Prostate Cancer Cells

Takaaki Harada,[1] *Lauren Giorgio,*[2] *Tiffany J. Harris,*[2] *Duc-Truc Pham,*[1] *Huy Tien Ngo,*[1] *Eleanor F. Need,*[2] *Brendon J. Coventry,*[3] *Stephen F. Lincoln,*[1] *Christopher J. Easton,*[4] *Grant Buchanan,*[2]* *and Tak W. Kee*[1]*

[1]Department of Chemistry, The University of Adelaide, Adelaide, South Australia, 5005, Australia

[2]Basil Hetzel Institute for Translational Health Research, Discipline of Surgery, Queen Elizabeth Hospital, The University of Adelaide, Woodville South, South Australia, 5011, Australia

[3]Discipline of Surgery, Royal Adelaide Hospital, The University of Adelaide, Adelaide, South Australia, 5005, Australia

[4]Research School of Chemistry, Australian National University, Canberra, ACT, 0200, Australia

* Corresponding authors

tak.kee@adelaide.edu.au, phone: +61 8 8313 5039, fax: +61 8 8313 4358

grant.buchanan@adelaide.edu.au, phone: +61 8 8133 4005, fax: +61 8 8222 6076

Keywords: Anti-cancer, Drug delivery, Cyclodextrin, Biocompatibility, Cell proliferation

Abstract

Diamide linked γ-cyclodextrin (γ-CD) dimers are proposed as molecular-scale delivery agents for the anti-cancer agent curcumin. *N,N'*-bis(6^{A}-deoxy-γ-cyclodextrin-6^{A}-yl)succinamide (66γCD$_2$su) and *N,N'*-bis(6^{A}-deoxy-γ-cyclodextrin-6^{A}-yl)urea (66γCD$_2$ur) markedly suppress the degradation of curcumin by forming a strong 1:1 cooperative binding complexes. The results presented in this study describe the potential efficacy of 66γCD$_2$su and 66γCD$_2$ur for intracellular curcumin delivery to cancer cells. Cellular viability assays demonstrated a dose-dependent anti-proliferative effect of curcumin in human prostate cancer (PC-3) cells that was preserved by the curcumin-66γCD$_2$su complex. In contrast, delivery of curcumin by 66γCD$_2$ur significantly delayed the anti-proliferative effect. We observed similar patterns of gene regulation in PC-3 cells for curcumin complexed with either 66γCD$_2$su or 66γCD$_2$ur in comparison to curcumin alone, although curcumin delivered by either 66γCD$_2$su or 66γCD$_2$ur induces a slightly higher upregulation of heme oxygenase-1. Highlighting their non-toxic nature, neither 66γCD$_2$su nor 66γCD$_2$ur carriers alone had any measurable effect on cell proliferation or candidate gene expression in PC-3 cells. Finally, confocal fluorescence imaging and uptake studies were used to study the intracellular delivery of curcumin by 66γCD$_2$su and 66γCD$_2$ur. Overall, these results demonstrate effective intracellular delivery and action of curcumin when complexed with 66γCD$_2$su and 66γCD$_2$ur, providing further evidence of their potential applications to deliver curcumin effectively in cancer and other treatment settings.

Introduction

Prostate cancer remains a worldwide health concern, with approximately 913,000 new cases diagnosed each year, or around 14% of all male cancers.[1] The treatment options for men diagnosed with early-stage prostate cancer include surgery and/or radiation, and are often curative. For men diagnosed with cancer that has already spread beyond the prostate gland, however, treatment options are essentially palliative, and often involve removal of the gland and/or surgical or chemical castration. While these treatments are initially effective, many patients eventually relapse, after which the only remaining treatments are chemotherapy or blockade of androgen metabolism, which have limited efficacy and significant side effects.[2-4] It is unsurprising, therefore, that there is considerable interest in developing adjuvant or alternative cancer agents to improve treatment response or prolong progression and/or quality of life, or have fewer side effects. One potential agent in this regard is the naturally occurring compound curcumin, found in the Indian spice plant turmeric (*Curcuma longa*), which has previously been shown to possess chemo-preventive properties with low toxicity.[5,6]

Turmeric contains a group of yellow pigments, namely curcuminoids, which are mainly comprised of curcumin (~77%), demethoxycurcumin (17%) and bisdemethoxycurcumin (3%).[7] In the past decade, curcumin has been investigated intensively and shown to have anti-cancer,[8-10] anti-inflammatory,[10,11] anti-Alzheimer's,[12] anti-cystic fibrosis,[13] and wound healing activities.[9,10] In a phase I clinical study, Cheng *et al.* demonstrated that curcumin is non-toxic up to 8 g/day when orally administrated for three months, but at that dose did not significantly affect a variety of either pre-malignant or high-risk lesions.[5] Poor bioavailability is likely to be a major contributor to the disparity between *in vitro* and *in vivo* effects of curcumin, which is poorly soluble in water (~11 μg/mL),[14,15] and prone to hydrolysis and fragmentation, resulting in significant degradation within 30 min.[16-19] These challenges must be overcome to increase the practical applicability of this compound. Previous studies have demonstrated effective stabilization of curcumin using a range of potential delivery agents, including micelles,[19-22]

liposomes,[23-25] polymers,[26-28] and proteins.[17,29-32] Each of these large-scale supramolecular assemblies may, however, limit intracellular delivery of curcumin, as they typically undergo significant structural perturbation upon contact with cellular membranes.[33] The development of molecular-scale delivery agents for curcumin and other agents is therefore of significant interest, because they have the potential to be more effective at delivering these agents to the intracellular milieu while maintaining structural integrity of the delivery agents.[33] Our previous study has shown that diamide linked γ-cyclodextrin dimers possess many desirable properties for molecular encapsulation and delivery of curcumin, including a high structural stability and the ability to suppress degradation of curcumin under physiological conditions.[16]

Cyclodextrins (CDs) are natural cyclic oligosaccharides that are FDA-approved,[34-36] and are already utilized in the food and cosmetic industries.[37] γ-Cyclodextrin (γ-CD), which consists of 8 glucopyranoside units in a toroidal structure, possesses a hydrophobic interior and hydrophilic exterior (Figure 1A). As such, γ-CD can act as a host to encapsulate and solubilize hydrophobic guest species in water through host-guest complexation.[38,39] Recently, Pham *et al.* established the synthesis of γ-CD dimers linked with either succinamide or urea substituted onto the $C6^A$ site of a glucopyranose unit in each of the γ-CD, namely *N,N'*-bis(6^A-deoxy-γ-cyclodextrin-6^A-yl)succinamide, $66\gamma CD_2su$, and *N,N'*-bis(6^A-deoxy-γ-cyclodextrin-6^A-yl)urea, $66\gamma CD_2ur$ (Figure 1B and 1C).[40] These diamide linked γ-CD dimers are excellent systems for drug delivery because (i) of their small size relative to other delivery agents mentioned above and (ii) the diamide linker can be hydrolyzed by intracellular enzymes to release the encapsulated species. The close proximity of the two γ-CDs in the dimers results in cooperative binding to the guest molecule. In the case of curcumin, the resulting molecular encapsulation by the diamide linked γ-CD dimers at the 1:1 molar ratio suppresses the rates of curcumin degradation substantially under physiological conditions.[16] Cooperative binding of the diamide linked γ-CD dimers to curcumin results in a high binding constant of 10^6 M^{-1}, which is indicative of an entrapment efficiency of nearly 100% in water. In addition, a high concentration of curcumin of at least 1.3 mg/mL (3.3 mM) in aqueous solution can be achieved with either $66\gamma CD_2su$ or $66\gamma CD_2ur$ at a 1:1 molar ratio, which is more than 100 times higher than the aqueous solubility of curcumin (11 μg/mL).[14,15] Moreover, this high concentration of curcumin is unachievable with single γ-CDs, demonstrating the importance of cooperative binding by $66\gamma CD_2su$ and $66\gamma CD_2ur$. Thus, they possess the potential to be effective and non-toxic delivery systems for curcumin.

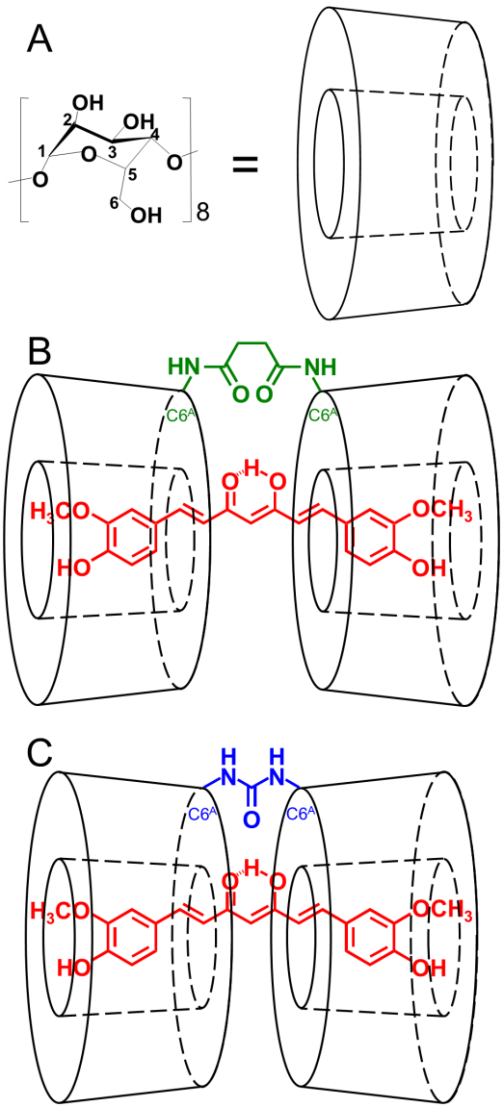

Figure 1: Structures of (A) γ-CD, and curcumin complexed in (B) 66γCD$_2$su and (C) 66γCD$_2$ur.

Here, we report for the first time the intracellular delivery of curcumin using 66γCD$_2$su and 66γCD$_2$ur and the biological consequences to human prostate cancer (PC-3) cells. Using cell viability assays, we observed a significant, dose-dependent decrease in cellular proliferation in response to encapsulated curcumin without any observable effect from the carrier 66γCD$_2$su or 66γCD$_2$ur alone. The intracellular delivery of curcumin to PC-3 cells by 66γCD$_2$su and 66γCD$_2$ur, and the maintenance of biological activity of curcumin delivered by these carriers, were verified by a variety of techniques, including confocal fluorescence imaging, uptake studies using fluorescence spectroscopy and expression of several well-characterized curcumin target genes. Overall, the results indicate the potential of 66γCD$_2$su and 66γCD$_2$ur as effective and non-toxic delivery agents for curcumin in cancer treatment.

Materials

Curcumin was obtained from LKT Laboratories (purity >98%). Methanol (AR grade, 99.5%) from Merck Pty Ltd was used as received. The phosphate buffer solution (50 mM) used in the stability study was prepared with deionized water from a Millipore Milli-Q NANO pure water system and the pH was adjusted to 7.4. The human prostate cancer (PC-3) cell line was obtained from American Type Culture Collection (VA, USA). RPMI 1640 cell culture medium with and without phenol red were purchased from Invitrogen (Mulgrave, VIC, Australia). Dimethyl sulfoxide (DMSO, $\geq$ 99.7%, sterile filtered), fetal bovine serum (FBS), dextran-coated charcoal stripped fetal bovine serum (DCC-FBS), bovine serum albumin (BSA) and 0.1% trypan blue diluted with PBS (endotoxin free) were purchased from Sigma-Aldrich (Castle Hill, NSW, Australia). RNA was extracted using the RNeasy mini kit (Qiagen, VIC, Australia) and cDNA generated using the iScript cDNA synthesis kit (Biorad, NSW, Australia). Cells were maintained in RPMI supplemented with 10% FBS. For cell treatments, phenol red-free (PRF) RPMI was supplemented with 10% DCC-FBS.

Synthesis of Diamide Linked γ-CD Dimers

The $C6^A$-to-$C6^A$ diamide linked γ-CD dimers, *N,N'*-bis(6^A-deoxy-γ-cyclodextrin-6^A-yl)succinamide, 66γCD_2su, and *N,N'*-bis(6^A-deoxy-γ-cyclodextrin-6^A-yl)urea, 66γCD_2ur, were synthesized using methods established by Pham *et al*.[40] Briefly, the native γ-CDs were substituted with 4-toluenesulfonylchloride for activation at the $C6^A$ position, which yielded 6^A-*O*-(4-methylbenzenesulfonyl)-γ-cyclodextrin (6γCDTs). For the synthesis of 66γCD_2su, the reaction between 6γCDTs and ammonium bicarbonate produced 6^A-amino-6^A-deoxy-γ-cyclodextrin, 6γ$CDNH_2$, which was then dimerized by the reaction with bis(4-nitrophenyl) succinate as the linker. For the synthesis of 66γCD_2ur, the reaction between 6γCDTs and sodium azide produced 6^A-azido-6^A-deoxy-γ-cyclodextrin, 6γCDN_3, which was then dimerized by the reaction with carbon dioxide as the linker.

Measurement of Cell Viability

A 50 mM solution of curcumin in DMSO and 8 mg/mL solutions of 66γCD_2su and 66γCD_2ur in PBS were used as stock solutions. PC-3 cells (5×10^3 cells/well in 24-well plates) were plated in phenol red free RPMI 1640 (PRF RPMI 1640) media containing 10% dextran-charcoal stripped fetal bovine serum (DCC-FBS) and allowed to attach for 24 h. Cells were washed with PBS once and treated in quadruplicates with curcumin (3.1 – 50.0 μM), 66γCD_2su (12.5 μM), 66γCD_2ur (12.5 μM), curcumin-66γCD_2su (12.5 μM) or curcumin-66γCD_2ur (12.5 μM) in PRF RPMI 1640 media containing 10% DCC-FBS, and the plates were incubated for 1 – 5 days. Owing to curcumin's low solubility and stability in PBS, it was delivered to PC-3 cells using a small quantity of DMSO. As a consequence, each solution contained a total of 0.03 vol% DMSO as vehicle control to maintain consistency in each study. The negligible quantity of DMSO was expected to have an insignificant effect on cell viability. The curcumin stock solution was mixed with either the 66γCD_2su or 66γCD_2ur solution in order to facilitate the diamide linked γ-CD dimer-curcumin complexation before being added to the medium. Viable and dead cells were manually counted using a hemocytometer on the day of treatment (Day 0) and at Days 1 – 5 post-treatment by trypan blue exclusion as described previously.[41,42]

Curcumin Target Gene Expression in PC-3 Cells

PC-3 cells (2×10^5 cells/well in 6 well plates) were plated in PRF RPMI 1640 containing 5% DCC-FBS and allowed to attach for 24 h. Cells were treated in triplicate for 12 h with curcumin (6.3 – 25.0 μM), 66γCD_2su (25.0 μM), 66γCD_2ur (25.0 μM), curcumin-66γCD_2su (6.3 – 25.0 μM) or curcumin-66γCD_2ur

(6.3 – 25.0 μM) in PRF RPMI 1640 containing 5% DCC-FBS. Each solution contained a total of 0.05 vol% DMSO as vehicle control for the reason stated above. For the studies involving a diamide linked γ-CD dimer, the control was either 25.0 μM 66γCD_2su or 66γCD_2ur, in addition to a total of 0.05 vol% DMSO without curcumin. RNA was extracted using the RNeasy mini kit and DNAse treated using the RNAse free DNAse kit according to the manufacturer's instructions (Qiagen, VIC, Australia). RNA was reverse transcribed using the iScript cDNA synthesis kit according to the manufacturer's protocol (Biorad, VIC, Australia). Quantitative real time PCR (QPCR) was performed using iQ SYBR green supermix (Biorad) on a Biorad CFX96 real time PCR machine. Data are presented as the average of three biological replicates in technical duplicates, with gene expression normalized to the reference genes *GAPDH* and *RPL32*.

Qualitative and Quantitative Cellular Uptake of Curcumin

The qualitative cellular uptake studies involved imaging PC-3 cells with curcumin with a laser scanning confocal fluorescence microscope (Leica TCS SP5). The purpose of these studies is to confirm cellular uptake of curcumin. PC-3 cells (1.6×10^3 cells/well in 8-well chamber slides) in PRF RPMI 1640 containing 10% DCC-FBS and allowed to attach for 24 h. Cells were washed once with PBS and treated with 12.5 μM curcumin, 66γCD_2su, 66γCD_2ur, curcumin-66γCD_2su or curcumin-66γCD_2ur in PRF RPMI 1640 containing 10% DCC-FBS, and incubated for 1 – 5 days. Each of these solutions contained a total of 0.08 vol% DMSO as vehicle control for the reason stated above. Prior to imaging, cells were washed with PBS twice (0.5 mL/well) so that only intracellular curcumin was detected. The excitation and emission wavelengths used were λ_{ex} = 405 nm and λ_{em} = 470 – 600 nm, respectively. The excitation source was a PicoQuant PDL 800-B pulse diode laser with a repetition rate of 4 MHz. The average excitation power used was 3 mW. The excitation light was focused onto the sample using a Leica HCX PL APO 63x N.A. 1.20 water-immersion objective with a 220 μm working distance. The emission was collected by the same objective, separated from the excitation source using a dichroic mirror and dispersed using a built-in spectrometer. Each image was acquired using line and frame averaging of 1 and 8, respectively. The images were 700 × 700 μm^2 and each image acquisition time was approximately 3 s. The first set of quantitative cellular uptake studies was performed using a FLUOstar OPTIMA microplate reader (λ_{ex} = 400 nm, λ_{em} = 520 nm). PC-3 cells (5×10^4 cells/well in 24-well plates) were plated in the same culture media and allowed to attach for 24 h. Cells were washed with PBS once and treated in sextuplicates with 12.5 μM curcumin, 66γCD_2su, 66γCD_2ur, curcumin-66γCD_2su or curcumin-66γCD_2ur in PBS, and incubated for the time periods. Cells were subsequently washed twice with PBS. At each incubation time point, 200 μL of chilled 100% methanol was used to lyse the cells in the six replicate wells. Lysates were combined and transferred to a well of a 96-well plate on ice in order to reduce methanol evaporation. Curcumin fluorescence intensity relative to untreated cells was measured. Data were normalized to the saturation intensity of curcumin (Supporting Information, Table S1) and was obtained by fitting with first-order binding kinetics. The second set of quantitative studies was aimed at investigating the role of BSA in cellular uptake of curcumin. A 4.0 mg/mL BSA solution was prepared in PBS, which corresponds to the concentration of BSA in PRF RPMI 1640 containing 10% DCC-FBS used in our cell viability and confocal fluorescence imaging assays.[43-45] Cells were incubated with either 0.0 or 4.0 mg/mL BSA solution supplemented with 12.5 μM curcumin, curcumin-66γCD_2su or curcumin-66γCD_2ur for 10 or 90 min, where fluorescence intensity was found to be within the error range of the half or full saturation value described above. The curcumin stock solution was mixed with either 66γCD_2su or 66γCD_2ur solution prior to dilution with the BSA solution. The curcumin

fluorescence intensity of 200 μL chilled 100% methanol lysates was measured using the microplate reader described above with identical wavelength settings. Fluorescence intensities were normalized to the half or full saturation intensity of each sample in PBS without BSA after 10-min or 90-min incubation, respectively.

Statistical Analyses

All data, except for cellular viability assays, are presented as mean ± standard deviation for three independently performed experiments unless described. The data from cellular viability assays are presented as mean ± standard error of the mean (SEM) of viable or dead cells per well in quadruplicates. Statistical analyses were performed by two-way ANOVA for paired comparisons of means. Values of $p > 0.05$ were indicative of insignificant differences whereas those of $p < 0.001$ were indicative of very significant differences.

Results

PC-3 viability in the presence of curcumin and encapsulated by diamide linked γ-CD dimers

The anti-proliferative effects of curcumin on PC-3 cells were evaluated using trypan blue exclusion, as described previously.[41,42] We observed a dose-dependent decrease in cell proliferation between 3.1 μM and 50.0 μM curcumin, with a 50% maximal inhibitory response (IC50) observed at 12.5 μM over a 5-day period (Figure 2A). The duration of our studies is consistent with that of previous studies.[46-51] Curcumin treatment did not appear to lead to an increased incidence of dead cells determined by trypan blue exclusion over the course of the experiments (Supporting Information; Figure S2). An IC50 concentration of 12.5 μM was determined and used for further investigation using 66γCD$_2$su and 66γCD$_2$ur as delivery agents.

The effect of curcumin encapsulated in either 66γCD$_2$su or 66γCD$_2$ur, namely curcumin-66γCD$_2$su and curcumin-66γCD$_2$ur, on PC-3 cells was investigated next over a 5-day period. Figure 2B shows the anti-proliferative effect of curcumin in the absence and presence of 66γCD$_2$su or 66γCD$_2$ur. Compared to vehicle, curcumin alone and curcumin-66γCD$_2$su were equally effective at inhibiting cell proliferation at all time points ($p > 0.05$). While curcumin-66γCD$_2$ur also inhibited cell proliferation effectively compared to vehicle at all time points ($p < 0.001$), it was only 73% as effective as curcumin or curcumin-66γCD$_2$su after Day 3 ($p < 0.001$; Figure 2B), indicating a delayed response. Importantly, neither 66γCD$_2$su nor 66γCD$_2$ur alone affected PC-3 cell proliferation compared to vehicle control ($p > 0.05$; Figure 2C).

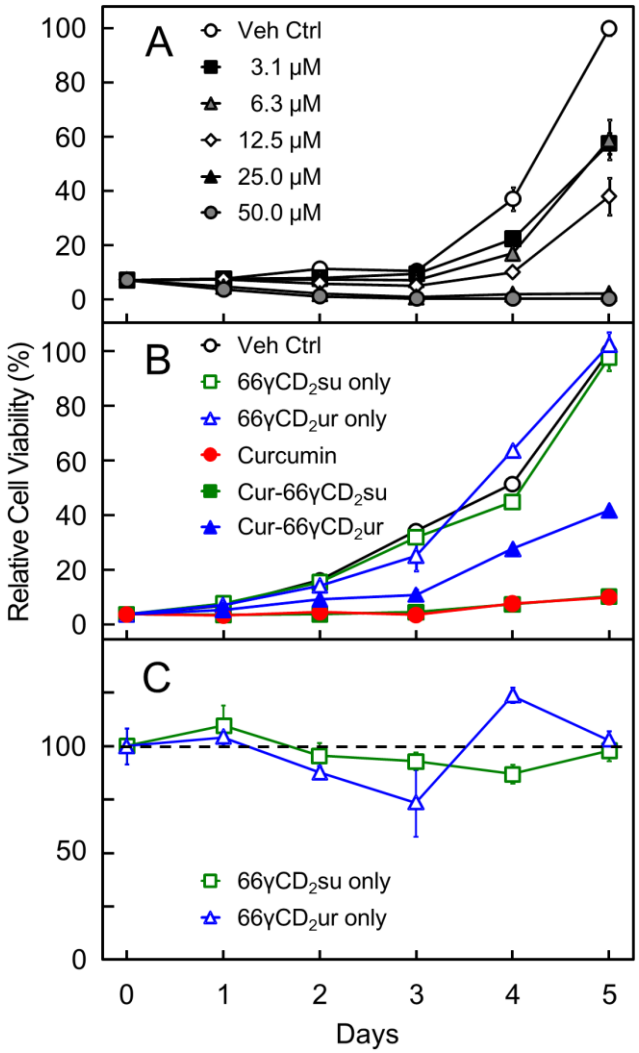

Figure 2: Cell viability assays performed using human prostate cancer PC-3 cells. (A) Viable PC-3 cells were treated with indicated concentrations of curcumin over 5 days, and viable cells were counted in the presence of trypan blue, demonstrating that curcumin exhibits dose-dependent anti-proliferative activity. (B) Viable PC-3 cells were counted using trypan blue assays after treatment with 12.5 μM curcumin, curcumin-66γCD$_2$su or curcumin-66γCD$_2$ur over 5 days. (C) Viable PC-3 cells were counted using trypan blue assays and treated with 66γCD$_2$su or 66γCD$_2$ur with respect to vehicle control (shown as dashed line), indicating their non-toxic nature ($p > 0.05$)

Curcumin-induced gene expression in the PC-3 cell line

Heme oxygenase 1 gene (*HMOX1*) is an inducible stress response gene forming part of the nuclear factor like 2 (NRF2) pathway, a primary cellular defense against cytotoxic effects of oxidative stress. Curcumin-induced expression of *HMOX1* has been well characterized in several cellular systems.[52-54] Here we used *HMOX1* regulation to infer and quantitate the intracellular delivery and biological activity of curcumin, curcumin-66γCD$_2$su and curcumin-66γCD$_2$ur in PC-3 cells. At 12.5 μM, a clear up-regulation of *HMOX1* expression with curcumin alone was observed relative to vehicle control (58 fold, $p < 0.001$; Figure 3A). Similar upregulation (53 or 70 fold) was observed with curcumin encapsulated in 66γCD$_2$su or 66γCD$_2$ur, respectively ($p < 0.001$). Furthermore, at 25.0 μM, both curcumin-66γCD$_2$su and curcumin-66γCD$_2$ur had significantly greater effect on *HMOX1* upregulation (140 fold) than curcumin alone (112 fold, $p < 0.001$). *HMOX1* expression did not increase above baseline levels in PC-3

cells treated with either 66γCD$_2$su or 66γCD$_2$ur alone (*i.e.*, 0 μM curcumin; Figure 3A and inset), consistent with the results in Figure 2. To support this finding further, we investigated 4 other curcumin target genes,[55-62] one of which was upregulated (*GADD45A*) and three down regulated (*TNFRSF10B, BRCA2* and *NFκBIA*) in response to curcumin treatment. The diamide linked γ-CD dimer encapsulated forms of curcumin were equally as effective as curcumin alone in increasing or decreasing expression of these candidate genes (Figures 3B-E), and again 66γCD$_2$su or 66γCD$_2$ur alone did not affect gene expression (Figure 3B-E). Together, these results demonstrate that encapsulation with 66γCD$_2$su or 66γCD$_2$ur permits intracellular delivery and biological activity of curcumin.

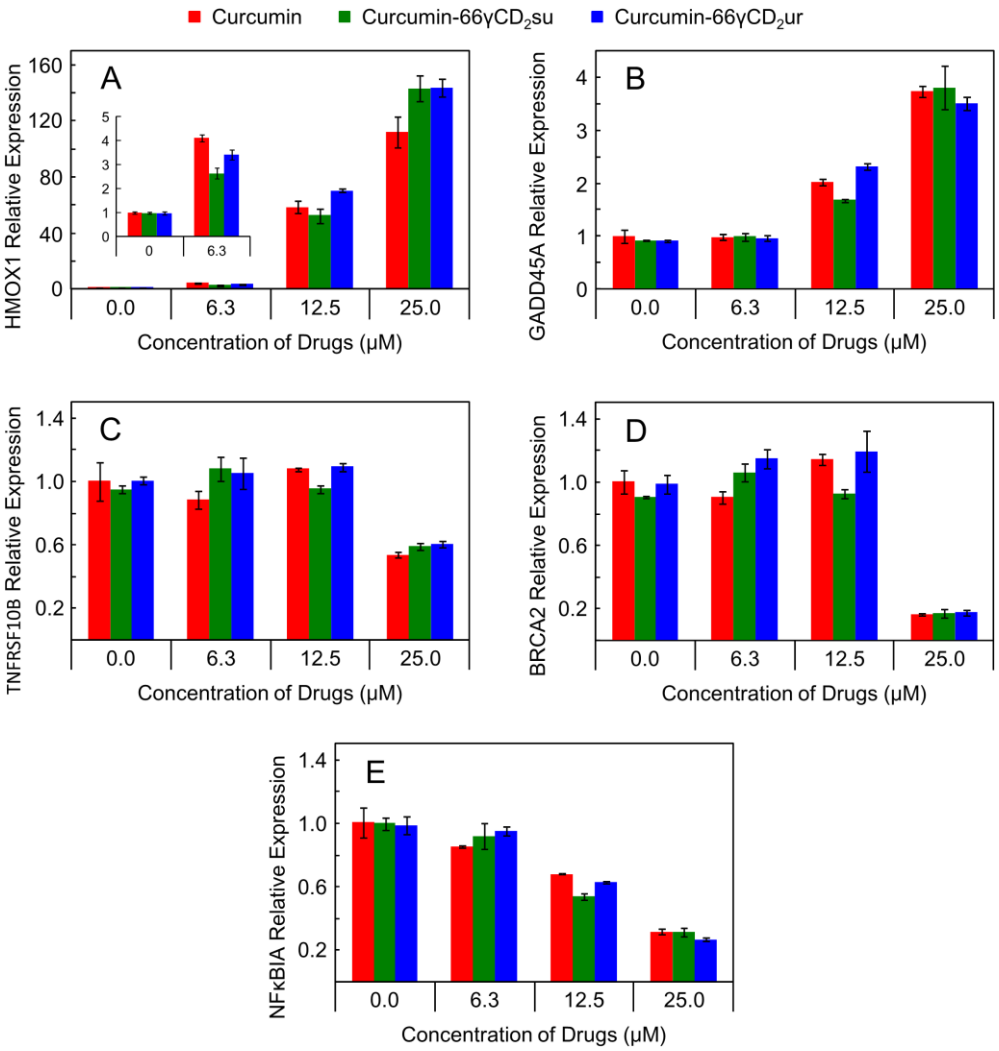

Figure 3: Relative expression of (A) *HMOX1*, (B) *GADD45A*, (C) *TNFRSF10B*, (D) *BRCA2* and (E) *NFκBIA* in PC-3 cells treated with different concentrations of curcumin (red), curcumin-66γCD$_2$su (green) or curcumin-66γCD$_2$ur (blue). The gene expression was normalized to those of *GAPDH* and *RPL32*. The 0.0 μM represents vehicle control with 0.05 vol% DMSO (red), 25.0 μM 66γCD$_2$su (green), and 25.0 μM 66γCD$_2$ur (blue).

Qualitative and Quantitative Cellular Uptake Studies of Curcumin

Next, we assessed the amount of curcumin delivered to PC-3 cells qualitatively using confocal fluorescence microscopy. Figure 4 shows fluorescence images of PC-3 cells treated with 12.5 μM curcumin, curcumin-66γCD$_2$su or curcumin-66γCD$_2$ur for 1 and 4 days. The fluorescence intensity at 1

day of each treatment was substantially greater than the detection limit (Figure 4, upper panels) while the intrinsic fluorescence of untreated cells was negligible (Supporting Information; Figure S3-5, panel A). Irrespective of 66γCD$_2$su or 66γCD$_2$ur encapsulation, curcumin fluorescence was still detectable within cells after single dose treatment at Day 4, with an intensity roughly half of that observed at Day 1, with slightly lower intensities for both treatments with encapsulated curcumin (Figure 4, lower panels).

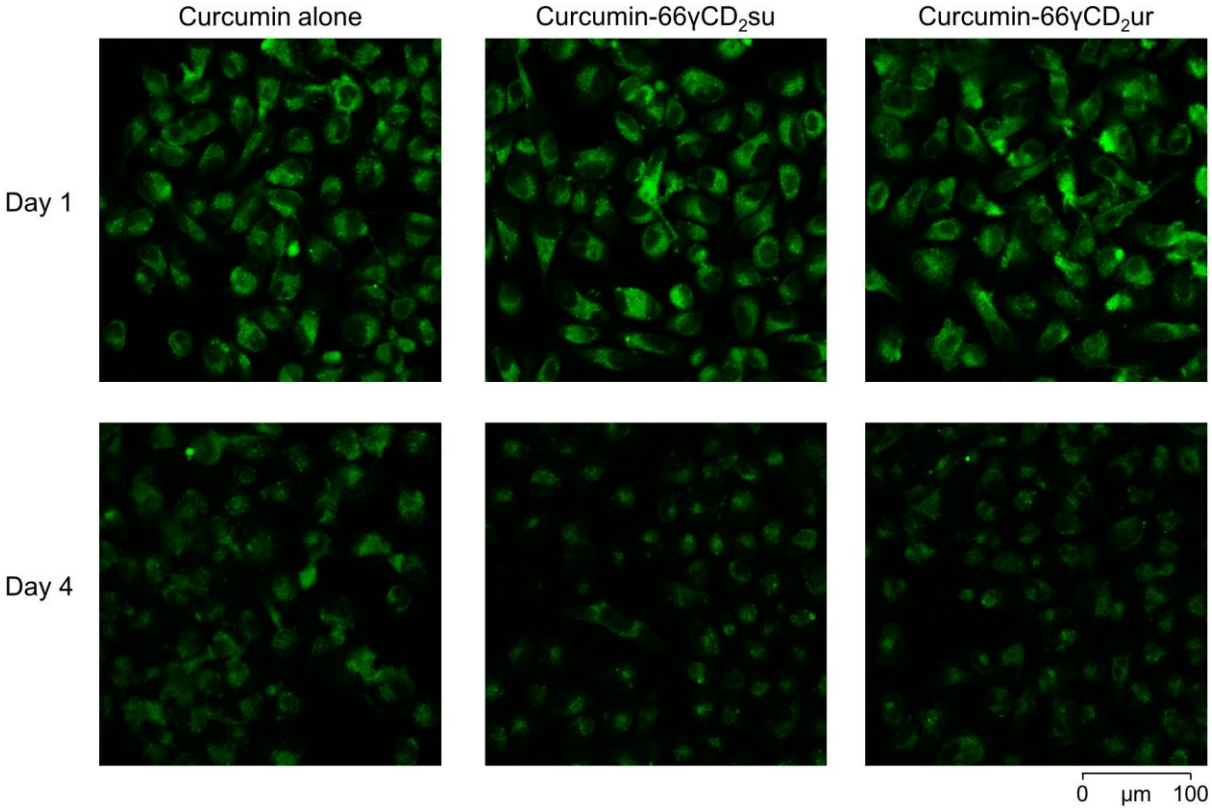

Figure 4: Confocal fluorescence images of PC-3 cells treated with 12.5 μM curcumin, curcumin-66γCD$_2$su and curcumin-66γCD$_2$ur 1 day (top) and 4 days (bottom) after single dose treatment.

Although fluorescence imaging revealed the intracellular presence of curcumin, the influence of serum proteins on curcumin delivery, specifically the effect of the most abundant protein in FBS, BSA, was not revealed. Therefore, the uptake of curcumin by PC-3 cells 10 and 90 min after treatment was measured using a fluorescent plate reader. The treatments involved using solutions of 12.5 μM curcumin, curcumin-66γCD$_2$su or curcumin-66γCD$_2$ur in PBS alone or PBS spiked with 4.0 mg/mL BSA, which is the approximate concentration found in 10% DCC-FBS/PRF RPMI 1640 and 5 times higher than the 12.5 M diamide linked γ-CD dimers used in our experiments.[43-45] The relative fluorescence intensity of each curcumin solution in the presence of BSA at 10 or 90 min was normalized to that in the absence of BSA (Figure 5). Importantly, the relative fluorescence intensity in cells treated with un-encapsulated curcumin was 72% lower when BSA was present in the solution ($p < 0.001$). However, BSA had a minor effect on the relative fluorescence intensity in cells treated with either curcumin-66γCD$_2$su or curcumin-66γCD$_2$ur (*n.s.*, $p > 0.05$), as shown in Figure 5. In addition, the fluorescence intensity of cells treated with curcumin alone in the presence of BSA resulted in a similar level to that of curcumin delivered by either 66γCD$_2$su or 66γCD$_2$ur (Supporting Information, Figure S6). Furthermore, the treatments were also applied to PC-3 cells in serum-free PBS to determine the amount of curcumin in cells within the

time scale that cellular proliferation was negligible. Consistent with first order binding kinetics, the fluorescent intensity following treatment with curcumin alone reached 50% of the maximum value within the first 10 min, and saturated around 90 min, increasing at a rate constant of 0.050 ± 0.012 min^{-1} (Supporting Information, Figure S7). The maximum fluorescence remained constant over an extended period of time (60 – 180 min; Supporting Information, Figure S8). In the presence of either 66γCD_2su or 66γCD_2ur (Supporting Information, Figure S7), the curcumin fluorescence intensity increased at a rate constant of 0.076 ± 0.031 min^{-1} and 0.029 ± 0.018 min^{-1}, respectively. The maximum fluorescence intensity of curcumin delivered by either 66γCD_2su or 66γCD_2ur is 5 – 9 times lower than that of curcumin alone.

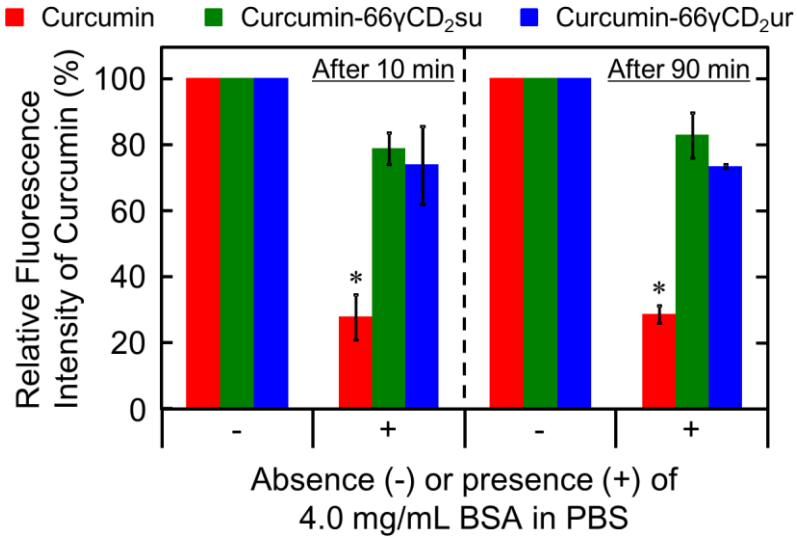

Figure 5: Effects of BSA on cellular uptake of curcumin in the absence (–) and presence (+) of either 66γCD_2su or 66γCD_2ur. PC-3 cells were treated with 12.5 μM of each solution prepared with either PBS alone or PBS spiked with 4.0 mg/mL BSA, for 10 (left) and 90 min (right). The asterisks in the figure represent statistically significant decrease in fluorescence intensity of curcumin due to the presence of BSA ($p < 0.001$).

Discussion

Curcumin, a naturally occurring yellow polyphenol, has been shown to have significant medicinal effects including anti-cancer and anti-inflammatory activities.[8-11] However, the poor solubility and stability of curcumin that limit the *in vivo* availability are major problems for the development of curcumin as a therapeutic agent. The association of curcumin with a delivery agent is an approach to address these issues. Our previous study showed effective and significant aqueous stabilization of curcumin using diamide linked γ-CD dimers, 66γCD_2su and 66γCD_2ur.[16] Here, we propose the use of 66γCD_2su and 66γCD_2ur as novel delivery systems for curcumin without perturbing its medicinal efficacy.

We demonstrated that curcumin inhibits the proliferation of PC-3 cells in a dose-dependent manner, which is consistent with previous studies.[63,64] Importantly, our results reveal that the use of the delivery agents 66γCD_2su and 66γCD_2ur does not prevent the anti-proliferative effect of curcumin, indicating effective intracellular delivery and biological activity of curcumin. In addition, we demonstrated that 66γCD_2su and 66γCD_2ur alone do not affect cellular proliferation or death, supporting a general non-toxic nature of these delivery agents. This observation is consistent with single γ-CDs being non-toxic,[34]

and the diamide linker of 66γCD$_2$su and 66γCD$_2$ur being hydrolyzed enzymatically in the cellular environment.[65-68] It is also important to stress that delivery of curcumin using 66γCD$_2$su and 66γCD$_2$ur here was achieved at a 1:1 molar ratio, whereas delivery systems with a much higher cyclodextrin-to-curcumin molar ratios have been reported in previous studies.[69-71] Curcumin delivery using 66γCD$_2$su and 66γCD$_2$ur is therefore more effective and efficient than other cyclodextrin-based delivery systems, and a higher concentration of encapsulated curcumin can be achieved.

Intracellular delivery of curcumin and the negligible effect of 66γCD$_2$su and 66γCD$_2$ur were observed on the expression of curcumin target genes. The increase or decrease in gene regulation was evident from curcumin treatment and exhibited a strong dependence on the dose of curcumin, which has been shown previously.[54] Our results showed that the gene expression of PC-3 cells treated with 66γCD$_2$su-curcumin or 66γCD$_2$ur-curcumin is also dose-dependent and comparable to curcumin alone, indicating that these delivery agents do not prevent the intracellular efficacy or uptake of curcumin. In addition, we demonstrated that neither 66γCD$_2$su nor 66γCD$_2$ur alone has any effect on these curcumin responsive target genes, which further supports their non-toxic nature up to 25.0 μM, consistent with our viability assay results.

Fluorescence imaging and spectroscopic studies provide further, direct evidence of curcumin-cell interaction owing to the sensitivity of the fluorescence properties of curcumin to the polarity of the surrounding environment.[22,72,73] For instance, the fluorescence quantum yields of curcumin in BSA and sodium dodecyl sulfate (SDS) micelles, which have hydrophobic characteristics similar to cell membranes, are approximately 2 – 5%, while that in a pH 7.4 phosphate buffer solution is negligible.[16,22,30] In addition, our previous study showed that curcumin is essentially non-fluorescent in the presence of either 66γCD$_2$su or 66γCD$_2$ur in buffer solution.[16] Our observation of intracellular fluorescence here therefore indicates that curcumin is present in hydrophobic regions, *e.g.*, membranes, within the intracellular space. The results can be used to directly assess the delivery of curcumin to PC-3 cells.

Confocal fluorescence images demonstrate a minor difference between the fluorescence intensity of curcumin alone and curcumin delivered by either 66γCD$_2$su or 66γCD$_2$ur, similar to our cellular viability and gene expression results. Together, all of these data demonstrate efficient intracellular delivery of curcumin by 66γCD$_2$su and 66γCD$_2$ur. Another interesting observation in the confocal fluorescence images is a lower fluorescence level in the nucleus, implying that curcumin is present at a higher concentration in the cytoplasm than the nucleus. This result was also observed in a previous study.[74] Moreover, the slightly lower fluorescence intensity of curcumin delivered by 66γCD$_2$su and 66γCD$_2$ur than curcumin alone at Day 4 is unlikely to arise from lower curcumin levels. This is because nearly identical anti-proliferative effects of curcumin alone and curcumin delivered by 66γCD$_2$su were observed, as shown in Figure 2b. It is likely that similar levels of curcumin were present in all cases.

We also considered the role of serum proteins in the cellular uptake of curcumin. It is possible that a significant proportion of curcumin in either 66γCD$_2$su or 66γCD$_2$ur are bound to serum proteins as the concentration of BSA was substantially higher than that of either 66γCD$_2$su or 66γCD$_2$ur in the medium. Previous studies showed that curcumin (in the absence of 66γCD$_2$su and 66γCD$_2$ur) is captured and stabilized by serum proteins and model membranes.[16,17,22,29,30,75] The stabilization of curcumin by these

systems may result in a similar level of anti-proliferative effect and fluorescence intensity of curcumin in the absence of 66γCD$_2$su and 66γCD$_2$ur. To further understand curcumin delivery to PC-3 cells we performed quantitative curcumin uptake studies.

Our results in Figure 5 indicate that a significant fraction of curcumin binds to BSA in the absence of either 66γCD$_2$su or 66γCD$_2$ur. Previous studies determined that the binding constants of curcumin to serum proteins are approximately 10^5 M^{-1}.[17,29,30] Therefore, the binding of curcumin to the hydrophobic pockets of BSA may be sufficiently strong to prevent curcumin from making contact with cell membranes and thereby inhibit transfer of curcumin by diffusion. In contrast, the intracellular delivery of 66γCD$_2$su- or 66γCD$_2$ur-complexed curcumin appears to be BSA-independent as there is only an insignificant decrease in curcumin uptake between the results with the absence and presence of BSA. This phenomenon is attributable to high binding constants of curcumin to either 66γCD$_2$su or 66γCD$_2$ur, of which are on the order of 10^6 M^{-1}.[16] Here, we propose that curcumin is directly delivered into PC-3 cells by either 66γCD$_2$su or 66γCD$_2$ur as follows. Curcumin may exist in the annuli of either 66γCD$_2$su or 66γCD$_2$ur or be transferred to the hydrophobic pocket of BSA, and/or bind to cell membranes, by diffusion. Our uptake results with and without BSA indicate that a high portion of curcumin remains in the annuli of 66γCD$_2$su and 66γCD$_2$ur rather than being transferred to BSA, in spite of a roughly five times higher BSA concentration. In addition, previous studies suggest a lack of interaction between either β-CD or diamide linked γ-CD dimers and the cell membrane based on SDS model membrane experiments.[16,75] Hence, the results here strongly suggest that 66γCD$_2$su and 66γCD$_2$ur deliver curcumin directly to the cell membrane, independent of the presence of BSA. Moreover, the fluorescence signal of curcumin alone in the presence of BSA is significantly weaker than that in its presence (Supporting Information, Figure S6), indicating that BSA reduces curcumin availability. However, the presence of BSA has a negligible effect on the fluorescence signals of curcumin in either 66γCD$_2$su or 66γCD$_2$ur (Supporting Information, Figure S6), supporting the high entrapment efficiency of the γ-CD dimers.

Our cellular uptake study in the serum-free environment further shows that curcumin and curcumin delivered by 66γCD$_2$su and 66γCD$_2$ur possess similar rate constants for uptake by PC-3 cells, indicating that similar cell membrane diffusion processes are involved for free curcumin and curcumin delivered using either 66γCD$_2$su or 66γCD$_2$ur. In the absence of the diamide linked γ-CD dimers, curcumin is able to partition into the cell membrane by diffusion,[16] which results in the maximum amount of curcumin in the cell. In contrast, in the presence of either 66γCD$_2$su or 66γCD$_2$ur, curcumin partitions largely into the diamide linked γ-CD dimers,[16] leading to an overall lower level of fluorescence because curcumin in the latter environment is essentially non-fluorescent.[16] However, observable fluorescence signal in addition to similar uptake rate constants illustrates that a moderate level of curcumin is released from 66γCD$_2$su or 66γCD$_2$ur by diffusion.

The advantage of the BSA-independent delivery of curcumin by 66γCD$_2$su and 66γCD$_2$ur is the control of effective dose of curcumin in cancer treatment. The direct delivery of curcumin to cells raises the possibility of protecting the highly labile curcumin against serum proteins and potentially lipoproteins in the circulatory system for an extended period of time by encapsulation. Furthermore, curcumin forms a more stable complex with 66γCD$_2$su and 66γCD$_2$ur than with BSA,[17] and our uptake results suggest a possible gradual increase in intracellular curcumin due to sustained delivery from either 66γCD$_2$su or 66γCD$_2$ur even in the presence of BSA. This phenomenon is consistent with the delayed and reduced

effects observed in our cell viability and fluorescence images. Therefore, our delivery agents, 66γCD_2su and 66γCD_2ur, potentially offer a prolonged delivery of curcumin in cancer therapy, and may therefore protect against rapid hepatic or renal clearance. Finally, while this study is concerned with the delivery of curcumin by 66γCD_2su and 66γCD_2ur *in vitro*, these agents may also be efficacious to deliver other therapeutic agents in other experimental systems.

A combination of either 66γCD_2su or 66γCD_2ur with curcumin will be investigated in our future *in vivo* studies to investigate their toxicity and pharmacological profiles, with an ultimate goal of developing curcumin-66γCD_2su and curcumin-66γCD_2ur as naturally derived chemotherapeutic drugs or their supplements.

Conclusions

We report here for the first time the direct intracellular delivery of curcumin using diamide linked γ-CD dimers, 66γCD_2su and 66γCD_2ur. These delivery agents offer molecular-scale encapsulation of curcumin at concentrations ranging from M to mM and a high structural integrity under physiological conditions. While encapsulation of curcumin using either 66γCD_2su or 66γCD_2ur strongly suppresses its degradation, cellular viability and uptake assays combined with gene expression and fluorescence microscopy reveal that 66γCD_2su and 66γCD_2ur alone do not produce measurable toxicity on viability or gene expression. The 66γCD_2su and 66γCD_2ur are both effective means to deliver curcumin into cells, resulting in inhibition of cellular proliferation, while initiating changes in gene expression similar to that exhibited by curcumin alone. Furthermore, the formation of 66γCD_2su and 66γCD_2ur with curcumin appears to protect curcumin from binding to BSA, which may result in a more efficient intracellular delivery via cell membranes. Together, our results demonstrate the promise of these novel non-toxic molecular-scale agents to deliver curcumin and other highly labile compounds to mammalian cells effectively, and therefore may present a more effective means of delivering these agents *in vivo*.

Acknowledgements

This work was supported in part by research grants from the Australian Research Council (DP0878100 and DP110101101), the Prostate Cancer Foundation of Australia (PG2210 to GB) and Cancer Australia (APP1032970 to GB and EFN). GB holds a Freemasons Foundation Centre for Men's Health postdoctoral fellowship and EFN holds a Hospital Research Foundation Early Career Fellowship. The authors acknowledge Ms. Lynette Waterhouse, Adelaide Microscopy, for induction with the Leica TCS SP5 confocal microscope. The authors also acknowledge Mr. Damien Leach at the Molecular Aging Laboratory for his support and advice on the cell studies. Ms. Allira Perks also contributed to this project through a Summer Research Scholarship supported by the University of Adelaide.

Supporting Information

Release of curcumin from 66γCD_2su and 66γCD_2ur, relative cell death determined by trypan blue exclusion assay, confocal fluorescence images of cells treated with nascent and encapsulated curcumin from Day 1 to Day 5 and curcumin uptake results. This material is available free of charge via the Internet at http://pubs.acs.org.

References

(1) Ferlay, J.; Shin, H.-R.; Bray, F.; Forman, D.; Mathers, C.; Parkin, D. M. Estimates of Worldwide Burden of Cancer in 2008: GLOBOCAN 2008. *Int. J. Cancer* **2010**, *127*, 2893-2917.

(2) Petrylak, D. P.; Tangen, C. M.; Hussain, M. H. A.; Lara, P. J.; Jones, J. A.; Taplin, M. E.; Burch, P. A.; Berry, D.; Moinpour, C.; Kohli, M.*et al.* Docetaxel and Estramustine Compared with Mitoxantrone and Prednisone for Advanced Refractory Prostate Cancer. *N. Engl. J. Med.* **2004**, *351*, 1513-1520.

(3) Jamieson, E. R.; Lippard, S. J. Structure, Recognition, and Processing of Cisplatin−DNA Adducts. *Chem. Rev.* **1999**, *99*, 2467-2498.

(4) Jung, Y. W.; Lippard, S. J. Direct Cellular Responses to Platinum-Induced DNA Damage. *Chem. Rev.* **2007**, *107*, 1387-1407.

(5) Cheng, A. L.; Hsu, C. H.; Lin, J. K.; Hsu, M. M.; Ho, Y. F.; Shen, T. S.; Ko, J. Y.; Lin, J. T.; Lin, B. R.; Wu, M. S.*et al.* Phase I Clinical Trial of Curcumin, A Chemopreventive Agent, in Patients with High-Risk or Pre-Malignant Lesions. *Anticancer Res.* **2001**, *21*, 2895-2900.

(6) Aggarwal, B. B.; Kumar, A.; Bharti, A. C. Anticancer Potential of Curcumin: Preclinical and Clinical Studies. *Anticancer Res.* **2003**, *23*, 363-398.

(7) Goel, A.; Kunnumakkara, A. B.; Aggarwal, B. B. Curcumin as "Curecumin": From kitchen to clinic. *Biochem. Pharmacol.* **2008**, *75*, 787-809.

(8) Kuttan, R.; Bhanumathy, P.; Nirmala, K.; George, M. C. Potential Anticancer Activity of Turmeric (Curcuma-longa). *Cancer Lett.* **1985**, *29*, 197-202.

(9) Anand, P.; Sundaram, C.; Jhurani, S.; Kunnumakkara, A. B.; Aggarwal, B. B. Curcumin and Cancer: An "Old-Age" Disease with an "Age-Old" Solution. *Cancer Lett.* **2008**, *267*, 133-164.

(10) Maheshwari, R. K.; Singh, A. K.; Gaddipati, J.; Srimal, R. C. Multiple Biological Activities of Curcumin: A Short Review. *Life Sci.* **2006**, *78*, 2081-2087.

(11) Srimal, R. C.; Dhawan, B. N. Pharmacology of Diferuloyl Methane (Curcumin), a Nonsteroidal Antiinflammatory Agent. *J. Pharm. Pharmacol.* **1973**, *25*, 447-452.

(12) Cole, G. M.; Lim, G. P.; Yang, F.; Teter, B.; Begum, A.; Ma, Q.; Harris-White, M. E.; Frautschy, S. A. Prevention of Alzheimer's Disease: Omega-3 Fatty Acid and Phenolic Anti-oxidant Interventions. *Neurobiol. Aging* **2005**, *26*, 133-136.

(13) Egan, M. E.; Pearson, M.; Weiner, S. A.; Rajendran, V.; Rubin, D.; Glockner-Pagel, J.; Canny, S.; Du, K.; Lukacs, G. L.; Caplan, M. J. Curcumin, A Major Constituent of Turmeric, Corrects Cystic Fibrosis Defects. *Science* **2004**, *304*, 600-602.

(14) Letchford, K.; Liggins, R.; Burt, H. Solubilization of Hydrophobic Drugs by Methoxy Poly(ethylene glycol)-block-polycaprolactone Diblock Copolymer Micelles: Theoretical and Experimental Data and Correlations. *J. Pharm. Sci.* **2008**, *97*, 1179-1190.

(15) Kaminaga, Y.; Nagatsu, A.; Akiyama, T.; Sugimoto, N.; Yamazaki, T.; Maitani, T.; Mizukami, H. Production of Unnatural Glucosides of Curcumin with Drastically Enhanced Water Solubility by Cell Suspension Cultures of Catharanthus Roseus. *FEBS Lett.* **2003**, *555*, 311-316.

(16) Harada, T.; Pham, D.-T.; Leung, M. H. M.; Ngo, H. T.; Lincoln, S. F.; Easton, C. J.; Kee, T. W. Cooperative Binding and Stabilization of the Medicinal Pigment Curcumin by Diamide Linked g-Cyclodextrin Dimers: A Spectroscopic Characterization. *J. Phys. Chem. B* **2011**, *115*, 1268-1274.

(17) Leung, M. H. M.; Kee, T. W. Effective Stabilization of Curcumin by Association to Plasma Proteins: Human Serum Albumin and Fibrinogen. *Langmuir* **2009**, *25*, 5773-5777.

(18) Wang, Y. J.; Pan, M. H.; Cheng, A. L.; Lin, L. I.; Ho, Y. S.; Hsieh, C. Y.; Lin, J. K. Stability of Curcumin in Buffer Solutions and Characterization of its Degradation Products. *J. Pharm. Biomed. Anal.* **1997**, *15*, 1867-1876.
(19) Leung, M. H. M.; Colangelo, H.; Kee, T. W. Encapsulation of Curcumin in Cationic Micelles Suppresses Alkaline Hydrolysis. *Langmuir* **2008**, *24*, 5672-5675.
(20) Mohanty, C.; Acharya, S.; Mohanty, A. K.; Dilnawaz, F.; Sahoo, S. K. Curcumin-Encapsulated MePEG/PCL Diblock Copolymeric Micelles: A Novel Controlled Delivery Vehicle for Cancer Therapy. *Nanomedicine* **2010**, *5*, 433-449.
(21) Tang, H. D.; Murphy, C. J.; Zhang, B.; Shen, Y. Q.; Sui, M. H.; Van Kirk, E. A.; Feng, X. W.; Murdoch, W. J. Amphiphilic Curcumin Conjugate-Forming Nanoparticles as Anticancer Prodrug and Drug Carriers: in vitro and in vivo Effects. *Nanomedicine* **2010**, *5*, 855-865.
(22) Wang, Z. F.; Leung, M. H. M.; Kee, T. W.; English, D. S. The Role of Charge in the Surfactant-Assisted Stabilization of the Natural Product Curcumin. *Langmuir* **2010**, *26*, 5520-5526.
(23) Takahashi, M.; Uechi, S.; Takara, K.; Asikin, Y.; Wada, K. Evaluation of an Oral Carrier System in Rats: Bioavailability and Antioxidant Properties of Liposome-Encapsulated Curcumin. *J. Agric. Food Chem.* **2009**, *57*, 9141-9146.
(24) Chen, C.; Johnston, T. D.; Jeon, H.; Gedaly, R.; McHugh, P. P.; Burke, T. G.; Ranjan, D. An in vitro Study of Liposomal Curcumin: Stability, Toxicity and Biological Activity in Human Lymphocytes and Epstein-Barr Virus-Transformed Human B-cells. *Int. J. Pharm.* **2009**, *366*, 133-139.
(25) Tønnesen, H. H.; Smistad, G.; Agren, T.; Karlsen, J. Studies on Curcumin and Curcuminoids XXIII. Effects of Curcumin on Liposomal Lipid-Peroxidation. *Int. J. Pharm.* **1993**, *90*, 221-228.
(26) Mathur, A. B.; Gupta, V. Silk Fibroin-Derived Nanoparticles for Biomedical Applications. *Nanomedicine* **2010**, *5*, 807-820.
(27) Yallapu, M. M.; Gupta, B. K.; Jaggi, M.; Chauhan, S. C. Fabrication of Curcumin Encapsulated PLGA Nanoparticles for Improved Therapeutic Effects in Metastatic Cancer Cells. *J. Colloid Interface Sci.* **2010**, *351*, 19-29.
(28) Das, R. K.; Kasoju, N.; Bora, U. Encapsulation of Curcumin in Alginate-Chitosan-Pluronic Composite Nanoparticles for Delivery to Cancer Cells. *Nanomed.: Nanotechnol. Biol. Med.* **2010**, *6*, 153-160.
(29) Sahu, A.; Kasoju, N.; Bora, U. Fluorescence Study of the Curcumin−Casein Micelle Complexation and its Application as a Drug Nanocarrier to Cancer Cells. *Biomacromolecules* **2008**, *9*, 2905-2912.
(30) Barik, A.; Priyadarsini, K. I.; Mohan, H. Photophysical Studies on Binding of Curcumin to Bovine Serum Albumin. *Photochem. Photobiol.* **2003**, *77*, 597-603.
(31) Esmaili, M.; Ghaffari, S. M.; Moosavi-Movahedi, Z.; Atri, M. S.; Sharifizadeh, A.; Farhadi, M.; Yousefi, R.; Chobert, J. M.; Haertle, T.; Moosavi-Movahedi, A. A. Beta Casein-Micelle as a Nano Vehicle for Solubility Enhancement of Curcumin; Food Industry Application. *Lwt-Food Sci. Technol.* **2011**, *44*, 2166-2172.
(32) Yazdi, S. R.; Corredig, M. Heating of Milk Alters the Binding of Curcumin to Casein Micelles. A Fluorescence Spectroscopy Study. *Food Chem.* **2012**, *132*, 1143-1149.
(33) Yang, L.; Alexandridis, P. Physicochemical Aspects of Drug Delivery and Release from Polymer-Based Colloids. *Curr. Opin. Colloid Interface Sci.* **2000**, *5*, 132-143.

(34) FDA. gamma cyclodexrin. Food and Drug Administration; **2000** [updated 2012 Jun 30; cited 2012 Aug 3]; Available from: http://www.accessdata.fda.gov/scripts/fcn/fcnDetailNavigation.cfm?rpt=grasListing&id=46.

(35) FDA. beta cyclodexrin. Food and Drug Administration; **2001** [updated 2012 Jun 30; cited 2012 Aug 3]; Available from: http://www.accessdata.fda.gov/scripts/fcn/fcnDetailNavigation.cfm?rpt=grasListing&id=74.

(36) FDA. alpha cyclodexrin. Food and Drug Administration; **2004** [updated 2012 Jun 30; cited 2012 Aug 3]; Available from: http://www.accessdata.fda.gov/scripts/fcn/fcnDetailNavigation.cfm?rpt=grasListing&id=155.

(37) Szejtli, J. Introduction and General Overview of Cyclodextrin Chemistry. *Chem. Rev.* **1998**, *98*, 1743-1753.

(38) Hirayama, F.; Uekama, K. Cyclodextrin-Based Controlled Drug Release System. *Adv. Drug Deliver. Rev.* **1999**, *36*, 125-141.

(39) Thompson, D. O. Cyclodextrins - Enabling Excipients: Their Present and Future Use in Pharmaceuticals. *Crit. Rev. Ther. Drug* **1997**, *14*, 1-104.

(40) Pham, D. T.; Ngo, H. T.; Lincoln, S. F.; May, B. L.; Easton, C. J. Synthesis of C6(A)-to-C6(A) and C3(A)-to-C3(A) Diamide Linked Gamma-cyclodextrin Dimers. *Tetrahedron* **2010**, *66*, 2895-2898.

(41) Marrocco, D. L.; Tilley, W. D.; Bianco-Miotto, T.; Evdokiou, A.; Scher, H. I.; Rifkind, R. A.; Marks, P. A.; Richon, V. M.; Butler, L. M. Suberoylanilide Hydroxamic Acid (Vorinostat) Represses Androgen Receptor Expression and Acts Synergistically with an Androgen Receptor Antagonist to Inhibit Prostate Cancer Cell Proliferation. *Mol. Cancer Ther.* **2007**, *6*, 51-60.

(42) Uliasz, T. F.; Hewett, S. J. A Microtiter Trypan Blue Absorbance Assay for the Quantitative Determination of Excitotoxic Neuronal Injury in Cell Culture. *J. Neurosci. Methods* **2000**, *100*, 157-163.

(43) Hayakawa, H.; Umehara, K.; Myrvik, Q. Oxidative Responses of Rabbit Alveolar Macrophages: Comparative Priming Activities of MIF/MAF, Sera, and Serum Components. *J. Leukoc. Biol.* **1989**, *45*, 231-238.

(44) Granato, A.; Gores, G.; Vilei, M. T.; Tolando, R.; Ferraresso, C.; Muraca, M. Bilirubin Inhibits Bile Acid Induced Apoptosis in Rat Hepatocytes. *Gut* **2003**, *52*, 1774-1778.

(45) Ueda, A.; Shimomura, M.; Ikeda, M.; Yamaguchi, R.; Tanishita, K. Effect of Glycocalyx on Shear-Dependent Albumin Uptake in Endothelial Cells. *Am. J. Physiol. Heart Circ. Physiol.* **2004**, *287*, H2287-H2294.

(46) Bang, Y. J.; Kim, S. J.; Danielpour, D.; Oreilly, M. A.; Kim, K. Y.; Myers, C. E.; Trepel, J. B. Cyclic-AMP Induces Transforming Growth-factor-beta-2 Gene-expression and Growth Arrest in the Human and Rogen-independent Prostate Carcinoma Cell Line PC-3. *Proc. Nat. Acad. Sc. U. S.* **1992**, *89*, 3556-3560.

(47) Bang, Y. J.; Pirnia, F.; Fang, W. G.; Kang, W. K.; Sartor, O.; Whitesell, L.; Ha, M. J.; Tsokos, M.; Sheahan, M. D.; Nguyen, P.*et al.* Terminal Neuroendocrine Differentiation of Human Prostate Carcinoma Cells in Response to Increased Intracellular Cyclic AMP. *Proc. Nat. Acad. Sc. U. S.* **1994**, *91*, 5330-5334.

(48) Calvert, R. C.; Shabbir, M.; Thompson, C. S.; Mikhailidis, D. P.; Morgan, R. J.; Burnstock, G. Immunocytochemical and Pharmacological Characterisation of P2-purinoceptor-mediated Cell Growth and Death in PC-3 Hormone Refractory Prostate Cancer Cells *Anticancer Res.* **2004**, *24*, 2853-2859.

(49) Jiang, Q.; Wong, J.; Fyrst, H.; Saba, J. D.; Ames, B. N. g-Tocopherol or Combinations of Vitamin E Forms Induce Cell Death in Human Prostate Cancer Cells by Interrupting Sphingolipid Synthesis. *Proc. Nat. Acad. Sc. U. S.* **2004**, *101*, 17825-17830.

(50) Paschka, A. G.; Butler, R.; Young, C. Y. F. Induction of Apoptosis in Prostate Cancer Cell Lines by the Green Tea Component, (-)-epigallocatechin-3-gallate. *Cancer Lett.* **1998**, *130*, 1-7.

(51) Rose, D. P.; Connolly, J. M. Effects of Fatty Acids and Eicosanoid Synthesis Inhibitors on the Growth of 2 Human Prostate Cancer Cell Lines. *Prostate* **1991**, *18*, 243-254.

(52) Thangapazham, R. L.; Shaheduzzaman, S.; Kim, K. H.; Passi, N.; Tadese, A.; Vahey, M.; Dobi, A.; Srivastava, S.; Maheshwari, R. K. Androgen Responsive and Refractory Prostate Cancer Cells Exhibit Distinct Curcumin Regulated Transcriptome. *Cancer Biol. Ther.* **2008**, *7*, 1429-1437.

(53) McNally, S. J.; Harrison, E. M.; Ross, J. A.; Garden, O. J.; Wigmore, S. J. Curcumin Induces Heme Oxygenase 1 through Generation of Reactive Oxygen Species, p38 Activation and Phosphatase Inhibition. *Int. J. Mol. Med.* **2007**, *19*, 165-172.

(54) Motterlini, R.; Foresti, R.; Bassi, R.; Green, C. J. Curcumin, an Antioxidant and Anti-inflammatory Agent, Induces Heme Oxygenase-1 and Protects Endothelial Cells against Oxidative Stress. *Free Radic. Biol. Med.* **2000**, *28*, 1303-1312.

(55) Aggarwal, B. B. Prostate Cancer and Curcumin - Add Spice to Your Life. *Cancer Biol. Ther.* **2008**, *7*, 1438-1442.

(56) Thangapazham, R. L.; Shaheduzzaman, S. M.; Kim, K. H.; Passi, N.; Dobi, A.; Srivastava, S.; Maheshwari, R. Androgen Responsive and Refractory Prostate Cancer Cells Exhibit Distinct Curcumin Regulated Transcriptome. *J. Urol.* **2008**, *179*, 190-191.

(57) Ravindran, J.; Subbaraju, G. V.; Ramani, M. V.; Sung, B. Y.; Aggarwal, B. B. Bisdemethylcurcumin and Structurally Related Hispolon Analogues of Curcumin Exhibit Enhanced Prooxidant, Anti-proliferative and Anti-inflammatory Activities in vitro. *Biochem. Pharmacol.* **2010**, *79*, 1658-1666.

(58) Shankar, S.; Chen, Q.; Sarva, K.; Siddiqui, I.; Srivastava, R. K.; J. Mol. Signal.: 2007; Vol. 2, p 1-14.

(59) Bachmeier, B. E.; Mirisola, V.; Romeo, F.; Generoso, L.; Esposito, A.; Dell'Eva, R.; Blengio, F.; Killian, P. H.; Albini, A.; Pfeffer, U. Reference Profile Correlation Reveals Estrogen-like Trancriptional Activity of Curcumin. *Cell. Physiol. Biochem.* **2010**, *26*, 471-482.

(60) Chirnomas, D.; Taniguchi, T.; de la Vega, M.; Vaidya, A. P.; Vasserman, M.; Hartman, A. R.; Kennedy, R.; Foster, R.; Mahoney, J.; Seiden, M. V.*et al.* Chemosensitization to Cisplatin by Inhibitors of the Fanconi Anemia/BRCA Pathway. *Mol. Cancer Ther.* **2006**, *5*, 952-961.

(61) Hour, T.-C.; Chen, J.; Huang, C.-Y.; Guan, J.-Y.; Lu, S.-H.; Pu, Y.-S. Curcumin Enhances Cytotoxicity of Chemotherapeutic Agents in Prostate Cancer Cells by Inducing p21WAF1/CIP1 and C/EBPβ Expressions and Suppressing NF-κB Activation. *Prostate* **2002**, *51*, 211-218.

(62) Mukhopadhyay, A.; Bueso-Ramos, C.; Chatterjee, D.; Pantazis, P.; Aggarwal, B. B. Curcumin Downregulates Cell Survival Mechanisms in Human Prostate Cancer Cell Lines. *Oncogene* **2001**, *20*, 7597-7609.

(63) Syrovets, T.; Gschwend, J. E.; Buchele, B.; Laumonnier, Y.; Zugmaier, W.; Genze, F.; Simmet, T. Inhibition of IkB Kinase Activity by Acetyl-boswellic Acids Promotes Apoptosis in Androgen-Independent PC-3 Prostate Cancer Cells in vitro and in vivo. *J. Biol. Chem.* **2005**, *280*, 6170-6180.

(64) Mukerjee, A.; Vishwanatha, J. K. Formulation, Characterization and Evaluation of Curcumin-loaded PLGA Nanospheres for Cancer Therapy. *Anticancer Res.* **2009**, *29*, 3867-3875.
(65) Janda, K. D.; Schloeder, D.; Benkovic, S. J.; Lerner, R. A. Induction of an Antibody that Catalyzes the Hydrolysis of an Amide Bond. *Science* **1988**, *241*, 1188-1191.
(66) Jencks, W. P.; Catalysis in Chemistry and Enzymology: McGraw-Hill: New York, 1969.
(67) Satterth, A. C.; Jencks, W. P. Mechanism of Aminolysis of Acetate Esters. *J. Am. Chem. Soc.* **1974**, *96*, 7018-7031.
(68) Fersht, A.; Enzyme Structure and Mechanism: W. H. Freeman & Company: London, 1985.
(69) Dhule, S. S.; Penfornis, P.; Frazier, T.; Walker, R.; Feldman, J.; Tan, G.; He, J.; Alb, A.; John, V.; Pochampally, R. Curcumin-Loaded γ-Cyclodextrin Liposomal Nanoparticles as Delivery Vehicles for Osteosarcoma. *Nanomed.: Nanotechnol. Biol. Med.* **2012**, *8*, 440-451.
(70) Yadav, V. R.; Prasad, S.; Kannappan, R.; Ravindran, J.; Chaturvedi, M. M.; Vaahtera, L.; Parkkinen, J.; Aggarwal, B. B. Cyclodextrin-Complexed Curcumin Exhibits Anti-inflammatory and Antiproliferative Activities Superior to those of Curcumin through Higher Cellular Uptake. *Biochem. Pharmacol.* **2010**, *80*, 1021-1032.
(71) Yallapu, M. M.; Jaggi, M.; Chauhan, S. C. b-Cyclodextrin-Curcumin Self-assembly Enhances Curcumin Delivery in Prostate Cancer Cells. *Colloids Surf., B* **2010**, *79*, 113-125.
(72) Chignell, C. F.; Bilskj, P.; Reszka, K. J.; Motten, A. G.; Sik, R. H.; Dahl, T. A. Spectral and Photochemical Properties of Curcumin. *Photochem. Photobiol.* **1994**, *59*, 295-302.
(73) Khopde, S. M.; Indira Priyadarsini, K.; Palit, D. K.; Mukherjee, T. Effect of Solvent on the Excited-State Photophysical Properties of Curcumin. *Photochem. Photobiol.* **2000**, *72*, 625-631.
(74) Anand, P.; Nair, H. B.; Sung, B. K.; Kunnumakkara, A. B.; Yadav, V. R.; Tekmal, R. R.; Aggarwal, B. B. Design of Curcumin-Loaded PLGA Nanoparticles Formulation with Enhanced Cellular Uptake, and Increased Bioactivity in vitro and Superior Bioavailability in vivo. *Biochem. Pharmacol.* **2010**, *79*, 330-338.
(75) Garcia-Rio, L.; Mendez, M.; Paleo, A. R.; Sardina, F. J. New Insights in Cyclodextrin: Surfactant Mixed Systems from the Use of Neutral and Anionic Cyclodextrin Derivatives. *J. Phys. Chem. B* **2007**, *111*, 12756-12764.

APPENDIX B

PRIMER SEQUENCES

Q = qRT-PCR, C = ChIP; all primers are listed as 5' to 3'

Use	Gene	Direction	Sequence
Q	ABCA6	F	CACACTGAGATTCTGAAGC
		R	CACAGGTTTGCTATCACC
Q	ABCC2	F	ACAGAGGCTGGTGGCAACC
		R	ACCATTACCTTGTCACTGTCCATGA
Q	ALAS1	F	AGATCAAAGAAACCCCTCCG
		R	AGCTGTGTGCCATCTGGACT
Q	AR	F	CTGGACACGACAACAACCAG
		R	CAGATCAGGGGCGAAGTAGA
Q	ATR	F	TGGGTCCTATGGGAACAGAG
		R	ACGCATCAGCCTCATTGTAA
Q	BRCA2	F	GTACAGGAAACAAGCTTCTGA
		R	GACTAACAGGTGGAGGTAAAG
Q	CDH11	F	AGAGGCCTACATTCTGAACG
		R	TTCTTTCTTTTGCCTTCTCAGG
Q	CLDN1	F	ATGGCCAACGCGGGGC
		R	ACGTAGTCTTTCCCGCTG
Q	CLSPN	F	AGGTGGAGGAAGGAGCGAA
		R	TTTCCCCTGCTGTGCCAT
Q	COL1A2	F	GCCACGTCCCTTCCCCCATTC
		R	AAGTCCGCGTATCCACAAAGCTGAGCAT
Q	COL4A6	F	GCTGGTCTTCTTTACCTTC
		R	TTCCCAATATTTTCACATCTTCTG
Q	COL8A1	F	CAGGAGTGGGCAAACCAGGAGTGA
		R	GGTCCAAGATCCCCAGGAACA
Q	EGF	F	TACTGCACGTGCCCTGTAGGATTT
		R	CACATTGCGTGGACAGGAAACAAG
C	FBXO32	F	GGCTCTCCAGCCGTGCATGA
		R	AGCAGGTGTGCACGTCCCTC
Q	FBXO32	F	CCCTTCAGCTCTGCAAACACTGTC
		R	CTCCAGTCAGCAGGGGGACC
Q	FGF1	F	AAGCCCGTCGGTGTCCATGG
		R	GATGGCACAGTGGATGGGAC
C	FKBP51	F	GCTCTGACTTATTGTTCTCTTACTGCCC
		R	TTGCTGTCAGCACATCGAGTTCA
Q	FKBP51	F	ATTATCCGGAGAACCAAACG
		R	CAAACATCCTTCCACCACAG
Q	GADD45A	F	GAGAGCAGAAGACCGAAAGGA
		R	CACAACACCACGTTATCGGG
Q	GAPDH	F	GTCATGGGTGTGAACCATGAGA
		R	GGTCATGAGTCCTTCCACGATAC

Q	HAS2	F	GATTCAGACACTATGCTTGACCCAGC
		R	CAACACCTCCAACCATGGGATCT
Q	HBEGF	F	GACCGGAAAGTCCGTGACTTGC
		R	TTTGGTGTGGCCAGTGCTTGTG
Q	HGF	F	TACTGCAGACCAATGTGCTA
		R	GCATTGTTTTCTTGCTTTAT
Q	HIST1H1D	F	TGCTCCTACCATTCCTGCAC
		R	TTGGCCTTGGGTTTGCCTTC
Q	HMOX1	F	ACCCAGGCAGAGAATGCTGAGTT
		R	CCTCCTCCAGGGCCACATAGATG
Q	HPRT1	F	GTTATGGCGACCCGCAG
		R	ACCCTTTCCAAATCCTCAGC
Q	IL33	F	CTGCCTGTCAACAGCAGTCT
		R	CTGGTCTGGCAGTGGTTTTT
Q	KLK3	F	GGCAGCATTGAACCAGAGGAG
		R	GCATGAACTTGGTCACCTTCTG
Q	MPRL32	F	GCATACGGGTCCTGGCAT
		R	ACATGCTTGCCATCCAACC
C	NC2	F	GTGAGTGCCCAGTTAGAGCATCTA
		R	GGAACCAGTGGGTCTTGAAGTG
Q	NFKBIA	F	AGAGAGTGAGGATGAGGAGAG
		R	ACACAGTCATCATAGGGCAG
Q	PIK3R1	F	ACTCTCTGAAATTTTCAGCCCTATG
		R	CGTTCATTCCATTCAGTTGAGATTA
Q	PNCA	F	TGAGGGCTTCGACACCTACC
		R	CTTTCTCCTGGTTTGGTGCTTC
Q	PPIA	F	TGCCAGTGGAAAAATCAGCCA
		R	CAAAGCAAATCTCGACACCTTG
Q	RAC1	F	CATGGCTAAGGAGATTGGTG
		R	CAGGCATTTTCTCTTCCTCT
Q	RAD17	F	AGCGAGAAAAAGAGGAAATC
		R	TGCCTTTCTAAAACTTGAGC
Q	RPL32	F	TTCCTGGTCCACAACGTCAAG
		R	TTGTGAGCGATCTCGGCAC
Q	SELPLG	F	CCCAGACCACATCTCTGTGA
		R	ACAGGGATGAGATGCAGACC
Q	TGFB3	F	GGCCCTTGCCCATACCTCCG
		R	AGCAAGGCGAGGCAGATGCT
Q	TP53	F	TAACAGTTCCTGCATGGGCGGC
		R	AGGACAGGCACAAACACGCACC
Q	VCAN	F	CTGCCTATGAAGATGGATTTG
		R	AAGGTGAATTTACTGGGGAC

REFERENCES

Adams, C., K. Totpal, D. Lawrence, S. Marsters, R. Pitti, S. Yee, S. Ross, L. Deforge, H. Koeppen, M. Sagolla, D. Compaan, H. Lowman, S. Hymowitz and A. Ashkenazi (2008). "Structural and functional analysis of the interaction between the agonistic monoclonal antibody Apomab and the proapoptotic receptor DR5." Cell Death and Differentiation **15**(4): 751-761.

Aggarwal, B. B. (2000). "Apoptosis and nuclear factor-κB: A tale of association and dissociation." Biochemical Pharmacology **60**(8): 1033-1039.

Aggarwal, B. B., A. Kumar and A. C. Bharti (2003). "Anticancer potential of curcumin: Preclinical and clinical studies." Anticancer Research **23**(1 A): 363-398.

AIHW (2013). "Cancer in Australia: Actual incidence data from 1991 to 2009 and mortality data from 1991 to 2010 with projections to 2012." Asia-Pacific Journal of Clinical Oncology **9**(3): 199-213.

Alimirah, F., R. Panchanathany, F. J. Davisy, J. Cheny and D. Choubey (2007). "Restoration of p53 expression in human cancer cell lines upregulates the expression of Notch1: Implications for cancer cell fate determination after genotoxic stress." Neoplasia **9**(5): 427-434.

Altenburg, J. D., A. A. Bieberich, C. Terry, K. A. Harvey, J. F. VanHorn, Z. Xu, V. Jo Davisson and R. A. Siddiqui (2011). "A synergistic antiproliferation effect of curcumin and docosahexaenoic acid in SK-BR-3 breast cancer cells: Unique signaling not explained by the effects of either compound alone." BMC Cancer **11**.

Anand, P., S. G. Thomas, A. B. Kunnumakkara, C. Sundaram, K. B. Harikumar, B. Sung, S. T. Tharakan, K. Misra, I. K. Priyadarsini, K. N. Rajasekharan and B. B. Aggarwal (2008). "Biological activities of curcumin and its analogues (Congeners) made by man and Mother Nature." Biochemical Pharmacology **76**(11): 1590-1611.

Andrzejewski, T., D. Deeb, X. Gao, A. Danyluk, A. S. Arbab, S. A. Dulchavsky and S. C. Gautam (2008). "Therapeutic efficacy of curcumin/TRAIL combination regimen for hormone-refractory prostate cancer." Oncology Research **17**(6): 257-267.

Arya, M., H. R. H. Patel, C. McGurk, R. Tatoud, H. Klocker, J. Masters and M. Williamson (2004). "The importance of the CXCL12-CXCR4 chemokine ligand-receptor interaction in prostate cancer metastasis." Journal of Experimental Therapeutics and Oncology **4**(4): 291-303.

Ashkenazi, A. (2002). "Targeting death and decoy receptors of the tumour-necrosis factor superfamily." Nature Reviews Cancer **2**(6): 420-430.

Ashkenazi, A. and R. S. Herbst (2008). "To kill a tumor cell: The potential of proapoptotic receptor agonists." Journal of Clinical Investigation **118**(6): 1979-1990.

Ashkenazi, A., R. C. Pai, S. Fong, S. Leung, D. A. Lawrence, S. A. Marsters, C. Blackie, L. Chang, A. E. McMurtrey, A. Hebert, L. DeForge, I. L. Koumenis, D. Lewis, L. Harris, J. Bussiere, H. Koeppen, Z. Shahrokh and R. H. Schwall (1999). "Safety and antitumor activity of recombinant soluble Apo2 ligand." Journal of Clinical Investigation **104**(2): 155-162.

Bachmeier, B. E., C. M. Iancu, P. H. Killian, E. Kronski, V. Mirisola, G. Angelini, M. Jochum, A. G. Nerlich and U. Pfeffer (2009). "Overexpression of the ATP binding cassette gene ABCA1 determines resistance to Curcumin in M14 melanoma cells." Molecular Cancer **8**.

Bachmeier, B. E., I. V. Mohrenz, V. Mirisola, E. Schleicher, F. Romeo, C. Höhneke, M. Jochum, A. G. Nerlich and U. Pfeffer (2008). "Curcumin downregulates the inflammatory cytokines CXCL1 and -2 in breast cancer cells via NFκB." Carcinogenesis **29**(4): 779-789.

Baguley, B. C. (2010). "Multiple drug resistance mechanisms in cancer." Molecular Biotechnology **46**(3): 308-316.

Balogun, E., M. Hoque, P. Gong, E. Killeen, C. J. Green, R. Foresti, J. Alam and R. Motterlini (2003). "Curcumin activates the haem oxygenase-1 gene via regulation of Nrf2 and the antioxidant-responsive element." Biochemical Journal **371**(3): 887-895.

Bander, N. H., M. I. Milowsky, D. M. Nanus, L. Kostakoglu, S. Vallabhajosula and S. J. Goldsmith (2005). "Phase I trial of 177Lutetium-labeled J591, a monoclonal antibody to prostate-specific membrane antigen, in patients with androgen-independent prostate cancer." Journal of Clinical Oncology **23**(21): 4591-4601.

Bar-Sela, G., R. Epelbaum and M. Schaffer (2010). "Curcumin as an anti-cancer agent: Review of the gap between basic and clinical applications." Current Medicinal Chemistry **17**(3): 190-197.

Barik, A., K. I. Priyadarsini and H. Mohan (2003). "Photophysical Studies on Binding of Curcumin to Bovine Serum Albumin." Photochemistry and Photobiology **77**(6): 597-603.

Barve, A., T. O. Khor, X. Hao, Y. S. Keum, C. S. Yang, B. Reddy and A. N. T. Kong (2008). "Murine prostate cancer inhibition by dietary phytochemicals - Curcumin and phenyethylisothiocyanate." Pharmaceutical Research **25**(9): 2181-2189.

Basu, P., S. Dutta, R. Begum, S. Mittal, P. D. Dutta, A. C. Bharti, C. K. Panda, J. Biswas, B. Dey, G. P. Talwar and B. C. Das (2013). "Clearance of cervical human papillomavirus infection by topical application of curcumin and curcumin containing polyherbal cream: A phase II randomized controlled study." Asian Pacific Journal of Cancer Prevention **14**(10): 5753-5759.

Beck, W. T., T. J. Mueller and L. R. Tanzer (1979). "Altered surface membrane glycoproteins in Vinca alkaloid-resistant human leukemic lymphoblasts." Cancer Research **39**(6 I): 2070-2076.

Beevers, C. S., L. Chen, L. Liu, Y. Luo, N. J. G. Webster and S. Huang (2009). "Curcumin disrupts the mammalian target of rapamycin-raptor complex." Cancer Research **69**(3): 1000-1008.

Beevers, C. S., F. Li, L. Liu and S. Huang (2006). "Curcumin inhibits the mammalian target of rapamycin-mediated signaling pathways in cancer cells." International Journal of Cancer **119**(4): 757-764.

Berg, C. D., G. L. Andriole, E. D. Crawford, R. L. Grubb, S. S. Buys, D. Chia, T. R. Church, M. N. Fouad, E. P. Gelmann, P. A. Kvale, D. J. Reding, J. L. Weissfeld, L. A. Yokochi, B. O'Brien, J. D. Clapp, J. M. Rathmell, T. L. Riley, R. B. Hayes, B. S. Kramer, G. Izmirlian, A. B. Miller, P. F. Pinsky, P. C. Prorok and J. K. Gohagan (2009). "Mortality results from a randomized prostate-cancer screening trial." New England Journal of Medicine **360**(13): 1310-1319.

Bhowmick, N. A., E. G. Neilson and H. L. Moses (2004). "Stromal fibroblasts in cancer initiation and progression." Nature **432**(7015): 332-337.

Bielak-Zmijewska, A., M. Koronkiewicz, J. Skierski, K. Piwocka, E. Radziszewska and E. Sikora (2000). "Effect of curcumin on the apoptosis of rodent and human nonproliferating and proliferating lymphoid cells." Nutrition and Cancer **38**(1): 131-138.

Bierhaus, A., Y. Zhang, P. Quehenberger, T. Luther, M. Haase, M. Müller, N. Mackman, R. Ziegler and P. P. Nawroth (1997). "The dietary pigment curcumin reduces endothelial tissue factor gene expression by inhibiting binding of AP-1 to the DNA and activation of NF-κB." Thrombosis and Haemostasis **77**(4): 772-782.

Blakemore, L. M., C. Boes, R. Cordell and M. M. Manson (2013). "Curcumin-induced mitotic arrest is characterized by spindle abnormalities, defects in chromosomal congression and DNA damage." Carcinogenesis **34**(2): 351-360.

Bock, C. and T. Lengauer (2012). "Managing drug resistance in cancer: Lessons from HIV therapy." Nature Reviews Cancer **12**(7): 494-501.

Bonkhoff, H. and K. Remberger (1996). "Differentiation pathways and histogenetic aspects of normal and abnormal prostatic growth: A stem cell model." Prostate **28**(2): 98-106.

Borley, N. and M. R. Feneley (2009). "Prostate cancer: Diagnosis and staging." Asian Journal of Andrology **11**(1): 74-80.

Bostwick, D. G. and J. Qian (2004). "High-grade prostatic intraepithelial neoplasia." Modern Pathology **17**(3): 360-379.

Braeuer, S. J., C. Büneker, A. Mohr and R. M. Zwacka (2006). "Constitutively activated nuclear factor-κB, but not induced NF-κB, leads to TRAIL resistance by up-regulation of X-linked inhibitor of apoptosis protein in human cancer cells." Molecular Cancer Research **4**(10): 715-728.

Brennen, W. N., J. T. Isaacs and S. R. Denmeade (2012). "Rationale behind targeting fibroblast activation protein-expressing carcinoma-associated fibroblasts as a novel chemotherapeutic strategy." Molecular Cancer Therapeutics **11**(2): 257-266.

Brennen, W. N., D. M. Rosen, H. Wang, J. T. Isaacs and S. R. Denmeade (2012). "Targeting carcinoma-associated fibroblasts within the tumor stroma with a fibroblast activation protein-activated prodrug." Journal of the National Cancer Institute **104**(17): 1320-1334.

Brown, J. M. and A. J. Giaccia (1998). "The unique physiology of solid tumors: Opportunities (and problems) for cancer therapy." Cancer Research **58**(7): 1408-1416.

Bubendorf, L., A. Schöpfer, U. Wagner, G. Sauter, H. Moch, N. Willi, T. C. Gasser and M. J. Mihatsch (2000). "Metastatic patterns of prostate cancer: An autopsy study of 1,589 patients." Human Pathology **31**(5): 578-583.

Buchanan, G., P. S. Craft, M. Yang, A. Cheong, J. Prescott, L. Jia, G. A. Coetzee and W. D. Tilley (2004). "PC-3 cells with enhanced androgen receptor signaling: A model for clonal selection in prostate cancer." Prostate **60**(4): 352-366.

Buchanan, G., R. A. Irvine, G. A. Coetzee and W. D. Tilley (2001). "Contribution of the androgen receptor to prostate cancer predisposition and progression." Cancer and Metastasis Reviews **20**(3-4): 207-223.

Buck, E., A. Eyzaguirre, M. Rosenfeld-Franklin, S. Thomson, M. Mulvihill, S. Barr, E. Brown, M. O'Connor, Y. Yao, J. Pachter, M. Miglarese, D. Epstein, K. K. Iwata, J. D. Haley, N. W. Gibson and Q. S. Ji (2008). "Feedback mechanisms promote cooperativity for small molecule inhibitors of epidermal and insulin-like growth factor receptors." Cancer Research **68**(20): 8322-8332.

Bush, J. A., K. J. J. Cheung Jr and G. Li (2001). "Curcumin induces apoptosis in human melanoma cells through a Fas receptor/caspase-8 pathway independent of p53." Experimental Cell Research **271**(2): 305-314.

Butler, L. M., M. M. Centenera, P. J. Neufing, G. Buchanan, C. S. Y. Choong, C. Ricciardelli, K. Saint, M. Lee, A. Ochnik, M. Yang, M. P. Brown and W. D. Tilley (2006). "Suppression of androgen receptor signaling in prostate cancer cells by an inhibitory receptor variant." Molecular Endocrinology **20**(5): 1009-1024.

Butler, M. S. (2004). "The role of natural product chemistry in drug discovery." Journal of Natural Products **67**(12): 2141-2153.

Camidge, D. R. (2008). "Apomab: An agonist monoclonal antibody directed against Death Receptor 5/TRAIL-Receptor 2 for use in the treatment of solid tumors." Expert Opinion on Biological Therapy **8**(8): 1167-1176.

Cano, P., A. Godoy, R. Escamilla, R. Dhir and S. A. Onate (2007). "Stromal-epithelial cell interactions and androgen receptor-coregulator recruitment is altered in the tissue microenvironment of prostate cancer." Cancer Research **67**(2): 511-519.

Cao, J., L. Jia, H. M. Zhou, Y. Liu and L. F. Zhong (2006). "Mitochondrial and nuclear DNA damage induced by curcumin in human hepatoma G2 cells." Toxicological Sciences **91**(2): 476-483.

Cara, S. and I. F. Tannock (2001). "Retreatment of patients with the same chemotherapy: Implications for clinical mechanisms of drug resistance." Annals of Oncology **12**(1): 23-27.

Carroll, R. E., R. V. Benya, D. K. Turgeon, S. Vareed, M. Neuman, L. Rodriguez, M. Kakarala, P. M. Carpenter, C. McLaren, F. L. Meyskens Jr and D. E. Brenner (2011). "Phase IIa clinical trial of curcumin for the prevention of colorectal neoplasia." Cancer Prevention Research **4**(3): 354-364.

Caubet, J. F., T. D. Tosteson, E. W. Dong, E. M. Naylon, G. W. Whiting, M. S. Ernstoff and S. D. Ross (1997). "Maximum androgen blockade in advanced prostate cancer: A meta-analysis of published randomized controlled trials using nonsteroidal antiandrogens." Urology **49**(1): 71-78.

Celis, J. E., P. Madsen, A. Celis, H. V. Nielsen and B. Gesser (1987). "Cyclin (PCNA, auxiliary protein of DNA polymerase δ) is a central component of the pathway(s) leading to DNA replication and cell division." FEBS Letters **220**(1): 1-7.

Chakravarti, A., J. S. Loeffler and N. J. Dyson (2002). "Insulin-like growth factor receptor I mediates resistance to anti-epidermal growth factor receptor therapy in primary human glioblastoma cells through continued activation of phosphoinositide 3-kinase signaling." Cancer Research **62**(1): 200-207.

Chang, H. Y., J. T. Chi, S. Dudoit, C. Bondre, M. Van De Rijn, D. Botstein and P. O. Brown (2002). "Diversity, topographic differentiation, and positional memory in human fibroblasts." Proceedings of the National Academy of Sciences of the United States of America **99**(20): 12877-12882.

Chaudhary, L. R. and K. A. Hruska (2003). "Inhibition of cell survival signal protein kinase B/Akt by curcumin in human prostate cancer cells." Journal of Cellular Biochemistry **89**(1): 1-5.

Chen, A. L., C. H. Hsu, J. K. Lin, M. M. Hsu, Y. F. Ho, T. S. She, J. Y. Ko, J. T. Lin, B. R. Lin, M. S. Wu, H. S. Yu, S. H. Jee, G. S. Chen, T. M. Chen, C. A. Chen, M. K. Lai, Y. S. Pu, M. H. Pan, Y. J. Wang, C. C. Tsai and C. Y. Hsieh (2001). "Phase I clinical trial of curcumin, a chemopreventive agent, in patients with high-risk or pre-malignant lesions." Anticancer Research **21**(4 B): 2895-2900.

Chen, C., T. D. Johnston, H. Jeon, R. Gedaly, P. P. McHugh, T. G. Burke and D. Ranjan (2009). "An in vitro study of liposomal curcumin: Stability, toxicity and biological activity in human lymphocytes and Epstein-Barr virus-transformed human B-cells." International Journal of Pharmaceutics **366**(1-2): 133-139.

Chen, D. R., H. W. Lai, S. Y. Chien, S. J. Kuo, L. M. Tseng, H. Y. Lin and C. W. Chi (2012). "The potential utility of curcumin in the treatment of HER-2-overexpressed breast cancer: An in vitro and in vivo comparison study with herceptin." Evidence-based Complementary and Alternative Medicine **2012**.

Chen, L., G. Tian, C. Shao, E. Cobos and W. Gao (2010). "Curcumin modulates eukaryotic initiation factors in human lung adenocarcinoma epithelial cells." Molecular Biology Reports **37**(7): 3105-3110.

Chen, W. T. and T. Kelly (2003). "Seprase complexes in cellular invasiveness." Cancer and Metastasis Reviews **22**(2-3): 259-269.

Chen, Y., C. L. Sawyers and H. I. Scher (2008). "Targeting the androgen receptor pathway in prostate cancer." Current Opinion in Pharmacology **8**(4): 440-448.

Cheng, T. S., W. C. Chen, Y. Y. Lin, C. H. Tsai, C. I. Liao, H. Y. Shyu, C. J. Ko, S. F. Tzeng, C. Y. Huang, P. C. Yang, P. W. Hsiao and M. S. Lee (2013). "Curcumin-targeting pericellular serine protease matriptase role in suppression of prostate cancer cell invasion, tumor growth, and metastasis." Cancer Prevention Research **6**(5): 495-505.

Chicheportiche, Y., P. R. Bourdon, H. Xu, Y. M. Hsu, H. Scott, C. Hession, I. Garcia and J. L. Browning (1997). "TWEAK, a new secreted ligand in the tumor necrosis factor family that weakly induces apoptosis." Journal of Biological Chemistry **272**(51): 32401-32410.

Chinni, S. R., S. Sivalogan, Z. Dong, J. C. Trindade Filho, X. Deng, R. D. Bonfil and M. L. Cher (2006). "CXCL12/CXCR4 signaling activates Akt-1 and MMP-9 expression in prostate cancer cells: The role of bone microenvironment-associated CXCL12." Prostate **66**(1): 32-48.

Chinni, S. R., H. Yamamoto, Z. Dong, A. Sabbota, R. D. Bonfil and M. L. Cher (2008). "CXCL12/CXCR4 transactivates HER2 in lipid rafts of prostate cancer cells and promotes growth of metastatic deposits in bone." Molecular Cancer Research **6**(3): 446-457.

Chmelar, R., G. Buchanan, E. F. Need, W. Tilley and N. M. Greenberg (2007). "Androgen receptor coregulators and their involvement in the development and progression of prostate cancer." International Journal of Cancer **120**(4): 719-733.

Chmielecki, J., J. Foo, G. R. Oxnard, K. Hutchinson, K. Ohashi, R. Somwar, L. Wang, K. R. Amato, M. Arcila, M. L. Sos, N. D. Socci, A. Viale, E. De Stanchina, M. S. Ginsberg, R. K. Thomas, M. G. Kris, A. Inoue, M. Ladanyi, V. A. Miller, F. Michor and W. Pao (2011). "Optimization of dosing for EGFR-mutant non-small cell lung cancer with evolutionary cancer modeling." Science Translational Medicine **3**(90).

Choi, H., Y. S. Chun, S. W. Kim, M. S. Kim and J. W. Park (2006). "Curcumin inhibits hypoxia-inducible factor-1 by degrading aryl hydrocarbon receptor nuclear translocator: A mechanism of tumor growth inhibition." Molecular Pharmacology **70**(5): 1664-1671.

Choi, H. Y., J. E. Lim and J. H. Hong (2010). "Curcumin interrupts the interaction between the androgen receptor and Wnt/β-catenin signaling pathway in LNCaP prostate cancer cells." Prostate Cancer and Prostatic Diseases **13**(4): 343-349.

Choudhuri, T., S. Pal, M. L. Agwarwal, T. Das and G. Sa (2002). "Curcumin induces apoptosis in human breast cancer cells through p53-dependent Bax induction." FEBS Letters **512**(1-3): 334-340.

Choudhuri, T., S. Pal, T. Das and G. Sa (2005). "Curcumin selectively induces apoptosis in deregulated cyclin D1-expressed cells at G 2 phase of cell cycle in a p53-dependent manner." Journal of Biological Chemistry **280**(20): 20059-20068.

Claessens, F., G. Verrijdt, E. Schoenmakers, A. Haelens, B. Peeters, G. Verhoeven and W. Rombauts (2001). "Selective DNA binding by the androgen receptor as a mechanism for hormone-specific gene regulation." Journal of Steroid Biochemistry and Molecular Biology **76**(1-5): 23-30.

Clayton, A., R. A. Evans, E. Pettit, M. Hallett, J. D. Williams and R. Steadman (1998). "Cellular activation through the ligation of intercellular adhesion molecule-1." Journal of Cell Science **111**(4): 443-453.

Cooke, P. S., P. F. Young and G. R. Cunha (1987). "Androgen dependence of growth and epithelial morphogenesis in neonatal mouse bulbourethral glands." Endocrinology **121**(6): 2153-2160.

Core, L. J. and J. T. Lis (2008). "Transcription regulation through promoter-proximal pausing of RNA polymerase II." Science **319**(5871): 1791-1792.

Cory, S. and J. M. Adams (2002). "The BCL2 family: Regulators of the cellular life-or-death switch." Nature Reviews Cancer **2**(9): 647-656.

Craft, N., Y. Shostak, M. Carey and C. L. Sawyers (1999). "A mechanism for hormone-independent prostate cancer through modulation of androgen receptor signaling by the HER-2/neu tyrosine kinase." Nature Medicine **5**(3): 280-285.

Culig, Z., A. Hobisch, M. V. Cronauer, C. Radmayr, J. Trapman, A. Hittmair, G. Bartsch and H. Klocker (1994). "Androgen receptor activation in prostatic tumor cell lines by insulin- like growth factor-I, keratinocyte growth factor, and epidermal growth factor." Cancer Research **54**(20): 5474-5478.

Culig, Z., A. Hobisch, A. Hittmair, H. Peterziel, A. C. B. Cato, G. Bartsch and H. Klocker (1998). "Expression, structure, and function of androgen receptor in advanced prostatic carcinoma." Prostate **35**(1): 63-70.

Cunha, G. R. (1994). "Role of mesenchymal-epithelial interactions in normal and abnormal development of the mammary gland and prostate." Cancer **74**(3): 1030-1044.

Cunha, G. R. (2008). "Mesenchymal-epithelial interactions: Past, present, and future." Differentiation **76**(6): 578-586.

Cunha, G. R., A. A. Donjacour, P. S. Cooke, S. Mee, R. M. Bigsby, S. J. Higgins and Y. Sugimura (1987). "The endocrinology and developmental biology of the prostate." Endocrine Reviews **8**(3): 338-362.

Dallas, N. A., L. Xia, F. Fan, M. J. Gray, P. Gaur, G. Van Buren Ii, S. Samuel, M. P. Kim, S. J. Lim and L. M. Ellis (2009). "Chemoresistant colorectal cancer cells, the cancer stem cell phenotype, and increased sensitivity to insulin-like growth factor-I receptor inhibition." Cancer Research **69**(5): 1951-1957.

Damiano, J. S., A. E. Cress, L. A. Hazlehurst, A. A. Shtil and W. S. Dalton (1999). "Cell adhesion mediated drug resistance (CAM-DR): Role of integrins and resistance to apoptosis in human myeloma cell lines." Blood **93**(5): 1658-1667.

Damiano, J. S., L. A. Hazlehurst and W. S. Dalton (2001). "Cell adhesion-mediated drug resistance (CAM-DR) protects the K562 chronic myelogenous leukemia cell line from apoptosis induced by BCR/ABL inhibition, cytotoxic drugs, and γ-irradiation." Leukemia **15**(8): 1232-1239.

Das, R. K., N. Kasoju and U. Bora (2010). "Encapsulation of curcumin in alginate-chitosan-pluronic composite nanoparticles for delivery to cancer cells." Nanomedicine: Nanotechnology, Biology, and Medicine **6**(1): e153-e160.

Datta, R., S. K. Halder and B. Zhang (2013). "Role of TGF-β signaling in curcumin-mediated inhibition of tumorigenicity of human lung cancer cells." Journal of Cancer Research and Clinical Oncology **139**(4): 563-572.

Davies, S. J. (2000). "Peritoneal solute transport - We know it is important, but what is it?" Nephrology Dialysis Transplantation **15**(8): 1120-1123.

Dawson, C. C., C. Intapa and M. A. Jabra-Rizk (2011). ""Persisters": Survival at the cellular level." PLoS Pathogens **7**(7).

De Marzo, A. M., A. K. Meeker, S. Zha, J. Luo, M. Nakayama, E. A. Platz, W. B. Isaacs and W. G. Nelson (2003). "Human prostate cancer precursors and pathobiology." Urology **62**(5 SUPPL. 1): 55-62.

Deeb, D., H. Jiang, X. Gao, M. S. Hafner, H. Wong, G. Divine, R. A. Chapman, S. A. Dulchavsky and S. C. Gautam (2004). "Curcumin sensitizes prostate cancer cells to tumor necrosis factor-related apoptosis-inducing ligand/Apo2L by inhibiting nuclear factor-κB through suppression of IκBα phosphorylation." Molecular Cancer Therapeutics **3**(7): 803-812.

Deeb, D., Y. X. Xu, H. Jiang, X. Gao, N. Janakiraman, R. A. Chapman and S. C. Gautam (2003). "Curcumin (diferuloyl-methane) enhances tumor necrosis factor-related apoptosis-inducing ligand-induced apoptosis in LNCaP prostate cancer cells." Molecular cancer therapeutics **2**(1): 95-103.

Degli-Esposti, M. A., W. C. Dougall, P. J. Smolak, J. Y. Waugh, C. A. Smith and R. G. Goodwin (1997). "The novel receptor TRAIL-R4 induces NF-κB and protects against TRAIL- mediated apoptosis, yet retains an incomplete death domain." Immunity **7**(6): 813-820.

Degli-Esposti, M. A., P. J. Smolak, H. Walczak, J. Waugh, C. P. Huang, R. F. DuBose, R. G. Goodwin and C. A. Smith (1997). "Cloning and characterization of TRAIL-R3, a novel member of the emerging TRAIL receptor family." Journal of Experimental Medicine **186**(7): 1165-1170.

Dehm, S. M. and D. J. Tindall (2006). "Molecular regulation of androgen action in prostate cancer." Journal of Cellular Biochemistry **99**(2): 333-344.

Demirovic, D. and S. I. S. Rattan (2011). "Curcumin induces stress response and hormetically modulates wound healing ability of human skin fibroblasts undergoing ageing in vitro." Biogerontology **12**(5): 437-444.

Deslypere, J. P., M. Young, J. D. Wilson and M. J. McPhaul (1992). "Testosterone and 5α-dihydrotestosterone interact differently with the androgen receptor to enhance transcription of the MMTV-CAT reporter gene." Molecular and Cellular Endocrinology **88**(1-3): 15-22.

Dhandapani, K. M., V. B. Mahesh and D. W. Brann (2007). "Curcumin suppresses growth and chemoresistance of human glioblastoma cells via AP-1 and NFκB transcription factors." Journal of Neurochemistry **102**(2): 522-538.

Dhillon, N., B. B. Aggarwal, R. A. Newman, R. A. Wolff, A. B. Kunnumakkara, J. L. Abbruzzese, C. S. Ng, V. Badmaev and R. Kurzrock (2008). "Phase II trial of curcumin in patients with advanced pancreatic cancer." Clinical Cancer Research **14**(14): 4491-4499.

Dhule, S. S., P. Penfornis, T. Frazier, R. Walker, J. Feldman, G. Tan, J. He, A. Alb, V. John and R. Pochampally (2012). "Curcumin-loaded γ-cyclodextrin liposomal nanoparticles as delivery vehicles for osteosarcoma." Nanomedicine: Nanotechnology, Biology, and Medicine **8**(4): 440-451.

Dickinson, D. A., K. E. Iles, H. Zhang, V. Blank and H. J. Forman (2003). "Curcumin alters EpRE and AP-1 binding complexes and elevates glutamate-cysteine ligase gene expression." The FASEB journal : official publication of the Federation of American Societies for Experimental Biology **17**(3): 473-475.

Divya, C. S. and M. R. Pillai (2006). "Antitumor action of curcumin in human papillomavirus associated cells involves downregulation of viral oncogenes, prevention of NFkB and AP-1 translocation, and modulation of apoptosis." Molecular Carcinogenesis **45**(5): 320-332.

Djavan, B., A. Zlotta, C. Kratzik, M. Remzi, C. Seitz, C. C. Schulman and M. Marberger (1999). "PSA, PSA density, PSA density of transition zone, free/total PSA ratio, and PSA velocity for early detection of prostate cancer in men with serum PSA 2.5 to 4.0 ng/mL." Urology **54**(3): 517-522.

Dorai, T., Y. C. Cao, B. Dorai, R. Buttyan and A. E. Katz (2001). "Therapeutic potential of curcumin in human prostate cancer. III. Curcumin inhibits proliferation, induces apoptosis, and inhibits angiogenesis of LNCaP prostate cancer cells in vivo." Prostate **47**(4): 293-303.

Dorai, T., N. Gehani and A. Katz (2000). "Therapeutic potential of curcumin in human prostate cancer - I. Curcumin induces apoptosis in both androgen-dependent and androgen-independent prostate cancer cells." Prostate Cancer and Prostatic Diseases **3**(2): 84-93.

Dorai, T., N. Gehani and A. Katz (2000). "Therapeutic potential of curcumin in human prostate cancer. II. Curcumin inhibits tyrosine kinase activity of epidermal growth factor receptor and depletes the protein." Molecular Urology **4**(1): 1-6.

Du, B., L. Jiang, Q. Xia and L. Zhong (2006). "Synergistic inhibitory effects of curcumin and 5-fluorouracil on the growth of the human colon cancer cell line HT-29." Chemotherapy **52**(1): 23-28.

Dudás, J., A. Fullár, A. Romani, C. Pritz, I. Kovalszky, V. Hans Schartinger, G. Mathias Sprinzl and H. Riechelmann (2013). "Curcumin targets fibroblast-tumor cell interactions in oral squamous cell carcinoma." Experimental Cell Research **319**(6): 800-809.

Dumas, E. O. and G. M. Pollack (2008). "Opioid tolerance development: A pharmacokinetic/pharmacodynamic perspective." AAPS Journal **10**(4): 537-551.

Dvorak, H. F., T. M. Sioussat, L. F. Brown, B. Berse, J. A. Nagy, A. Sotrel, E. J. Manseau, L. Van De Water and D. R. Senger (1991). "Distribution of vascular permeability factor (vascular endothelial growth factor) in tumors: Concentration in tumor blood vessels." Journal of Experimental Medicine **174**(5): 1275-1278.

Eckstein, N., K. Servan, B. Hildebrandt, A. Pölitz, G. Von Jonquières, S. Wolf-Kümmeth, I. Napierski, A. Hamacher, M. U. Kassack, J. Budczies, M. Beier, M. DieteL, B. Royer-Pokora, C. Denkert and H. D. Royer (2009). "Hyperactivation of the insulin-like growth factor receptor I signaling pathway Is an essential event for cisplatin resistance of ovarian cancer cells." Cancer Research **69**(7): 2996-3003.

Emery, J. G., P. McDonnell, M. B. Burke, K. C. Deen, S. Lyn, C. Silverman, E. Dul, E. R. Appelbaum, C. Eichman, R. DiPrinzio, R. A. Dodds, I. E. James, M. Rosenberg, J. C. Lee and P. R. Young (1998). "Osteoprotegerin is a receptor for the cytotoxic ligand TRAIL." Journal of Biological Chemistry **273**(23): 14363-14367.

Escudier, B., T. Eisen, W. M. Stadler, C. Szczylik, S. Oudard, M. Siebels, S. Negrier, C. Chevreau, E. Solska, A. A. Desai, F. Rolland, T. Demkow, T. E. Hutson, M. Gore, S. Freeman, B. Schwartz, M. Shan, R. Simantov and R. M. Bukowski (2007). "Sorafenib in advanced clear-cell renal-cell carcinoma." New England Journal of Medicine **356**(2): 125-134.

Esmaili, M., S. M. Ghaffari, Z. Moosavi-Movahedi, M. S. Atri, A. Sharifizadeh, M. Farhadi, R. Yousefi, J. M. Chobert, T. Haertlé and A. A. Moosavi-Movahedi (2011). "Beta casein-micelle as a nano vehicle for solubility enhancement of curcumin; food industry application." LWT - Food Science and Technology **44**(10): 2166-2172.

Fajardo, A. M., D. A. MacKenzie, M. Ji, L. M. Deck, D. L. V. Jagt, T. A. Thompson and M. Bisoffi (2012). "The curcumin analog ca27 down-regulates androgen receptor through an oxidative stress mediated mechanism in human prostate cancer cells." Prostate **72**(6): 612-625.

Feltquate, D., L. Nordquist, C. Eicher, M. Morris, O. Smaletz, S. Slovin, T. Curley, A. Wilton, M. Fleisher, G. Heller and H. I. Scher (2006). "Rapid androgen cycling as treatment for patients with prostate cancer." Clinical Cancer Research **12**(24): 7414-7421.

Ferlay, J., H. R. Shin, F. Bray, D. Forman, C. Mathers and D. M. Parkin (2010). "Estimates of worldwide burden of cancer in 2008: GLOBOCAN 2008." International Journal of Cancer **127**(12): 2893-2917.

Fizazi, K., H. I. Scher, A. Molina, C. J. Logothetis, K. N. Chi, R. J. Jones, J. N. Staffurth, S. North, N. J. Vogelzang, F. Saad, P. Mainwaring, S. Harland, O. B. Goodman, C. N. Sternberg, J. H. Li, T. Kheoh, C. M. Haqq and J. S. de Bono (2012). "Abiraterone acetate for treatment of metastatic castration-resistant prostate cancer: Final overall survival analysis of the COU-AA-301 randomised, double-blind, placebo-controlled phase 3 study." The Lancet Oncology **13**(10): 983-992.

Flechsig, P., M. Dadrich, S. Bickelhaupt, J. Jenne, K. Hauser, C. Timke, P. Peschke, E. W. Hahn, H. J. Grone, J. Yingling, M. Lahn, U. Wirkner and P. E. Huber (2012). "LY2109761 attenuates radiation-induced pulmonary murine fibrosis via reversal of TGF-β and BMP-associated proinflammatory and proangiogenic signals." Clinical Cancer Research **18**(13): 3616-3627.

Freedman, M. L., C. A. Haiman, N. Patterson, G. J. McDonald, A. Tandon, A. Waliszewska, K. Penney, R. G. Steen, K. Ardlie, E. M. John, I. Oakley-Girvan, A. S. Whittemore, K. A. Cooney, S. A. Ingles, D. Altshuler, B. E. Henderson and D. Reich (2006). "Admixture mapping identifies 8q24 as a prostate

cancer risk locus in African-American men." Proceedings of the National Academy of Sciences of the United States of America **103**(38): 14068-14073.

Fulda, S. and K. M. Debatin (2006). "Extrinsic versus intrinsic apoptosis pathways in anticancer chemotherapy." Oncogene **25**(34): 4798-4811.

Gann, P. H., C. H. Hennekens, J. Ma, C. Longcope and M. J. Stampfer (1996). "Prospective study of sex hormone levels and risk of prostate cancer." Journal of the National Cancer Institute **88**(16): 1118-1126.

Gao, X., D. Deeb, H. Jiang, Y. B. Liu, S. A. Dulchavsky and S. C. Gautam (2005). "Curcumin differentially sensitizes malignant glioma cells to TRAIL/Apo2L-mediated apoptosis through activation of procaspases and release of cytochrome c from mitochondria." Journal of Experimental Therapeutics and Oncology **5**(1): 39-48.

García-Martínez, J., A. Aranda and J. E. Pérez-Ortín (2004). "Genomic run-on evaluates transcription rates for all yeast genes and identifies gene regulatory mechanisms." Molecular Cell **15**(2): 303-313.

Garin-Chesa, P., L. J. Old and W. J. Rettig (1990). "Cell surface glycoprotein of reactive stromal fibroblasts as a potential antibody target in human epithelial cancers." Proceedings of the National Academy of Sciences of the United States of America **87**(18): 7235-7239.

Ghobrial, I. M., T. E. Witzig and A. A. Adjei (2005). "Targeting apoptosis pathways in cancer therapy." Ca-A Cancer Journal for Clinicians **55**(3): 178-194.

Gjertson, C. K. and P. C. Albertsen (2011). "Use and assessment of PSA in prostate cancer." Medical Clinics of North America **95**(1): 191-200.

Glasspool, R. M., J. M. Teodoridis and R. Brown (2006). "Epigenetics as a mechanism driving polygenic clinical drug resistance." British Journal of Cancer **94**(8): 1087-1092.

Gleason, D. F., G. T. Mellinger and L. J. Ardving (1974). "Prediction of prognosis for prostatic adenocarcinoma by combined histological grading and clinical staging." Journal of Urology **111**(1): 58-64.

Gleave, M. E., N. Bruchovsky, M. J. Moore and P. Venner (1999). "Prostate cancer: 9. Treatment of advanced disease." CMAJ **160**(2): 225-232.

Gleixner, K. V., M. Mayerhofer, A. Vales, A. Gruze, G. Hörmann, S. Cerny-Reiterer, E. Lackner, E. Hadzijusufovic, H. Herrmann, A. K. Iyer, M. T. Krauth, W. F. Pickl, B. Marian, R. Panzer-Grümayer, C. Sillaber, H. Maeda, C. Zielinski and P. Valent (2009). "Targeting of Hsp32 in solid tumors and leukemias: A novel approach to optimize anticancer therapy." Current Cancer Drug Targets **9**(5): 675-689.

Glickman, M. S. and C. L. Sawyers (2012). "Converting cancer therapies into cures: Lessons from infectious diseases." Cell **148**(6): 1089-1098.

Gonzales, A. M. and R. A. Orlando (2008). "Curcumin and resveratrol inhibit nuclear factor-kappaB-mediated cytokine expression in adipocytes." Nutrition and Metabolism **5**(1).

Greaves, M. (2009). "Darwin and evolutionary tales in leukemia. The Ham-Wasserman Lecture." Hematology / the Education Program of the American Society of Hematology. American Society of Hematology. Education Program: 3-12.

Gulbins, E., A. Jekle, K. Ferlinz, H. Grassmé and F. Lang (2000). "Physiology of apoptosis." American Journal of Physiology - Renal Physiology **279**(4 48-4): 605-615.

Guo, H., Y. M. Xu, Z. Q. Ye, J. H. Yu and X. Y. Hu (2013). "Curcumin induces cell cycle arrest and apoptosis of prostate cancer cells by regulating the expression of IκBα, c-Jun and androgen receptor." Pharmazie **68**(6): 431-434.

Gupta, S. C., G. Kismali and B. B. Aggarwal (2013). "Curcumin, a component of turmeric: From farm to pharmacy." BioFactors **39**(1): 2-13.

Gururaj, A. E., M. Belakavadi, D. A. Venkatesh, D. Marmé and B. P. Salimath (2002). "Molecular mechanisms of anti-angiogenic effect of curcumin." Biochemical and Biophysical Research Communications **297**(4): 934-942.

Györffy, B., P. Surowiak, O. Kiesslich, C. Denkert, R. Schäfer, M. Dietel and H. Lage (2006). "Gene expression profiling of 30 cancer cell lines predicts resistance towards 11 anticancer drugs at clinically achieved concentrations." International Journal of Cancer **118**(7): 1699-1712.

Häggman, M. J., J. A. Macoska, K. J. Wojno and J. E. Oesterling (1997). "The relationship between prostatic intraepithelial neoplasia and prostate cancer: Critical issues." Journal of Urology **158**(1): 12-22.

Haider, S. G. (2007). "Leydig cell steroidogenesis: Unmasking the functional importance of mitochondria." Endocrinology **148**(6): 2581-2582.

Han, G., G. Buchanan, M. Ittmann, J. M. Harris, X. Yu, F. J. DeMayo, W. Tilley and N. M. Greenberg (2005). "Mutation of the androgen receptor causes oncogenic transformation of the prostate." Proceedings of the National Academy of Sciences of the United States of America **102**(4): 1151-1156.

Hanahan, D. and R. A. Weinberg (2011). "Hallmarks of cancer: The next generation." Cell **144**(5): 646-674.

Hankey, B. F., E. J. Feuer, L. X. Clegg, R. B. Hayes, J. M. Legler, P. C. Prorok, L. A. Ries, R. M. Merrill and R. S. Kaplan (1999). "Cancer surveillance series: Interpreting trends in prostate cancer - Part I: Evidence of the effects of screening in recent prostate cancer incidence, mortality, and survival rates." Journal of the National Cancer Institute **91**(12): 1017-1024.

Harada, T., L. Giorgio, T. J. Harris, D. T. Pham, H. T. Ngo, E. F. Need, B. J. Coventry, S. F. Lincoln, C. J. Easton, G. Buchanan and T. W. Kee (2013). "Diamide linked γ-cyclodextrin dimers as molecular-scale delivery systems for the medicinal pigment curcumin to prostate cancer cells." Molecular Pharmaceutics **10**(12): 4481-4490.

Harada, T., D. T. Pham, M. H. M. Leung, H. T. Ngo, S. F. Lincoln, C. J. Easton and T. W. Kee (2011). "Cooperative binding and stabilization of the medicinal pigment curcumin by diamide linked γ-cyclodextrin dimers: A spectroscopic characterization." Journal of Physical Chemistry B **115**(5): 1268-1274.

Hartojo, W., A. L. Silvers, D. G. Thomas, C. W. Seder, L. Lin, H. Rao, Z. Wang, J. K. Greenson, T. J. Giordano, M. B. Orringer, A. Rehemtulla, M. S. Bhojani, D. G. Beer and A. C. Chang (2010). "Curcumin promotes apoptosis, increases chemosensitivity, and inhibits nuclear factor κB in esophageal adenocarcinoma." Translational Oncology **3**(2): 99-108.

Hasima, N. and B. B. Aggarwal (2012). "Cancer-linked targets modulated by curcumin." International Journal of Biochemistry and Molecular Biology **3**(4): 328-351.

Hatcher, H., R. Planalp, J. Cho, F. M. Torti and S. V. Torti (2008). "Curcumin: From ancient medicine to current clinical trials." Cellular and Molecular Life Sciences **65**(11): 1631-1652.

Hejazi, J., R. Rastmanesh, F. A. Taleban, S. H. Molana and G. Ehtejab (2013). "A pilot clinical trial of radioprotective effects of curcumin supplementation in patients with prostate cancer." Journal of Cancer Science and Therapy **5**(10): 320-324.

Heldin, C. H., K. Rubin, K. Pietras and A. Östman (2004). "High interstitial fluid pressure - An obstacle in cancer therapy." Nature Reviews Cancer **4**(10): 806-813.

Hendrayani, S. F., H. H. Al-Khalaf and A. Aboussekhra (2013). "Curcumin triggers p16-dependent senescence in active breast cancer-associated fibroblasts and suppresses their paracrine procarcinogenic effects." Neoplasia (United States) **15**(6): 631-640.

Henry, M. D., S. Wen, M. D. Silva, S. Chandra, M. Milton and P. J. Worland (2004). "A prostate-specific membrane antigen-targeted monoclonal antibody-chemotherapeutic conjugate designed for the treatment of prostate cancer." Cancer Research **64**(21): 7995-8001.

Henshall, S. M., D. I. Quinn, C. S. Lee, D. R. Head, D. Golovsky, P. C. Brenner, W. Delprado, P. D. Stricker, J. J. Grygiel and R. L. Sutherland (2001). "Altered expression of androgen receptor in the malignant epithelium and adjacent stroma is associated with early relapse in prostate cancer." Cancer Research **61**(2): 423-427.

Herbst, R. S., S. G. Eckhardt, R. Kurzrock, S. Ebbinghaus, P. J. O'Dwyer, M. S. Gordon, W. Novotny, M. A. Goldwasser, T. M. Tohnya, B. L. Lum, A. Ashkenazi, A. M. Jubb and D. S. Mendelson (2010). "Phase I dose-escalation study of recombinant human Apo2L/TRAIL, a dual proapoptotic receptor agonist, in patients with advanced cancer." Journal of Clinical Oncology **28**(17): 2839-2846.

Herman, J. G., H. L. Stadelman and C. E. Roselli (2009). "Curcumin blocks CCL2-induced adhesion, motility and invasion, in part, through down-regulation of CCL2 expression and proteolytic activity." International Journal of Oncology **34**(5): 1319-1327.

Hershey, J. W. B. (1991). "Translational control in mammalian cells." Annual Review of Biochemistry **60**: 717-755.

Hilchie, A. L., S. J. Furlong, K. Sutton, A. Richardson, M. R. J. Robichaud, C. A. Giacomantonio, N. D. Ridgway and D. W. Hoskin (2010). "Curcumin-induced apoptosis in PC3 prostate carcinoma cells is caspase-independent and involves cellular ceramide accumulation and damage to mitochondria." Nutrition and Cancer **62**(3): 379-389.

Hill, R., Y. Song, R. D. Cardiff and T. Van Dyke (2005). "Selective evolution of stromal mesenchyme with p53 loss in response to epithelial tumorigenesis." Cell **123**(6): 1001-1011.

Hoheisel, J. D. (2006). "Microarray technology: Beyond transcript profiling and genotype analysis." Nature Reviews Genetics **7**(3): 200-210.

Holder, G. M., J. L. Plummer and A. J. Ryan (1978). "The metabolism and excretion of curcumin (1,7-bis-(4-hydroxy-3-methoxyphenyl)-1,6-heptadiene-3,5-dione) in the rat." Xenobiotica **8**(12): 761-768.

Hong, J. H., K. S. Ahn, E. Bae, S. S. Jeon and H. Y. Choi (2006). "The effects of curcumin on the invasiveness of prostate cancer in vitro and in vivo." Prostate Cancer and Prostatic Diseases **9**(2): 147-152.

Hoogstraat, M., M. S. De Pagter, G. A. Cirkel, M. J. Van Roosmalen, T. T. Harkins, K. Duran, J. Kreeftmeijer, I. Renkens, P. O. Witteveen, C. C. Lee, I. J. Nijman, T. Guy, R. Van't Slot, T. N. Jonges, M. P. Lolkema, M. J. Koudijs, R. P. Zweemer, E. E. Voest, E. Cuppen and W. P. Kloosterman (2014). "Genomic and transcriptomic plasticity in treatment-naïve ovarian cancer." Genome Research **24**(2): 200-211.

Hotte, S. J., H. W. Hirte, E. X. Chen, L. L. Siu, L. H. Le, A. Corey, A. Lacobucci, M. MacLean, L. Lo, N. L. Fox and A. M. Oza (2008). "A phase 1 study of mapatumumab (fully human monoclonal antibody to TRAIL-R1) in patients with advanced solid malignancies." Clinical Cancer Research **14**(11): 3450-3455.

Hu, P., P. Huang and M. W. Chen (2013). "Curcumin attenuates cyclooxygenase-2 expression via inhibition of the NF-κb pathway in lipopolysaccharide-stimulated human gingival fibroblasts." Cell Biology International **37**(5): 443-448.

Hu, X. L., D. H. Hu, Y. B. Han, W. X. Cai, X. Z. Bai, C. Z. Yang and P. Ji (2008). "Effect of curcumin on the collagen synthesis of keloid fibroblasts." Journal of Clinical Rehabilitative Tissue Engineering Research **12**(46): 9024-9027.

Huang, J., C. Wu, P. A. Di Sant'Agnese, J. L. Yao, L. Cheng and Y. Na (2007). "Function and molecular mechanisms of neuroendocrine cells in prostate cancer." Analytical and Quantitative Cytology and Histology **29**(3): 128-138.

Huggins, C. and C. V. Hodges (2002). "Studies on prostatic cancer: I. The effect of castration, of estrogen and of androgen injection on serum phosphatases in metastatic carcinoma of the prostate. 1941." Journal of Urology **168**(1): 9-12.

Hugosson, J., S. Carlsson, G. Aus, S. Bergdahl, A. Khatami, P. Lodding, C. G. Pihl, J. Stranne, E. Holmberg and H. Lilja (2010). "Mortality results from the Göteborg randomised population-based prostate-cancer screening trial." The Lancet Oncology **11**(8): 725-732.

Hussain, A. R., M. Ahmed, N. A. Al-Jomah, A. S. Khan, P. Manogaran, M. Sultana, J. Abubaker, L. C. Platanias, K. S. Al-Kuraya and S. Uddin (2008). "Curcumin suppresses constitutive activation of nuclear factor-κB and requires functional Bax to induce apoptosis in Burkitt's lymphoma cell lines." Molecular Cancer Therapeutics **7**(10): 3318-3329.

Hwang, B. M., E. M. Noh, J. S. Kim, J. M. Kim, Y. O. You, J. K. Hwang, K. B. Kwon and Y. R. Lee (2013). "Curcumin inhibits UVB-induced matrix metalloproteinase-1/3 expression by suppressing the MAPK-p38/JNK pathways in human dermal fibroblasts." Experimental Dermatology **22**(5): 371-374.

Jaisin, Y., A. Thampithak, B. Meesarapee, P. Ratanachamnong, A. Suksamrarn, L. Phivthong-ngam, N. Phumala-Morales, S. Chongthammakun, P. Govitrapong and Y. Sanvarinda (2011). "Curcumin I protects the dopaminergic cell line SH-SY5Y from 6-hydroxydopamine-induced neurotoxicity through attenuation of p53-mediated apoptosis." Neuroscience Letters **489**(3): 192-196.

Jakobovits, A. (2008). Monoclonal antibody therapy for prostate cancer. **181:** 237-256.

Jee, S. H., S. C. Shen, C. R. Tseng, H. C. Chiu and M. L. Kuo (1998). "Curcumin induces a p53-dependent apoptosis in human basal cell carcinoma cells." Journal of Investigative Dermatology **111**(4): 656-661.

Jin, S., H. Zhao, F. Fan, P. Blanck, W. Fan, A. B. Colchagie, A. J. Fornace Jr and Q. Zhan (2000). "BRCA1 activation of the GADD45 promoter." Oncogene **19**(35): 4050-4057.

Jin, Z. and W. S. El-Deiry (2005). "Overview of cell death signaling pathways." Cancer Biology and Therapy **4**(2): 139-163.

Johansson, A. C., A. Ansell, F. Jerhammar, M. B. Lindh, R. Grénman, E. Munck-Wikland, A. Östman and K. Roberg (2012). "Cancer-associated fibroblasts induce matrix metalloproteinase-mediated cetuximab resistance in head and neck squamous cell carcinoma cells." Molecular Cancer Research **10**(9): 1158-1168.

Juliano, R. L. and V. Ling (1976). "A surface glycoprotein modulating drug permeability in Chinese hamster ovary cell mutants." BBA - Biomembranes **455**(1): 152-162.

Jutooru, I., G. Chadalapaka, P. Lei and S. Safe (2010). "Inhibition of NFκB and pancreatic cancer cell and tumor growth by curcumin is dependent on specificity protein down-regulation." Journal of Biological Chemistry **285**(33): 25332-25344.

Kalluri, R. and M. Zeisberg (2006). "Fibroblasts in cancer." Nature Reviews Cancer **6**(5): 392-401.

Kamat, A. M., G. Sethi and B. B. Aggarwal (2007). "Curcumin potentiates the apoptotic effects of chemotherapeutic agents and cytokines through down-regulation of nuclear factor-κB and nuclear factor-κB-regulated gene products in IFN-α-sensitive and IFN-α-resistant human bladder cancer cells." Molecular Cancer Therapeutics **6**(3): 1022-1030.

Kaminaga, Y., A. Nagatsu, T. Akiyama, N. Sugimoto, T. Yamazaki, T. Maitani and H. Mizukami (2003). "Production of unnatural glucosides of curcumin with drastically enhanced water solubility by cell suspension cultures of Catharanthus roseus." FEBS Letters **555**(2): 311-316.

Kandioler-Eckersberger, D., C. Ludwig, M. Rudas, S. Kappel, E. Janschek, C. Wenzel, H. Schlagbauer-Wadl, M. Mittlböck, M. Gnant, G. Steger and R. Jakesz (2000). "TP53 mutation and p53 overexpression for prediction of response to neoadjuvant treatment in breast cancer patients." Clinical Cancer Research **6**(1): 50-56.

Kang, H. J., S. H. Lee, J. E. Price and L. S. Kim (2009). "Curcumin suppresses the paclitaxel-induced nuclear factor-B in breast cancer cells and potentiates the growth inhibitory effect of paclitaxel in a breast cancer nude mice model." Breast Journal **15**(3): 223-229.

Kang, Z., J. J. Chen, Y. Yu, B. Li, S. Y. Sun, B. Zhang and L. Cao (2011). "Drozitumab, a human antibody to death receptor 5, has potent antitumor activity against rhabdomyosarcoma with the expression of caspase-8 predictive of response." Clinical Cancer Research **17**(10): 3181-3192.

Kantoff, P. W., C. S. Higano, N. D. Shore, E. R. Berger, E. J. Small, D. F. Penson, C. H. Redfern, A. C. Ferrari, R. Dreicer, R. B. Sims, Y. Xu, M. W. Frohlich and P. F. Schellhammer (2010). "Sipuleucel-T immunotherapy for castration-resistant prostate cancer." New England Journal of Medicine **363**(5): 411-422.

Kanwar, R. K., C. H. A. Cheung, J. Y. Chang and J. R. Kanwar (2010). "Recent advances in anti-survivin treatments for cancer." Current Medicinal Chemistry **17**(15): 1509-1515.

Karagiannis, G. S., T. Poutahidis, S. E. Erdman, R. Kirsch, R. H. Riddell and E. P. Diamandis (2012). "Cancer-associated fibroblasts drive the progression of metastasis through both paracrine and mechanical pressure on cancer tissue." Molecular Cancer Research **10**(11): 1403-1418.

Kelley, S. K., L. A. Harris, D. Xie, L. Deforge, K. Totpal, J. Bussiere and J. A. Fox (2001). "Preclinical studies to predict the disposition of Apo2L/tumor necrosis factor-related apoptosis-inducing ligand in humans: Characterization of in vivo efficacy, pharmacokinetics, and safety." Journal of Pharmacology and Experimental Therapeutics **299**(1): 31-38.

Khar, A., A. M. Ali, B. V. V. Pardhasaradhi, C. Varalakshmi, R. Anjum and A. L. Kumari (2001). "Induction of stress response renders human tumor cell lines resistant to curcumin-mediated apoptosis: Role of reactive oxygen intermediates." Cell Stress and Chaperones **6**(4): 368-376.

Khayat, D., Z. Dux, R. Anavi, Y. Shlomo, I. P. Witz and M. Ran (1984). "Circulating cellfree Fcγ2b/γ1 receptor in normal mouse serum: Its detection and specificity." Journal of Immunology **132**(5): 2496-2501.

Khor, T. O., Y. Huang, T. Y. Wu, L. Shu, J. Lee and A. N. T. Kong (2011). "Pharmacodynamics of curcumin as DNA hypomethylation agent in restoring the expression of Nrf2 via promoter CpGs demethylation." Biochemical Pharmacology **82**(9): 1073-1078.

Khor, T. O., Y. S. Keum, W. Lin, J. H. Kim, R. Hu, G. Shen, C. Xu, A. Gopalakrishnan, B. Reddy, X. Zheng, A. H. Conney and A. N. T. Kong (2006). "Combined inhibitory effects of curcumin and phenethyl isothiocyanate on the growth of human PC-3 prostate xenografts in immunodeficient mice." Cancer Research **66**(2): 613-621.

Killian, P. H., E. Kronski, K. M. Michalik, O. Barbieri, S. Astigiano, C. P. Sommerhoff, U. Pfeffer, A. G. Nerlich and B. E. Bachmeier (2012). "Curcumin inhibits prostate cancer metastasis in vivo by targeting the inflammatory cytokines CXCL1 and -2." Carcinogenesis **33**(12): 2507-2519.

Kloesch, B., T. Becker, E. Dietersdorfer, H. Kiener and G. Steiner (2013). "Anti-inflammatory and apoptotic effects of the polyphenol curcumin on human fibroblast-like synoviocytes." International Immunopharmacology **15**(2): 400-405.

Koivisto, P., M. Kolmer, T. Visakorpi and O. P. Kallioniemi (1998). "Androgen receptor gene and hormonal therapy failure of prostate cancer." American Journal of Pathology **152**(1): 1-9.

Konishi, N., K. Shimada, E. Ishida and M. Nakamura (2005). "Molecular pathology of prostate cancer." Pathology International **55**(9): 531-539.

Korutla, L., J. Y. Cheung, J. Mendelsohn and R. Kumar (1995). "Inhibition of ligand-induced activation of epidermal growth factor receptor tyrosine phosphorylation by curcumin." Carcinogenesis **16**(8): 1741-1745.

Kuang, Y. and D. R. Walt (2005). "Monitoring "promiscuous" drug effects on single cells of multiple cell types." Analytical Biochemistry **345**(2): 320-325.

Kucik, D. F. and C. Wu (2005). "Cell-adhesion assays." Methods in molecular biology (Clifton, N.J.) **294**: 43-54.

Kukreja, P., A. B. Abdel-Mageed, D. Mondal, K. Liu and K. C. Agrawal (2005). "Up-regulation of CXCR4 expression in PC-3 cells by stromal-derived factor-1α (CXCL12) increases endothelial adhesion and transendothelial migration: Role of MEK/ERK signaling pathway-dependent NF-κB activation." Cancer Research **65**(21): 9891-9898.

Kunnumakkara, A. B., S. Guha, S. Krishnan, P. Diagaradjane, J. Gelovani and B. B. Aggarwal (2007). "Curcumin potentiates antitumor activity of gemcitabine in an orthotopic model of pancreatic cancer through suppression of proliferation, angiogenesis, and inhibition of nuclear factor-κB-regulated gene products." Cancer Research **67**(8): 3853-3861.

Kunwar, A., A. Barik, B. Mishra, K. Rathinasamy, R. Pandey and K. I. Priyadarsini (2008). "Quantitative cellular uptake, localization and cytotoxicity of curcumin in normal and tumor cells." Biochimica et Biophysica Acta - General Subjects **1780**(4): 673-679.

Kurata, T., K. Tamura, H. Kaneda, T. Nogami, H. Uejima, G. Asai, K. Nakagawa and M. Fukuoka (2004). "Effect of re-treatment with gefitinib ('Iressa', ZD1839) after acquisition of resistance [1]." Annals of Oncology **15**(1): 173.

Kurzrock, E. A., L. S. Baskin and G. R. Cunha (1999). "Ontogeny of the male urethra: Theory of endodermal differentiation." Differentiation **64**(2): 115-122.

Labrie, F., V. Luu-The, C. Labrie and J. Simard (2001). "DHEA and its transformation into androgens and estrogens in peripheral target tissues: Intracrinology." Frontiers in Neuroendocrinology **22**(3): 185-212.

Labrinidis, A., P. Diamond, S. Martin, S. Hay, V. Liapis, I. Zinonos, N. A. Sims, G. J. Atkins, C. Vincent, V. Ponomarev, D. M. Findlay, A. C. W. Zannettino and A. Evdokiou (2009). "Apo2L/TRAIL inhibits tumor growth and bone destruction in a murine model of multiple myeloma." Clinical Cancer Research **15**(6): 1998-2009.

Lambert, G., L. Estévez-Salmeron, S. Oh, D. Liao, B. M. Emerson, T. D. Tlsty and R. H. Austin (2011). "An analogy between the evolution of drug resistance in bacterial communities and malignant tissues." Nature Reviews Cancer **11**(5): 375-382.

Landais, I., S. Hiddingh, M. McCarroll, C. Yang, A. Sun, M. S. Turker, J. P. Snyder and M. E. Hoatlin (2009). "Monoketone analogs of curcumin, a new class of Fanconi anemia pathway inhibitors." Molecular Cancer **8**.

LeBeau, A. M., W. N. Brennen, S. Aggarwal and S. R. Denmeade (2009). "Targeting the cancer stroma with a fibroblast activation protein-activated promelittin protoxin." Molecular Cancer Therapeutics **8**(5): 1378-1386.

Lee, J., M. Fassnacht, S. Nair, D. Boczkowski and E. Gilboa (2005). "Tumor immunotherapy targeting fibroblast activation protein, a product expressed in tumor-associated fibroblasts." Cancer Research **65**(23): 11156-11163.

Lee, J. M. and A. Bernstein (1995). "Apoptosis, cancer and the p53 tumour suppressor gene." Cancer and Metastasis Reviews **14**(2): 149-161.

Lee, K. H., F. Abas, N. B. Mohamed Alitheen, K. Shaari, N. H. Lajis, D. A. Israf and A. Syahida (2014). "Chemopreventive effects of a curcumin-like diarylpentanoid [2,6-bis(2,5-dimethoxybenzylidene)cyclohexanone] in cellular targets of rheumatoid arthritis in vitro." International Journal of Rheumatic Diseases.

Leighl, N. B., L. Paz-Ares, J. Y. Douillard, C. Peschel, A. Arnold, A. Depierre, A. Santoro, D. C. Betticher, U. Gatzemeier, J. Jassem, J. Crawford, D. Tu, A. Bezjak, J. S. Humphrey, M. Voi, S. Galbraith, K. Hann, L. Seymour and F. A. Shepherd (2005). "Randomized phase III study of matrix metalloproteinase inhibitor BMS-275291 in combination with paclitaxel and carboplatin in advanced non-small-cell lung cancer: National Cancer Institute of Canada-Clinical Trials Group Study BR. 18." Journal of Clinical Oncology **23**(12): 2831-2839.

Letchford, K., R. Liggins and H. Burt (2008). "Solubilization of hydrophobic drugs by methoxy poly(ethylene glycol)-block-polycaprolactone diblock copolymer micelles: Theoretical and experimental data and correlations." Journal of Pharmaceutical Sciences **97**(3): 1179-1190.

Leung, M. H. M., H. Colangelo and T. W. Kee (2008). "Encapsulation of curcumin in cationic micelles suppresses alkaline hydrolysis." Langmuir **24**(11): 5672-5675.

Leung, M. H. M. and T. W. Kee (2009). "Effective stabilization of curcumin by association to plasma proteins: Human serum albumin and fibrinogen." Langmuir **25**(10): 5773-5777.

Lev-Ari, S., L. Strier, D. Kazanov, L. Madar-Shapiro, H. Dvory-Sobol, I. Pinchuk, B. Marian, D. Lichtenberg and N. Arber (2005). "Celecoxib and curcumin synergistically inhibit the growth of colorectal cancer cells." Clinical Cancer Research **11**(18): 6738-6744.

Lewis, K. (2013). "Platforms for antibiotic discovery." Nature Reviews Drug Discovery **12**(5): 371-387.

Li, R., T. Wheeler, H. Dai, A. Frolov, T. Thompson and G. Ayala (2004). "High level of androgen receptor is associated with aggressive clinicopathologic features and decreased biochemical recurrence-free survival in prostate: Cancer patients treated with radical prostatectomy." American Journal of Surgical Pathology **28**(7): 928-934.

Li, Y., C. X. Li, H. Ye, F. Chen, J. Melamed, Y. Peng, J. Liu, Z. Wang, H. C. Tsou, J. Wei, P. Walden, M. J. Garabedian and P. Lee (2008). "Decrease in stromal androgen receptor associates with androgen-independent disease and promotes prostate cancer cell proliferation and invasion." Journal of Cellular and Molecular Medicine **12**(6B): 2790-2798.

Liang, D., Y. Ma, J. Liu, C. G. Trope, R. Holm, J. M. Nesland and Z. Suo (2012). "The hypoxic microenvironment upgrades stem-like properties of ovarian cancer cells." BMC Cancer **12**.

Lièvre, A., J. B. Bachet, D. Le Corre, V. Boige, B. Landi, J. F. Emile, J. F. Côté, G. Tomasic, C. Penna, M. Ducreux, P. Rougier, F. Penault-Llorca and P. Laurent-Puig (2006). "KRAS mutation status is predictive of response to cetuximab therapy in colorectal cancer." Cancer Research **66**(8): 3992-3995.

Lin, L., Q. Shi, A. K. Nyarko, K. F. Bastow, C. C. Wu, C. Y. Su, C. C. Y. Shih and K. H. Lee (2006). "Antitumor agents. 250. Design and synthesis of new curcumin analogues as potential anti-prostate cancer agents." Journal of Medicinal Chemistry **49**(13): 3963-3972.

Lin, Y. G., A. B. Kunnumakkara, A. Nair, W. M. Merritt, L. Y. Han, G. N. Armaiz-Pena, A. A. Kamat, W. A. Spannuth, D. M. Gershenson, S. K. Lutgendorf, B. B. Aggarwal and A. K. Sood (2007). "Curcumin inhibits tumor growth and angiogenesis in ovarian carcinoma by targeting the nuclear factor-κB pathway." Clinical Cancer Research **13**(11): 3423-3430.

Liu, E., J. Wu, W. Cao, J. Zhang, W. Liu, X. Jiang and X. Zhang (2007). "Curcumin induces G2/M cell cycle arrest in a p53-dependent manner and upregulates ING4 expression in human glioma." Journal of Neuro-Oncology **85**(3): 263-270.

Liu, S., Z. Wang, Z. Hu, X. Zeng, Y. Li, Y. Su, C. Zhang and Z. Ye (2011). "Anti-tumor activity of curcumin against androgen-independent prostate cancer cells via inhibition of NF-κB and AP-1 pathway in vitro." Journal of Huazhong University of Science and Technology - Medical Science **31**(4): 530-534.

Liu, Y. C., I. T. Chiang, F. T. Hsu and J. J. Hwang (2012). "Using NF-κB as a molecular target for theranostics in radiation oncology research." Expert Review of Molecular Diagnostics **12**(2): 139-146.

Loeffler, M., J. A. Krüger, A. G. Niethammer and R. A. Reisfeld (2006). "Targeting tumor-associated fibroblasts improves cancer chemotherapy by increasing intratumoral drug uptake." Journal of Clinical Investigation **116**(7): 1955-1962.

Lu, H. F., K. C. Lai, S. C. Hsu, H. J. Lin, M. D. Yang, Y. L. Chen, M. J. Fan, J. S. Yang, P. Y. Cheng, C. L. Kuo and J. G. Chung (2009). "Curcumin induces apoptosis through FAS and FADD, in caspase-3-dependent and -independent pathways in the N18 mouse-rat hybrid retina ganglion cells." Oncology Reports **22**(1): 97-104.

Lu, J. J., Y. J. Cai and J. Ding (2011). "Curcumin induces DNA damage and caffeine-insensitive cell cycle arrest in colorectal carcinoma HCT116 cells." Molecular and Cellular Biochemistry **354**(1-2): 247-252.

Lu, W. D., Y. Qin, C. Yang, L. Li and Z. X. Fu (2013). "Effect of curcumin on human colon cancer multidrug resistance in vitro and in vivo." Clinics **68**(5): 694-701.

Lubahn, D. B., D. R. Joseph, M. Sar, J. Tan, H. N. Higgs, R. E. Larson, F. S. French and E. M. Wilson (1988). "The human androgen receptor: Complementary deoxyribonucleic acid cloning, sequence analysis and gene expression in prostate." Molecular Endocrinology **2**(12): 1265-1275.

Magalska, A., A. Brzezinska, A. Bielak-Zmijewska, K. Piwocka, G. Mosieniak and E. Sikora (2006). "Curcumin induces cell death without oligonucleosomal DNA fragmentation in quiescent and proliferating human CD8+ cells." Acta Biochimica Polonica **53**(3): 531-538.

Maher, C. A., C. Kumar-Sinha, X. Cao, S. Kalyana-Sundaram, B. Han, X. Jing, L. Sam, T. Barrette, N. Palanisamy and A. M. Chinnaiyan (2009). "Transcriptome sequencing to detect gene fusions in cancer." Nature **458**(7234): 97-101.

Majumdar, A. P. N., S. Banerjee, J. Nautiyal, B. B. Patel, V. Patel, J. Du, Y. Yu, A. A. Elliott, E. Levi and F. H. Sarkar (2009). "Curcumin synergizes with resveratrol to inhibit colon cancer." Nutrition and Cancer **61**(4): 544-553.

Makridakis, N. M., R. K. Ross, M. C. Pike, L. E. Crocitto, L. N. Kolonel, C. L. Pearce, B. E. Henderson and J. K. V. Reichardt (1999). "Association of mis-sense substitution in SRD5A2 gene with prostate cancer in African-American and Hispanic men in Los Angeles, USA." Lancet **354**(9183): 975-978.

Marcu, M. G., Y. J. Jung, S. Lee, E. J. Chung, M. J. Lee, J. Trepel and L. Neckers (2006). "Curcumin is an inhibitor of p300 histone acetylatransferase." Medicinal Chemistry **2**(2): 169-174.

Marsters, S. A., J. P. Sheridan, R. M. Pitti, J. Brush, A. Goddard and A. Ashkenazi (1998). "Identification of a ligand for the death-domain-containing receptor Apo3." Current Biology **8**(9): 525-528.

Mayerhofer, M., K. V. Gleixner, J. Mayerhofer, G. Hoermann, E. Jaeger, K. J. Aichberger, R. G. Ott, K. Greish, H. Nakamura, S. Derdak, P. Samorapoompichit, W. F. Pickl, V. Sexl, H. Esterbauer, I. Schwarzinger, C. Sillaber, H. Maeda and P. Valent (2008). "Targeting of heat shock protein 32 (Hsp32)/heme oxygenase-1 (HO-1) in leukemic cells in chronic myeloid leukemia: A novel approach to overcome resistance against imatinib." Blood **111**(4): 2200-2210.

McNeal, J. E. (1981). "The zonal anatomy of the prostate." Prostate **2**(1): 35-49.

Meads, M. B., R. A. Gatenby and W. S. Dalton (2009). "Environment-mediated drug resistance: A major contributor to minimal residual disease." Nature Reviews Cancer **9**(9): 665-674.

Mellado, B., J. Codony, M. J. Ribal, L. Visa and P. Gascón (2009). "Molecular biology of androgen-independent prostate cancer: The role of the androgen receptor pathway." Clinical and Translational Oncology **11**(1): 5-10.

Michel, D., J. M. Chitanda, R. Balogh, P. Yang, J. Singh, U. Das, A. El-Aneed, J. Dimmock, R. Verrall and I. Badea (2012). "Design and evaluation of cyclodextrin-based delivery systems to incorporate poorly soluble curcumin analogs for the treatment of melanoma." European Journal of Pharmaceutics and Biopharmaceutics **81**(3): 548-556.

Milowsky, M. I., D. M. Nanus, L. Kostakoglu, S. Vallabhajosula, S. J. Goldsmith and N. H. Bander (2004). "Phase I trial of yttrium-90-labeled anti-prostate-specific membrane antigen monoclonal antibody J591 for androgen-independent prostate cancer." Journal of Clinical Oncology **22**(13): 2522-2531.

Miyazaki, T., Y. Miyazaki, K. Izumikawa, H. Kakeya, S. Miyakoshi, J. E. Bennett and S. Kohno (2006). "Fluconazole treatment is effective against a Candida albicans erg3/erg3 mutant in vivo despite in vitro resistance." Antimicrobial Agents and Chemotherapy **50**(2): 580-586.

Mohanty, C., S. Acharya, A. K. Mohanty, F. Dilnawaz and S. K. Sahoo (2010). "Curcumin-encapsulated MePEG/PCL diblock copolymeric micelles: A novel controlled delivery vehicle for cancer therapy." Nanomedicine **5**(3): 433-449.

Montironi, R., R. Mazzucchelli, A. Lopez-Beltran, L. Cheng and M. Scarpelli (2007). "Mechanisms of Disease: High-grade prostatic intraepithelial neoplasia and other proposed preneoplastic lesions in the prostate." Nature Clinical Practice Urology **4**(6): 321-332.

Moon, D. O., M. O. Kim, Y. H. Choi, Y. M. Park and G. Y. Kim (2010). "Curcumin attenuates inflammatory response in IL-1β-induced human synovial fibroblasts and collagen-induced arthritis in mouse model." International Immunopharmacology **10**(5): 605-610.

Müerköster, S. S., V. Werbing, D. Koch, B. Sipos, O. Ammerpohl, H. Kalthoff, M. S. Tsao, U. R. Fölsch and H. Schäfer (2008). "Role of myofibroblasts in innate chemoresistance of pancreatic carcinoma - Epigenetic downregulation of caspases." International Journal of Cancer **123**(8): 1751-1760.

Mukhopadhyay, A., C. Bueso-Ramos, D. Chatterjee, P. Pantazis and B. B. Aggarwal (2001). "Curcumin downregulates cell survival mechanisms in human prostate cancer cell lines." Oncogene **20**(52): 7597-7609.

Mullan, P. B., J. E. Quinn and D. P. Harkin (2006). "The role of BRCA1 in transcriptional regulation and cell cycle control." Oncogene **25**(43): 5854-5863.

Murphy, D. G., T. Ahlering, W. J. Catalona, H. Crowe, J. Crowe, N. Clarke, M. Cooperberg, D. Gillatt, M. Gleave, S. Loeb, M. Roobol, O. Sartor, T. Pickles, A. Wootten, P. C. Walsh and A. J. Costello (2014). "The Melbourne Consensus Statement on the early detection of prostate cancer." BJU International **113**(2): 186-188.

Nakamura, K., Y. Yasunaga, T. Segawa, D. Ko, J. W. Moul, S. Srivastava and J. S. Rhim (2002). "Curcumin down-regulates AR gene expression and activation in prostate cancer cell lines." International journal of oncology **21**(4): 825-830.

Nanus, D. M., M. I. Milowsky, L. Kostakoglu, P. M. Smith-Jones, S. Vallabahajosula, S. J. Goldsmith, N. H. Bander, J. B. Nelson, W. R. Sellers, M. Roach Iii, P. W. Kantoff, W. K. Oh and M. R. Smith (2003). "Clinical use of monoclonal antibody HuJ591 therapy: Targeting prostate specific membrane antigen." Journal of Urology **170**(6 II): S84-S89.

Narayanan, N. K., D. Nargi, C. Randolph and B. A. Narayanan (2009). "Liposome encapsulation of curcumin and resveratrol in combination reduces prostate cancer incidence in PTEN knockout mice." International Journal of Cancer **125**(1): 1-8.

Need, E. F., H. I. Scher, A. A. Peters, N. L. Moore, A. Cheong, C. J. Ryan, G. A. Wittert, V. R. Marshall, W. D. Tilley and G. Buchanan (2009). "A novel androgen receptor amino terminal region reveals two classes of amino/carboxyl interaction-deficient variants with divergent capacity to activate responsive sites in chromatin." Endocrinology **150**(6): 2674-2682.

Need, E. F., L. A. Selth, T. J. Harris, S. N. Birrell, W. D. Tilley and G. Buchanan (2012). "Research resource: Interplay between the genomic and transcriptional networks of androgen receptor and estrogen receptor α in luminal breast cancer cells." Molecular Endocrinology **26**(11): 1941-1952.

Nicolas, E., V. Morales, L. Magnaghi-Jaulin, A. Harel-Bellan, H. Richard-Foy and D. Trouche (2000). "RbAp48 belongs to the histone deacetylase complex that associates with the retinoblastoma protein." Journal of Biological Chemistry **275**(13): 9797-9804.

Niu, Y., S. Altuwaijri, S. Yeh, K. P. Lai, S. Yu, K. H. Chuang, S. P. Huang, H. Lardy and C. Chang (2008). "Targeting the stromal androgen receptor in primary prostate tumors at earlier stages." Proceedings of the National Academy of Sciences of the United States of America **105**(34): 12188-12193.

Nowell, P. C. (1976). "The clonal evolution of tumor cell populations. Acquired genetic lability permits stepwise selection of variant sublines and underlies tumor progression." Science **194**(4260): 23-28.

O'Sullivan-Coyne, G., G. C. O'Sullivan, T. R. O'Donovan, K. Piwocka and S. L. McKenna (2009). "Curcumin induces apoptosis-independent death in oesophageal cancer cells." British Journal of Cancer **101**(9): 1585-1595.

Ohtsu, H., Z. Xiao, J. Ishida, M. Nagai, H. K. Wang, H. Itokawa, C. Y. Su, C. Shih, T. Chiang, E. Chang, Y. Lee, M. Y. Tsai, C. Chang and K. H. Lee (2002). "Antitumor agents. 217. Curcumin analogues as novel androgen receptor antagonists with potential as anti-prostate cancer agents." Journal of Medicinal Chemistry **45**(23): 5037-5042.

Olapade-Olaopa, E. O., D. K. Moscatello, E. H. MacKay, D. P. Sandhu, T. R. Terry, A. J. Wong and F. K. Habib (2004). "Alterations in the expression of androgen receptor, wild type-epidermal growth factor receptor and a mutant epidermal growth factor receptor in human prostate cancer." African journal of medicine and medical sciences **33**(3): 245-253.

Olapade-Olaopa, E. O., C. A. Muronda, E. H. MacKay, A. P. Danso, D. P. Sandhu, T. R. Terry and F. K. Habib (2004). "Androgen receptor protein expression in prostatic tissues in Black and Caucasian men." Prostate **59**(4): 460-468.

Olumi, A. F., G. D. Grossfeld, S. W. Hayward, P. R. Carroll, T. D. Tlsty and G. R. Cunha (1999). "Carcinoma-associated fibroblasts direct tumor progression of initiated human prostatic epithelium." Cancer Research **59**(19): 5002-5011.

Oppenheimer, A. (1937). "TURMERIC (CURCUMIN) IN BILIARY DISEASES." The Lancet **229**(5924): 619-621.

Orio Jr, F., B. Térouanne, V. Georget, S. Lumbroso, C. Avances, C. Siatka and C. Sultan (2002). "Potential action of IGF-1 and EGF on androgen receptor nuclear transfer and transactivation in normal and cancer human prostate cell lines." Molecular and Cellular Endocrinology **198**(1-2): 105-114.

Owen, D. H. and D. F. Katz (2005). "A review of the physical and chemical properties of human semen and the formulation of a semen simulant." Journal of Andrology **26**(4): 459-469.

Paland, N., I. Kamer, I. Kogan-Sakin, S. Madar, N. Goldfinger and V. Rotter (2009). "Differential influence of normal and cancer-associated fibroblasts on the growth of human epithelial cells in an in vitro cocultivation model of prostate cancer." Molecular Cancer Research **7**(8): 1212-1223.

Pan, G., J. Ni, Y. F. Wei, G. I. Yu, R. Gentz and V. M. Dixit (1997). "An antagonist decoy receptor and a death domain-containing receptor for TRAIL." Science **277**(5327): 815-818.

Panchal, H. D., K. Vranizan, C. Y. Lee, J. Ho, J. Ngai and P. S. Timiras (2008). "Early anti-oxidative and anti-proliferative curcumin effects on neuroglioma cells suggest therapeutic targets." Neurochemical Research **33**(9): 1701-1710.

Park, C., D. O. Moon, I. W. Choi, B. T. Choi, T. J. Nam, C. H. Rhu, T. K. Kwon, W. H. Lee, G. Y. Kim and Y. H. Choi (2007). "Curcumin induces apoptosis and inhibits prostaglandin E 2 production in synovial fibroblasts of patients with rheumatoid arthritis." International Journal of Molecular Medicine **20**(3): 365-372.

Park, J., V. Ayyappan, E. K. Bae, C. Lee, B. S. Kim, B. K. Kim, Y. Y. Lee, K. S. Ahn and S. S. Yoon (2008). "Curcumin in combination with bortezomib synergistically induced apoptosis in human multiple myeloma U266 cells." Molecular Oncology **2**(4): 317-326.

Park, S., D. H. Cho, L. Andera, N. Suh and I. Kim (2013). "Curcumin enhances TRAIL-induced apoptosis of breast cancer cells by regulating apoptosis-related proteins." Molecular and Cellular Biochemistry **383**(1-2): 39-48.

Pavlaki, M. and S. Zucker (2003). "Matrix metalloproteinase inhibitors (MMPIs): The beginning of phase I or the termination of phase III clinical trials." Cancer and Metastasis Reviews **22**(2-3): 177-203.

Peng, X., C. L. Wood, E. M. Blalock, K. C. Chen, P. W. Landfield and A. J. Stromberg (2003). "Statistical implications of pooling RNA samples for microarray experiments." BMC Bioinformatics **4**.

Pham, D. T., H. T. Ngo, S. F. Lincoln, B. L. May and C. J. Easton (2010). "Synthesis of C6A-to-C6A and C3A-to-C3A diamide linked γ-cyclodextrin dimers." Tetrahedron **66**(15): 2895-2898.

Piantino, C. B., F. A. Salvadori, P. P. Ayres, R. B. Kato, V. Srougi, K. R. Leite and M. Srougi (2009). "An evaluation of the anti-neoplastic activity of curcumin in prostate cancer cell lines." International Braz J Urol **35**(3): 354-360.

Piccolella, M., V. Crippa, E. Messi, M. J. Tetel and A. Poletti (2014). "Modulators of estrogen receptor inhibit proliferation and migration of prostate cancer cells." Pharmacological Research **79**: 13-20.

Pisano, M., G. Pagnan, M. A. Dettori, S. Cossu, I. Caffa, I. Sassu, L. Emionite, D. Fabbri, M. Cilli, F. Pastorino, G. Palmieri, G. Delogu, M. Ponzoni and C. Rozzo (2010). "Enhanced anti-tumor activity of a new curcumin-related compound against melanoma and neuroblastoma cells." Molecular Cancer **9**.

Pitti, R. M., S. A. Marsters, S. Ruppert, C. J. Donahue, A. Moore and A. Ashkenazi (1996). "Induction of apoptosis by Apo-2 ligand, a new member of the tumor necrosis factor cytokine family." Journal of Biological Chemistry **271**(22): 12687-12690.

Piwocka, K., A. Bielak-Zmijewska and E. Sikora (2002). Curcumin induces caspase-3-independent apoptosis in human multidrug-resistant cells. **973:** 250-254.

Plummer, R., G. Attard, S. Pacey, L. Li, A. Razak, R. Perrett, M. Barrett, I. Judson, S. Kaye, N. L. Fox, W. Halpern, A. Corey, H. Calvert and J. De Bono (2007). "Phase 1 and pharmacokinetic study of lexatumumab in patients with advanced cancers." Clinical Cancer Research **13**(20): 6187-6194.

Pontiggia, O., R. Sampayo, D. Raffo, A. Motter, R. Xu, M. J. Bissell, E. B. De Kier Joffé and M. Simian (2012). "The tumor microenvironment modulates tamoxifen resistance in breast cancer: A role for soluble stromal factors and fibronectin through β1 integrin." Breast Cancer Research and Treatment **133**(2): 459-471.

Pound, C. R., A. W. Partin, M. A. Eisenberger, D. W. Chan, J. D. Pearson and P. C. Walsh (1999). "Natural history of progression after PSA elevation following radical prostatectomy." Journal of the American Medical Association **281**(17): 1591-1597.

Pratt, W. B. and D. O. Toft (1997). "Steroid receptor interactions with heat shock protein and immunophilin chaperones." Endocrine Reviews **18**(3): 306-360.

Premanand, C., M. Rema, M. Z. Sameer, M. Sujatha and M. Balasubramanyam (2006). "Effect of curcumin on proliferation of human retinal endothelial cells under in vitro conditions." Investigative Ophthalmology and Visual Science **47**(5): 2179-2184.

Prins, G. S. (2000). "Molecular biology of the androgen receptor." Mayo Clinic Proceedings **75**(SUPPL.): S32-S35.

Pure, E., C. J. Durie, C. K. Summerill and J. C. Unkeless (1984). "Identification of soluble Fc receptors in mouse serum and the conditioned medium of stimulated B cells." Journal of Experimental Medicine **160**(6): 1836-1849.

Qin, C. H., Y. G. Li, J. Wu and H. J. He (2012). "Curcumin reverses adriamycin-resistance of thermotolerant hepatocarcinoma cells by down-regulating P-glycoprotein and heat shock protein 70." Progress in Biochemistry and Biophysics **39**(2): 151-160.

Qiu, J., Y. F. Fu, Q. Cheng, X. D. Cheng, X. Xie and W. G. Lü (2012). "Reversing paclitaxel-resistance of SKOV3-TR30 cell line by curcumin." National Medical Journal of China **92**(27): 1926-1928.

Rahman, S., S. Cao, K. J. Steadman, M. Wei and H. S. Parekh (2012). "Native and ß-cyclodextrin-enclosed curcumin: Entrapment within liposomes and their in vitro cytotoxicity in lung and colon cancer." Drug Delivery **19**(7): 346-353.

Raith, K. and G. Hochhaus (2004). "Drugs used in the treatment of opioid tolerance and physical dependence: A review." International Journal of Clinical Pharmacology and Therapeutics **42**(4): 191-203.

Ramachandran, C. and W. You (1999). "Differential sensitivity of human mammary epithelial and breast carcinoma cell lines to curcumin." Breast Cancer Research and Treatment **54**(3): 269-278.

Rao, C. V., A. Rivenson, B. Simi and B. S. Reddy (1995). Chemoprevention of colon cancer by dietary curcumin. **768:** 201-204.

Rashmi, R., T. R. Santhosh Kumar and D. Karunagaran (2003). "Human colon cancer cells differ in their sensitivity to curcumin-induced apoptosis and heat shock protects them by inhibiting the release of apoptosis-inducing factor and caspases." FEBS Letters **538**(1-3): 19-24.

Rauh-Adelmann, C., K. M. Lau, N. Sabeti, J. P. Long, S. C. Mok and S. M. Ho (2000). "Altered expression of BRCA1, BRCA2, and a newly identified BRCA2 exon 12 deletion variant in malignant human ovarian, prostate, and breast cancer cell lines." Molecular Carcinogenesis **28**(4): 236-246.

Ravindran, J., S. Prasad and B. B. Aggarwal (2009). "Curcumin and cancer cells: How many ways can curry kill tumor cells selectively?" AAPS Journal **11**(3): 495-510.

Redmond, K. M., T. R. Wilson, P. G. Johnston and D. B. Longley (2008). "Resistance mechanisms to cancer chemotherapy." Frontiers in Bioscience **13**(13): 5138-5154.

Ricciardelli, C., C. S. Choong, G. Buchanan, S. Vivekanandan, P. Neufing, J. Stahl, V. R. Marshall, D. J. Horsfall and W. D. Tilley (2005). "Androgen receptor levels in prostate cancer epithelial and peritumoral stromal cells identify non-organ confined disease." Prostate **63**(1): 19-28.

Riccioni, R., L. Pasquini, G. Mariani, E. Saulle, A. Rossini, D. Diverio, E. Pelosi, A. Vitale, A. Chierichini, M. Cedrone, R. Foà, F. Lo Coco, C. Peschle and U. Testa (2005). "TRAIL decoy receptors mediate resistance of acute myeloid leukemia cells to TRAIL." Haematologica **90**(5): 612-624.

Ricke, E. A., K. Williams, Y. F. Lee, S. Couto, Y. Wang, S. W. Hayward, G. R. Cunha and W. A. Ricke (2012). "Androgen hormone action in prostatic carcinogenesis: Stromal androgen receptors mediate prostate cancer progression, malignant transformation and metastasis." Carcinogenesis **33**(7): 1391-1398.

Risbridger, G. P. and R. A. Taylor (2008). "Minireview: Regulation of prostatic stem cells by stromal niche in health and disease." Endocrinology **149**(9): 4303-4306.

Rocks, N., S. Bekaert, I. Coia, G. Paulissen, M. Gueders, B. Evrard, J. C. Van Heugen, P. Chiap, J. M. Foidart, A. Noel and D. Cataldo (2012). "Curcumin-cyclodextrin complexes potentiate gemcitabine effects in an orthotopic mouse model of lung cancer." British Journal of Cancer **107**(7): 1083-1092.

Rodemann, H. P. and G. A. Muller (1991). "Characterization of human renal fibroblasts in health and disease: II. In vitro growth, differentiation, and collagen synthesis of fibroblasts from kidneys with interstitial fibrosis." American Journal of Kidney Diseases **17**(6): 684-686.

Rong, G., H. Kang, Y. Wang, T. Hai and H. Sun (2013). "Candidate Markers That Associate with Chemotherapy Resistance in Breast Cancer through the Study on Taxotere-Induced Damage to Tumor Microenvironment and Gene Expression Profiling of Carcinoma-Associated Fibroblasts (CAFs)." PLoS ONE **8**(8).

Roninson, I. B., J. E. Chin, K. Choi, P. Gros, D. E. Housman, A. Fojo, D. W. Shen, M. M. Gottesman and I. Pastan (1986). "Isolation of human mdr DNA sequences amplified in multidrug-resistant KB carcinoma cells." Proceedings of the National Academy of Sciences of the United States of America **83**(12): 4538-4542.

Rosenwald, I. B. (1996). "Upregulated expression of the genes encoding translation initiation factors eIF-4E and eIF-2α in transformed cells." Cancer Letters **102**(1-2): 113-123.

Rosenwald, I. B., M. J. Hutzler, S. Wang, L. Savas and A. E. Fraire (2001). "Expression of eukaryotic translation initiation factors 4E and 2α is increased frequently in bronchioloalveolar but not in squamous cell carcinomas of the lung." Cancer **92**(8): 2164-2171.

Rothfuss, A. and G. Speit (2002). "Overexpression of heme oxygenase-1 (HO-1) in V79 cells results in increased resistance to hyperbaric oxygen (HBO)-induced DNA damage." Environmental and Molecular Mutagenesis **40**(4): 258-265.

Rowe, D. L., T. Ozbay, R. M. O'Regan and R. Nahta (2009). "Modulation of the BRCA1 protein and induction of apoptosis in triple negative breast cancer cell lines by the polyphenolic compound curcumin." Breast Cancer: Basic and Clinical Research **3**(1): 61-75.

Rozzo, C., M. Fanciulli, C. Fraumene, A. Corrias, T. Cubeddu, I. Sassu, S. Cossu, V. Nieddu, G. Galleri, E. Azara, M. A. Dettori, D. Fabbri, G. Palmieri and M. Pisano (2013). "Molecular changes induced by the curcumin analogue D6 in human melanoma cells." Molecular Cancer: 37.

Rushworth, S. A. and D. J. MacEwan (2008). "HO-1 underlies resistance of AML cells to TNF-induced apoptosis." Blood **111**(7): 3793-3801.

Ryu, H. W., S. P. Kim, K. S. Lee and J. W. Cho (2012). "Curcumin induced decreased expression of type I collagen in human skin fibroblast through down-regulation of Smad2/3 expressions." Korean Journal of Dermatology **50**(1): 1-7.

Saha, S., A. Adhikary, P. Bhattacharyya, T. Das and G. Sa (2012). "Death by design: Where curcumin sensitizes drug-resistant tumours." Anticancer Research **32**(7): 2567-2584.

Sahu, A., N. Kasoju and U. Bora (2008). "Fluorescence study of the curcumin-casein micelle complexation and its application as a drug nanocarrier to cancer cells." Biomacromolecules **9**(10): 2905-2912.

Sakulterdkiat, T., C. Srisomsap, R. Udomsangpetch, J. Svasti and K. Lirdprapamongkol (2012). "Curcumin resistance induced by hypoxia in HepG2 cells is mediated by multidrug-resistance-associated proteins." Anticancer Research **32**(12): 5337-5342.

Sallman, D. A., X. Chen, B. Zhong, D. L. Gilvary, J. Zhou, S. Wei and J. Y. Djeu (2007). "Clusterin mediates TRAIL resistance in prostate tumor cells." Molecular Cancer Therapeutics **6**(11): 2938-2947.

Salvesen, G. S. and C. S. Duckett (2002). "IAP proteins: Blocking the road to death's door." Nature Reviews Molecular Cell Biology **3**(6): 401-410.

Sawyers, C. L. (2007). "Where lies the blame for resistance - Tumor or host?" Nature Medicine **13**(10): 1144-1145.

Scharstuhl, A., H. A. M. Mutsaers, S. W. C. Pennings, W. A. Szarek, F. G. M. Russel and F. A. D. T. G. Wagener (2009). "Curcumin-induced fibroblast apoptosis and in vitro wound contraction are regulated by antioxidants and heme oxygenase: Implications for scar formation." Journal of Cellular and Molecular Medicine **13**(4): 712-725.

Scher, H. I., K. Fizazi, F. Saad, M. E. Taplin, C. N. Sternberg, K. Miller, R. De Wit, P. Mulders, K. N. Chi, N. D. Shore, A. J. Armstrong, T. W. Flaig, A. Fléchon, P. Mainwaring, M. Fleming, J. D. Hainsworth, M. Hirmand, B. Selby, L. Seely and J. S. De Bono (2012). "Increased survival with enzalutamide in prostate cancer after chemotherapy." New England Journal of Medicine **367**(13): 1187-1197.

Scher, H. I. and C. L. Sawyers (2005). "Biology of progressive, castration-resistant prostate cancer: Directed therapies targeting the androgen-receptor signaling axis." Journal of Clinical Oncology **23**(32): 8253-8261.

Schmitt, B., T. J. Wilt, P. F. Schellhammer, V. DeMasi, O. Sartor, E. D. Crawford and C. L. Bennett (2001). "Combined androgen blockade with nonsteroidal antiandrogens for advanced prostate cancer: a systematic review." Urology **57**(4): 727-732.

Schröder, F. H., J. Hugosson, M. J. Roobol, T. L. J. Tammela, S. Ciatto, V. Nelen, M. Kwiatkowski, M. Lujan, H. Lilja, M. Zappa, L. J. Denis, F. Recker, A. Páez, L. Määttänen, C. H. Bangma, G. Aus, S. Carlsson, A. Villers, X. Rebillard, T. Van Der Kwast, P. M. Kujala, B. G. Blijenberg, U. H. Stenman, A. Huber, K. Taari, M. Hakama, S. M. Moss, H. J. De Koning and A. Auvinen (2012). "Prostate-cancer mortality at 11 years of follow-up." New England Journal of Medicine **366**(11): 981-990.

Scott, A. M., G. Wiseman, S. Welt, A. Adjei, F. T. Lee, W. Hopkins, C. R. Divgi, L. H. Hanson, P. Mitchell, D. N. Gansen, S. M. Larson, J. N. Ingle, E. W. Hoffman, P. Tanswell, G. Ritter, L. S. Cohen, P. Bette, L. Arvay, A. Amelsberg, D. Vlock, W. J. Rettig and L. J. Old (2003). "A phase I dose-escalation study of sibrotuzumab in patients with advanced or metastatic fibroblast activation protein-positive cancer." Clinical Cancer Research **9**(5): 1639-1647.

Scott, S. L., J. D. Earle and P. H. Gumerlock (2003). "Functional p53 Increases Prostate Cancer Cell Survival after Exposure to Fractionated Doses of Ionizing Radiation." Cancer Research **63**(21): 7190-7196.

Sebens, S. and H. Schäfer (2012). "The Tumor Stroma as Mediator of Drug Resistance - A Potential Target to Improve Cancer Therapy?" Current Pharmaceutical Biotechnology **13**(11): 2259-2272.

Sertel, S., T. Eichhorn, J. Bauer, K. Hock, P. K. Plinkert and T. Efferth (2012). "Pharmacogenomic determination of genes associated with sensitivity or resistance of tumor cells to curcumin and curcumin derivatives." Journal of Nutritional Biochemistry **23**(8): 875-884.

Sethi, T., R. C. Rintoul, S. M. Moore, A. C. MacKinnon, D. Salter, C. Choo, E. R. Chilvers, I. Dransfield, S. C. Donnelly, R. Strieter and C. Haslett (1999). "Extracellular matrix proteins protect small cell lung cancer cells against apoptosis: A mechanism for small cell lung cancer growth and drug resistance in vivo." Nature Medicine **5**(6): 662-668.

Shah, S., S. Prasad and K. E. Knudsen (2012). "Targeting pioneering factor and hormone receptor cooperative pathways to suppress tumor progression." Cancer Research **72**(5): 1248-1259.

Shain, K. H. and W. S. Dalton (2001). "Cell adhesion is a key determinant in de Novo multidrug resistance (MDR): New targets for the prevention of acquired MDR." Molecular Cancer Therapeutics **1**(1): 69-78.

Shankar, S., Q. Chen, K. Sarva, I. Siddiqui and R. K. Srivastava (2007). "Curcumin enhances the apoptosis-inducing potential of TRAIL in prostate cancer cells: Molecular mechanisms of apoptosis, migration and angiogenesis." Journal of Molecular Signaling **2**.

Shankar, S., S. Ganapathy, Q. Chen and R. K. Srivastava (2008). "Curcumin sensitizes TRAIL-resistant xenografts: Molecular mechanisms of apoptosis, metastasis and angiogenesis." Molecular Cancer **7**.

Shankar, S. and R. K. Srivastava (2007). "Involvement of Bcl-2 family members, phosphatidylinositol 3'-kinase/AKT and mitochondrial p53 in curcumin (diferulolylmethane)- induced apoptosis in prostate cancer." International Journal of Oncology **30**(4): 905-918.

Sharma, R. A., S. A. Euden, S. L. Platton, D. N. Cooke, A. Shafayat, H. R. Hewitt, T. H. Marczylo, B. Morgan, D. Hemingway, S. M. Plummer, M. Pirmohamed, A. J. Gescher and W. P. Steward (2004). "Phase I clinical trial of oral curcumin: Biomarkers of systemic activity and compliance." Clinical Cancer Research **10**(20): 6847-6854.

Sharma, S. V., D. Y. Lee, B. Li, M. P. Quinlan, F. Takahashi, S. Maheswaran, U. McDermott, N. Azizian, L. Zou, M. A. Fischbach, K. K. Wong, K. Brandstetter, B. Wittner, S. Ramaswamy, M. Classon and J. Settleman (2010). "A Chromatin-Mediated Reversible Drug-Tolerant State in Cancer Cell Subpopulations." Cell **141**(1): 69-80.

Shaulian, E. and M. Karin (2001). "AP-1 in cell proliferation and survival." Oncogene **20**(19 REV. ISS. 2): 2390-2400.

Shaw, A., J. Papadopoulos, C. Johnson and W. Bushman (2006). "Isolation and characterization of an immortalized mouse urogenital sinus mesenchyme cell line." Prostate **66**(13): 1347-1358.

Shen, D. W., A. Fojo, J. E. Chin, I. B. Roninson, N. Richert, I. Pastan and M. M. Gottesman (1986). "Human multidrug-resistant cell lines: Increased mdr1 expression can precede gene amplification." Science **232**(4750): 643-645.

Shen, M. M. and C. Abate-Shen (2010). "Molecular genetics of prostate cancer: New prospects for old challenges." Genes and Development **24**(18): 1967-2000.

Shi, Q., C. C. Y. Shih and K. H. Lee (2009). "Novel anti-prostate cancer curcumin analogues that enhance androgen receptor degradation activity+." Anti-Cancer Agents in Medicinal Chemistry **9**(8): 904-912.

Shishodia, S., H. M. Amin, R. Lai and B. B. Aggarwal (2005). "Curcumin (diferuloylmethane) inhibits constitutive NF-κB activation, induces G1/S arrest, suppresses proliferation, and induces apoptosis in mantle cell lymphoma." Biochemical Pharmacology **70**(5): 700-713.

Shoba, G., D. Joy, T. Joseph, M. Majeed, R. Rajendran and P. S. S. R. Srinivas (1998). "Influence of piperine on the pharmacokinetics of curcumin in animals and human volunteers." Planta Medica **64**(4): 353-356.

Shu, L., T. O. Khor, J. H. Lee, S. S. S. Boyanapalli, Y. Huang, T. Y. Wu, C. L. L. Saw, K. L. Cheung and A. N. T. Kong (2011). "Epigenetic CpG demethylation of the promoter and reactivation of the expression of neurog1 by curcumin in prostate LNCaP cells." AAPS Journal **13**(4): 606-614.

Shukla, S., H. Zaher, A. Hartz, B. Bauer, J. A. Ware and S. V. Ambudkar (2009). "Curcumin inhibits the activity of ABCG2/BCRP1, a multidrug resistance-linked ABC drug transporter in mice." Pharmaceutical Research **26**(2): 480-487.

Signoretti, S. and M. Loda (2006). "Defining cell lineages in the prostate epithelium." Cell Cycle **5**(2): 138-141.

Simian, M., Y. Hirai, M. Navre, Z. Werb, A. Lochter and M. J. Bissell (2001). "The interplay of matrix metalloproteinases, morphogens and growth factors is necessary for branching of mammary epithelial cells." Development **128**(16): 3117-3131.

Singh, N., A. Shrivastav and R. K. Sharma (2009). "Curcumin induces caspase and calpain-dependent apoptosis in HT29 human colon cancer cells." Molecular Medicine Reports **2**(4): 627-631.

Singh, S., U. P. Singh, W. E. Grizzle and J. W. Lillard Jr (2004). "CXCL12-CXCR4 interactions modulate prostate cancer cell migration, metalloproteinase expression and invasion." Laboratory Investigation **84**(12): 1666-1676.

Sinha, R., D. E. Anderson, S. S. McDonald and P. Greenwald (2003). "Cancer risk and diet in India." Journal of Postgraduate Medicine **49**(3): 222-228.

Slovin, S. F., W. K. Kelly, A. Wilton, M. Kattan, P. Myskowski, J. Mendelsohn and H. I. Scher (2009). "Anti-epidermal growth factor receptor monoclonal antibody cetuximab plus doxorubicin in the treatment of metastatic castration-resistant prostate cancer." Clinical Genitourinary Cancer **7**(3): 77-82.

Smaletz, O., H. I. Scher, E. J. Small, D. A. Verbel, A. McMillan, K. Regan, W. K. Kelly and M. W. Kattan (2002). "Nomogram for overall survival of patients with progressive metastatic prostate cancer after castration." Journal of Clinical Oncology **20**(19): 3972-3982.

Smith-Jones, P. M., S. Vallabhajosula, V. Navarro, D. Bastidas, S. J. Goldsmith and N. H. Bander (2003). "Radiolabeled monoclonal antibodies specific to the extracellular domain of prostate-specific membrane antigen: Preclinical studies in nude mice bearing LNCaP human prostate tumor." Journal of Nuclear Medicine **44**(4): 610-617.

Smith, D. S. and W. J. Catalona (1995). "Interexaminer variability of digital rectal examination in detecting prostate cancer." Urology **45**(1): 70-74.

Smyth, G. K., J. Michaud and H. S. Scott (2005). "Use of within-array replicate spots for assessing differential expression in microarray experiments." Bioinformatics **21**(9): 2067-2075.

Sneharani, A. H., S. A. Singh and A. G. A. Rao (2009). "Interaction of αS1-casein with curcumin and its biological Implications." Journal of Agricultural and Food Chemistry **57**(21): 10386-10391.

Sodergard, R., T. Backstrom, V. Shanbhag and H. Carstensen (1982). "Calculation of free and bound fractions of testosterone and estradiol-17β to human plasma proteins at body temperature." Journal of Steroid Biochemistry **16**(6): 801-810.

Sokoloff, R., K. C. Norton, C. L. Gasior, K. M. Marker and L. S. Grauer (2000). "A dual-monoclonal sandwich assay for prostate-specific membrane antigen: Levels in tissues, seminal fluid and urine." Prostate **43**(2): 150-157.

Soloway, M. and M. Roach Iii (2005). "Prostate cancer progression after therapy of primary curative intent: A review of data from the prostate-specific antigen era." Cancer **104**(11): 2310-2322.

Song, K., S. Peng, Z. Sun, H. Li and R. Yang (2011). "Curcumin suppresses TGF-β signaling by inhibition of TGIF degradation in scleroderma fibroblasts." Biochemical and Biophysical Research Communications **411**(4): 821-825.

Sonnenberg, M., H. van der Kuip, S. Haubeiß, P. Fritz, W. Schroth, G. Friedel, W. Simon, T. E. Mürdter and W. E. Aulitzky (2008). "Highly variable response to cytotoxic chemotherapy in carcinoma-associated fibroblasts (CAFs) from lung and breast." BMC Cancer **8**.

Sreenivasan, S., S. Ravichandran, U. Vetrivel and S. Krishnakumar (2013). "Modulation of multidrug resistance 1 expression and function in retinoblastoma cells by curcumin." Journal of Pharmacology and Pharmacotherapeutics **4**(2): 103-109.

Srihari Rao, T., N. Basu and H. H. Siddiqui (1982). "Anti-inflammatory activity of curcumin analogues." Indian Journal of Medical Research **75**(4): 574-578.

Srimal, R. C. and B. N. Dhawan (1973). "Pharmacology of diferuloyl methane (curcumin), a non steroidal anti inflammatory agent." Journal of Pharmacy and Pharmacology **25**(6): 447-452.

Stamey, T. A., C. M. Yemoto, J. E. McNeal, B. M. Sigal and I. M. Johnstone (2000). "Prostate cancer is highly predictable: A prognostic equation based on all morphological variables in radical prostatectomy specimens." Journal of Urology **163**(4): 1155-1160.

Stankiewicz, A. R., G. Lachapelle, C. P. Z. Foo, S. M. Radicioni and D. D. Mosser (2005). "Hsp70 inhibits heat-induced apoptosis upstream of mitochondria by preventing Bax translocation." Journal of Biological Chemistry **280**(46): 38729-38739.

Steeghs, N., J. W. R. Nortier and H. Gelderblom (2007). "Small molecule tyrosine kinase inhibitors in the treatment of solid tumors: An update of recent developments." Annals of Surgical Oncology **14**(2): 942-953.

Stetler-Stevenson, W. G., S. Aznavoorian and L. A. Liotta (1993). "Tumor cell interactions with the extracellular matrix during invasion and metastasis." Annual Review of Cell Biology **9**: 541-573.

Stone, N. N., E. P. DeAntoni and F. D. Crawford (1994). "Screening for prostate cancer by digital rectal examination and prostate- specific antigen: Results of Prostate Cancer Awareness Week, 1989-1992." Urology **44**(6 SUPPL.): 18-25.

Strano, S., S. Dell'Orso, S. Di Agostino, G. Fontemaggi, A. Sacchi and G. Blandino (2007). "Mutant p53: An oncogenic transcription factor." Oncogene **26**(15): 2212-2219.

Strieter, R. M., R. Wiggins, S. H. Phan, B. L. Wharram, H. J. Showell, D. G. Remick, S. W. Chensue and S. L. Kunkel (1989). "Monocyte chemotactic protein gene expression by cytokine-treated human fibroblasts and endothelial cells." Biochemical and Biophysical Research Communications **162**(2): 694-700.

Su, C. C., J. S. Yang, C. C. Lu, J. H. Chiang, C. L. Wu, J. J. Lin, K. C. Lai, T. C. Hsia, H. F. Lu, M. J. Fan and J. G. Chung (2010). "Curcumin inhibits human lung large cell carcinoma cancer tumour growth in a murine xenograft model." Phytotherapy Research **24**(2): 189-192.

Sun, J. and Z. y. Zhao (2011). "Effect of curcumin on keloid fibroblasts cycle and nuclear factor-kappa B signaling pathways." Journal of Clinical Rehabilitative Tissue Engineering Research **15**(11): 2026-2029.

Sun, Y., J. Campisi, C. Higano, T. M. Beer, P. Porter, I. Coleman, L. True and P. S. Nelson (2012). "Treatment-induced damage to the tumor microenvironment promotes prostate cancer therapy resistance through WNT16B." Nature Medicine **18**(9): 1359-1368.

Sun, Z. J., G. Chen, W. Zhang, X. Hu, Y. Liu, Q. Zhou, L. X. Zhu and Y. F. Zhao (2011). "Curcumin dually inhibits both mammalian target of rapamycin and nuclear factor-κB pathways through a crossed phosphatidylinositol 3-kinase/Akt/IκB kinase complex signaling axis in adenoid cystic carcinoma." Molecular Pharmacology **79**(1): 106-118.

Sundram, V., S. C. Chauhan, M. Ebeling and M. Jaggi (2012). "Curcumin attenuates β-catenin signaling in prostate cancer cells through activation of protein kinase D1." PLoS ONE **7**(4).

Suzuki, K., P. Bose, R. Y. Leong-Quong, D. J. Fujita and K. Riabowol (2010). "REAP: A two minute cell fractionation method." BMC Research Notes **3**.

Syng-Ai, C., A. L. Kumari and A. Khar (2004). "Effect of curcumin on normal and tumor cells: Role of glutathione and bcl-2." Molecular Cancer Therapeutics **3**(9): 1101-1108.

Szejtli, J. (1998). "Introduction and general overview of cyclodextrin chemistry." Chemical Reviews **98**(5): 1743-1753.

Takahashi, M., S. Uechi, K. Takara, Y. Asikin and K. Wada (2009). "Evaluation of an oral carrier system in rats: Bioavailability and antioxidant properties of liposome-encapsulated curcumin." Journal of Agricultural and Food Chemistry **57**(19): 9141-9146.

Takeda, K., K. Okumura and M. J. Smyth (2007). "Combination antibody-based cancer immunotherapy." Cancer Science **98**(9): 1297-1302.

Tang, F., C. Barbacioru, E. Nordman, B. Li, N. Xu, V. I. Bashkirov, K. Lao and M. A. Surani (2010). "RNA-Seq analysis to capture the transcriptome landscape of a single cell." Nature Protocols **5**(3): 516-535.

Tang, H., C. J. Murphy, B. Zhang, Y. Shen, M. Sui, E. A. Van Kirk, X. Feng and W. J. Murdoch (2010). "Amphiphilic curcumin conjugate-forming nanoparticles as anticancer prodrug and drug carriers: In vitro and in vivo effects." Nanomedicine **5**(6): 855-865.

Tanner, M. J., R. C. Welliver Jr, M. Chen, M. Shtutman, A. Godoy, G. Smith, B. M. Mian and R. Buttyan (2011). "Effects of androgen receptor and androgen on gene expression in prostate stromal fibroblasts and paracrine signaling to prostate cancer cells." PLoS ONE **6**(1).

Tannock, I. F., R. De Wit, W. R. Berry, J. Horti, A. Pluzanska, K. N. Chi, S. Oudard, C. Théodore, N. D. James, I. Turesson, M. A. Rosenthal and M. A. Eisenberger (2004). "Docetaxel plus prednisone or mitoxantrone plus prednisone for advanced prostate cancer." New England Journal of Medicine **351**(15): 1502-1512.

Tarin, D. and C. B. Croft (1969). "Ultrastructural features of wound healing in mouse skin." Journal of Anatomy **105**(1): 189-190.

Teiten, M. H., F. Gaascht, M. Cronauer, E. Henry, M. Dicato and M. Diederich (2011). "Anti-proliferative potential of curcumin in androgen-dependent prostate cancer cells occurs through modulation of the Wingless signaling pathway." International Journal of Oncology **38**(3): 603-611.

Teiten, M. H., A. Gaigneaux, S. Chateauvieux, A. M. Billing, S. Planchon, F. Fack, J. Renaut, F. Mack, C. P. Muller, M. Dicato and M. Diederich (2012). "Identification of differentially expressed proteins in curcumin-treated prostate cancer cell lines." OMICS A Journal of Integrative Biology **16**(6): 289-300.

Thakkar, H., X. Chen, F. Tyan, S. Gim, H. Robinson, C. Lee, S. K. Pandey, C. Nwokorie, N. Onwudiwe and R. K. Srivastava (2001). "Pro-survival function of Akt/protein kinase B in prostate cancer cells. Relationship with trail resistance." Journal of Biological Chemistry **276**(42): 38361-38369.

Thangapazham, R. L., S. Shaheduzzaman, K. H. Kim, N. Passi, A. Tadese, M. Vahey, A. Dobi, S. Srivastava and R. K. Maheshwari (2008). "Androgen responsive and refractory prostate cancer cells exhibit distinct curcumin regulated transcriptome." Cancer Biology and Therapy **7**(9): 1429-1437.

Thayyullathil, F., S. Chathoth, A. Hago, M. Patel and S. Galadari (2008). "Rapid reactive oxygen species (ROS) generation induced by curcumin leads to caspase-dependent and -independent apoptosis in L929 cells." Free Radical Biology and Medicine **45**(10): 1403-1412.

Thomas, X., B. Anglaret, J. P. Magaud, J. Epstein and E. Archimbaud (1998). "Interdependence between cytokines and cell adhesion molecules to induce interleukin-6 production by stromal cells in myeloma." Leukemia and Lymphoma **32**(1-2): 107-119.

Thompson, T. C., T. L. Timme, D. Kadmon, S. H. Park, S. Egawa and K. Yoshida (1993). "Genetic predisposition and mesenchymal-epithelial interactions in ras + myc-induced carcinogenesis in reconstituted mouse prostate." Molecular Carcinogenesis **7**(3): 165-179.

Thornberry, N. A. and Y. Lazebnik (1998). "Caspases: Enemies within." Science **281**(5381): 1312-1316.

Tilley, W. D., G. Buchanan, T. E. Hickey and J. M. Bentel (1996). "Mutations in the androgen receptor gene are associated with progression of human prostate cancer to androgen independence." Clinical Cancer Research **2**(2): 277-285.

Tilley, W. D., M. Marcelli, J. D. Wilson and M. J. McPhaul (1989). "Characterization and expression of a cDNA encoding the human androgen receptor." Proceedings of the National Academy of Sciences of the United States of America **86**(1): 327-331.

Tolcher, A. W., M. Mita, N. J. Meropol, M. Von Mehren, A. Patnaik, K. Padavic, M. Hill, T. Mays, T. McCoy, N. L. Fox, W. Halpern, A. Corey and R. B. Cohen (2007). "Phase I pharmacokinetic and biologic correlative study of mapatumumab, a fully human monoclonal antibody with agonist activity to tumor necrosis factor-related apoptosis-inducing ligand receptor-1." Journal of Clinical Oncology **25**(11): 1390-1395.

Tomi, M., M. Mori, M. Tachikawa, K. Katayama, T. Terasaki and K. I. Hosoya (2005). "L-type amino acid transporter 1-mediated L-leucine transport at the inner blood-retinal barrier." Investigative Ophthalmology and Visual Science **46**(7): 2522-2530.

Tonneson, H. H., G. Smistad, T. Agren and J. Karlsen (1993). "Studies on curcumin and curcuminoids. XXIII: Effects of curcumin on liposomal lipid peroxidation." International Journal of Pharmaceutics **90**(3): 221-228.

Tourkina, E., P. Gooz, J. C. Oates, A. Ludwicka-Bradley, R. M. Silver and S. Hoffman (2004). "Curcumin-induced apoptosis in scleroderma lung fibroblasts: Role of protein kinase Cε." American Journal of Respiratory Cell and Molecular Biology **31**(1): 28-35.

Traverso, N., R. Ricciarelli, M. Nitti, B. Marengo, A. L. Furfaro, M. A. Pronzato, U. M. Marinari and C. Domenicotti (2013). "Role of glutathione in cancer progression and chemoresistance." Oxidative Medicine and Cellular Longevity.

Trimboli, A. J., C. Z. Cantemir-Stone, F. Li, J. A. Wallace, A. Merchant, N. Creasap, J. C. Thompson, E. Caserta, H. Wang, J. L. Chong, S. Naidu, G. Wei, S. M. Sharma, J. A. Stephens, S. A. Fernandez, M. N. Gurcan, M. B. Weinstein, S. H. Barsky, L. Yee, T. J. Rosol, P. C. Stromberg, M. L. Robinson, F. Pepin, M. Hallett, M. Park, M. C. Ostrowski and G. Leone (2009). "Pten in stromal fibroblasts suppresses mammary epithelial tumours." Nature **461**(7267): 1084-1091.

Trotta, A. P., E. F. Need, L. M. Butler, L. A. Selth, M. A. O'Loughlin, G. A. Coetzee, W. D. Tilley and G. Buchanan (2012). "Subdomain structure of the co-chaperone SGTA and activity of its androgen receptor client." Journal of Molecular Endocrinology **49**(2): 57-68.

Trotta, A. P., E. F. Need, L. A. Selth, S. Chopra, C. B. Pinnock, D. A. Leach, G. A. Coetzee, L. M. Butler, W. D. Tilley and G. Buchanan (2013). "Knockdown of the cochaperone SGTA results in the suppression of androgen and PI3K/Akt signaling and inhibition of prostate cancer cell proliferation." International Journal of Cancer **133**(12): 2812-2823.

Tsai, K. K. C., J. Stuart, Y. Y. E. Chuang, J. B. Little and Z. M. Yuan (2009). "Low-dose radiation-induced senescent stromal fibroblasts render nearby breast cancer cells radioresistant." Radiation Research **172**(3): 306-313.

Tyagi, R. K., Y. Lavrovsky, S. C. Ahn, C. S. Song, B. Chatterjee and A. K. Roy (2000). "Dynamics of intracellular movement and nucleocytoplasmic recycling of the ligand-activated androgen receptor in living cells." Molecular Endocrinology **14**(8): 1162-1174.

Urbanucci, A., S. Marttila, O. A. Jänne and T. Visakorpi (2012). "Androgen receptor overexpression alters binding dynamics of the receptor to chromatin and chromatin structure." Prostate **72**(11): 1223-1232.

Vairapandi, M., A. G. Balliet, A. J. Fornace Jr, B. Hoffman and D. A. Liebermann (1996). "The differentiation primary response gene MyD118, related to GADD45, encodes for a nuclear protein which interacts with PCNA and p21(WAF1/CIP1)." Oncogene **12**(12): 2579-2594.

Vanaja, D. K., S. H. Mitchell, D. O. Toft and C. Y. F. Young (2002). "Effect of geldanamycin on androgen receptor function and stability." Cell Stress and Chaperones **7**(1): 55-64.

Verma, S. P., E. Salamone and B. Goldin (1997). "Curcumin and genistein, plant natural products, show synergistic inhibitory effects on the growth of human breast cancer MCF-7 cells induced by estrogenic pesticides." Biochemical and Biophysical Research Communications **233**(3): 692-696.

Visakorpi, T., E. Hyytinen, P. Koivisto, M. Tanner, R. Keinanen, C. Palmberg, A. Palotie, T. Tammela, J. Isola and O. P. Kallioniemi (1995). "In vivo amplification of the androgen receptor gene and progression of human prostate cancer." Nature Genetics **9**(4): 401-406.

Voelkel-Johnson, C., D. L. King and J. S. Norris (2002). "Resistance of prostate cancer cells to soluble TNF-related apoptosis-inducing ligand (TRAIL/Apo2L) can be overcome by doxorubicin or adenoviral delivery of full-length TRAIL." Cancer Gene Therapy **9**(2): 164-172.

Wahl, H., L. Tan, K. Griffith, M. Choi and J. R. Liu (2007). "Curcumin enhances Apo2L/TRAIL-induced apoptosis in chemoresistant ovarian cancer cells." Gynecologic Oncology **105**(1): 104-112.

Wakelee, H. A., A. Patnaik, B. I. Sikic, M. Mita, N. L. Fox, R. Miceli, S. J. Ullrich, G. A. Fisher and A. W. Tolcher (2009). "Phase I and pharmacokinetic study of lexatumumab (HGS-ETR2) given every 2 weeks in patients with advanced solid tumors." Annals of Oncology **21**(2): 376-381.

Walczak, H., R. E. Miller, K. Ariail, B. Gliniak, T. S. Griffith, M. Kubin, W. Chin, J. Jones, A. Woodward, T. Le, C. Smith, P. Smolak, R. G. Goodwin, C. T. Rauch, J. C. L. Schuh and D. H. Lynch (1999). "Tumoricidal activity of tumor necrosis factor-related apoptosis-inducing ligand in vivo." Nature Medicine **5**(2): 157-163.

Walker, W. H. and J. Cheng (2005). "FSH and testosterone signaling in Sertoli cells." Reproduction **130**(1): 15-28.

Wang, D., M. S. Veena, K. Stevenson, C. Tang, B. Ho, J. D. Suh, V. M. Duarte, K. F. Faull, K. Mehta, E. S. Srivatsan and M. B. Wang (2008). "Liposome-encapsulated curcumin suppresses growth of head and neck squamous cell carcinoma in vitro and in xenografts through the inhibition of nuclear factor κB by an AKT-independent pathway." Clinical Cancer Research **14**(19): 6228-6236.

Wang, P., L. Zhang, H. Peng, Y. Li, J. Xiong and Z. Xu (2013). "The formulation and delivery of curcumin with solid lipid nanoparticles for the treatment of on non-small cell lung cancer both in vitro and in vivo." Materials Science and Engineering C **33**(8): 4802-4808.

Wang, Q., C. G. Bailey, C. Ng, J. Tiffen, A. Thoeng, V. Minhas, M. L. Lehman, S. C. Hendy, G. Buchanan, C. C. Nelson, J. E. J. Rasko and J. Holst (2011). "Androgen receptor and nutrient signaling pathways coordinate the demand for increased amino acid transport during prostate cancer progression." Cancer Research **71**(24): 7525-7536.

Wang, S. and W. S. El-Deiry (2003). "TRAIL and apoptosis induction by TNF-family death receptors." Oncogene **22**(53 REV. ISS. 7): 8628-8633.

Wang, Y., D. Sudilovsky, B. Zhang, P. C. Haughney, M. A. Rosen, D. S. Wu, T. J. Cunha, R. Dahiya, G. R. Cunha and S. W. Hayward (2001). "A human prostatic epithelial model of hormonal carcinogenesis." Cancer Research **61**(16): 6064-6072.

Wang, Y. J., M. H. Pan, A. L. Cheng, L. I. Lin, Y. S. Ho, C. Y. Hsieh and J. K. Lin (1997). "Stability of curcumin in buffer solutions and characterization of its degradation products." Journal of Pharmaceutical and Biomedical Analysis **15**(12): 1867-1876.

Wang, Z., M. H. M. Leung, T. W. Kee and D. S. English (2010). "The role of charge in the surfactant-assisted stabilization of the natural product curcumin." Langmuir **26**(8): 5520-5526.

Watson, J. L., A. Greenshields, R. Hill, A. Hilchie, P. W. Lee, C. A. Giacomantonio and D. W. Hoskin (2010). "Curcumin-induced apoptosis in ovarian carcinoma cells is p53-independent and involves p38 mitogen-activated protein kinase activation and downregulation of Bcl-2 and survivin expression and akt signaling." Molecular Carcinogenesis **49**(1): 13-24.

Watson, J. L., R. Hill, P. W. Lee, C. A. Giacomantonio and D. W. Hoskin (2008). "Curcumin induces apoptosis in HCT-116 human colon cancer cells in a p21-independent manner." Experimental and Molecular Pathology **84**(3): 230-233.

Weber, W. M., L. A. Hunsaker, S. F. Abcouwer, L. M. Deck and D. L. Vander Jagt (2005). "Anti-oxidant activities of curcumin and related enones." Bioorganic and Medicinal Chemistry **13**(11): 3811-3820.

Weigel, N. L. and Y. Zhang (1998). "Ligand-independent activation of steroid hormone receptors." Journal of Molecular Medicine **76**(7): 469-479.

Welch, H. G. and P. C. Albertsen (2009). "Prostate cancer diagnosis and treatment after the introduction of prostate-specific antigen screening: 1986-2005." Journal of the National Cancer Institute **101**(19): 1325-1329.

Welt, S., C. R. Divgi, A. M. Scott, P. Garin-Chesa, R. D. Finn, M. Graham, E. A. Carswell, A. Cohen, S. M. Larson, L. J. Old and W. J. Rettig (1994). "Antibody targeting in metastatic colon cancer: A phase I study of monoclonal antibody F19 against a cell-surface protein of reactive tumor stromal fibroblasts." Journal of Clinical Oncology **12**(6): 1193-1203.

Wen, Y., C. T. Wang, T. T. Ma, Z. Y. Li, L. N. Zhou, B. Mu, F. Leng, H. S. Shi, Y. O. Li and Y. Q. Wei (2010). "Immunotherapy targeting fibroblast activation protein inhibits tumor growth and increases survival in a murine colon cancer model." International Journal of Psychoanalysis **91**(5): 2325-2332.

Whittemore, A. S., A. H. Wu, L. N. Kolonel, E. M. John, R. P. Gallagher, G. R. Howe, D. W. West, C. Z. Teh and T. Stamey (1995). "Family history and prostate cancer risk in black, white, and Asian men in the United States and Canada." American Journal of Epidemiology **141**(8): 732-740.

Wikström, P., J. Marusic, P. Stattin and A. Bergh (2009). "Low stroma androgen receptor level in normal and tumor prostate tissue is related to poor outcome in prostate cancer patients." Prostate **69**(8): 799-809.

Wiley, S. R., K. Schooley, P. J. Smolak, W. S. Din, C. P. Huang, J. K. Nicholl, G. R. Sutherland, T. D. Smith, C. Rauch, C. A. Smith and R. G. Goodwin (1995). "Identification and characterization of a new member of the TNF family that induces apoptosis." Immunity **3**(6): 673-682.

Wilson, E. M. and F. S. French (1976). "Binding properties of androgen receptors. Evidence for identical receptors in rat testis, epididymis, and prostate." Journal of Biological Chemistry **251**(18): 5620-5629.

Wiseman, B. S. and Z. Werb (2002). "Development: Stromal effects on mammary gland development and breast cancer." Science **296**(5570): 1046-1049.

Wolk, A. (2005). "Diet, lifestyle and risk of prostate cancer." Acta Oncologica **44**(3): 277-281.

Wu, H. C., J. T. Hsieh, M. E. Gleave, N. M. Brown, S. Pathak and L. W. K. Chung (1994). "Derivation of androgen-independent human LNCaP prostatic cancer cell sublines: Role of bone stromal cells." International Journal of Cancer **57**(3): 406-412.

Wu, S. H., L. W. Hang, J. S. Yang, H. Y. Chen, H. Y. Lin, J. H. Chiang, C. C. Lu, J. L. Yang, T. Y. Lai, Y. C. Ko and J. G. Chung (2010). "Curcumin induces apoptosis in human non-small cell lung cancer NCI-H460 cells through ER stress and caspase cascade- and mitochondria-dependent pathways." Anticancer Research **30**(6): 2125-2133.

Xiong, Y., G. J. Hannon, H. Zhang, D. Casso, R. Kobayashi and D. Beach (1993). "p21 is a universal inhibitor of cyclin kinases." Nature **366**(6456): 701-704.

Xu, G., Y. Chu, N. Jiang, J. Yang and F. Li (2012). "The three dimensional quantitative structure activity relationships (3D-QSAR) and docking studies of curcumin derivatives as androgen receptor antagonists." International Journal of Molecular Sciences **13**(5): 6138-6155.

Xu, Y. X., K. R. Pindolia, N. Janakiraman, R. A. Chapman and S. C. Gautam (1997). "Curcumin inhibits IL1α and TNF-α induction of AP-1 and NF-kB DNA-binding activity in bone marrow stromal cells." Hematopathology and Molecular Hematology **11**(1): 49-62.

Xu, Y. X., K. R. Pindolia, N. Janakiraman, C. J. Noth, R. A. Chapman and S. C. Gautam (1997). "Curcumin, a compound with anti-inflammatory and anti oxidant properties, down-regulates chemokine expression in bone marrow stromal cells." Experimental Hematology **25**(5): 413-422.

Yadav, V. R., S. Prasad, R. Kannappan, J. Ravindran, M. M. Chaturvedi, L. Vaahtera, J. Parkkinen and B. B. Aggarwal (2010). "Cyclodextrin-complexed curcumin exhibits anti-inflammatory and antiproliferative activities superior to those of curcumin through higher cellular uptake." Biochemical Pharmacology **80**(7): 1021-1032.

Yallapu, M. M., B. K. Gupta, M. Jaggi and S. C. Chauhan (2010). "Fabrication of curcumin encapsulated PLGA nanoparticles for improved therapeutic effects in metastatic cancer cells." Journal of Colloid and Interface Science **351**(1): 19-29.

Yallapu, M. M., M. Jaggi and S. C. Chauhan (2010). "Poly(β-cyclodextrin)/Curcumin Self-Assembly: A Novel Approach to Improve Curcumin Delivery and its Therapeutic Efficacy in Prostate Cancer Cells." Macromolecular Bioscience **10**(10): 1141-1151.

Yan, H., X. Chen, Q. Zhang, J. Qin, H. Li, C. Liu, T. Calhoun-Davis, L. Della Coletta, J. Klostergaard, I. Fokt, S. Skora, W. Priebe, Y. Bi and D. G. Tang (2011). "Drug-tolerant cancer cells show reduced tumor-initiating capacity: Depletion of CD44 + cells and evidence for epigenetic mechanisms." PLoS ONE **6**(9).

Yano, S., E. Nakataki, S. Ohtsuka, M. Inayama, H. Tomimoto, N. Edakuni, S. Kakiuchi, N. Nishikubo, H. Muguruma and S. Sone (2005). "Retreatment of lung adenocarcinoma patients with gefitinib who had experienced favorable results from their initial treatment with this selective epidermal growth factor receptor inhibitor: A report of three cases." Oncology Research **15**(2): 107-111.

Yarden, R. I. and L. C. Brody (1999). "BRCA1 interacts with components of the histone deacetylase complex." Proceedings of the National Academy of Sciences of the United States of America **96**(9): 4983-4988.

Ye, M. X., Y. L. Zhao, Y. Li, Q. Miao, Z. K. Li, X. L. Ren, L. Q. Song, H. Yin and J. Zhang (2012). "Curcumin reverses cis-platin resistance and promotes human lung adenocarcinoma A549/DDP cell apoptosis through HIF-1α and caspase-3 mechanisms." Phytomedicine **19**(8-9): 779-787.

Younes, A., J. M. Vose, A. D. Zelenetz, M. R. Smith, H. A. Burris, S. M. Ansell, J. Klein, W. Halpern, R. Miceli, E. Kumm, N. L. Fox and M. S. Czuczman (2010). "A Phase 1b/2 trial of mapatumumab in patients with relapsed/refractory non-Hodgkin's lymphoma." British Journal of Cancer **103**(12): 1783-1787.

Yu, S., G. Shen, O. K. Tin, J. H. Kim and A. N. T. Kong (2008). "Curcumin inhibits Akt/mammalian target of rapamycin signaling through protein phosphatase-dependent mechanism." Molecular Cancer Therapeutics **7**(9): 2609-2620.

Yu, S., C. R. Yeh, Y. Niu, H. C. Chang, Y. C. Tsai, H. L. Moses, C. R. Shyr, C. Chang and S. Yeh (2012). "Altered prostate epithelial development in mice lacking the androgen receptor in stromal fibroblasts." Prostate **72**(4): 437-449.

Zannettino, A. C. W., J. R. Rayner, L. K. Ashman, T. J. Gonda and P. J. Simmons (1996). "A powerful new technique for isolating genes encoding cell surface antigens using retroviral expression cloning." Journal of Immunology **156**(2): 611-620.

Zeisberg, M., F. Strutz and G. A. Müller (2000). "Role of fibroblast activation in inducing interstitial fibrosis." Journal of Nephrology **13**(3 SUPPL.): S111-S120.

Zhang, D., C. Huang, C. Yang, R. J. Liu, J. Wang, J. Niu and D. Brömme (2011). "Antifibrotic effects of curcumin are associated with overexpression of cathepsins K and L in bleomycin treated mice and human fibroblasts." Respiratory Research **12**(154).

Zhang, H., Y. Xiong and D. Beach (1993). "Proliferating cell nuclear antigen and p21 are components of multiple cell cycle kinase complexes." Molecular Biology of the Cell **4**(9): 897-906.

Zhang, L. and B. Fang (2005). "Mechanisms of resistance to TRAIL-induced apoptosis in cancer." Cancer Gene Therapy **12**(3): 228-237.

Zhang, Y., J. Han, C. Lu and J. Liang (2005). "Extraction and antiseptic effect of curcumin on foods." Nongye Gongcheng Xuebao/Transactions of the Chinese Society of Agricultural Engineering **21**(2): 144-148.

Ziada, A., A. Barqawi, L. M. Glode, M. Varella-Garcia, F. Crighton, S. Majeski, M. Rosenblum, M. Kane, L. Chen and E. D. Crawford (2004). "The use of trastuzumab in the treatment of hormone refractory prostate cancer; phase II trial." Prostate **60**(4): 332-337.

Zinonos, I., A. Labrinidis, M. Lee, V. Liapis, S. Hay, V. Ponomarev, P. Diamond, A. C. W. Zannettino, D. M. Findlay and A. Evdokiou (2009). "Apomab, a fully human agonistic antibody to DR5, exhibits potent antitumor activity against primary and metastatic breast cancer." Molecular Cancer Therapeutics **8**(10): 2969-2980.

Zou, H., Y. Li, X. Liu and X. Wang (1999). "An APAf-1 · cytochrome C multimeric complex is a functional apoptosome that activates procaspase-9." Journal of Biological Chemistry **274**(17): 11549-11556.